



Universitat Autònoma de Barcelona

**ADVERTIMENT.** L'accés als continguts d'aquesta tesi queda condicionat a l'acceptació de les condicions d'ús establertes per la següent llicència Creative Commons:  [http://cat.creativecommons.org/?page\\_id=184](http://cat.creativecommons.org/?page_id=184)

**ADVERTENCIA.** El acceso a los contenidos de esta tesis queda condicionado a la aceptación de las condiciones de uso establecidas por la siguiente licencia Creative Commons:  <http://es.creativecommons.org/blog/licencias/>

**WARNING.** The access to the contents of this doctoral thesis it is limited to the acceptance of the use conditions set by the following Creative Commons license:  <https://creativecommons.org/licenses/?lang=en>



**Universitat Autònoma  
de Barcelona**

Escola d'Enginyeria

Departament d'Enginyeria Química, Biològica i Ambiental

GICOM (Composting Research Group)

Environmental Science and Technology studies

**Sophorolipids production by solid-state fermentation: from  
lab-scale to pilot plant**

**PhD Thesis**

**Pedro Jiménez Peñalver**

Supervised by:

Dr. Teresa Gea Leiva

Dr. Xavier Font Segura

Bellaterra, Cerdanyola del Vallés, Barcelona

September 2017





**Universitat Autònoma  
de Barcelona**

**Teresa Gea Leiva**, profesora titular, y **Xavier Font Segura**, profesor agregado, del Departament d'Enginyeria Química, Biològica i Ambiental de la Universitat Autònoma de Barcelona.

Certifican:

que, el graduado en Química y máster en Química Agrícola y Nuevos Alimentos **Pedro Jiménez Peñalver** ha realizado bajo nuestra dirección el trabajo con el título “Sophorolipids production by solid-state fermentation: from lab-scale to pilot plant” que se presenta en esta memoria, la cual constituye su tesis para optar al Grado de Doctor en Ciencia y Tecnología Ambiental por la Universitat Autònoma de Barcelona.

Y para que se tenga conocimiento y conste a efectos oportunos, presentamos en la Escola d'Enginyeria de la Universitat Auònoma de Barcelona la citada Tesis firmando el presente certificado.

Dra. Teresa Gea Leiva

Dr. Xavier Font Segura

Bellaterra, Septiembre 2017



A mi madre y a mi padre,

por ser mis maestros,

por estar incondicionalmente a mi lado,

por dar un sentido mayúsculo a la palabra FAMILIA.

---



## **Agradecimientos**

Al Ministerio de Economía y Competitividad por la financiación de los proyectos marco de esta tesis (CTM2012-33663 y CTM2015-69513-R) y por la financiación económica del doctorado (BES-2013-064852).

A mis directores de tesis Teresa Gea y Xavier Font, a Antoni Sánchez y al resto de miembros del grupo de investigación en compostatge (GICOM).

A Richard Gross, a Amanda Koh, y a Mohammad Ibrahim del Rensselaer Polytechnic Institute (Troy, NY).

A todos los estudiantes que han colaborado en esta tesis (Noel, Gyuwon, Juan, Elan, Jina, Silvia, Jordi, Laura, Raphaela, Ana, Jose Luis y Marta). Muy especialmente a Marta, cuyo trabajo queda recogido en el Capítulo 8 de esta memoria.

Al Departament d'Enginyeria Química Biològica i Ambiental (doctorandos, profesores, técnicos, secretaría, y personal de limpieza).

A las empresas Lípidos Santiga S.A. (LIPSA) y a AB Azucarera Iberia S.L. por proveernos de residuos para la realización de los experimentos.

Al Servei d'Anàlisi Química (Alba Eustaquio) y al Servei de Microscòpia (Alejandro Sánchez).





## **Agradecimientos extraoficiales**

Tener una idea genial. Leer unos papers. Planear un experimento. Recoger residuos. Triturar paja. Preparar mezclas. Poner el autoclave. Reservar el agitador. Poner el autoclave con lo que se te olvidó la primera vez. Plaquear. Comprobar el correo. Entregar comandas. Pedir la vez para calentar en los microondas. Bajar al Chema. Reírse. Inocular en la cámara de flujo. Fermentar. Recoger pedidos. Ir a la caseta. Extraer el soforolípido. Pesar las grasas. Limpiar. Analizar datos. Hacer gráficas. Discutir los resultados. Frustrarse. Odiar al dios de los soforolípidos. Pensar en dejar el doctorado una vez más. Respirar hondo. Aprender de los errores. Coger fuerzas. Volver a empezar.

\*\*\*

Comencé esta aventura, el doctorado, hace ya casi 4 años. Años en los que no solo he peleado para adquirir el título de doctor, si es que eso algo significa, sino que además ha sido una etapa de madurez personal, un tránsito entre la juventud y la adultez. Mi padre pensará en este punto que no madure tanto, no sea que me caiga del árbol. Pero oye, así lo siento. ¿Que qué ha pasado en estos años? Te lo cuento.

Corría el año 2013 cuando el dios de los soforolípidos con su poder infinito me sedujo para que hiciera un doctorado. De una lista de más de mil proyectos comencé a señalar aquellos que más me llamaban la atención. De entre los finalistas descarté el de Murcia, por razones que no voy a dejar por escrito por no herir sensibilidades, y después aquellos situados en la Comunidad de Madrid, pues el cuerpo me pedía un cambio de aires. Y allí quedó mi destino: Barcelona. En pleno auge independentista no es de extrañar que en mi entrevista telefónica preguntara al jefe del grupo hasta qué punto era importante hablar catalán. Este me dijo que no me preocupara por eso, que la ciencia era un ámbito internacional. Meses más tarde y tras la confirmación de que me habían seleccionado, descubriría que en ese “ámbito internacional” se encontraban representados prácticamente todos los países de América Central y del Sur. Y así ha pasado, que me voy sin hablar catalán, pero imitando perfectamente los acentos

sudamericanos. Y no será porque no me he empeñado duro en la dichosa ese sorda: Manressa, Terrasa, Cervessa.

Volvamos a situarnos de nuevo. Eran principios de diciembre de 2013, y mi yo de 23 años recorría las calles de Sabadell por la noche tirando de dos maletones bajo un buen chaparrón. Era mi primer día emancipado. Tras media hora caminando y calado hasta los huesos llegué hasta mi pisito de soltero situado en un barrio estupendo de Sabadell Nord donde los canis me recibieron con un leve movimiento de cabeza. Allí sobreviví los 6 primeros meses.

Comenzaron mis primeros días en la uni. Días de ubicarme, conocer a gente, intentar encajar. Si a alguien tengo que destacar de esos días, y de los que han venido después, es a mi directora de tesis. Digo directora por decir algo, pues ha sido mi coach, psicóloga, jefa, amiga, y un sinfín de cosas más. Ha sido sin lugar a dudas la persona de la que más he aprendido estos años, y desde luego la que más me ha visto crecer tanto a nivel personal como profesional (Papá, pregúntale ya verás cómo es cierto lo de que he madurado). Recuerdo con cariño cómo me escribía cada noche por WhatsApp para preguntarme si ya había cenado. Estoy seguro de que por aquel entonces pensabas: este se me vuelve a Madrid en cualquier momento.

Pero aguanté. Me costó, pero aguanté. Me hice a los espacios, me hice a los compañeros, encontré gente con la que comer... Y entonces, sin poder definir muy bien cuándo, comenzó un huracán de acontecimientos que aún hoy sigue imparable. Mis compañeros de la uni se acabaron convirtiendo en mis amigos, y por último en mi familia. ¡Incluso con algunos llegué a compartir piso durante 3 largos años! (Bendito Piso Iso...). ¿En qué momento dejé de decir “voy con los de la uni” a “voy con mis amigos de Barcelona”?

Tengo muchos, y muy buenos, recuerdos de esta etapa. La vez que fuimos a la Patum de Berga donde casi morimos aplastados. Las tesis y sus correspondientes pica picas. Aquella vez que hicimos una pequeña ruta en Kayaks de 5 horitas y su correspondiente intento fallido de rescatar unas gafas de sol. Cuando hicimos noche en aquel refugio en medio de un lago. El campeonato de Volley playa en el que, cabe recordar, ganó mi equipo. La vez que contratamos unos mariachis para una cena de tesis. ¡Y cuando contratamos a los gaiteros! Aquel paseo en otoño por La Fageda. Mi paso por la CUP como bastoner. El Fort Pienc. Las famosas paellas de la ETSE en

pleno julio bajo la sombra de la higuera. Los dimecres de pastís. Los momentos de musical en el laboratorio. La plancha del Chema. Los “cumpleaños feliz” en la cafetería. Las revueltas contra las puertas disuasorias. La estancia en Troy. Las limpiezas de la cámara fría donde, da igual cuántas veces se limpiara, siempre aparecía una muestra congelada del 2013. Los “recién”, las “demoras”, las cosas “malogradas”. La centrifuga y sus 6 vueltas y media. Los correos de Pili de “Benvinguts companys, QUIÉN HA ROTO...?” La Luisa y sus dolores de articulaciones. La Fina y sus conversaciones matinales. Los videos de tesis. La anarquía del cuarto de autoclaves. Las reservas de azúcar del despacho de la segunda planta. Las reuniones que comienzan con “Bueno... ¿Cómo va la Candi?”. Los jamones robados. Los debates eternos a la hora de la comida. Las escapadas al Chumi. Aprender a escribir sin dudar la palabra COMPOSTATGE. Los segundos en los que el tribunal anunciaba que tu amigo/a ya era doctor/a. Las llegadas. Las despedidas. Los reencuentros.

Y aquí estoy en mi terraza de Poble Sec, testigo fiel de los últimos coletazos del doctorado y de mi amor profundo por la ciudad de Barcelona, escribiendo las últimas palabras en una memoria que recoge mi trabajo, la mitad de mi vida, de estos casi 4 años. Aquí terminan las pesadillas cuando los reactores no funcionaban como debían, los cabreos cuando el personal no hacía un buen uso de los equipos, o la frustración al ver que el trabajo realizado no se correspondía con los resultados. Pero también terminan todas las cosas extraordinarias que he vivido en esta etapa. Tengo mucho que agradecer y me faltan palabras para poder describir lo que cada uno de vosotros, los que os habéis imaginado junto a mi mientras leíais estos recuerdos, ha significado para mi en estos años. Gracias por ser unos excelentes compañeros de trabajo y unos extraordinarios amigos, gracias por hacerme reír, gracias por enseñarme los rincones más bonitos de Catalunya, gracias por hacerme sentir querido, gracias por ayudarme, gracias por escucharme, gracias por animarme cuando me quejaba por enésima vez de lo que odiaba el doctorado, gracias por abrirme los ojos sobre tantos temas, gracias por mostrarme la mejor cara de la cultura catalana, gracias por tantos buenos momentos juntos. Me siento tremendamente afortunado de haber caído en este departamento para hacer la tesis. ¿Quizás el dios de los sofrolípidos lo tenía ya todo planeado?

En estos años he aprendido muchas cosas, más allá del mundo científico, que difícilmente hubiera podido aprender en otro ámbito y que, desde luego, me serán muy

útiles para seguir creciendo como persona y como profesional. Después de 9 largos años de vida universitaria, de haber estado en 5 universidades y en 4 grupos de investigación, toca emprender un nuevo vuelo. Gracias a todos los que me habéis dado los conocimientos y la fortaleza necesarios para enfrentarme con determinación a lo que esté por venir.

\*\*\*

## Overview of the Thesis

This work proposes a potential alternative approach to produce sophorolipids (SLs), a type of biosurfactant, which are presented as an alternative to chemically-produced surfactants due to their higher efficiency and better environmental compatibility. Two strategies have been performed in this work to increase their cost-performance relative to petroleum based surfactants, which determines their commercial viability. Both are based in the production of SLs by the solid-state fermentation (SSF) of solid hydrophobic substrates by the yeast *Starmerella bombicola*.

The first strategy was to use winterization oil cake (WOC), an oil cake that comes from the oil refining industry, to decrease the price of the substrates and, therefore, the final production costs of SLs. Sugar-beet molasses was used as co-substrate and wheat straw was chosen as inert support. The process was optimized in terms of substrates ratio, aeration rate and inoculum size at 0.5-L scale to obtain a yield of 0.261 g of SLs per g of substrate at day 10. The optimized process was successfully scale-up to a 40-L packed-bed bioreactor but problems associated with heat removal were found during the scale-up to a 100-L intermittently-mixed bioreactor. The chemical structure and interfacial properties of the SL natural mixture produced from the WOC were studied during a research stay at the Rensselaer Polytechnic Institute (RPI) in NY, USA.

The second strategy consisted in the use of stearic acid (C18:0) to obtain SLs with a specific structure that improves the physicochemical properties of the SL natural mixture and, therefore, their performance. Sugar-beet molasses was used as co-substrate and polyurethane foam (PUF) functioned as inert support. The effect of PUF density and water holding capacity was assessed and the process was optimized in terms of substrate and inoculum ratio to obtain a final yield of 0.211 g of SLs per g of substrate. SLs produced herein had high contents of diacetylated acidic and lactonic C18:0 SLs.

There were significant correlations between the SL yield and the oxygen consumed (COC). This suggests that the respiration parameter COC, can be used as an indirect measurement of the production of SLs for the on-line monitoring of SSF processes.

This thesis represents the beginning of a new research line focused on the production of SLs by SSF in the Composting Research Group (GICOM) at the Department of Chemical, Biological and Environmental Engineering of the Universitat Autònoma de Barcelona.



## Resumen de la Tesis

En este trabajo se propone una tecnología alternativa para producir soforolípidos (SLs), un tipo de biosurfactante, presentados como alternativa a los surfactantes producidos químicamente debido a su mayor eficiencia y mejor perfil medioambiental. En este trabajo se han explorado dos estrategias para mejorar la relación coste-eficiencia de los SLs respecto a los surfactantes producidos químicamente, que es lo que determina su viabilidad económica. Ambas estrategias están basadas en la producción de SLs mediante la fermentación en estado sólido (FES) de *Starmerella bombicola*.

La primera estrategia consistió en el uso de un residuo de winterización (RW) con el fin de disminuir el precio de los sustratos. Se utilizó melaza de azúcar como co-sustrato y paja de trigo como soporte inerte. El proceso fue optimizado en base a la ratio de sustratos, la velocidad de aireación y el tamaño del inóculo a escala de 100-g obteniendo un rendimiento de 0.261 g de SLs por g de sustrato a día 10. El proceso fue escalado satisfactoriamente a un biorreactor de lecho fijo de 40-L, pero se observaron problemas asociados con la eliminación del calor durante el escalado a un biorreactor de 100-L. Los SLs producidos a partir del RW fueron caracterizados durante una estancia en el Rensselaer Polytechnic Institute (RPI) en NY, EEUU.

La segunda estrategia consistió en el uso de ácido esteárico (C18:0) para obtener SLs con una estructura específica que mejore las propiedades fisicoquímicas de la mezcla natural de SLs y, por tanto, su eficiencia. Se utilizó melaza de azúcar como co-sustrato y espuma de poliuretano como soporte inerte. Se evaluó el efecto de la densidad de la espuma de poliuretano y la capacidad de retención hídrica y el proceso fue optimizado en base a la ratio de sustratos e inóculo obteniendo un rendimiento final de 0.211 g de SLs por g de sustrato. Los SLs producidos presentaron contenidos elevados de SLs diacetilados C18:0 ácido y lactónico.

Se observaron correlaciones significativas entre el rendimiento de SLs y el oxígeno consumido (COA). Esto sugiere que el COA puede ser usado como medida indirecta de la producción de SLs para la monitorización on-line de procesos de FES.

Esta tesis representa el comienzo de una nueva línea de investigación centrada en la producción de SLs por FES en el Grupo de Investigación en Compostaje (GICOM) del Departamento de Ingeniería Química, Biológica y Ambiental de la Universitat Autònoma de Barcelona.





## **Resum de la Tesi**

En aquest treball es proposa una tecnologia alternativa per a la producció de soforolípid (SLs), un tipus de biosurfactant, presentats com a alternativa als surfactants produïts químicament degut a la seva major eficiència i millor perfil mediambiental. En aquest treball s'han dut a terme dues estratègies per a millorar la relació de cost-eficiència dels SLs respecte als surfactants produïts químicament, que és el que determina la seva viabilitat econòmica. Ambdues estratègies estan basades en la producció de SLs mitjançant la fermentació en estat sòlid.

La primera estratègia va consistir en el ús d'un residu de winterització (RW) amb l'objectiu de disminuir el preu dels substrats i, per tant, el cost final de producció dels SLs. Es va utilitzar melassa de sucre com a co-substrat i palla de blat com a suport inert. El procés va ser optimitzat en base al rati de substrats, la velocitat d'aeració i a la mida de l'inòcul a escala de 100-g, obtenint-se un rendiment de 0.261 g per g de substrat al dia 10. El procés optimitzat, va ser escalat satisfactòriament a un bioreactor de llit fix de 40-L, però posteriorment, es van observar problemes associats amb l'eliminació de calor durant l'escalat a un bioreactor de 100-L amb barreja intermitent. L'estructura química i les propietats interfacials de la barreja natural dels SLs produït a partir del RW es va estudiar durant una estança al Rensselaer Polytechnic Institute (NY, USA).

La segona estratègia consistí en l'ús de àcid esteàric (C18:0) per a l'obtenció de SLs amb una estructura específica que millori les propietats fisicoquímiques de la barreja natural de SLs i, per tant, la seva eficiència. Es va utilitzar melassa de sucre com a co-substrat i escuma de poliuretà com a suport inert. L'efecte de la densitat de l'escuma de poliuretà i la capacitat de retenció hídrica van ser avaluades i el procés va ser optimitzat en base al rati de substrats e inòcul, obtenint-se un rendiment final de 0.211 g de SLs per g de substrat. Els SLs produïts contenien elevades quantitats de SLs C18:0.

Es van observar correlacions significatives entre el rendiment de SLs i l'oxigen consumit (COA). Això suggereix que el COA pot ser utilitzat com a mesura indirecta de la producció de SLs per a la monitorització en línia de processos de FES.

Aquesta tesi representa el començament d'una nova línia d'investigació centrada en la producció de SLs per FES en el Grup de Investigació en Compostatge (GICOM) del Departament d'Enginyeria Química, Biològica i Ambiental de la Universitat Autònoma de Barcelona.



# Content

## CHAPTER 1

<b><i>Introduction</i></b> .....	<b>1</b>
1.1. Biosurfactants: description and market overview .....	3
1.2. Sophorolipids as the most promising biosurfactants .....	6
1.3. Production of sophorolipids by solid-state fermentation .....	10
1.3.1. What is solid-state fermentation? .....	10
1.3.2. The potential of agro-industrial wastes in SSF .....	12
1.3.3. Biosurfactants by SSF .....	13
1.3.4. Sophorolipids by SSF: pros and cons .....	17

## CHAPTER 2

<b><i>Research objectives</i></b> .....	<b>21</b>
---	-----------

## CHAPTER 3

<b><i>Materials and methods</i></b> .....	<b>25</b>
3.1. Materials .....	27
3.1.1. Agro-industrial wastes and by-products .....	27
3.1.2. Strain <i>Starmerella bombicola</i> .....	28
3.2. Fermentation systems .....	31
3.2.1. Fermentation System I: 0.5-L scale .....	32
3.2.2. Fermentation System II: 40-L bioreactor .....	33
3.2.3. Fermentation System III: 100-L bioreactor .....	35
3.3. Respiration indices .....	37
3.4. Standard Analytical Methods .....	38
3.4.1. pH .....	38
3.4.2. Water content and dry matter .....	38
3.4.3. Organic matter .....	38

3.4.4. Bulk density .....	39
3.4.5. Water holding capacity .....	39
3.5. Specific methods for the monitoring of SSF processes .....	40
3.5.1. SL yield .....	40
3.5.2. Fat content .....	42
3.5.3. Glucose content .....	42
3.5.4. Reducing sugar content (DNS method) .....	43
3.5.5. Total sugar content (anthrone method) .....	43
3.5.6. Nitrogen content .....	44
3.5.7. Viable cell numbers .....	45
3.5.8. Scanning electron microscopy .....	45
3.6. Specific methods for the characterization of SLs .....	45
3.6.1. Structural characterization .....	45
3.6.2. SL purification .....	46
3.6.3. Interfacial properties .....	47
3.6.4. Synthesis of ethyl ester SL .....	49

## **CHAPTER 4**

<i>Sophorolipids from winterization oil cake by SSF: how we get here</i> .....	<b>53</b>
4.1. Materials .....	55
4.2. Experiments .....	57
4.3. Results and discussion .....	58
4.3.1. Step 1: SLs by SSF using glucose and oleic acid .....	58
4.3.2. Step 2: Screening of agro-industrial wastes and by-products as substrates ..	67
4.3.3. Step 3: Testing wheat straw as the inert support .....	71
4.4. Conclusions .....	76

## CHAPTER 5

<i>Sphorolipids from winterization oil cake by SSF: process optimization</i> .....	79
5.1. Materials .....	81
5.2. Experiments .....	82
5.3. Results and discussion .....	84
5.3.1 Optimizing the aeration rate and the ratio of substrates.....	84
5.3.2. Effect of inoculum size and sterilization.....	89
5.3.3. Monitoring SL production under optimized conditions.....	90
5.3.4. Effect of intermittent mixing on SL production.....	94
5.3.5. Process monitoring variables .....	98
5.3.6. Process versatility.....	98
5.4. Conclusions.....	101

## CHAPTER 6

<i>Sphorolipids from winterization oil cake by SSF: scale-up</i> .....	103
6.1. Materials .....	105
6.2. Experiments .....	106
6.3. Results and discussion .....	107
6.3.1. Effect of temperature on SL production.....	107
6.3.2. Scale-up to the 40-L bioreactor.....	109
6.3.3. Scale-up to the 100-L bioreactor.....	113
6.3.4. SL production by SSF: yields .....	118
6.4. Conclusions.....	119

## CHAPTER 7

<i>Sphorolipids from winterization oil cake by SSF: characterization</i> .....	121
7.1. Materials .....	123
7.2. Experiments .....	124

7.3. Results and discussion .....	125
7.3.1. Structural characterization by FTIR, <sup>1</sup> H-NMR and LC-MS .....	125
7.3.2. Purification and quantification .....	131
7.3.3. Comparison with SLs produced by SmF .....	133
7.3.4. Surface tension lowering capacity .....	135
7.3.5. Emulsion properties .....	138
7.3.6. Displacement activity .....	142
7.3.7. Interfacial properties of the ethyl ester SL .....	143
7.4. Conclusions.....	148

## **CHAPTER 8**

### ***Sophorolipids from stearic acid by SSF: process optimization and characterization*** 151

8.1. Materials .....	153
8.2. Experiments .....	154
8.3. Results and discussion .....	155
8.3.1. Effect of PUF density .....	155
8.3.2. Optimization of substrates ratio and inoculum size .....	156
8.3.3. Effect of PUF saturation in SL yield.....	159
8.3.4. Time course .....	160
8.3.5. Characterization of SLs from stearic acid.....	166
8.4. Conclusions.....	172

## **CHAPTER 9**

### ***Conclusions and future work***..... 173

### ***References***..... 179

### ***Annexes***..... 193

I. Fat characterization of the winterization oil cake.....	195
II. Calibration curves .....	197

III. Surface tension curves at temperatures ranging from 15 to 50 °C.....	201
IV. Ethyl ester SL characterization.....	203
V. Scanning electron microscope pictures of polyurethane foam cubes .....	205
VI. Surface tension curve of the SLs from stearic acid .....	207





## List of abbreviations

Abbreviation	Definition	Units
BD	Bulk density	$\text{g L}^{-1}$
CMC	Critical micelle concentration	
COC	Cumulative oxygen consumption	$\text{g O}_2 \text{ g}^{-1}\text{DM} /$ $\text{g O}_2 \text{ g}^{-1}\text{substrates}$
DM	Dry matter	%
EESL	Ethyl ester sophorolipid	
$^1\text{H-NMR}$	Proton Nuclear Magnetic Resonance	
FTIR	Fourier transform infrared spectroscopy	
HPLC	High pressure liquid chromatography	
LC-MS	Liquid chromatography – mass spectrometry	
MEL	Mannosylerythritol lipid	
MS	Mass spectrometry	
mST	Minimal surface tension	
MOL	Sugar beet molasses	
OM	Organic matter	%
OUR	Oxygen uptake rate	$\text{mg O}_2 \text{ g}^{-1}\text{DM h}^{-1} /$ $\text{mg O}_2 \text{ g}^{-1}\text{substrates h}^{-1}$
PUF	Polyurethane foam	
RL	Rhamnolipid	
SA	Stearic acid	
SEM	Scanning electron microscope	
SL	Sophorolipid	
SmF	Submerged fermentation	
SSF	Solid-state fermentation	
TIC	Total ion chromatogram	
TLC	Thin layer chromatography	
WC	Water content	%
WHC	Water holding capacity	$\text{g water g}^{-1}\text{material}$
WOC	Winterization oil cake	



# CHAPTER 1

---

## *Introduction*



### 1.1. Biosurfactants: description and market overview

Surfactants or surface active molecules are one of the most important bulk chemicals with a current world production estimated at 15 million tonnes per year and a growing market that is expected to reach \$36.1 billion by 2020 (Acmite Market Intelligence, 2013). They are amphiphilic molecules that decrease the interfacial tension between two different phases (air-liquid, liquid-liquid, solid-liquid, etc.). This characteristic property of surfactants results in the reduction of repulsive forces between dissimilar phases and allows the two phases to mix and interact more easily (Soberón-Chávez, 2011). Thus, these molecules can act as detergents, wetting agents, emulsifiers, foaming agents, and dispersants. Surfactants are used in almost every product of human daily life: approximately half of the total production is used in household and laundry detergents, and the other half is used in cosmetics, foods, textiles, agriculture, paper industry, pharmaceuticals, etc. (Van Bogaert et al., 2011b).

The usage of surfactants in such large quantities present several environmental and health burdens associated with their production and use. Regarding their production, most synthetic surfactants are synthesized from petroleum, a non-renewable source, through chemical synthesis routes that can be environmentally hazardous. Also, these molecules inevitably end in the environment after use, which have a potential negative impact in the aquatic systems due to their high toxicity and low rate of biodegradation (Knepper, et al., 2003; Mann and Bidwell, 2001). The ecotoxicity, bio-accumulation and low biodegradability of these molecules have become issues of major concern in the last decades, which have led to more stringent policies and the withdrawal of several surfactants from the market. For example, the production and use of nonylphenol and nonylphenol ethoxylate were banned in the European Union in 2003 due to their negative effects on health and the environment (European Union, 2003; Soares et al., 2008).

Biosurfactants, surface-active molecules produced by a variety of microorganisms, are presented as an alternative to synthetic surfactants. First, because they can be produced from cheap renewable feedstocks, or even waste materials, by fermentation. Second, because biosurfactants have shown better foaming properties and stable activity at extremes of pH, salinity and temperature. And third, because they are readily biodegradable and display low toxicity, and hence, have greater environmental

compatibility (Mukherjee et al., 2006). In this sense, biosurfactants are preferred over synthetic surfactants to be applied for the remediation of contaminated soils (Bordas et al., 2005; Wang and Mulligan, 2009) or to enhance oil recovery (Pornsunthorntawee et al., 2008), and their use can be extended to the synthesis of new polymers and bioplastics, in detergents and cosmetics, in foods and beverages, and even in the pharmaceutical industry (Singh et al., 2007).

Biosurfactants appear in the nature as a wide variety of molecules with key physiological roles in the growth of microorganisms. For example, they are important for motility, cell-cell interactions and cellular differentiation, substrate accession and the avoidance of toxic elements and compounds (Van Hamme et al., 2006). It has also been described that biosurfactants can act as carbon and energy reservoir or may simply be by-products released in response to environmental changes (Hommel et al., 1994b). It is believed that only a small fraction of biosurfactants have been characterized to date and, therefore, their functions involved in the growth of microorganisms could be even more. The increasing research in areas as genomics, proteomics and metabolomics will provide more information about structures and functions of biosurfactants in the nature (Van Hamme et al., 2006).

In general, biosurfactants are classified in two major groups: low-molecular-weight biosurfactants, composed generally by glycolipids and lipopeptides; and high-molecular-weight biosurfactants, which are polysaccharides and lipopolysaccharides, and proteins and lipoproteins (Figure 1.1) (Van Hamme et al., 2006). It is reasonable to assume that different groups of biosurfactants with different chemical structures have different surface properties. For example, low-molecular-weight biosurfactants are more effective lowering the interfacial and surface tension while high-molecular-weight biosurfactants are better stabilizing oil-in-water emulsions (Ron and Rosenberg, 2001).

To date, most research has been focused on the process development to produce glycolipids and lipopeptides by submerged fermentation (SmF). Glycolipids are the most studied biosurfactants and are constituted by carbohydrates attached with long-chain fatty acids or hydroxylated fatty acids by a glycosidic bond. There are plenty of studies about the production of rhamnolipids (RLs) by *Pseudomonas aeruginosa* (Haba et al., 2014; Radzuan et al., 2017; Sathi Reddy et al., 2016), mannosylerythritol lipids (MELs) by *Pseudozyma antarctica* (Faria et al., 2015; Morita et al., 2007), and

sophorolipids (SLs) by *Starmerella bombicola* (previously *Candida bombicola*) (Daverey and Pakshirajan, 2009; Rispoli et al., 2010). In the case of lipopeptides, they are constituted by a lipid attached to a polypeptide chain and most research has been focused on the production of surfactin by different strains of *Bacillus* (Slivinski et al., 2012; Zhi et al., 2017).

Recently, these biosurfactants have found their way to the market and are currently produced and used commercially by several companies. For example, RLs are produced by Jeneil Biosurfactant Company LLC (USA) and Rhamnolipid, Inc. (USA) for their use in cleaning products, agriculture, food products, cosmetics and pharmaceuticals (Soberón-Chávez, 2011). MELs are produced by Henkel (Germany) for their usage in cleaning products and cosmetics (Randhawa and Rahman, 2014). In the case of SLs, they are currently produced by Ecover (Belgium), Soliance (France), SyntheZyme (USA) or Kaneka Co. (Japan) for their application in detergents, cosmetics, pest control and more (Van Bogaert and Soetaert, 2011).

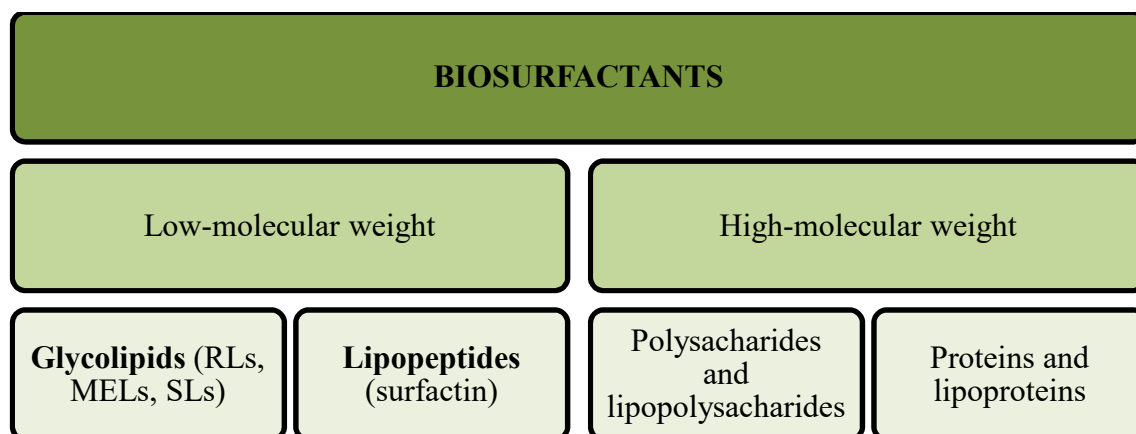


**Figure 1.1.** Classification of biosurfactants (RLs, rhamnolipids; MELs, mannosylerythritol lipids; and SLs, sophorolipids).

It is clear that there is an increasing tendency for the creation of green companies that not only supply green chemicals to other industries but also develop new products as detergents or cosmetics more environmentally friendly. This tendency may be explained from three different points of view. From a social point of view, there is a growing environmental awareness and a higher interest in products with a better environmental profile. From a political point of view, many countries are developing



more stringent policies regarding the use of certain chemically-synthesized molecules and, therefore, there is a necessity to replace the banned chemicals by others with a better environmental and health profile. Also, there is an increasing public investment for the development of bioprocesses and biorefineries to produce bioproducts such as enzymes, biosurfactants, biopesticides, bioplastics, etc. From an economical point of view, the new bio-based economy framework is an opportunity for the creation not only of new companies but also qualified jobs. However, there are still several technological challenges to overcome in order to achieve more sustainable and efficient processes that can compete with the optimized petrochemical production chains (Mussatto, 2017).

## **1.2. Sophorolipids as the most promising biosurfactants**

As mentioned before, SLs are a glycolipid type microbial biosurfactants that provide an environmentally friendly alternative to chemically-produced surfactants used in a wide variety of applications. SLs show excellent surface and interfacial tension properties which make them ideal to be used in formulations of cleaning products or cosmetics. Additionally, they have good anti-microbial, anti-inflammatory, anti-HIV and even anti-cancer effects, which allow these molecules to be used even in the pharmaceutical industry (Chen et al., 2006; Díaz De Rienzo et al., 2015; Rashad et al., 2014; Shah et al., 2005).

SLs are preferred over other biosurfactants for two main reasons. First, because high production yields (over 400 g L<sup>-1</sup>) and substrate conversion (70%) can be achieved by fermentation. And second, because SLs are produced by non-pathogenic yeast species, which is in contrast with RLs. The most widely studied specie and most efficient SL producer is *Starmerella bombicola*, which was isolated from the honey of a bumblebee (Spencer et al., 1970). The strain ATCC 22214 available in culture collections is the one preferred because it has shown the best yields (Van Bogaert et al., 2011b). Other species such as *Candida apicola*, *Pichia anomala* or *Wickerhamiella domercqiae* have also been identified as SL producers but low yields have been reported (Chen et al., 2006; Gorin et al., 1961; Thaniyavarn et al., 2008). From a biological point of view, SLs are produced extracellularly as secondary metabolites during the stationary growth phase and may be used as a carbon and energy reservoir for the yeast (Hommel et al., 1994b).

SL molecules consist of a sophorose (diglucose with a  $\beta$ -1,2 bond) bound to a hydroxylated fatty acid (mainly C18:1) through a glycosidic linkage (Figure 1.2). It is well-known that SLs are produced as a mixture of slightly different molecules with two main points of variation: acetylation in the sophorose moiety and lactonization. The acetylation may occur at the 6' or 6'' positions of the sophorose. The fatty acid tail might be free (acid form) or forming an internal esterification between the carboxylic end of the fatty acid and the 4'' position of the sophorose (lactonic form). Other variations that occur are the fatty acid chain length (generally 16 or 18 carbon atoms) and degree of unsaturation (0, 1, or 2 double bonds). As would be anticipated, differences in the SL structure impact their biological and physicochemical properties. For example, lactonic SLs have better surface tension properties and antimicrobial activity, whereas the acidic ones display better foam production and solubility (Van Bogaert et al., 2011b).

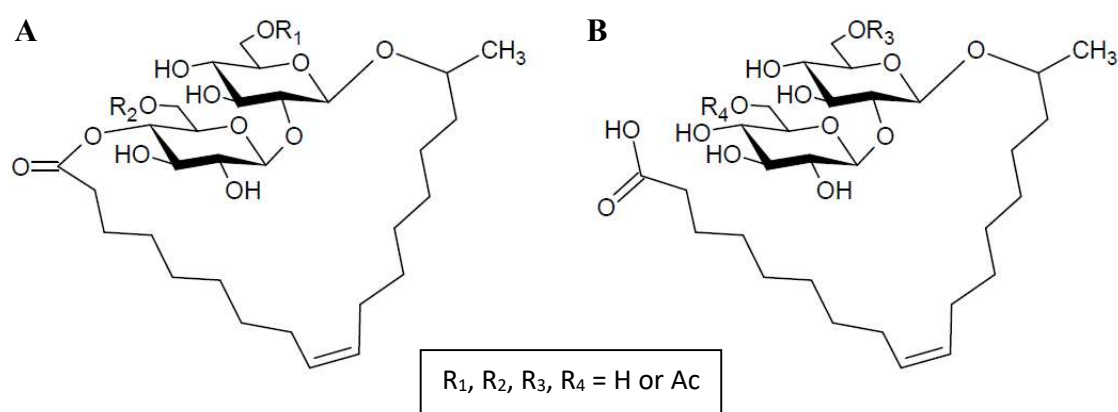


**Figure 1.2.** Structure of C18:1 sophorolipids (A) lactonic form and (B) free acid form.

The suggested SL biosynthesis pathway is shown in Figure 1.3. As can be observed, there are two main inputs: a hydrophilic carbon source, activated glucoses, and a hydrophobic carbon source, fatty acids. The fatty acids can be directly supplemented to the media or can be supplied as triglyceride or a fatty acid methyl- or ethyl ester which will undergo extracellular hydrolysis by a lipase (Van Bogaert et al., 2011b). If hydrophobic carbon source is not available, fatty acids will be synthesized *de novo* from acetyl-CoA derived from the glycolysis (Van Bogaert et al., 2008). However, it is well-known that better yields are achieved when both hydrophilic and hydrophobic

carbon sources are in the fermentation media. It should be remarked that glucoses are not directly incorporated to the SL structure, but firstly directed to the glycolysis (Hommel et al., 1994a). This explains why the structure of the sophorose moiety cannot be modified by simply changing glucose by other carbohydrates (Klekner et al., 1991). In contrast, the SL fatty acid moiety can be altered to a certain extent by changing the hydrophobic carbon source (Ashby et al., 2008).

SLs are conventionally produced in SmFs using glucose as the hydrophilic carbon source and a high oleic acid feedstock (C18:1) as the hydrophobic carbon source (Kim et al., 2009; Koh and Gross, 2016a). Generally, oleic acid or vegetable oils rich in oleic acid as rapeseed oil are used for optimal productions (Kim et al., 2009). The fermentation media is also supplemented with a nitrogen source as yeast extract or urea and small amounts of minerals as Mg, Fe, Ca, Zn and Na (Van Bogaert et al., 2011b).

To expand the market of SLs, research should be focused on the improvement of their cost-performance relative to petroleum based surfactants, which determines their commercial viability. This can be achieved adopting two strategies: (i) the use of cheaper renewable feedstocks or even waste materials as substrates, and (ii) the production of modified SLs with better biological and physicochemical properties and, therefore, better performance.

The first strategy is the use of solid hydrophobic wastes to decrease the price of the substrates and, therefore, the final production costs of SLs. Conventional substrates used for SL synthesis (glucose, oleic acid, yeast extract, etc.) affect considerably to the total production costs. Substrates account from 10 to 30% of the final price of a bioproduct in most biotechnological processes (Mukherjee et al., 2006). These conventional substrates can be substituted by cheaper renewable feedstocks or even waste materials but lower yields are generally obtained. For example, glucose can be replaced by sucrose (Klekner et al., 1991), sugarcane molasses (Daverey and Pakshirajan, 2009; Takahashi et al., 2011), soy molasses (Solaiman et al., 2004; Solaiman et al., 2007), deproteinized whey (Daniel et al., 1998; Daverey and Pakshirajan, 2010), cheese whey (Zhou and Kosaric, 1995) or biomass hydroxylates (Konishi et al., 2015; Samad et al., 2015). As the hydrophobic carbon source, the use of a biodiesel by-product stream (Ashby et al., 2005), waste frying oil (Fleurackers, 2006; Maddikeri et al., 2015; Shah et al., 2007), animal fat (Deshpande and Daniels, 1995) or industrial fatty acid residues (Felse et al.,

2007) have been successfully explored to produce SLs under SmF. Proper calculations should be done to ensure that the production costs of the SLs are lower using these low-cost materials.

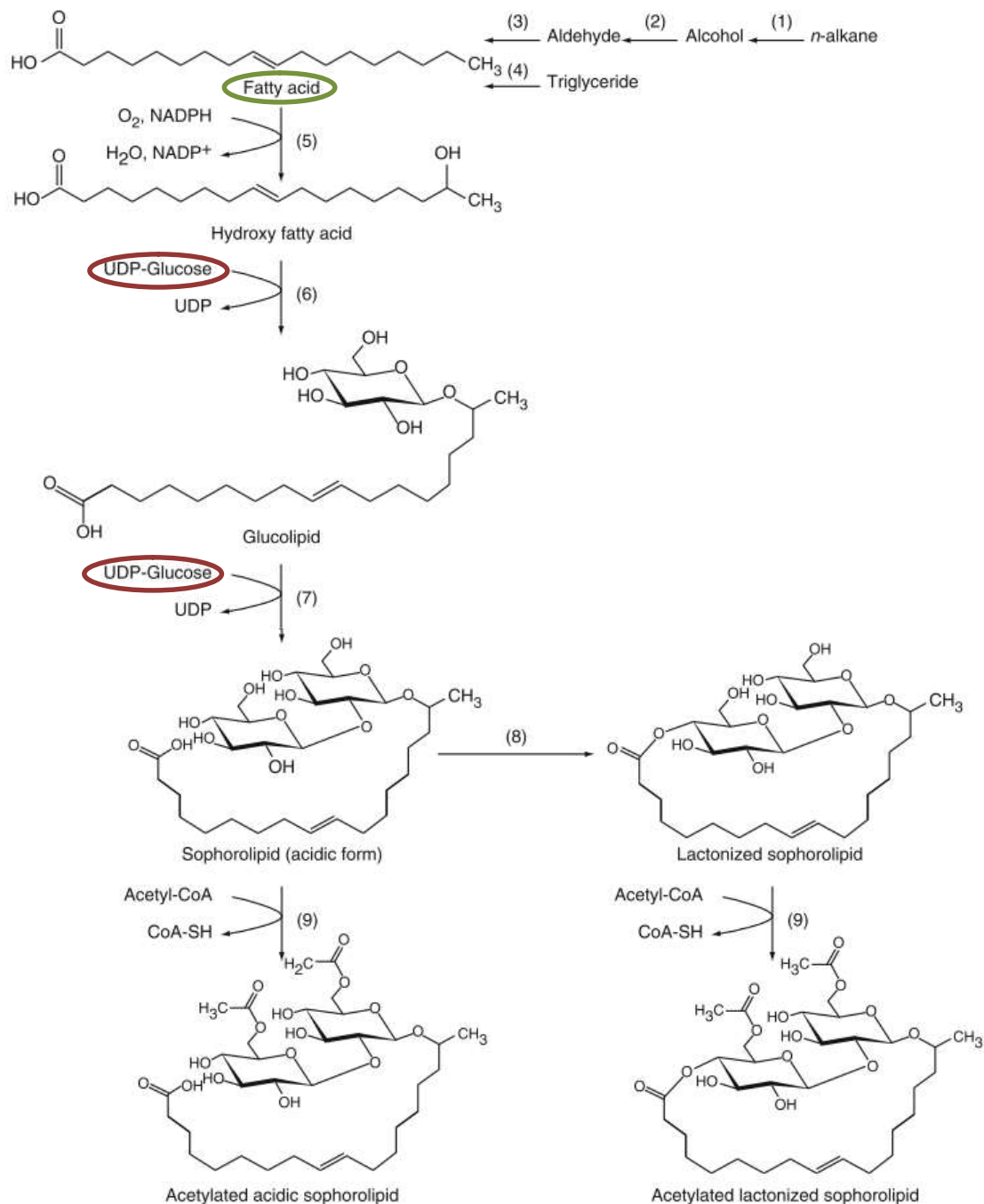


**Figure 1.3.** Proposed sophorolipid biosynthesis pathway: (1) cytochrome P450 monooxygenase, (2) alcohol-dehydrogenase, (3) aldehyde-dehydrogenase, (4) lipase, (5) cytochrome P450 monooxygenase, (6) glucosyltransferase I, (7) glucosyltransferase II, (8) lactonesterase, (9) acetyltransferase. Source: Van Bogaert and Soetaert, (2011).

The second strategy consists in production of modified SLs with a specific structure. As would be anticipated, differences in the SL structure impact their biological and physicochemical properties, which is especially important in improving their cost-performance in selected applications (Koh and Gross, 2016a). Modified SLs can be obtained either by post-fermentative modification (Peng et al., 2015; Zhang et al., 2004), or during the microbial synthesis. Examples of the latter are the use of genetically modified strains (Van Bogaert et al., 2016; Roelants et al., 2016) and the variation in the hydrophobic carbon source which can change the SL hydrophobic tail composition (Ashby et al., 2008; Hu and Ju, 2001). However, some potential hydrophobic carbon sources are solids at the fermentation temperature (e.g. stearic acid, C18:0, melting point 69.3 °C) which complicates their use as substrate in SmF processes. In such instances, solid-state fermentation (SSF) provides a potentially useful alternative fermentation approach. This approach would be also appropriate for solid hydrophobic wastes as oil cakes from the oil refining industries.

### **1.3. Production of sophorolipids by solid-state fermentation**

#### **1.3.1. What is solid-state fermentation?**

Solid-state fermentation (SSF) is defined as a heterogeneous process with a solid, a liquid and a gaseous phase where microorganisms grow in the absence or near absence of free water (Thomas et al., 2013). The solid phase could be either a substrate that acts as the source of carbon and other nutrients, or an inert support with an impregnated media with nutrients (Figure 1.4). The inert support might have a natural origin as sugarcane bagasse or wheat bran (Parekh and Pandit, 2012; Slivinski et al., 2012); or be synthetic as perlite, vermiculite, polyurethane foams or polystyrene (Gautam, 2002; Hernández-Rodríguez et al., 2009; Martin del Campo et al., 2015; Mata-Gómez et al., 2015). The usage of inert supports ensures a more or less constant physical structure of the solid phase during the fermentation process since they are not degraded by microorganisms. It avoids heat and mass transfer problems due to compaction, which are normally observed when substrates are used as the carbon source. An additional advantage of using inert supports is that the bioproduct is recovered more easily and with fewer impurities, and the inert support might be reused (Ooijkaas et al., 2000).

Also, SSF systems with inert supports allow a better optimization, control and monitoring of the process since all the nutrients in the SSF system are known.

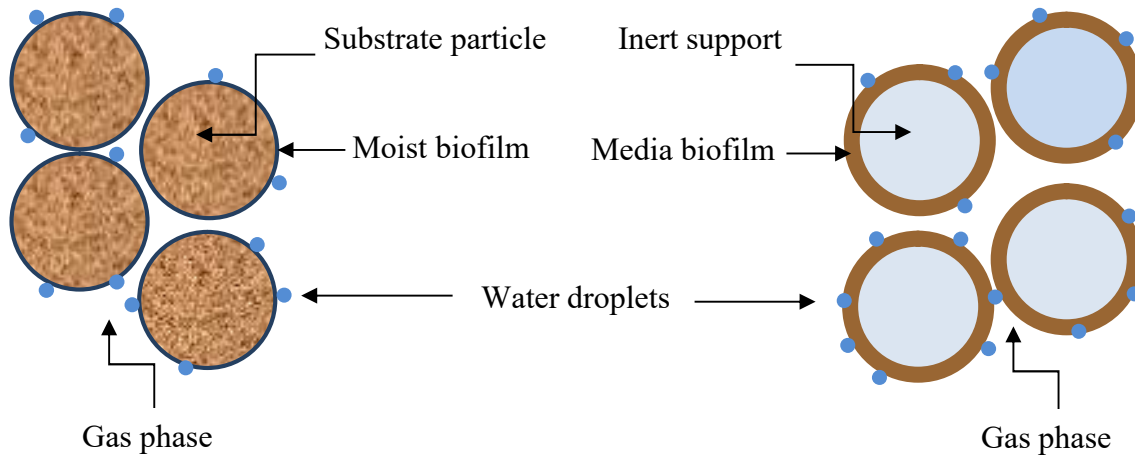


**Figure 1.4.** SSF systems when the solid phase is a substrate (left) or an inert support impregnated with media (right).

Despite the multiple advantages that inert supports offer, the use of substrates as the carbon source seems to be more attractive for researchers. From an economical point of view, this system seems cheaper since the use of an inert support impregnated with media is costlier than the use of a substrate, which are normally low-cost agro-industrial residues or by-products. Also, the time needed to prepare the SSF mixture is lower (Mitchell et al., 2006). From an environmental point of view, the usage of substrates seems more attractive as a way to valorize these agro-industrial residues or by-products as will be discussed below. Either if the solid phase is a substrate or an inert support impregnated with media, it must possess enough moisture to support the growth and the metabolic activity of the microorganisms. The SSF system also includes a gas phase which passes within the solid phase providing oxygen to the microorganisms and exhausting the carbon dioxide from their metabolic activity (Figure 1.4).

There are various types of microorganisms used in the SSF process including fungi, yeasts, and bacteria. However, fungi and yeast are the most commonly reported because SSF can provide an habitat similar to its natural one, which has low water activity in the fermentation media (Yazid et al., 2017). Besides the water activity, there are several other physicochemical factors that are essential for optimal growth and activity of the

microorganism as temperature, pH, moisture, aeration rate and, the most important, the nature of solid substrates.

There has been an increasing interest over the past decade in SSF for processes for production of biochemicals such as enzymes, biosurfactants, organic acids, bioplastics, biopolymers, biopesticides or pigments and aroma compounds (Thomas et al., 2013), and pretreatment of lignocellulose to increase its recalcitrance for saccharification (de Barros et al., 2017). SSF has proven successfully for the production of several compounds at high yields that are sometimes higher than those obtained in SmF (Mussatto et al., 2015). This has spurred work in SSF bioreactor design to increase its efficiency (Mitchell et al., 2006; Rodríguez-Jasso et al., 2013). Consequently, some SSF processes are already performed at the commercial scale in the food industry or for waste management and bioremediation processes.

### **1.3.2. The potential of agro-industrial wastes in SSF**

As mentioned before, agro-industrial residues or by-products are normally used as substrates in SSF processes. It firstly adds an economical value to these residues or by-products, and secondly solves the problem of their disposal, which would cause pollution. To date, most agro-industrial residues are treated biologically in processes as composting or anaerobic digestion, which are implemented all over the world (Haug, 1993). However, the potential of some of these agro-industrial wastes could be better exploited by other technologies as SSF.

Authorities as the European Commission or at the United States of America are including policies for general waste prevention, waste recycling and biological treatments for the reduction of final disposal in landfills. Specifically, the Waste Framework Directive (2008/98/CE) of the European Commission requires that all the urban and industrial wastes generated must be treated in a way that protects the environment and human health (European Union, 2003). These policies have motivated the industries to find a solution to the residues they generate to avoid taxes for waste disposal and become more environmentally friendly at the same time. For example, the well-known company Procter & Gamble (USA), which produces personal and home care products, has recently announced that any of their manufacturing sites would send wastes to landfills by 2020 (Procter and Gamble, 2017). Currently the 56% of their

global production sites has achieved this goal by converting liquid wastes into biogas or solid wastes into compost. The most important achievement has been the use of residues from the corn harvesting to obtain bioethanol that is later included in their products. This is just an example of the zero-waste philosophy that is being pursued by some industries in the new bio-based economy framework.

The interest to achieve the goal of zero-waste disposal is not only pursued by big international industries, but also by relatively small local companies. In the case of Barcelona, our research group (GICOM) has been working in the last years with several agro-industrial local industries to valorize their wastes by SSF. For example, soy fiber from the food industry has been proven successfully to produce proteases amylases and biopesticides using the strain *Bacillus thuringiensis* (Abraham et al., 2013; Ballardo et al., 2016; Cerda et al., 2016a). Hair waste from the tanning industry was used together with an anaerobically digested sludge to produce proteases in 10-L bioreactors (Abraham et al., 2014; Yazid et al., 2016). Coffee husk from the food industry was proven as a feasible substrate to obtain cellulases (Cerda et al., 2017). In this work, a SSF system of 4.5L bioreactors was operated continuously by sequential batch operation using the fermented solids from one batch to inoculate the following batch. Martínez et al. (2017) used a mixture of sugarcane bagasse and sugar beet molasses inoculated with *Kluyveromyces marxianus* to produce aroma compounds which can be used in the fragrance and flavor sector. A winterization oil cake (WOC), an oil cake that comes from the oil-refining industry, was used to produce lipases using a raw sludge as inoculum and co-substrate (Santis-Navarro et al., 2011). This WOC is a fat-rich residue obtained by cooling sunflower oil to 5 °C for 24 h, followed by the removal of waxes by filtering with perlite. Currently, this waste is being sold as cattle food with an economical income for the industry of just 20€ per ton. However, it seems that the high fat content of the WOC (60-70%) would allow the valorization of this residue in several other ways. For example, it could be used as the hydrophobic carbon source in the synthesis of SLs.

### 1.3.3. Biosurfactants by SSF

There has been considerable attention on the production of biosurfactants in recent years, as can be deduced from the growing number of scientific publications in this



issue (Figure 1.5). Similarly, there have been an increasing interest in SSF processes, especially in the last decade (Figure 1.5). However, there are just few studies regarding the production of biosurfactants by SSF. Table 1.1 summarizes all the studies found in the literature focused on the production of biosurfactants by SSF. As can be observed, research has only been focused on the production of the glycolipids SLs and RLs; and lipopeptides, especially surfactin. These biosurfactants are indeed the ones with higher industrial interest as explained in the previous section.

Only three studies have been published on the production of SLs by SSF. Parekh and Pandit (2012) produced SLs using glucose and oleic acid as substrates (blended with wheat bran) and obtained a maximum SL yield of 0.180 g per g of substrate at day 8 of fermentation. Similar yields were obtained when the oleic acid was substituted by mango kernel fat as the hydrophobic carbon source (Parekh et al., 2012). Interestingly, the SL yield was 3 times higher than the obtained by SmF using the same amount of mango kernel fat which confirms that SSF is a more suitable technology for solid substrates. These authors also produced SLs from stearic acid (C18:0) under SmF and SSF and obtained 2.5 times higher substrate conversion into SLs by SSF (0.085 g g<sup>-1</sup> substrates, day 10). Rashad et al. (2014) used a medium based on a mixture of sunflower oil cake and soybean oil moistened with a nutrient medium. These authors obtained a maximum yield of 0.221 g per g of substrates at day 8 when using the same extraction method as that used by Parekh and Pandit (2012) and Parekh et al. (2012).

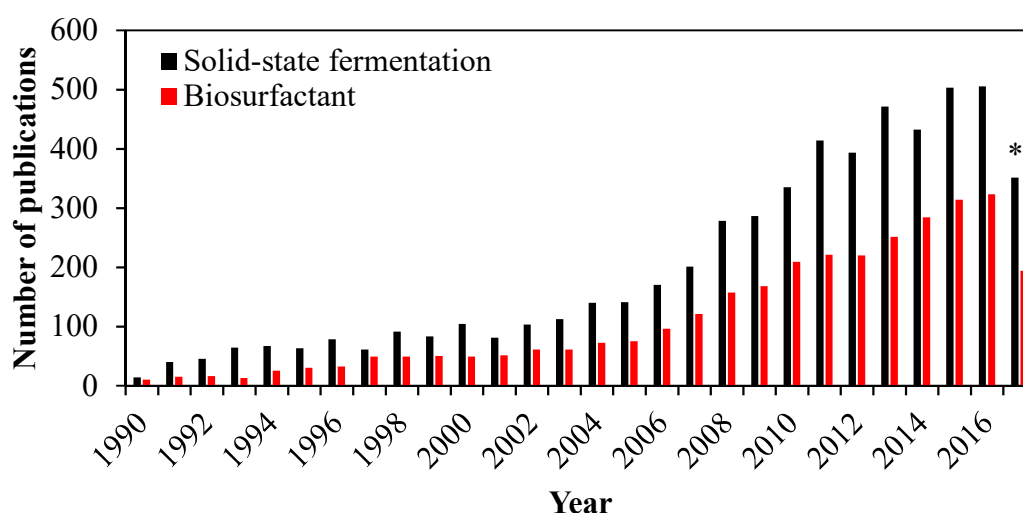


**Figure 1.5.** Number of publications per year about biosurfactants and solid-state fermentation. Source: [www.webofknowledge.com](http://www.webofknowledge.com). \*Last time consulted: 01/09/17.

**Table 1.1.** Summary of different biosurfactants produced by solid-state fermentation.

<b>Biosurfactant</b>	<b>Substrates</b>	<b>Amount of substrates (g)</b>	<b>Microorganism</b>	<b>Yield (g g<sup>-1</sup> substrates)</b>	<b>Reference</b>
Sophorolipids	Glucose and oleic acid	4	<i>Starmerella bombicola</i>	0.180	(Parekh and Pandit, 2012)
	blended with wheat bran		ATCC 22214		
	Glucose and mango kernel	4	<i>Starmerella bombicola</i>	0.175	(Parekh et al., 2012)
	fat blended with wheat bran		ATCC 22214		
	Glucose and stearic acid	4	<i>Starmerella bombicola</i>	0.085	(Parekh et al., 2012)
blended with wheat bran		ATCC 22214			
Rhamnolipids	Sunflower oil cake and crude soybean oil	10	<i>Starmerella bombicola</i>	0.221	(Rashad et al., 2014)
			ATCC 22214		
Surfactin	Sugarcane bagasse and corn bran	10	<i>Pseudomonas aeruginosa</i>	-	(Camilios-Neto et al., 2011)
			UFPEDA 614		
Surfactin	Mahua oil cake	5	<i>Serratia rubidaea</i>	-	(Nalini and Parthasarathi, 2014)
			SNAU02		
Surfactin	Okara and sugarcane bagasse as the bulking agent	14	<i>Bacillus pumilus</i> UFPEDA	0.003	(Slivinski et al., 2012)
			448		

**Table 1.1 (continuation).** Summary of different biosurfactants produced by solid-state fermentation.

<b>Biosurfactant</b>	<b>Substrates</b>	<b>Amount of substrates (g)</b>	<b>Microorganism</b>	<b>Yield (g g<sup>-1</sup> substrates)</b>	<b>Reference</b>
Surfactin	Rice straw and soybean flour	9	<i>Bacillus amyloliquefaciens</i>	0.050	(Zhu et al., 2012)
	Rice straw and soybean flour	9,000	<i>Bacillus amyloliquefaciens</i> XZ-173	0.015	(Zhu et al., 2013)
Lipopeptides	Potato peels	5	<i>Bacillus subtilis</i>	0.067	(Das and Mukherjee, 2007)
	Pre-treated molasses	5	<i>Brevibacterium aureum</i> MSA13	-	(Seghal Kiran et al., 2010)
	Fish flour and potato waste flour	10	<i>Bacillus subtilis</i> SPB1	0.028	(Mnif et al., 2013)
Biosurfactant	Olive leaf residues and olive cake flour	10	<i>Bacillus subtilis</i> SPB1	0.031	(Zouari et al., 2014)
	Peanut oil cake	5	<i>Bacillus cereus</i> SNAU01	-	(Nalini et al., 2016)
Biosurfactant	Sunflower seed shells	5	<i>Pleurotus djamor</i>	-	(Velioglu and Ozturk Urek, 2015)

These three studies and the rest listed in Table 1.1 were performed using small amounts (4-14 g) of substrates and, as such, did not deal with scale-up issues such as compaction. Only one study performed the scale-up of the process into a 50-L bioreactor using rice straw and soybean flour to produce surfactin (Zhu et al., 2013). However, these authors used a SmF bioreactor for this purpose and provided little information about the setup, operation and monitoring of the fermentation process. To our knowledge, this is the only work performed at pilot scale regarding the production of biosurfactants by SSF, which demonstrates the lack of information on this topic.

#### **1.3.4. Sophorolipids by SSF: pros and cons**

SSF shows certain potential advantages to produce biosurfactants, and more specifically SLs, over SmF despite the small number of works performed on this topic. These advantages are: (i) the feasibility to work with solid hydrophobic substrates, (ii) neither foaming nor viscosity complicates the fermentation process, and (iii) there are less water requirements and better oxygen transfer to the fermentation media.

Regarding the first point, SSF allows the use of solid hydrophobic substrates which are difficult to use in SmF processes. These solid substrates might be wastes or by-products such as oil cakes (Nalini and Parthasarathi, 2014) or pure substrates as stearic acid (Parekh et al., 2012). As already mentioned, the use of these two kind of substrates would increase the cost-performance of SLs relative to petroleum-based surfactants.

Regarding the second point, SSF avoids potential problems of foaming and viscosity which are typically found in SmF bioreactors. Foam appears due to the agitation and forced aeration used in the bioreactor and affects negatively to the fermentation process due to the reduction in the efficiency of gas transfer between the gas and liquid phases and the loss of cells that tend to accumulate within the foam. Normally, foaming is combatted through the addition of anti-foaming agents, which are expensive and decrease the oxygen and carbon dioxide transfer between gas and liquid phases (Winterburn and Martin, 2012). Foam can also be broken with mechanical devices. However, this is not effective when large quantities of foam are produced, as in the case of biosurfactant production processes (Krieger et al., 2010). Foam does not form in SSF systems since the air passes within particles and is not entered through a liquid containing biosurfactant.

Viscosity of the medium can gradually increase during SmF processes due to the associated formation of exopolysaccharides (Thomas et al., 2013). Viscosity is especially important when bioreactors are operated in the fed-batch mode due to the continuous addition of substrates and the accumulation of the product in the fermentation broth. Viscosity hinders agitation and gas transfer in the fermentation media. Problems associated with foaming and viscosity can be minimized by the periodical removal of SLs from the bioreactor during the fermentation following the methodology proposed by Dolman et al. (2017). These authors separate SLs gravimetrically from the fermentation broth because of their different density.

Finally, regarding the third point, SSF processes display better oxygen transfer to the solid bed and have low water requirements (Krieger et al., 2010). It is well-known that oxygen transfer in SmF processes is very limited due to the low solubility of oxygen in water. It forces the usage of high aeration rates into the reactor that highly exceeds the requirements of the microorganisms. Also, SmF processes require big volumes of water to produce low-concentrated products. Water requirements can be decreased by increasing the volumetric production of the bioreactor which can be achieved working in the fed-batch mode (Dolman et al., 2017; Maddikeri et al., 2015).

Despite the potential advantages that SSF shows versus SmF, there are several challenges which must be addressed before the developing of large-scale SSF processes: (i) the design of bioreactors with high rates of heat removal, (ii) the monitoring of the fermentation process, and (iii) the development of an economic and environmentally friendly methodology for the downstream.

Regarding the first point, the design of large-scale bioreactors with high rates of heat removal is essential to maintain the temperature of the SSF mixture as close as possible to the optimal temperature for microbial growth and product formation. In this sense, aeration rate plays a key role in heat removal in large-scale processes due to the ineffectiveness of water jackets or cooling coils to remove heat from solids (Krieger et al., 2010). However, high aeration rates greatly affect the water content of the SSF mixture in the reactor creating gradients along the solid mixture. For this reason, rotating drums or agitated bioreactors seem to be the most appropriate configurations for processes sensitive to high temperatures (Mitchell et al., 2006). It should be noticed that this kind of bioreactors are not appropriate when working with filamentous fungi

since the fungal hyphae can be damaged when the bed is mixed. In contrast, bacteria and yeast are much less susceptible to mechanical damage during mixing. Currently, there are few commercially available bioreactors for SSF processes, which is in contrast with the wide variety of SmF bioreactors available in the market.

Regarding the second point, monitoring of the SSF process to produce biosurfactants remains as a challenge. Biomass determination is specially complicated with fungi since the fungal hyphae typically penetrate the substrate making it impossible to separate them. In the case of bacteria and yeast, extraction from the media is easier but biomass quantification is still not accurate since part of the biomass tends to be retained in the solids and some solids are also extracted from the residual solid substrate. Microbial activity can be indirectly monitor by measuring oxygen consumption. Respirometry has been used for the monitoring of some SSF processes but not for biosurfactants (Cerda et al., 2017).

Monitoring of biosurfactant production can be performed by various methods. For example, the removal of large samples from the SSF mixture and the extraction of the biosurfactant as one would do at the end of the process. Also, water can be added to a small sample and determine the surface lowering capacity. However, this is a coarse method that provides not accurate data since surface tension keeps constant above certain surfactant concentrations. Similarly, the emulsification index can be used for monitoring (Nalini and Parthasarathi, 2014). Another method for the monitoring of biosurfactant production is the use of HPLC methods. This is probably the most accurate manner but their use is complicated for these biosurfactants that are produced as mixtures, as in the case of SLs (Hu and Ju, 2001).

Finally, regarding the third point, another key challenge is the development of an economic and environmentally friendly methodology for the downstream. SLs can be easily separated from SmFs since they are heavier than water, allowing to centrifuge them down or to just decant them from the fermentation medium (Van Bogaert et al., 2011b). So far, at lab scale, SLs are extracted from the solid mixture with organic solvents as ethyl acetate or ethanol as an analytical tool to measure the production (Parekh and Pandit, 2012). However, this methodology is unfeasible to be used in large-scale processes since a huge amount of solvents would be needed, even if they are recycled, and the final solids would be impregnated in solvent hampering their disposal

(Krieger et al., 2010) or valorization. Supercritical fluid extraction could be presented as an alternative. This technology has been studied for the recovery of other products from SSF processes but not for biosurfactants (Martins et al., 2011). It should be noticed that the fermented solid might be used directly in some applications at the end of the process such as in bioremediation of soils (Singh et al., 2007). In these applications, SL extraction and purification would not be needed.

Table 1.2 summarizes the pros and cons described above.

**Table 1.2.** Pros and cons of sophorolipid production by SSF.

<b>Pros</b>	<b>Cons</b>
Use of solid hydrophobic substrates	Few commercially available bioreactors
No problems of foaming or viscosity	Imprecise tools for the monitoring
Better oxygen transfer and low water requirements than SmF processes	Difficulty to recover the product

## CHAPTER 2

---

### *Research objectives*





This research has been developed within the research line “From waste to products” of the research group GICOM at UAB. The consolidated background of GICOM on the composting and valorization of organic wastes was used as the starting point of this study. This is the first work of the research group based on the production of biosurfactants by solid-state fermentation, and one of the few in which the organic materials are inoculated with a pure strain.

The main goal of this research is to study the production of sophorolipids through solid-state fermentation with *S. bombicola* at lab and pilot scale using both pure substrates and agro-industrial wastes and by-products.

To go deeper and reach this main goal, several specific objectives were also set and are presented below divided in two main lines:

(i) Production of SLs using wastes and by-products:

- To learn how to produce SLs in a SSF mixture based on pure substrates.
- To search and screen national agro-industrial wastes or by-products as suitable substrates to produce SLs by SSF.
- To optimize the most promising SSF mixture to maximize SL yield and to get a better understanding of the process dynamics at 0.5-L scale.
- To scale-up the process to a 40-L and a 100-L bioreactors.
- To determine the structure and concentration of the SLs contained in the SL natural mixture and to purify the most abundant SL.
- To study the interfacial properties of the SL natural mixture in terms of surface tension lowering capacity, emulsion properties and displacement activity.

- To obtain SLs by SmF and to compare the SLs obtained with the ones obtained by SSF.
- To investigate the potential correlations between SL yield and monitoring variables.

(ii) Production of SLs using pure substrate:

- To produce SLs by an SSF system using stearic acid as the hydrophobic carbon source and to optimize the process to maximize SL yield.
- To characterize the SLs produced using stearic acid in terms of structure and interfacial properties.

## CHAPTER 3

---

### *Materials and methods*



## Summary

This chapter describes the yeast strain and the agro-industrial wastes and by-products used for SSF, the setup of the Fermentation Systems where experiments were performed, and the general methodologies used during this research. Some specific materials, setup and methodologies are reported in detail at the corresponding chapter.

## 3.1. Materials

### 3.1.1. Agro-industrial wastes and by-products

The agro-industrial wastes and by-products used in this research were a winterization oil cake (WOC), a bleaching oil cake (BOC), and sugar-beet molasses (MOL). The WOC provided by the oil refinery LIPSA (Lípidos Santiga S.A., Barcelona, Spain) is obtained by cooling sunflower oil to 5 °C for 24 h, followed by the removal of waxes by filtering with perlite. The chemical composition of the WOC depends on the efficiency of the winterization process and the quality of the raw oil. Therefore, WOC composition, in terms of waxes and other fats, can vary slightly among different batches. Fat content of WOC was determined for every new batch of waste and ranged from 60 to 70% db. According to the information provided by LIPSA, most of these fats corresponds to sunflower oil that remains in the perlite after filtration, and only a low percentage corresponds to waxes. Fats from WOC were characterized by Lluís Jané Busquets Laboratori d'Anàlisi S.L. (Barcelona). Results showed that waxes represent only the 4% of the WOC (Annex I). The fatty acids profile of the sunflower oil remained in the WOC was also determined by Lluís Jané Busquets Laboratori d'Anàlisi S.L. (Barcelona). Results indicated that around the 80% of total fatty acids corresponds with oleic acid (Table 3.1), which indicates that the oil in the WOC is a high oleic sunflower oil (Flagella et al., 2002). The complete profile of fatty acids is detailed in Annex I.

BOC, also known as spent bleaching earth, was also provided by LIPSA. This waste is obtained after the discoloration of vegetable oils. MOL were generously provided by the sugar company AB Azucarera Iberia S.L. (Madrid, Spain). This by-product corresponds to the syrup left from the final crystallization stage of the sugar

beets and has a high content in sugars. Sugar content of MOL was determined for every new batch of by-product and showed a value of around 78% db.

WOC, BOC and MOL were stored in a fridge chamber (4 °C) for a maximum of 4 months. No changes were observed in their physicochemical properties during this time. Physical appearance of the substrates is illustrated in Figure 3.1. Specific details on the characterization of WOC, BOC and MOL are described at each chapter.

**Table 3.1.** Fatty acid composition of the sunflower oil remained in the winterization oil cake.

Fatty acid	Palmitic acid C16:0	Stearic acid C18:0	Oleic acid C18:1	Linoleic acid C18:2
Composition (%)	4.62	2.77	80.88	7.67

### 3.1.2. Strain *Starmerella bombicola*

#### Yeast strain

*Starmerella bombicola* ATCC 22214 was obtained from the American Type Culture Collection (ATCC, Manassas, USA). The strain was rehydrated according to the instructions provided by ATCC, maintained at -80 °C in cryovials with 10% (v/v) glycerol. A new streak plate was cultivated for each experiment. The method of the seed lot system was used to maintain the genetic stability of the strain (Figure 3.1). More information about the seed lot system and general information about cryopreservation can be found elsewhere (Simione, 2009).

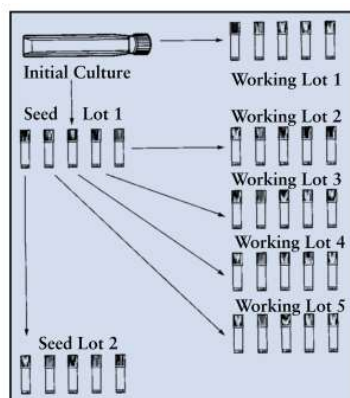


**Figure 3.1.** Seed lot system used for the preservation of the yeast *Starmerella bombicola*. Figure from: (Simione, 2009).

### Inoculum preparation

The strain, inoculated from a glycerol stock, was grown on agar streak plates, for 48 h at 30 °C, that contained (g L<sup>-1</sup>): dextrose, 10; peptone, 5; malt extract, 3; yeast extract, 3; agar, 20. To prepare the inoculum, a loop full of freshly grown yeast from agar streak plates (Figure 3.2), was transferred to a 250-mL Erlenmeyer flask with 50 mL of sterile medium. The medium contained (g L<sup>-1</sup>): dextrose, 10; peptone, 5; malt extract, 3; yeast extract, 3. The culture was incubated in an orbital incubator shaker at 30 °C, 180 rpm for 48 h (Figure 3.2). For the experiments of Chapter 6, the inoculum was grown on 1-L Erlenmeyer flasks with 200 mL of sterile medium. A summary of the process for inoculum preparation is shown in Figure 3.3.

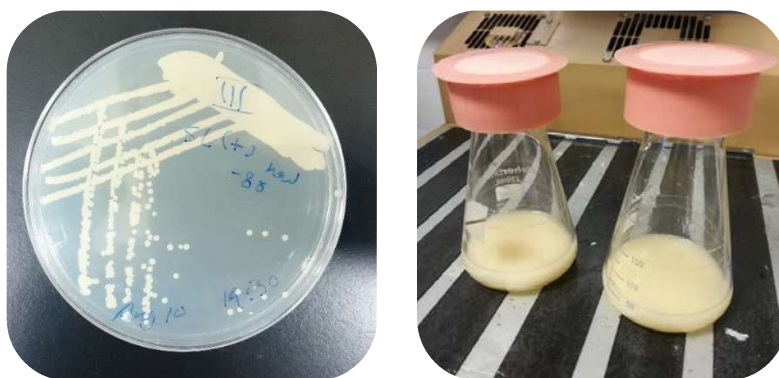


**Figure 3.2.** Agar streak plate with the yeast *Starmerella bombicola* after 48 h of incubation (left) and fresh inoculum (right).

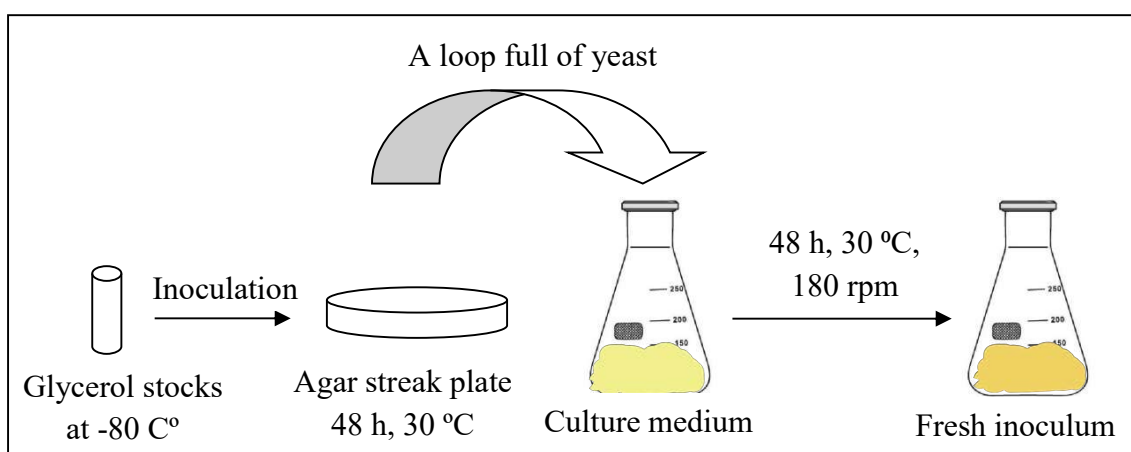


**Figure 3.3.** Scheme of the steps followed for the growth of the yeast *Starmerella bombicola*.



Some important things to keep in mind when preparing the inoculum are:

- Dextrose (D-glucose) should be sterilized separately from the rest of the culture medium to avoid the Maillard reaction. For that, a solution of dextrose at 50% w/v is prepared (50 g of dextrose diluted until 100 mL with distilled water). The dextrose should be slowly added into the water in agitation to avoid the formation of blocks of dextrose, which are difficult to dilute. Complete dilution of the dextrose is not achieved until the solution is sterilized. The solution of glucose is added to the rest of the agar or culture medium after sterilization in a laminar flow cabinet or directly to the Erlenmeyer Flasks where the inoculum is going to grow.
- Streak plates should be incubated and preserved at 4 °C facing down, i.e., with the part of the agar on the top. So, if condensation of water occurs it will be collected in the side without agar.
- The same vial at -80 °C can be used multiple times to seed new streak plates. However, this process is not recommended to be performed for more than 3 times.
- More useful information about microbiology can be find elsewhere (Koneman et al., 2006).

### **Evaluation of the inoculum**

Two tasks were performed routinely to confirm a proper growth of the inoculum:

- Optical density:

The Measurement of the optical density (OD) of a fresh growth inoculum gives an estimation of the concentration of cells in the culture media, i.e., the cell density of the inoculum. Similar ODs should be obtained every time the inoculum is prepared to get reproducible results between different batches of experiments.

OD was measured at 600 nm in a spectrophotometer (Cary 50 Bio, UV-Visible Spectrophotometer). The culture medium was used as the blank. Inoculum samples were diluted with distilled water to confine the absorbance readings to the range 0.1 - 0.35 optical density as required by the Lambert-Beer law. For that, the sample of

inoculum was normally diluted x50 times. OD of the inoculum was calculated according to Equation 3.1. Values were between 20-25 for all the fermentations carried out in this research, which corresponds with a biomass content around 4 g L<sup>-1</sup>.

$$OD = Abs_{600} \cdot N \quad (\text{Eq. 3.1})$$

where: OD, optical density at 600 nm; Abs<sub>600</sub>, absorbance at 600 nm; N, number of dilutions.

- Optical microscopy:

Optical microscopy is a good tool to check if the inoculum is contaminated by other microorganisms. The size and morphology of the cells of *S. bombycola* can be differentiated from other microorganisms. Some pictures taken with a lens of x100 are illustrated in Figure 3.4.

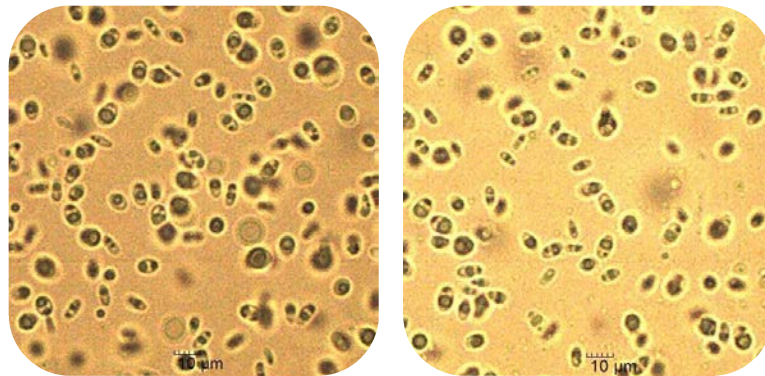


**Figure 3.4.** Pictures of the inoculum *Starmarella bombycola* obtained with an optical microscope.

### 3.2. Fermentation systems

Different fermentation systems have been used in this work. Most experiments have been performed at 0.5-L scale in the Fermentation System I. The scale-up was performed in a 40-L packed-bed bioreactor with 3 trays (Fermentation System II) and in a 100-L intermittently-mixed bioreactor (Fermentation System III).

In all the Fermentation Systems, humidified air was continuously supplied to the reactors by means of an air flow meter (Bronkhorst, Spain). The air entered the

bioreactor below the bed, passing through the solid bed and exiting at the top. The oxygen concentration in the exhaust gases was measured by an oxygen detector (O2-A2, Alphasense, UK) and recorded in a personal computer. This data was used for the calculation of the oxygen uptake rate (OUR) and the cumulative oxygen consumption (COC) as explained in Chapter 3, section 3.3.

### 3.2.1. Fermentation System I: 0.5-L scale

The Fermentation System I was design, built and well described in previous studies by Ponsá et al. (2010); based on the methodology proposed by Adani et al. (2006). In summary, this system allows to perform SSF experiments at 0.5-L scale in well-controlled conditions and to monitor on-line the process through respirometry. The temperature was controlled by submerging the reactors in a water bath at 30 °C. Figure 3.5 shows the experimental setup of one line of the Fermentation System I.

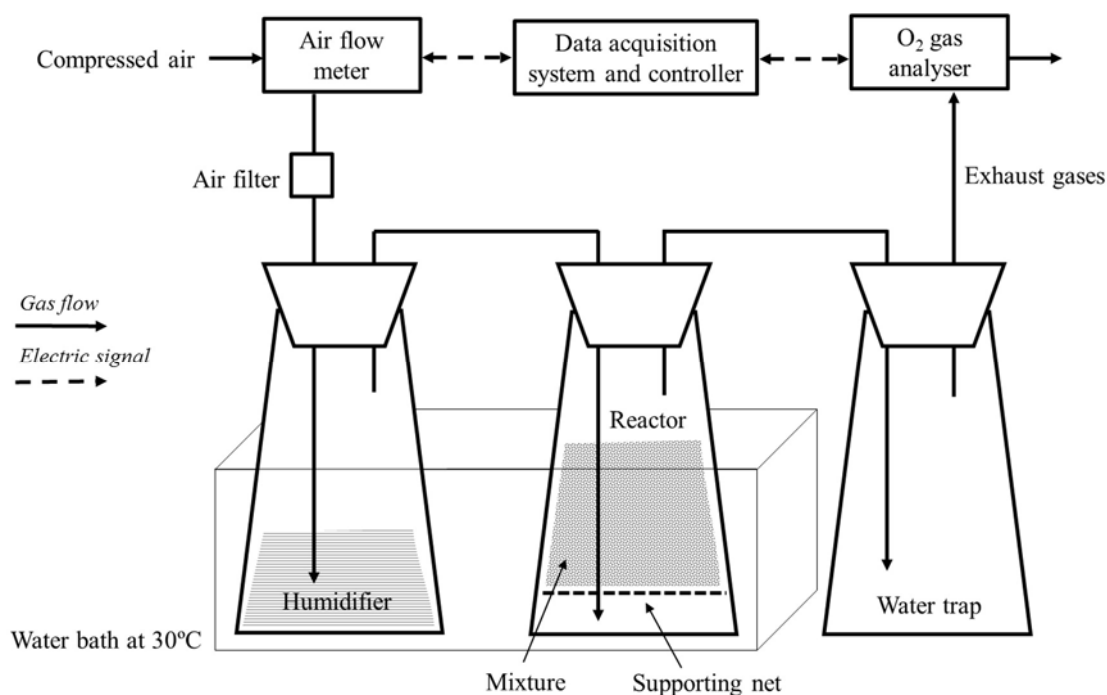


**Figure 3.5.** Experimental setup of the Fermentation System I.

The laboratory of the GICOM group has 27 lines like the one previously described. Each of them has its own air flow meter and oxygen detector. Several modifications have been performed during these years, for example the installation of air filters to

avoid contamination or the change of reactors from 0.5-L Erlenmeyer Flasks to 0.45-L cylindrical polypropylene packed-bed bioreactors (13 cm height and 7 cm diameter), which were made specifically for this group (Figure 3.6). All the modifications are explained more in detail in the corresponding chapters.



**Figure 3.6.** Pictures of the Fermentation System I when the reactor is a 0.5-L Erlenmeyer Flask (left) or a 450-mL cylindrical polypropylene packed-bed reactor (right).

### 3.2.2. Fermentation System II: 40-L bioreactor

The Fermentation System II was a cylindrical polypropylene fixed-bed bioreactor with a total volume of 40 L (24 cm height and 46 cm diameter) divided in 3 trays (8 cm height each). It has capacity for 6 kg of fermentation mixture (2 kg per tray). Temperature inside each tray was on-line monitored using temperature sensors (DS18B20 sensor, BricoGeek, Spain) which were placed in the center point of each tray ( $r = 0$  cm). The vapor condensing device is a glass bottle of 2-L placed inside a fridge and is used to condensate the moisture from the exhaust gases. Figure 3.7 shows the experimental setup of the Fermentation System II.

The Fermentation System II is indeed a commercial vermicomposter which has been adapted to be used as a bioreactor. For example, the exit used to drain lixiviates is used as the entrance of the air. Also, exterior holes were sealed to force the inlet air to pass through the three trays, which was possible due to the perforated base of the trays. Finally, the trays were perforated to place the temperature sensors. Figure 3.8 illustrates some pictures of the Fermentation System II.

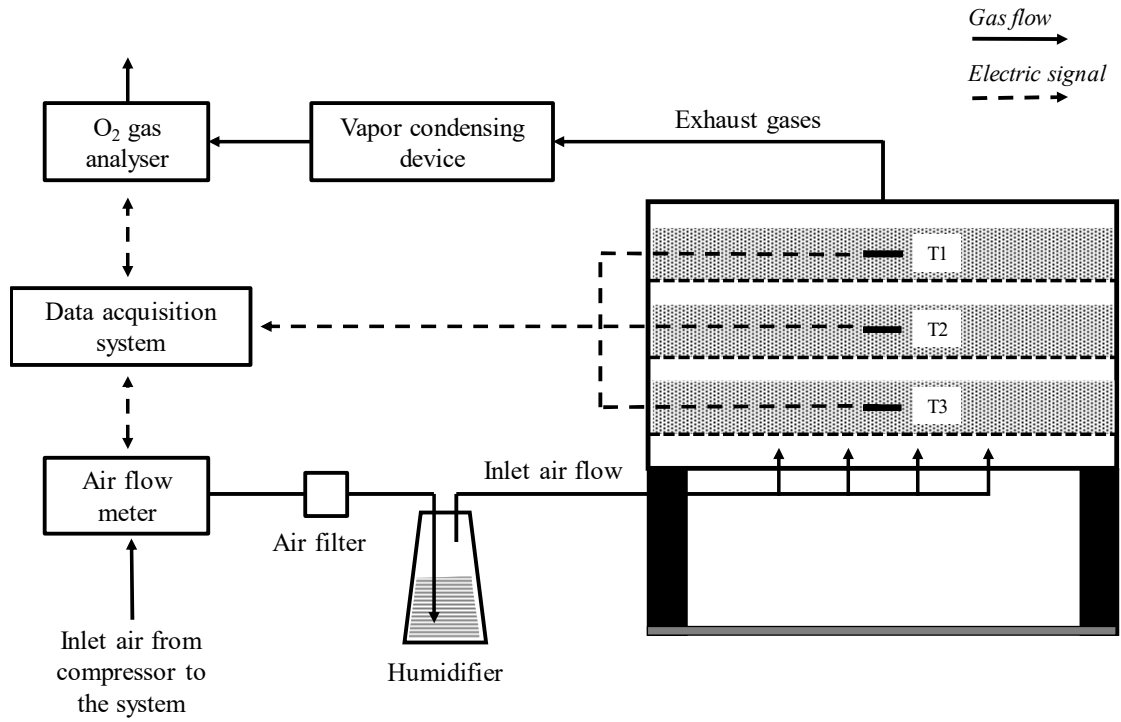


Figure 3.7. Experimental setup of the Fermentation System II.

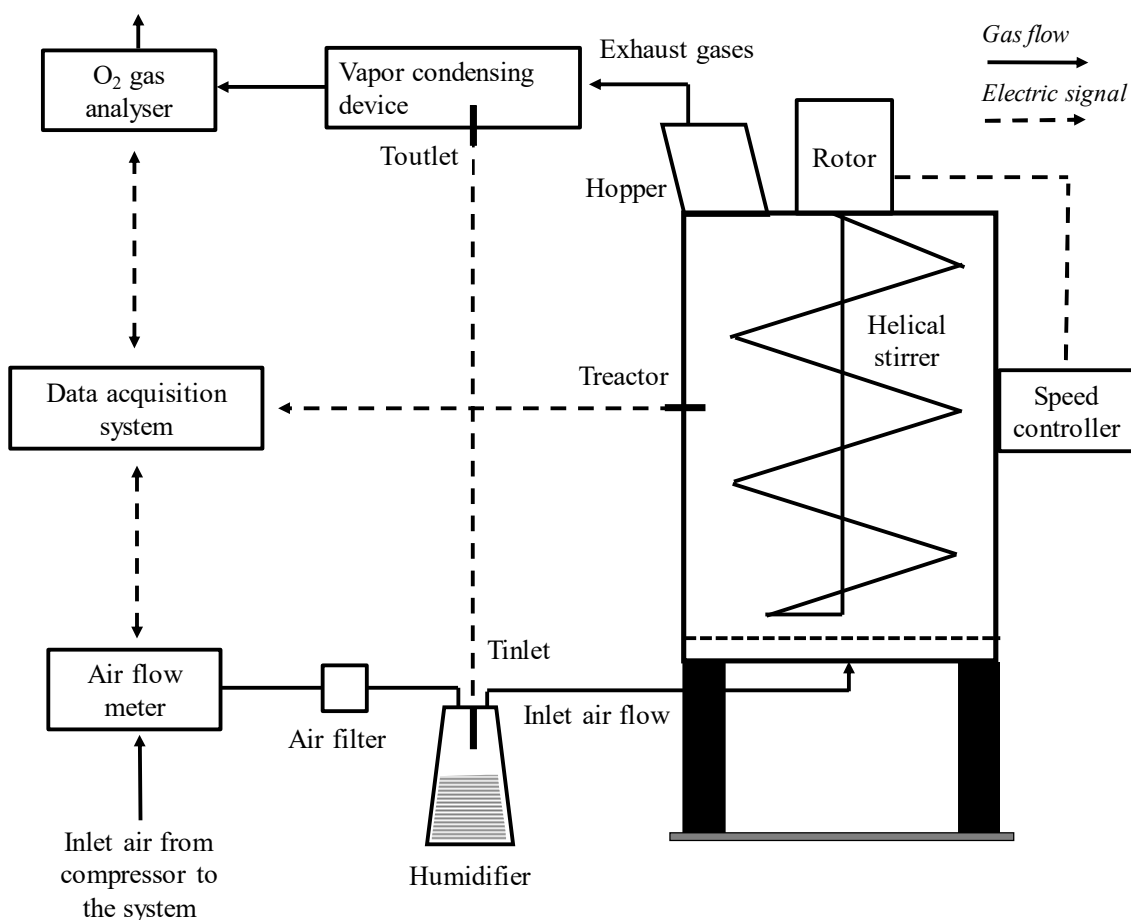


Figure 3.8. Pictures of the Fermentation System II.

### 3.2.3. Fermentation System III: 100-L bioreactor

The Fermentation System III was a cylindrical stainless steel intermittently-mixed bioreactor with a total volume of 100 L (80 cm height and 46 cm diameter) with a helical stirrer in the center (80 cm height). The stirrer is connected to a rotor situated on top of the bioreactor and its speed is controlled by a speed controller situated in the exterior wall of the bioreactor. There is a hopper situated on top of the bioreactor to introduce the SSF mixture. Temperature was on-line monitored in the inlet air flow, the reactor and the exhaust gases using temperature sensors (DS18B20 sensor, BricoGeek, Spain). The vapor condensing device is the one used in the Fermentation System II. Figure 3.9 shows the experimental setup of the Fermentation System III and Figure 3.10 illustrates some pictures of the bioreactor.

This bioreactor was designed and built by Industrias AJA de Lliçà, S.L. (Barcelona), and the set-up was performed by the PhD student.



**Figure 3.9.** Experimental setup of the Fermentation System III.

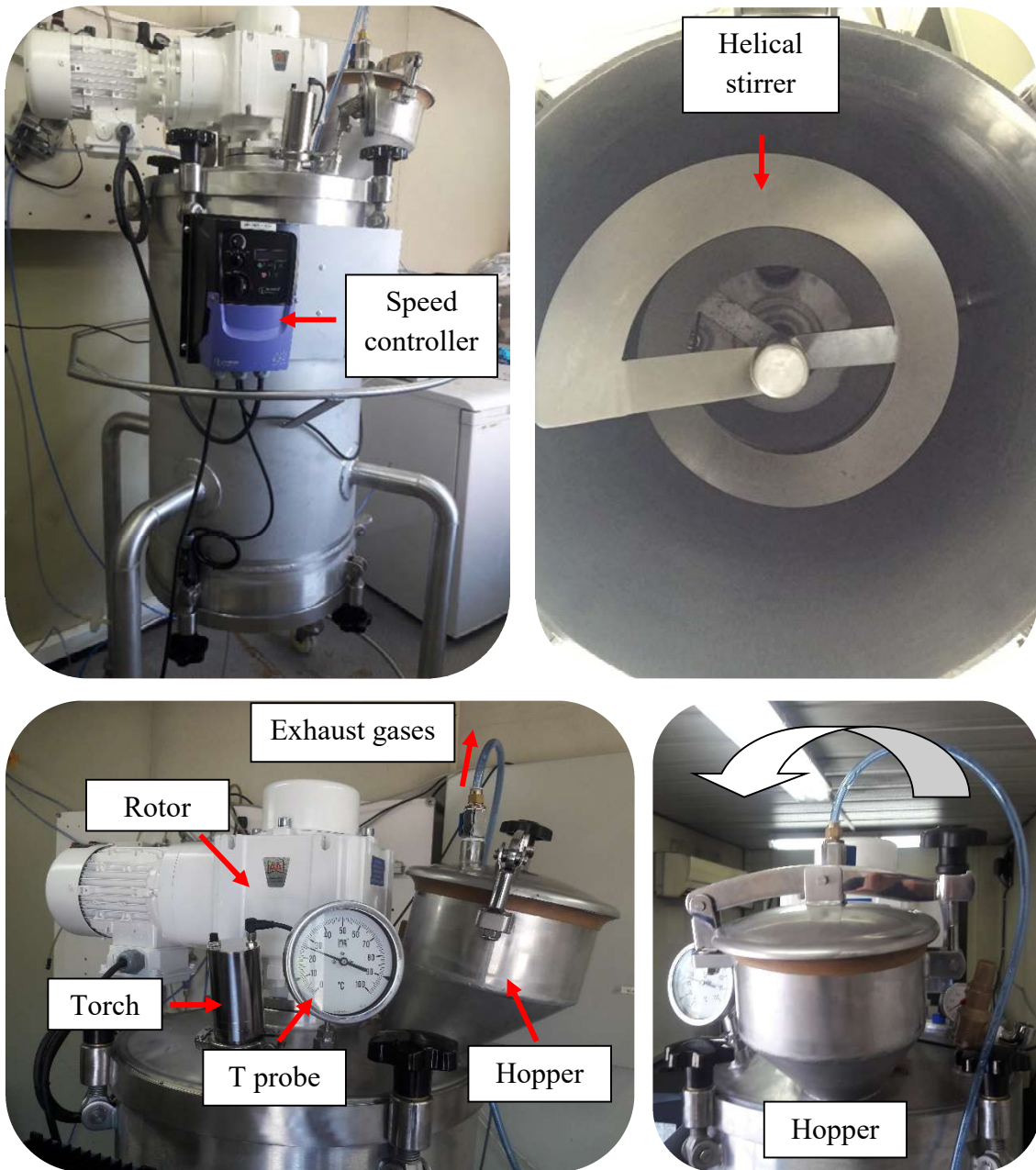


Figure 3.10. Pictures of the Fermentation System II.

### 3.3. Respiration indices

Respiration indices, oxygen uptake rate (OUR) and cumulative oxygen consumption (COC), have been used to indirectly study the biological activity during the SSF processes (Ponsá et al., 2010).

#### 3.3.1. Oxygen uptake rate

Oxygen uptake rate (OUR) can be calculated from oxygen and aeration rate data at a given time (Equation 3.2):

$$\text{OUR}_t = \frac{\Delta\text{O}_2 \cdot F \cdot 31.98 \cdot 60 \cdot 1,000^a}{1,000^b \cdot 22.4 \cdot \text{DM}} \quad (\text{Eq. 3.2})$$

where:

$\text{OUR}_t$  = oxygen uptake rate at a given time,  $\text{mg O}_2 \text{ g}^{-1}\text{DM h}^{-1}$

$\Delta\text{O}_2$  = oxygen content variation between airflow in and the exhaust gases of the reactor, volumetric fraction

$F$  = aeration rate,  $\text{mL min}^{-1}$

31.98 = oxygen molecular weight,  $\text{g mol}^{-1}$

60 = conversion factor,  $\text{min h}^{-1}$

1,000<sup>a</sup> = conversion factor,  $\text{mg g}^{-1}$

1,000<sup>b</sup> = conversion factor,  $\text{mL L}^{-1}$

22.4 = volume occupied by one mol of ideal gas under normal conditions (1 atm and 273 K), L

DM = dry matter of sample loaded in the reactor, g

OUR will be represented herein as  $\text{OUR}_{1h}$ , which is the average of  $\text{OUR}_t$  values in 1 h of fermentation. In Chapter 8, OUR will be expressed as  $\text{mg O}_2 \text{ g}^{-1}\text{substrates h}^{-1}$ . In this case DM of Equation 3.2 corresponds to the dry matter of substrates loaded in the reactor (g).

#### 3.3.2. Cumulative oxygen consumption

Cumulative oxygen consumption (COC) during  $n$  days can be calculated as described in Equation 3.3:



$$\text{COC} = \int_0^n \text{OUR}_t \cdot dt \quad (\text{Eq. 3.3})$$

### 3.4. Standard Analytical Methods

Regular parameters were determined according to the standard procedures included in the “Test Methods for the Examination of Composting and Compost” (The US Department of Agriculture and The US Composting Council, 2001). All the results were calculated as a mean of three replicates and presented as mean  $\pm$  standard deviation.

#### 3.4.1. pH

pH was determined in the aqueous extract obtained after mixing the sample with distilled water in a 1:5 w/v ratio. The sample was first extracted with distilled water (250 rpm, 30 min) and then centrifuged (3,500 rpm, 10 min). pH was measured with an electrometric pH meter (Crison®, micropH2001).

#### 3.4.2. Water content and dry matter

To calculate the water content (WC) and dry matter (DM) samples were oven dried in a capsule at 105 °C for 24 h, then weighted and calculated by using Equations 3.4 and 3.5:

$$\text{WC (\%)} = \frac{P_i - P_f}{P_i - P_o} \cdot 100 \quad (\text{Eq. 3.4})$$

$$\text{DM (\%)} = 100 - \text{WC (\%)} \quad (\text{Eq. 3.5})$$

Where:  $P_i$ , initial wet weight of the sample (g);  $P_f$ , final dry weight of the sample (g);  $P_o$ , capsule weight (g).

#### 3.4.3. Organic matter

To calculate organic matter (OM) dry samples were ignited at 550 °C in the presence of excess air for 4 h and calculated as described in Equation 3.6:

$$\text{OM (\%)} = \frac{P_i - P_a}{P_i - P_o} \cdot 100 \quad (\text{Eq. 3.6})$$

where:  $P_i$ , initial weight of the dry sample (g);  $P_a$ , weight of the ashes (g);  $P_o$ , capsule weight (g).

#### 3.4.4. Bulk density

Bulk density (BD) is defined as the weight per unit of volume of sample. BD was calculated on wet basis dividing the sample weight by the sample volume as shown in Equation 3.7:

$$\text{BD} = \frac{P}{V} \quad (\text{Eq. 3.7})$$

where: BD, bulk density ( $\text{g L}^{-1}$ ); P, wet weight of the sample (g); V, sample volume (L).

#### 3.4.5. Water holding capacity

Water holding capacity (WHC) is defined as the capacity of a material to retain water. Firstly, the material was copiously washed with distilled water, and dried at 65 °C for 24 h. Then, a known mass of material was transferred to a cylindrical tube with a net on the bottom and was saturated with water. The material was allowed to drain for 1 h. The resulting sample weight gained due to retained moisture represents the relative WHC of the material. Calculations were done according to Equation 3.8:

$$\text{WHC} = \frac{P_f - P_i}{P_i} \quad (\text{Eq. 3.8})$$

where: WHC, water holding capacity ( $\text{g water g}^{-1}$  material);  $P_f$ , final wet weight of the material (g);  $P_i$ , initial dry weight of the material (g).

### 3.5. Specific methods for the monitoring of SSF processes

#### 3.5.1. SL yield

SLs were extracted from the fermentation medium as shown in Figure 3.11. Basically, a given amount of the mixture was mixed with ethyl acetate in a 1:4 (w/v) ratio at 200 rpm for 1 h. This extraction protocol was repeated three times. Solvent extractions were pooled together, dried with a small amount of Na<sub>2</sub>SO<sub>4</sub> anhydrous, filtered through a Whatman paper Grade 1, and vacuum-dried at 40 °C with a rotary evaporator (Figure 3.12). The amber colored, honey like semi-crystalline SLs were washed twice with 20 ml of *n*-hexane to remove any remaining oily residue or hydrophobic substances such as fatty acids and alcohols formed during the fermentation. Partially purified SLs were obtained after vaporizing the residual hexane at 40 °C under vacuum (Hu and Ju, 2001). Final product was stored at 4 °C. The ethyl acetate and the *n*-hexane recovered after rotary evaporation were reused in consecutive extractions.

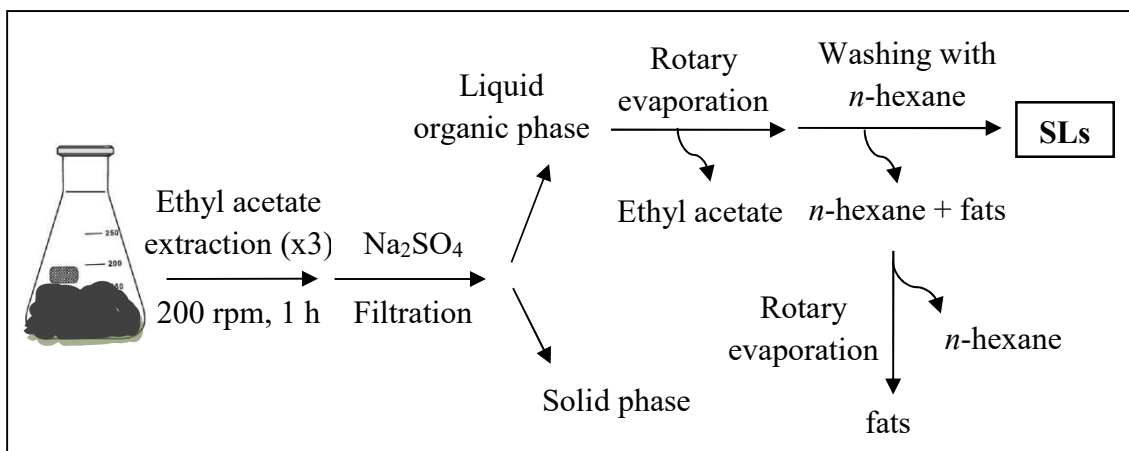


**Figure 3.11.** Scheme of the procedure for SL extraction from SSF.

SL yield was expressed as grams of SLs per gram of dry sample using the following equation 3.10:

$$\text{SL yield} = \frac{P_f - P_i}{P} \cdot \frac{100}{\text{DM}} \quad (\text{Eq. 3.10})$$

where: SL yield ( $\text{g g}^{-1}\text{DM}$ ); Pf, weight of the round bottom flask with the SLs (g); Pi, weight of the round bottom flask empty (g); P, wet weight of the sample (g); DM, dry matter of the fermentation (%).

SL yield was also expressed as grams of SLs per gram of substrates. Calculations were done according to Equation 3.11:

$$\text{SL yield} = \frac{\text{Pf} - \text{Pi}}{\text{P}} \cdot \frac{\text{Pt}}{\text{Ps}} \quad (\text{Eq. 3.11})$$

where: SL yield ( $\text{g g}^{-1}$  substrates); Pf, weight of the round bottom flask with the SLs (g); Pi, weight of the round bottom flask (g); P, wet weight of the sample (g); Pt, total wet weight of the fermentation (g); Ps, total weight of the substrates of the fermentation (g).

In Chapter 8, SL yield was also expressed as grams of SLs per L. Calculations were done according to Equation 3.12:

$$\text{SL yield} = \frac{\text{Pf} - \text{Pi}}{\text{P}} \cdot \frac{\text{Pt}}{\text{V}} \quad (\text{Eq. 3.12})$$

where: SL yield ( $\text{g L}^{-1}$ ); Pf, weight of the round bottom flask with the SLs (g); Pi, weight of the round bottom flask (g); P, wet weight of the sample (g); Pt, total wet weight of the fermentation (g); V, volume of the fermentation (L).



**Figure 3.12.** Pictures of the rotary evaporator (left), a round bottom flask during the evaporation of the ethyl acetate (center), and the SLs (right).

### 3.5.2. Fat content

Fat content was measured using a standard Soxhlet method with *n*-hexane as organic solvent (The U.S. Environmental Protection Agency, Method 9071B). The extraction was carried out by mixing 5 g of dry sample with 3 g of sodium sulphate anhydrous in a cellulose cartridge, and using Soxhlet E-816 (Büchi) with the solvent *n*-hexane ( $\geq 95\%$  of purity, Sigma-Aldrich) during 4 hours (Figure 3.13).



**Figure 3.13.** Pictures of the Soxhlet E-816 (Büchi) during the extraction of fats.

Results were presented as grams of fats per gram of dry sample using the following equation 3.13:

$$\text{Fat content} = \frac{P_f - P_i}{P} \quad (\text{Eq. 3.13})$$

where: fat content ( $\text{g g}^{-1}\text{DM}$ );  $P_f$ , weight of the flask with the fat (g);  $P_i$ , weight of the flask (g);  $P$ , weight of the dry sample added to the cartridge (g).

### 3.5.3. Glucose content

Glucose was extracted from dry samples by mixing a known amount of sample with distilled water in a 1:10 (w/v) ratio. The mixture was incubated (15 min, 50 °C) in a water bath shaker and then centrifuged (10 min, 4,000 rpm). The supernatant was recovered and the extraction was carried out two more times. The supernatants were pooled together and filtered with a 0.45  $\mu\text{m}$  membrane filter. Finally, total volume of the recovered supernatant was measured. Concentration of glucose in the supernatant

was determined by an on line biochemistry analyzer YSI 2700. The glucose content was determined according to the following equation 3.14:

$$\text{Glucose content} = \frac{C}{P} \cdot V \quad (\text{Eq. 3.14})$$

where: glucose content ( $\text{g g}^{-1}\text{DM}$ ); C, concentration of glucose given by the analyser YSI ( $\text{g L}^{-1}$ ); P, weight of the dry sample (g); V, total volume of the supernatant (L).

#### 3.5.4. Reducing sugar content (DNS method)

Reducing sugars were determined according to DNS method (Miller, 1959). The reducing sugars were extracted from the dried solids as explained in section 3.5.3. Then, 3 mL of DNS reagent were added to 1 mL of supernatant in 25-mL glass tubes, and the mixture was boiled for 5 min. The sample was cooled and 20 mL of distilled water was added. Absorbance was measured at 540 nm in a spectrophotometer (Cary 50 Bio, UV-Visible Spectrophotometer). For the blank, 1 mL of distilled water was used instead of 1 mL of supernatant. Calibration curve was prepared using glucose with concentrations ranging from 0 to 2  $\text{g L}^{-1}$  (Annex II). The reducing sugar content was expressed as grams of glucose-equivalent per gram of dry matter according to the following equation 3.15:

$$\text{Reducing sugar content} = \frac{C}{P} \cdot V \quad (\text{Eq. 3.15})$$

where: reducing sugar content ( $\text{g g}^{-1}\text{DM}$ ); C, concentration of glucose-equivalents ( $\text{g L}^{-1}$ ); P, weight of the dry sample (g); V, total volume of the supernatant (L).

#### 3.5.5. Total sugar content (anthrone method)

Total sugar content was estimated using the anthrone method (Scott and Melvin, 1953). The sugars were extracted from the dried solids as explained in section 3.5.3. Anthrone reagent was prepared by dissolving 200 mg anthrone in 100 mL ice cold 95% sulphuric acid and was prepared fresh before use. 4 mL of anthrone reagent was added to 1 ml of supernatant in 25-mL glass tubes and the reaction mixture was heated for 8

min in a boiling water bath and cooled rapidly. The absorbance of the green coloured solution was measured at 630 nm using a spectrophotometer (Cary 50 Bio, UV-Visible Spectrophotometer). For the blank, 1 mL of distilled water was used instead of 1 mL of supernatant. Calibration curve was prepared using glucose with concentrations ranging from 0 to 0.1 g L<sup>-1</sup> (Annex II). Figure 3.14 illustrates the range of colours from yellow to dark green obtained for the calibration curve.

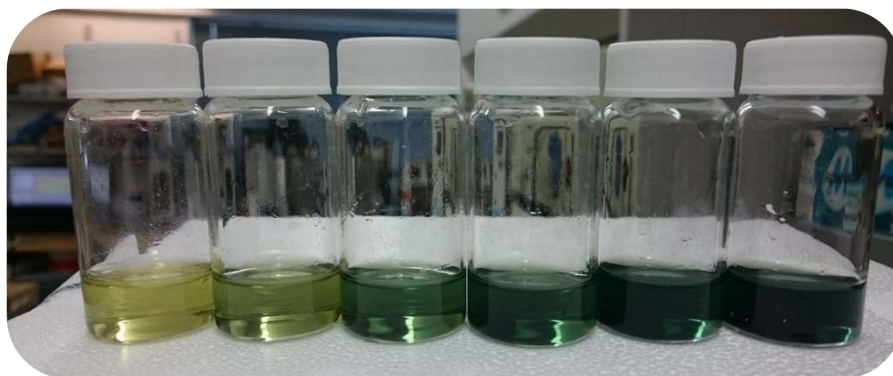


**Figure 3.14.** Picture of the calibration curve for the anthrone method.

The total sugar content was expressed as gram of glucose-equivalent per gram of dry matter according to the following equation 3.16:

$$\text{Total sugar content} = \frac{C}{P} \cdot V \quad (\text{Eq. 3.16})$$

where: total sugar content (g g<sup>-1</sup>DM); C, concentration of glucose-equivalents (g L<sup>-1</sup>); P, weight of the dry sample (g); V, total volume of the supernatant (L).

### 3.5.6. Nitrogen content

Nitrogen content in the dry sample was determined by the Servei d'Anàlisi Química (SAQ) of the Universitat Autònoma de Barcelona using gas chromatography. The nitrogen content was expressed as grams of nitrogen per gram of dry matter.

### 3.5.7. Viable cell numbers

Viable cell numbers were quantified by mixing 1 g of material with 9 mL of culture solution (peptone 1 g L<sup>-1</sup> and sodium chloride 8.5 g L<sup>-1</sup>) in a vortex mixer for 1 min. Serial dilutions were prepared from this mixture, then plated on agar streak plates and incubated at 30 °C during 72 h. Manual counting of viable cells was performed afterwards. Analysis were performed in triplicates and results were expressed as colony forming units (CFU) per gram of initial dry substrates according to the following equation 3.17:

$$\text{CFUs} = \frac{N}{P} \cdot D \cdot \frac{Pt}{S} \quad (\text{Eq. 3.17})$$

where: colony forming units (CFUs g<sup>-1</sup>substrates); N, number of viable cells (CFU); P, weight of material (g); D, dilution factor; Pt, total weight of fermentation (g); S, total weight of initial dry substrates (g).

### 3.5.8. Scanning electron microscopy

Scanning electron microscope (SEM) analyses were performed using a Zeiss digital scanning microscope EVO (Germany). Samples were fixed according to the methodology described by Varesche et al. (1997).

## 3.6. Specific methods for the characterization of SLs

### 3.6.1. Structural characterization

#### Fourier transform infrared spectroscopy

Structural characterization by Fourier transform infrared spectroscopy (FTIR) was performed using a FTIR Spectrophotometer (Tensor 27, Bruker). The instrument had an attenuated total reflection accessory (ATR Specac Golden Gate) which avoids the use of KBr pellets. The infrared spectrum was recorded from 600 to 4,000 cm<sup>-1</sup>. These analyses were performed in the Servei d'Anàlisi Química of the Universitat Autònoma de Barcelona.



### Proton nuclear magnetic resonance

Structural characterization by proton nuclear magnetic resonance ( $^1\text{H-NMR}$ ) was carried out using  $\text{CDCl}_3$  (Robot 250 MHz NMR Spectrometer, Bruker). This analysis was performed by the Servei de Resonància Magnètica of the Universitat Autònoma de Barcelona.

### Mass spectrometry

Mass spectrometry (MS) (microTOF-QTM, Bruker Daltonics, Germany) was used to identify the structures of the SLs of the SL natural mixture. SLs were dissolved in methanol ( $1 \text{ mg mL}^{-1}$ ) and passed through a  $0.22\text{-}\mu\text{m}$  membrane filter. The sample was directly infused into the mass spectrometer using a syringe pump to obtain the overall mass spectra. SL molecules were ionized by electrospray (negative ion mode) and further collected in an ion trap where their mass/charge ( $m/z$ ) values were detected. These analyses were performed by the Servei d'Anàlisi Química of the Universitat Autònoma de Barcelona.

### Liquid chromatography-mass spectrometry

Separation of SL molecules was performed by high pressure liquid chromatography (HPLC) (Prominence Series, Shimadzu) using a  $150 \text{ mm} \times 2.1 \text{ mm}$  Symmetry C8  $3.5\mu\text{m}$  column. A linear gradient elution was used from acetonitrile (5 mM  $\text{NH}_4\text{Ac}$ )/water (5 mM  $\text{NH}_4\text{Ac}$ ) 50/50 (v/v) to acetonitrile (5 mM  $\text{NH}_4\text{Ac}$ )/water (5 mM  $\text{NH}_4\text{Ac}$ ) 100/0 (v/v) for 17 min. The flow rate was  $0.30 \text{ mL min}^{-1}$ . The response of the SLs was measured with a UV-Visible diode-array detector at 205 nm. The effluent was connected to a mass spectrometer (microTOF-QTM, Bruker Daltonics) where the SLs were ionized by electrospray (negative ion mode) and further collected in an ion trap where their mass/charge ( $m/z$ ) values were detected. The samples were dissolved in 50:50 acetonitrile/water at a concentration of  $1 \text{ g L}^{-1}$  and filtered through a  $0.2 \mu\text{m}$  membrane filter before injection.

#### 3.6.2. SL purification

SL purification was performed by silica gel column using a glass column packed with slurry containing silica gel with  $\text{CHCl}_3$ :methanol 95:5, which was the initial

mobile phase (Figure 3.15). Chromatography was carried out by loading the column with the sample dissolved with the initial mobile phase, and its elution was carried out with  $\text{CHCl}_3$ :methanol using a gradient system (5 – 20% methanol) (Daverey and Pakshirajan, 2010). Fractions of 100 mL collected from the column were analyzed by thin layer chromatography (TLC) with  $\text{CHCl}_3$ :methanol (9:1) as the mobile solvent (Figure 3.15). Fractions containing identical SLs were pooled and the solvent was removed by evaporation. The resulting SL was lyophilized overnight and stored at 4 °C.

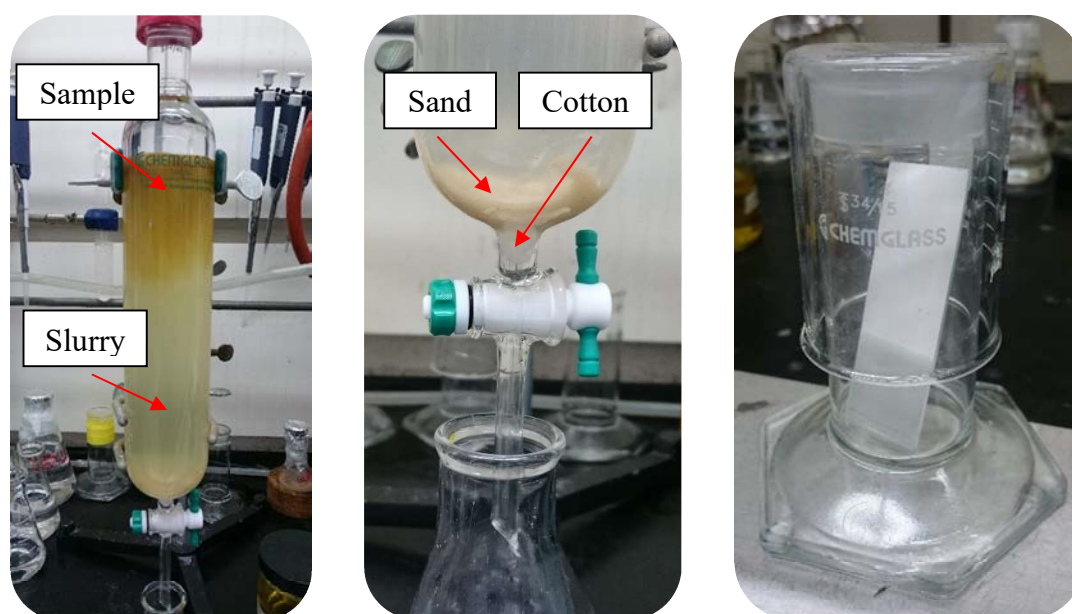


**Figure 3.15.** Pictures of the setup for the silica gel column chromatography (left and middle) and for the thin layer chromatography (right).

### 3.6.3. Interfacial properties

#### Emulsification activity

Emulsification activity was measured using a modified method of Cirigliano & Carman (1984). Briefly, 1 mL sample containing the surfactant ( $1 \text{ g L}^{-1}$ ) was mixed with 1 mL solvent. Thereafter, the mixture was shaken vigorously in a vortex mixer for 2 min and allowed to sit for 10 min before measuring its turbidity at 600 nm in a spectrophotometer (Cary 50 Bio, UV-Visible Spectrophotometer). Emulsification activity was therefore expressed as the absorbance of the mixture at 600 nm. A cuvette

with the 1 g L<sup>-1</sup> surfactant solution was used as blank. All water used for these experiments was Millipore deionized water.

### **Emulsion properties**

Emulsions were prepared and evaluated following a methodology previously described by Koh et al. (2016a). Emulsions were prepared using a IKA T25 shear homogenizer (24,000 rpm, 60 s). Average emulsion droplet sizes were determined with a Malvern Zetasizer ZSP (Worcestershire, UK) with a 173° backscatter angle detector. Samples were diluted 100 times in deionized water to minimize multiple scattering effects. Droplet sizes are reported as the emulsion z-average diameter in nanometres. Emulsion phase stability was recorded by photographs with a Nikon D5200 camera fitted with a Nikon AF-S Micro Nikkor 60 mm lens.

Almond oil from the *Prunus dulcis* tree and lemon oil from California were purchased from Sigma-Aldrich (St. Louis, MO, USA). The same batches were used herein for all the analysis and were stored at 4 °C in amber glass bottles to prevent degradation and loss of volatile compounds. The commercial non-ionic surfactant Triton X-100 was purchased from Sigma-Aldrich (St. Louis, MO, USA). All water used for these experiments was Millipore deionized water.

### **Surface tension**

Minimum surface tension (mST) and critical micelle concentration (CMC) were estimated using a surface tensiometer (K100, Krüss) by the Wilhelmy plate method. The Wilhelmy plate used was length: 10 mm, width: 19.9 mm and thickness: 0.2 mm (model PL01, Krüss, Germany). CMC was calculated from the relationship between the log of SL concentration and the corresponding surface tension. Measurements of surface tensions were performed in surfactant concentrations ranging from 0 to 500 mg L<sup>-1</sup> and the result reported is the average of triplicate analysis. All water used for these experiments was Millipore deionized water.

### **Displacement activity**

To investigate SL diesel spreading, an 8.8-cm-diameter petri dish was filled with 20 mL of deionized water. Subsequently, diesel (20 µL) was added to the petri dish that

spread such that it covered the full surface of the aqueous phase. Then, 20  $\mu\text{L}$  of surfactant solution was dropped onto the center of the oil-covered dish of water from a height of 5.5 cm. For the next 5 min, the radius of diesel spreading, herein called displacement activity, was measured after 30 and 300 s. The final spreading diameter is reported. Surfactant solutions containing SLs or Triton X-100 at 0.1 and 0.5  $\text{mg mL}^{-1}$  were used. Spreading experiments were performed at ambient temperature.

### 3.6.4. Synthesis of ethyl ester SL

The ethyl ester SL (EESL) was prepared following a procedure described earlier (Bisht et al., 1999). In summary, 2 g of the crude SL natural mixture was added to a 0.2 N sodium ethoxide solution in 10 mL of ethanol. The reaction mixture was stirred at 80  $^{\circ}\text{C}$  for 1 h under a nitrogen atmosphere. TLC was used to monitor the progress of the reaction ( $\text{CHCl}_3$ :methanol, 9:1). The reaction was stopped when all the diacetylated lactonic C18:1 SL was converted to EESL (Figure 3.16). Then, the reaction mixture was acidified (pH 4) with glacial acetic acid. The residue was then purified as described in section 3.7.2. The pure EESL was found to be white crystalline in nature.

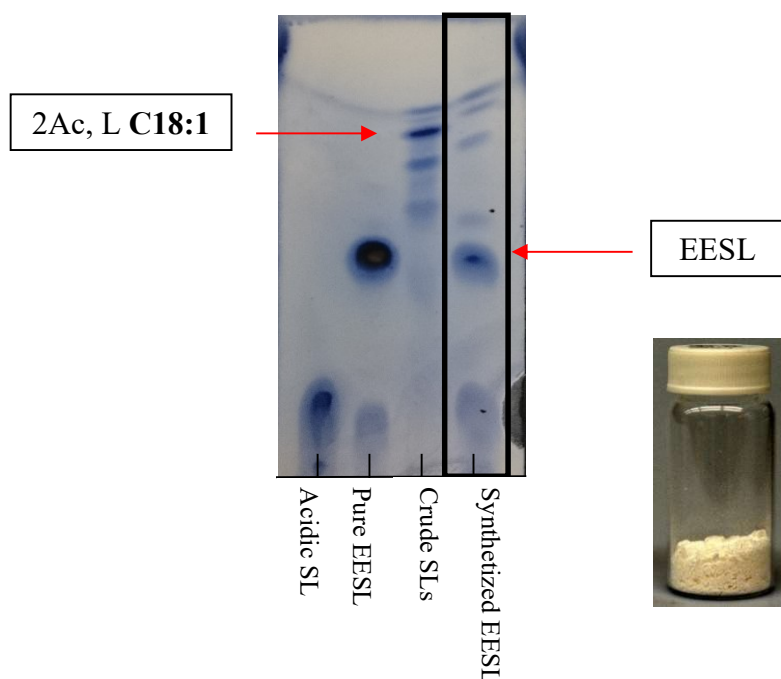
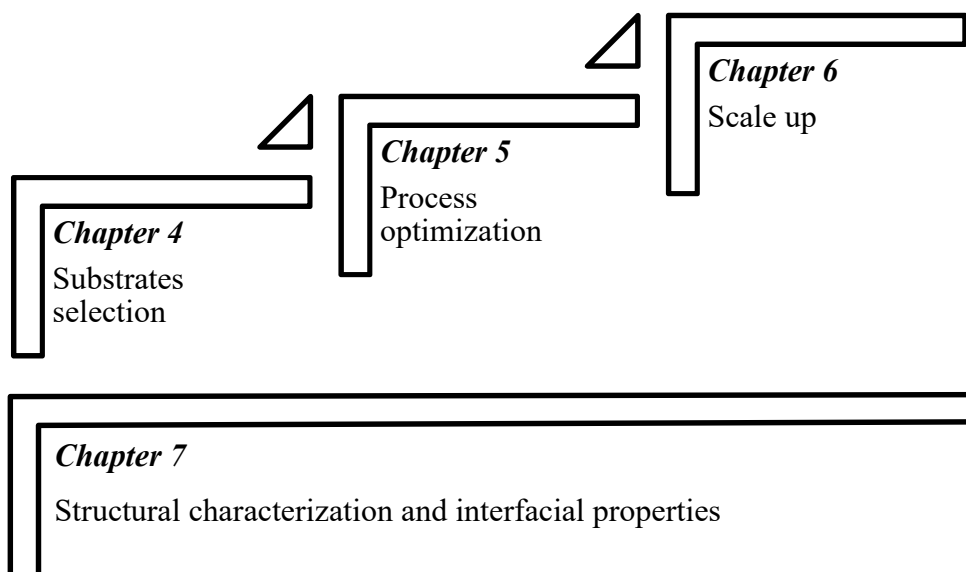


**Figure 7.16.** TLC plate at the end of the reaction of EESL synthesis.

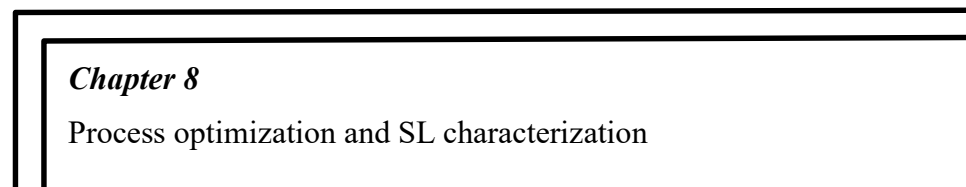


# RESULTS

## BLOCK I: PRODUCTION OF SLs FROM A WINTERAZATION OIL CAKE



## BLOCK II: PRODUCTION OF SLs FROM STEARIC ACID





## CHAPTER 4

---

*Sophorolipids from winterization oil cake by SSF: how we get here*

*Part of this chapter has been presented as a poster on the international congress: 7<sup>th</sup> European Meeting on Chemical Industry and Environment, 2015, Tarragona.*

*Application of solid-state fermentation for the production of sophorolipids from industrial wastes.*

*Jiménez-Peñalver, P., Font, X., Gea, T.*





## **Summary**

In this chapter the feasibility of SSF to produce SLs was explored using both pure substrates and agro-industrial wastes or by-products. Firstly, the production of SLs was performed in a SSF mixture based on glucose and oleic acid, which are the conventional substrates used for the synthesis of SLs under SmF. These pure substrates were blended with wheat bran, which functioned as the inert support giving consistency to the solid mixture. Secondly, glucose and oleic acid were replaced by some agro-industrial wastes or by-products which could work as low-cost hydrophilic and hydrophobic carbon sources for SLs synthesis. Sugar beet molasses, a by-product of the sugar industry, was tested as the hydrophilic carbon source. Waste cooking olive oil and a winterization oil cake were tested as hydrophobic carbon sources. Finally, wheat straw was tested as the inert support for the fermentation of sugar beet molasses and the winterization oil cake, which were the most promising substrates, and results were compared with those obtained for wheat bran. Process dynamics were followed biologically by monitoring the oxygen consumption, and chemically by measuring SL yield, consumption of glucose and fats, pH and water content. The identity of these molecules was confirmed by FTIR.

## **4.1. Materials**

Glucose and oleic acid were of analytical grade and provided by Sigma-Aldrich (St. Louis, MO, USA). The substrates used were sugar-beet molasses (MOL), waste cooking olive oil (OIL) and winterization oil cake (WOC). Olive oil was purchased in a local market and used for frying at home. The OIL was centrifuged (10,000 rpm, 10 min) to eliminate the impurities. More information about the materials MOL and WOC can be found in Chapter 3, section 3.1.1. Wheat bran and wheat straw were purchased in a local market and used as the inert support for the substrates. Wheat straw was shredded and sieved. Particles between 5 and 30 mm were used. Water holding capacity (WHC) of wheat bran and wheat straw was 2.6 and 2.4 g water g<sup>-1</sup> of material, respectively. Physical appearance of the substrates and the inert supports are illustrated in Figure 4.1, and their main characteristics are summarized in Table 4.1. Toothpicks (100% DM) were purchased in a local market and used as a bulking agent to increase the porosity of the samples. All materials were autoclaved before use (121 °C, 30 min).



**Figure 4.1.** Physical appearance of the sugar beet molasses (up left), waste cooking oil (up center), winterization oil cake (up right), wheat bran (down left) and wheat straw (down right).

**Table 4.1.** Main characteristics of the substrates and the inert supports.

	Substrates			Inert supports	
	Sugar beet molasses	Waste cooking oil	Winterization oil cake	Wheat bran	Wheat straw (commercial)
<b>Wet basis</b>					
pH	6.79±0.06	n.a.	4.75±0.01	6.43±0.01	6.29±0.01
Water content (%)	16.9±0.8	0	0	7.9±0.2	4.4±0.9
Dry matter (%)	83.1±0.8	100	100	92.1±0.2	95.6±0.9
<b>Dry basis</b>					
Organic matter (%)	87.3±2.1	100	59.8±3.1	95.4±1.0	93.0±2.2
Fat content (%)	n.d.	<b>100</b>	<b>60.0±0.4</b>	4.9±0.30	2.1±0.4
Glucose content (%)	0.24±0.01	n.a.	n.d.	n.d.	n.d.
Reducing sugars (%)	4.18±0.06	n.a.	n.a.	n.a.	n.a.
Sugar content (%)	<b>78.4±2.8</b>	n.a.	n.a.	7.2±0.8	11.4±1.3
Nitrogen content (%)	<b>1.89±0.01</b>	n.d.	n.d.	2.86±0.10	1.18±0.22

Abbreviations: n.d., not detected; n.a., not analyzed. Data presented as mean ± standard deviation.

## 4.2. Experiments

Figure 4.2 shows a scheme of the three experimental steps explained in this chapter. Firstly, the production of SLs was performed in a SSF mixture based on glucose and oleic acid blended with wheat bran. Secondly, the conventional substrates glucose and oleic acid were substituted by MOL and OIL or WOC respectively to test the feasibility of these agro-industrial materials to produce SLs. Finally, wheat straw was tested as the inert support for the most promising substrates.

All the experiments were performed at 0.5-L scale in 0.5-L Erlenmeyer Flasks at 30 °C in the Fermentation System I described in Chapter 3, section 3.2.1. OUR and COC were calculated from the oxygen concentration of the exhaust gases as described in Chapter 3, section 3.3. At sampling times, the whole content of one reactor was collected and manually homogenized with a metal spatula. Then, 5 g were used to measure pH, 10 g were used to analyse SL content, and the rest of the sample was oven-dried at 105 °C to measure the water content according to the methods described in Chapter 3, section 3.4 and 3.5. The glucose and fat contents of the dry sample were then determined (Chapter 3, section 3.5). Identity of the SLs was confirmed by FTIR as described in Chapter 3, section 3.6.1. For easy reading, experimental conditions for each step are presented in the corresponding section (4.3.1, 4.3.2 and 4.3.3).

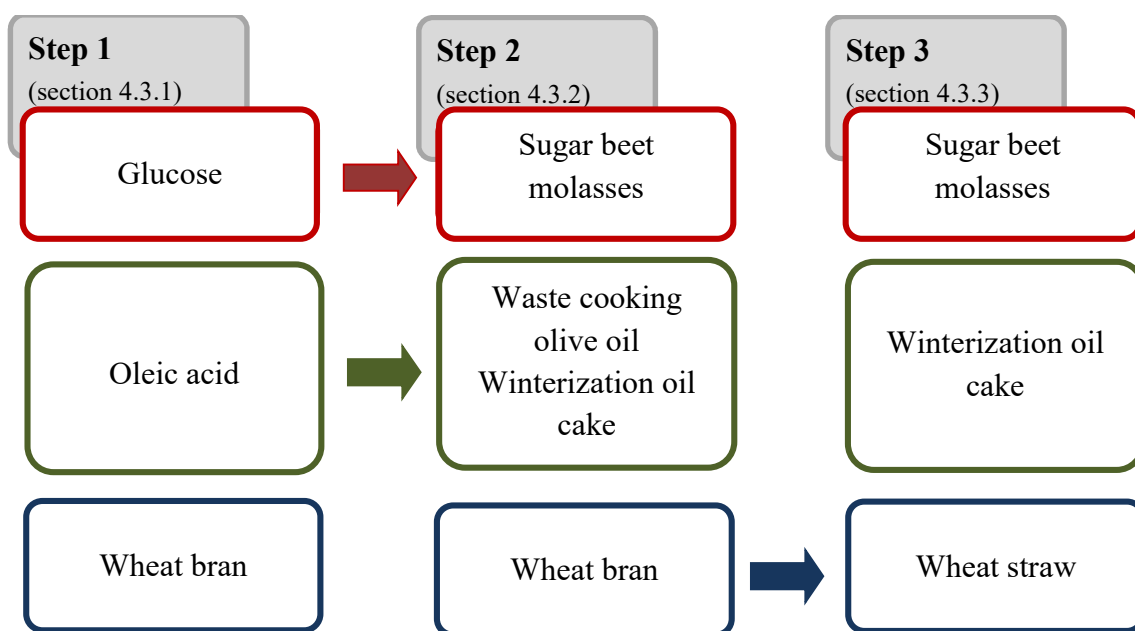


**Figure 4.2.** Scheme of the steps followed in the experiments described in Chapter 4.

### 4.3. Results and discussion

#### 4.3.1. Step 1: SLs by SSF using glucose and oleic acid

The solid mixture based on glucose and oleic acid blended with wheat bran was chosen as the starting point of our research for two main reasons: first, because glucose and oleic acid are extensively used in the literature for the production of SLs under SmF (Ashby et al., 2008; Daverey and Pakshirajan, 2009; Felse et al., 2007); and second, because a previous work had demonstrated the efficiency of this mixture for the production of SLs under SSF at a smaller scale (Parekh and Pandit, 2012). Hence, the objective of this experiment was not to prove the feasibility of SSF to obtain SLs from glucose and oleic acid but to adapt the published information to our Fermentation System I (Chapter 3, section 3.2.1) and to get some knowledge about the process itself. This includes the learning of basic aspects of microbiology, the monitoring of the process through respirometry, the evaluation of protocols for the extraction, quantification and structural identification of the SLs molecules, and the validation of other protocols as the ones used for the determination of glucose and fat content.

#### Experiments

In this experiment, SSF was based on 10 g of glucose and 10 g of oleic acid blended with 30 g of wheat bran powder, which was used as the inert support. The proportion 1:1:3 between glucose, oleic acid and wheat bran was based on a previous work published by Parekh and Pandit (2012). In our study the scale of the SSF mixture was 5 times higher than the work mentioned and toothpicks were added in a 10% w/w to increase the porosity of the solid mixture and avoid compaction. The SSF mixture was prepared as shown in Figure 4.3 under sterile conditions (laminar flow chamber). First, 30 g of wheat bran were autoclaved in a 1-L glass beaker. Next, the wheat bran was blended with 40 mL of a sterile 250 g L<sup>-1</sup> glucose solution, 10 g of sterile oleic acid and 10 mL of freshly prepared inoculum. The mixture was carefully homogenised with a metal spatula. Finally, 10 g of toothpicks were added to the mixture to increase the porosity of the medium and the whole mixture was manually homogenised. The freshly prepared fermentation mixture was transferred to the reactor. Final appearance of the SSF mixture is shown in Figure 4.4.

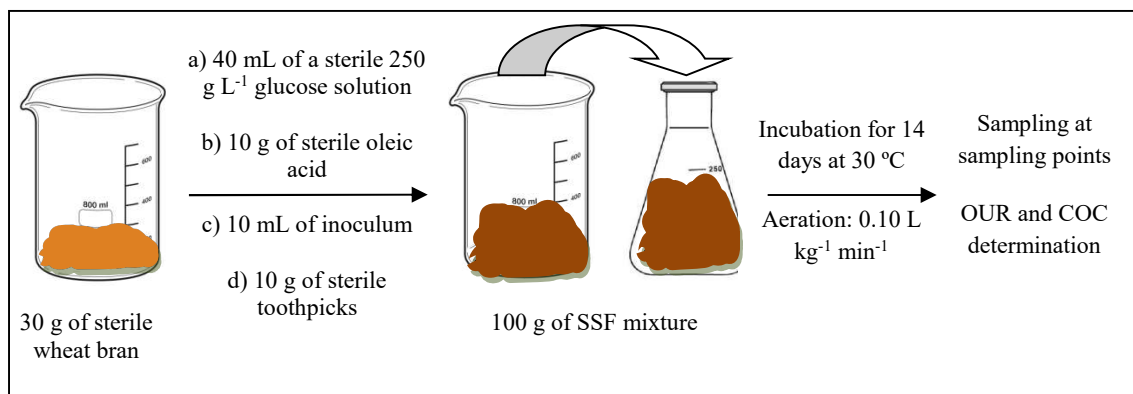


**Figure 4.3.** Scheme of SSF mixture preparation



**Figure 4.4.** SSF mixture based on glucose and oleic acid blended with wheat bran.

In summary, a total of 60 mL of media (substrates, inoculum and water) were added to 30 g of inert support. This means that each gram of inert support held 2 mL of media. Since the WHC of the wheat bran was determined to be 2.6 g of water per gram of inert support, the fermentation was carried out at the 75% of the WHC of the wheat bran.

Seven reactors were prepared as described above and one of them was terminated at each sampling point (days 0, 2, 4, 6, 9, 13, 14). Continuous aeration of 0.10 L kg<sup>-1</sup> min<sup>-1</sup> was provided to the reactors. Three consecutive extractions were performed to evaluate SL yield and the efficiency of the extraction method. Emulsion activity of the produced SLs was determined towards hexadecane and sunflower oil according to the method described in Chapter 3, section 3.6.3. Results were compared with those obtained with a commercial SL and the commercial surfactants Triton X-100 and Tween 20. Results were analyzed by one-way ANOVA followed by Duncan's test ( $p < 0.05$  confidence

level) using SPSS 15.0 for Windows. All these materials were purchased in Sigma-Aldrich (St. Louis, MO, USA).

### Process dynamics

SLs were satisfactorily produced in a SSF mixture composed by glucose and oleic acid blended with wheat bran at 0.5-L scale. SLs were amber coloured, honey like semi-crystalline molecules (Figure 4.5). Figure 4.6 shows SL yield evolution in the fermentation. The maximum yield was reached on day 6, with a total amount of 0.063 g g<sup>-1</sup>DM, which corresponds to 0.158 g g<sup>-1</sup> of wet substrates. This yield agrees with the reported by Parekh and Pandit (2012) who produced 0.180 g g<sup>-1</sup> of wet substrates using a similar fermentation media than the one used in this experiment but in a 5-times smaller scale.

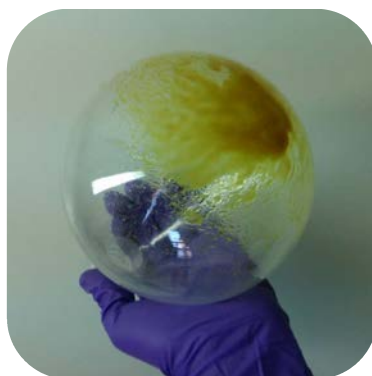


**Figure 4.5.** Appearance of the final extract containing SLs after *n*-hexane washing.

As shown in Figure 4.6, SL yield slightly decreased with the time course of the fermentation after day 6. It can be assumed that synthesis of SLs is hindered after this point because nutrients are either depleted or unavailable for the yeast. Two hypothesis arise to explain the decrement in the SL yield observed after day 6. The first one is that *S. bombicola* is consuming the SLs produced due to the depletion of available nutrients. It has been reported that one of the reasons why SLs are synthesized is to be used as external carbon and energy storage molecules (Hommel et al., 1994b). The second hypothesis points to the growth of other microorganisms which are taking advantage of nutrients unavailable for the yeast and even consuming the SLs produced. In fact, growth of black and green fungi was observed at the latter days of fermentation (Figure

4.7). The origin of these microorganisms would come from the Fermentation System I itself (Chapter 3, section 3.2.1) as it is used by other users who work either with other microorganisms or under non-sterile conditions. This would suggest an inefficient sterilization of the System before the beginning of the experiment. Also, as demonstrated in the following experiments, the use of wheat bran promotes the growth of fungi even when sterilized, which is a major issue considering that these fungi might be not only degrading SLs but also competing with the yeast for the nutrients. Both hypothesis described in this paragraph might be occurring at the same time.

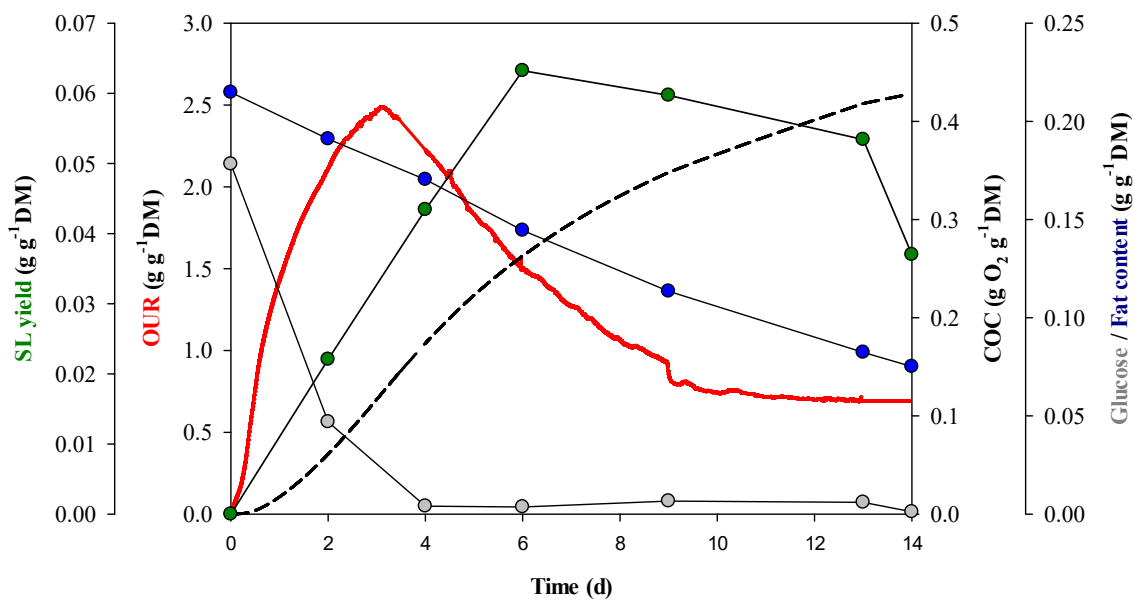


**Figure 4.6.** SSF profile of the process: OUR and COC profiles and time course of SL yield and fat and glucose contents.



**Figure 4.7.** Fungi found in the reactors sampled at days 13 (left) and 14 (right) of the fermentation.



The fermentations were monitored on-line during the 14 days using the respirometer parameters OUR and COC (Figure 4.6). OUR reached its maximum value after 3 days ( $2.39 \pm 0.10 \text{ mg O}_2 \text{ g}^{-1}\text{DM h}^{-1}$ , average  $\pm$  standard deviation for 5 fermentations), and the oxygen consumed at the end of the fermentation was  $0.430 \text{ g O}_2 \text{ g}^{-1} \text{ DM}$ . However, the oxygen consumed to reach the maximum SL yield (day 6) was around the half of the final one. The growth of other microorganisms in the fermentation mixture would contribute to the oxygen uptake after reaching the maximum SL yield.

Figure 4.6 also shows the profile of glucose and fat content expressed as grams per gram of total dry matter in the fermentation mixture. Around 75% of the glucose was consumed at day 2 of fermentation, and it was almost depleted at day 4. Thus, glucose content remains below the 4% after day 4. Remaining glucose probably corresponds to an inaccessible fraction for the yeast cells. Conversely, fat content was more gradually degraded. It should be noticed that fat content corresponds mainly to oleic acid, as the low fat content of the wheat bran constitutes less than the 9% of the total fats of the SSF mixture (Table 4.1). Approximately, one third part of the initial oleic acid was consumed at day 6, when maximum SL yield was achieved, and about two third parts at the end of the fermentation. This oleic acid may be used for synthesis of SLs, that are later consumed, consumed by other microorganisms or oxidized to  $\text{CO}_2$  (Van Bogaert et al., 2011b).

A linear relationship was found when SL yield ( $\text{g g}^{-1}\text{DM}$ ) was plotted versus COC ( $\text{g O}_2 \text{ g}^{-1}\text{DM}$ ) and versus fat consumed ( $\text{g g}^{-1}\text{DM}$ ) with determination coefficients ( $R^2$ ) of 0.977 and 0.996, respectively. These correlations are valid until day 6 when maximum SL yield was obtained. Linear correlations between SL yield and COC and fat consumed have also been found in the following experiments described in this chapter, and will be discussed more in detail in Chapter 5.

The pH dropped from an initial value of 6.0 to values between 4.2 and 4.5 after day 2. Fermentations with *S. bombicola* are associated with a pH drop (Van Bogaert et al., 2011b). At the end of fermentation (days 13 and 14), pH increased to 5.5 coinciding with the decrease in SL yield and the growth of other microorganisms. The water content of the SSF mixtures remained at values of approximately 50% during the whole process, which confirms the effectiveness of the use of humidified air to avoid moisture

losses. It should be noticed that in this experiment SSF mixtures were not supplemented with nitrogen or minerals such as Mg, Na or K which are essential for the growth of the yeast. It means that nitrogen and essential minerals were provided by the inert support. Nitrogen content of the wheat bran was determined in 2.86% db (Table 4.1). Also, according to supplier information, wheat bran is rich in proteins (13.4% wb) and minerals as Na, Mg, Fe and Zn.

### Efficiency of the SL extraction methodology

This experiment was used to assess the efficiency of the methodology for SL extraction. For that, three consecutive extractions were performed and quantified at each sampling point. Figure 4.8 shows the fraction of SLs extracted in each of the three extractions at each of the samplings along the time course of the fermentation. On average, 78% of SL yield was extracted in the first extraction, 17% in the second one, and a 5% in the last one.

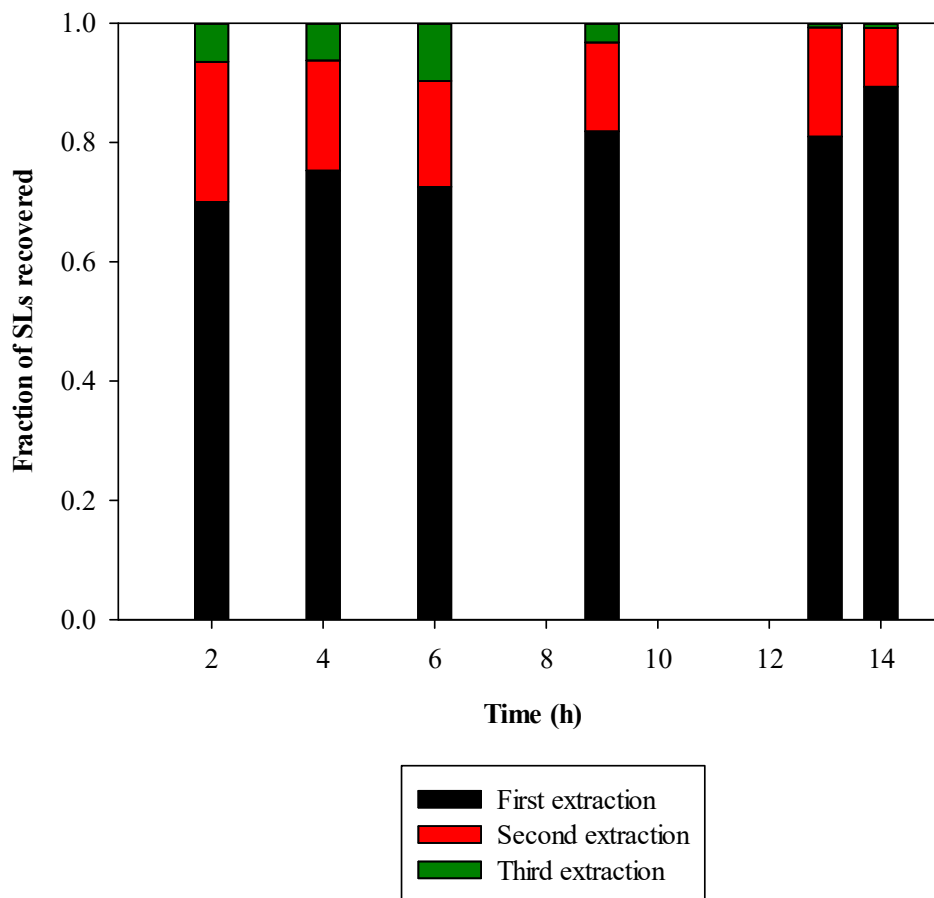


**Figure 4.8.** Fraction of SLs extracted in each of the three extractions performed at each sampling point of the time course of the fermentation.

Interestingly, it was observed that the efficiency of the first extraction increased with the time course of the fermentation. It turned out that the fraction of SL yield of the first extraction was highly dependent on the fat content of the fermentation mixture: the lower the fat content, the higher recovery in the first extraction. Figure 4.9 shows fat content ( $\text{g g}^{-1}\text{DM}$ ) plotted vs. the fraction of SLs recovered of the first extraction. The linear regression of the experimental points has a poor determination coefficient ( $R^2 = 0.805$ ), which could be explained due to the lack of triplicates. However, the tendency is clear and indicates that the efficiency of the first extraction in the fermented mixture increases when the oleic acid is consumed. According to the regression curve obtained ( $y = -1.35x + 0.958$ ), in a hypothetical SSF mixture without fat content, up to 96% of the SLs would be extracted in the first extraction.

In summary, these data suggest that the election of the number of extractions for SL recovery from a SSF is dependent on the fat content of the SSF mixture, and therefore it varies depending on the initial composition of the SSF mixture and the substrate conversion rates of the process. For the case of the SSF mixture of this experiment we can conclude that 3 extractions would be enough to recover the SLs. In the upcoming experiments, 3 extractions will be performed to determine SL yield.

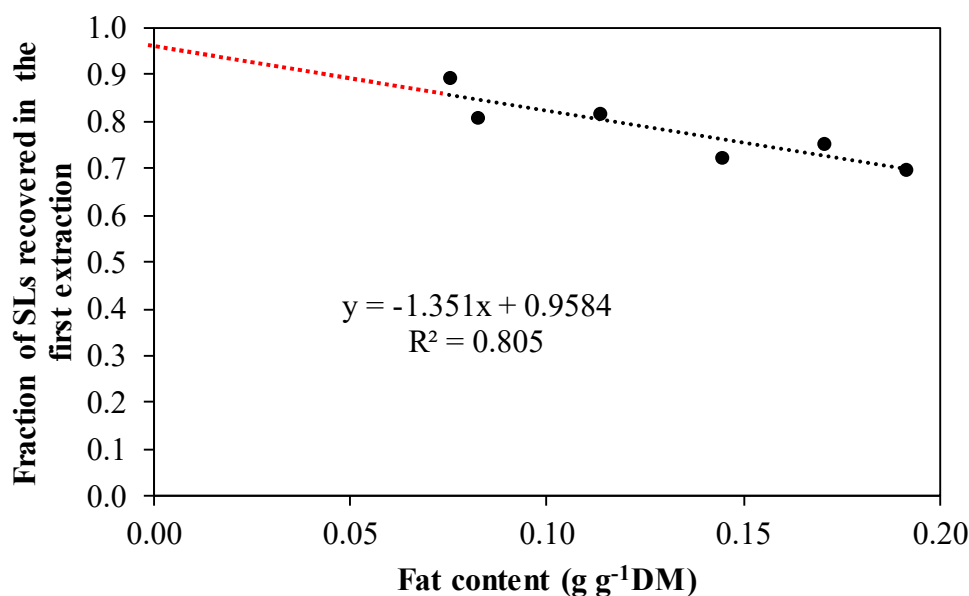


**Figure 4.9.** Fat content ( $\text{g g}^{-1}\text{DM}$ ) plotted vs. fraction of SLs recovered during the first extraction.

## Structural identification by FTIR

The SLs obtained were initially identified and characterized by FTIR (Figure 4.10). The spectrum revealed a broad band at  $3369\text{ cm}^{-1}$ , which corresponds to the O-H stretch (Figure 1.2). Asymmetrical stretching ( $\nu_{\text{as}}\text{ CH}_2$ ) and symmetrical stretching ( $\nu_{\text{s}}\text{ CH}_2$ ) of methylene were observed at  $2923\text{ cm}^{-1}$  and  $2853\text{ cm}^{-1}$ , respectively. The C=O absorption band at  $1736\text{ cm}^{-1}$  may include contributions from lactones, esters or acids. The stretch of the C-O band of C(=O)-O-C in lactones appeared at  $1169\text{ cm}^{-1}$ . The C=O absorption band at  $1236\text{ cm}^{-1}$  of acetyl esters and the band at  $1368\text{ cm}^{-1}$  for the symmetrical bending of the methyl groups of the acetyl esters indicate that our SL natural mixture contains acetylated sophorose moieties. The band at  $1454\text{ cm}^{-1}$  corresponds to the C-O-H in-plane bending of carboxylic acid (-COOH) and may indicate the presence of small quantities of unused fatty acids that were left after hexane washings or the contribution of acid SLs. Finally, a C-O stretch from C-O-H groups of sugars was observed at  $1033\text{--}1075\text{ cm}^{-1}$ . All the bands mentioned together with the correspondent stretch and the functional group involved are summarize in Table 4.2.

The structural characterization obtained by FTIR analysis was similar to the structural characterization reported previously by other authors (Daverey and Pakshirajan, 2010; Rashad et al., 2014), which confirmed that the product obtained belongs to the SLs.

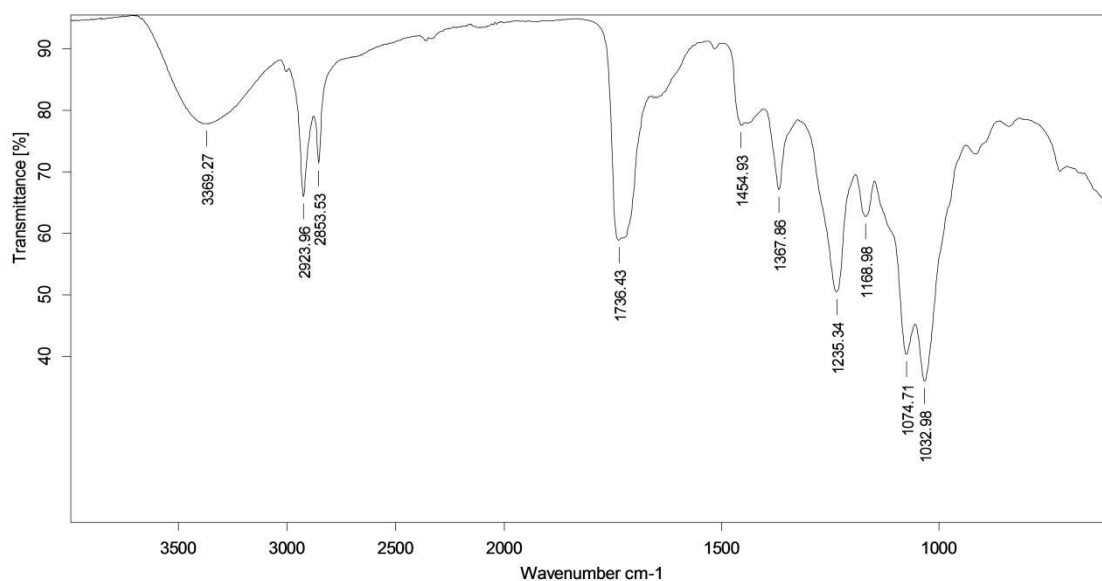


**Figure 4.10.** FTIR spectra of the SLs produced from glucose and oleic acid.

**Table 4.2.** Frequencies of the FTIR spectra with the correspondent stretch, functional group and structure.

Frequency (cm <sup>-1</sup> )	Stretch	Functional group	Structure
3369	O-H	-OH	Acids and glucoses
2923	$\nu_{\text{as}}$ CH <sub>2</sub>	-CH <sub>2</sub> -	Fatty acid chain moiety
2853	$\nu_{\text{s}}$ CH <sub>2</sub>	-CH <sub>2</sub> -	Fatty acid chain moiety
1736	C=O	-C(=O)-O-X (X=H or R)	Lactones, esters and acids
1454	C-O-H	-COOH	Acids
1368	$\delta_{\text{s}}$ CH <sub>3</sub>	R-O-C(=O)-CH <sub>3</sub>	Acetyl group
1236	C=O	R-O-C(=O)-CH <sub>3</sub>	Acetyl esters
1169	C-O	R'-C(=O)-O-R''	Lactones
1033-1075	C-O	C-O-H	Glucoses (sophorose moiety)

#### Emulsification activity of the SLs produced and comparison with commercial surfactants

Emulsification activity of the SLs produced in this experiment was evaluated towards hexadecane and sunflower oil. The results were compared with those obtained using a commercial SL and two synthetic commercial surfactants: Triton X-100 and Tween 20. As shown in Figure 4.11, there were no significant differences in the emulsification activity between the experimental SL and the commercial SL towards both hexadecane and sunflower oil according to Duncan's test ( $p < 0.05$ ). However, their emulsion activities were lower than those obtained for the synthetic surfactants for both solvents (Figure 4.11).

It is well-known that the emulsification capacity of any surfactant depends not only on the structure of the surfactant but also on the solvent system used. In the case of the SLs, both experimental and commercial, their emulsion activities are higher with hexadecane than with sunflower oil. This means that SLs are better solubilizing hexadecane than sunflower oil. Similar emulsion activities of SLs towards sunflower oil are reported in the literature (Daverey and Pakshirajan, 2009; Mahanty et al., 2006). Further experiments and discussion about the emulsification properties of SLs will be described in Chapter 7.

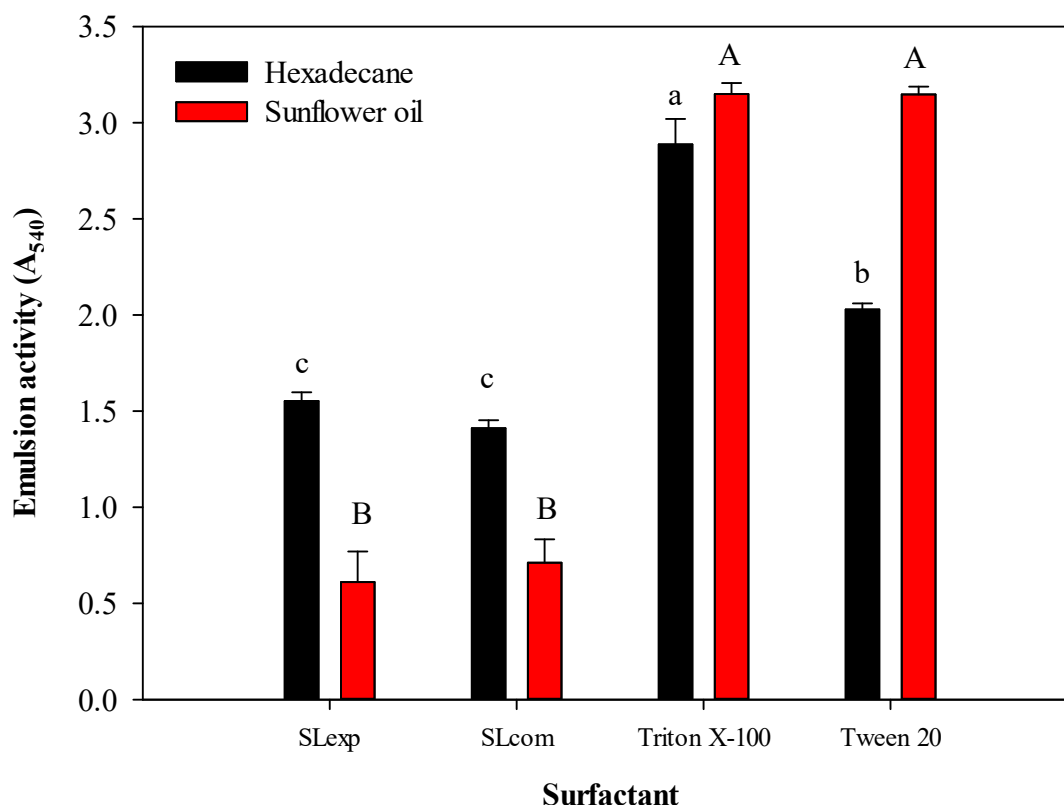


**Figure 4.11.** Emulsion activity of the experimental SL (SLexp), commercial SL (SLcom), and two other commercial surfactants towards hexadecane and sunflower oil. Results are expressed as mean  $\pm$  standard deviation of three replicates. Means with the same letters are statistically equal according to Duncan's test ( $p < 0.05$ ).

#### 4.3.2. Step 2: Screening of agro-industrial wastes and by-products as substrates

Once we learnt the basics to perform a SSF to obtain SLs using pure substrates we went a step further and explored the possibility of substituting the pure substrates glucose (G) and oleic acid (OLEIC) by agro-industrial wastes or by-products. Sugar beet molasses (MOL), a by-product of the sugar industry, was tested as the hydrophilic carbon sources of the synthesis due to its high sugar content (Table 4.1). Waste cooking olive oil (OIL) and a winterization oil cake (WOC) were tested as the hydrophobic carbon source because of their high fat content (Table 4.1).

#### Experiments

A total of 6 different SSF mixtures were tested as summarized in Table 4.3. In a first batch, we tested G+OLEIC, G+OIL and G+WOC (3 reactors). In a second batch,

we repeated the mixtures with glucose (3 reactors) and we tested MOL+O, MOL+OIL and MOL+WOC (3 reactors). It means that results of fermentations with glucose were obtained in duplicates. The control (G+OLEIC) was prepared as described previously in Step 1. The rest of the SSF mixtures were prepared following the same scheme with minor modifications. For those containing MOL, 40 mL of a sterile 250 g L<sup>-1</sup> MOL solution was added instead of the glucose solution. For those containing OIL, 10 g of sterile OIL were added instead of the oleic acid. Finally, for those containing WOC, 20 g of sterile wheat bran and 20 g of sterile WOC were used instead of the 30 g of wheat bran and the 10 g of oleic acid used in the control.

Reactors were continuously aerated with 0.20 L kg<sup>-1</sup> min<sup>-1</sup>. Aeration rate was doubled with respect to the experiment of Step 1 because low oxygen concentrations were measured in the exhaust gases (6-7%) in the moment of maximum biological activity. A higher airflow ensures that the process is not limited by oxygen. All the reactors were sampled at day 5 of fermentation.

**Table 4.3.** Abbreviations of the SSF mixtures studied.

		Hydrophilic source	
		Glucose	Sugar beet molasses
		Oleic acid	G+OLEIC
			MOL+OLEIC
<b>Hydrophobic source</b>	Waste cooking olive oil	G+OIL	MOL+OIL
	Winterization oil cake	G+WOC	MOL+WOC

## Results

Figure 4.12 shows SL yield obtained in the SSF mixtures after 5 days of fermentation. Results are expressed in terms of g of SLs per g of DM and per g of substrates. As expected, highest SL yield of 0.114 g g<sup>-1</sup> of wet substrates was obtained for the mixture based on glucose and oleic acid. This yield agrees with the results obtained in the previous experiment (section 4.3.1). SL yield decreased when oleic acid was replaced by any of the studied hydrophobic wastes: the lower the purity of the hydrophobic waste, the lower the SL yield in terms of g per g of substrates (OLEIC > OIL > WOC). This trend was observed for SSF mixtures with glucose and MOL. However, in terms of g of SL per g of DM, mixtures with WOC performed better than

the ones with OIL and very similar to mixtures with OLEIC. As described in the experimental section, the amount of WOC used was twice the amount of OIL (20 g vs. 10 g per 100 g of SSF mixture), which means that the fat content was higher (20%) in fermentations with WOC (Table 4.1). This would explain the higher SL yield expressed in this units.

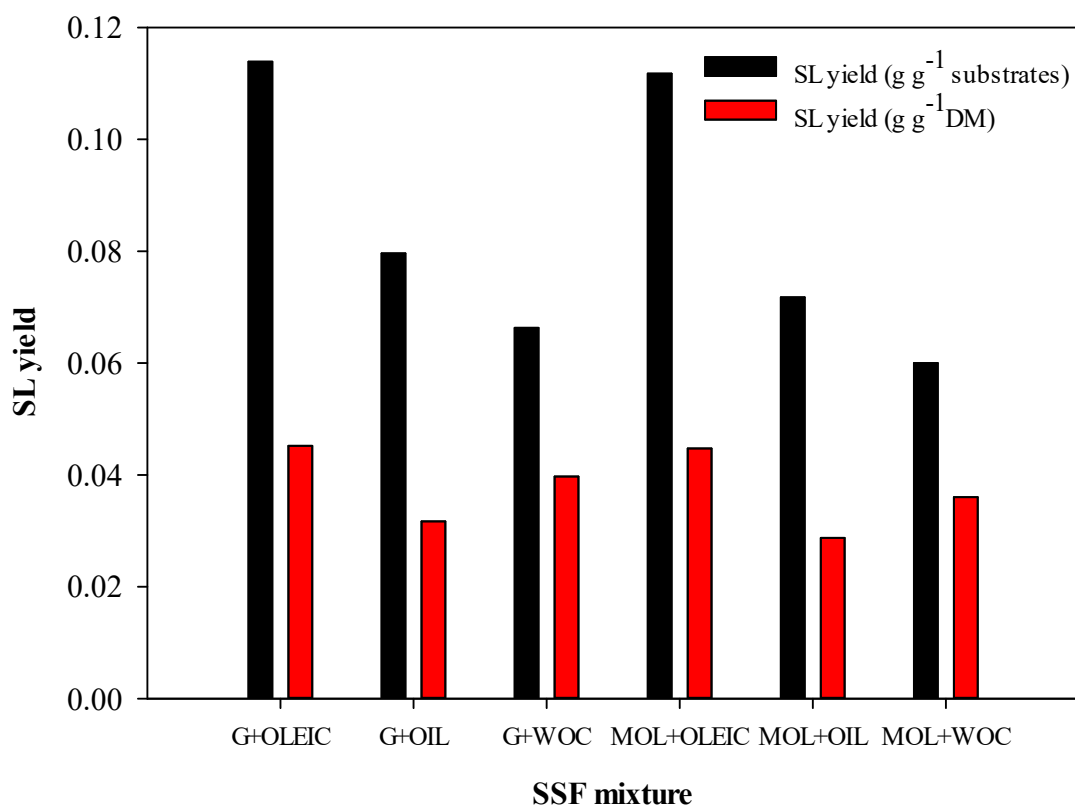


**Figure 4.12.** SL yield obtained at day 5 of fermentation for the different SFF mixtures (G, glucose; MOL, sugar beet molasses; OLEIC, oleic acid; OIL, waste cooking olive oil; and WOC, winterization oil cake). Results with glucose are the average of two replicates.

When glucose was replaced by MOL the SL yield obtained was very similar. The use of MOL in SL production has been studied previously in SmF with good results (Felse et al., 2007; Solaiman et al., 2004; Solaiman et al., 2007; Takahashi et al., 2011). Molasses (from sugar beet, sugar cane, soy, etc.) is a substrate composed mainly by sugars, which makes it ideal as a replacement of glucose in fermentations. The sugar content of the MOL used in this study was around 78% db (Table 4.1). Additionally, molasses have a high content in nitrogen and micronutrients such as Mg, K or Na which



decreases or even avoids the need for mineral supplementation to the yeast (Van Bogaert et al., 2011b). Nitrogen content of the MOL used in this experiment was 1.89% db (Table 4.1).

The mixture based on MOL and WOC was selected for further experiments due to its feasibility to be used for SLs production. Logically, SSF mixtures containing glucose or oleic acid were not considered for further research because the aim of this study is the valorisation of wastes or by-products from the agro-industrial industry.

### Structural identification by FTIR

The identity of the SLs produced from the different SSF mixtures was confirmed by FTIR analysis. The structural characterization obtained by FTIR was similar to the structural characterization obtained for the control (G+OLEIC), which confirmed that all the products obtained belong to the SLs. As an example, spectra of the SLs obtained in the mixtures where glucose was used as the hydrophilic carbon source of the synthesis is shown in Figure 4.13.

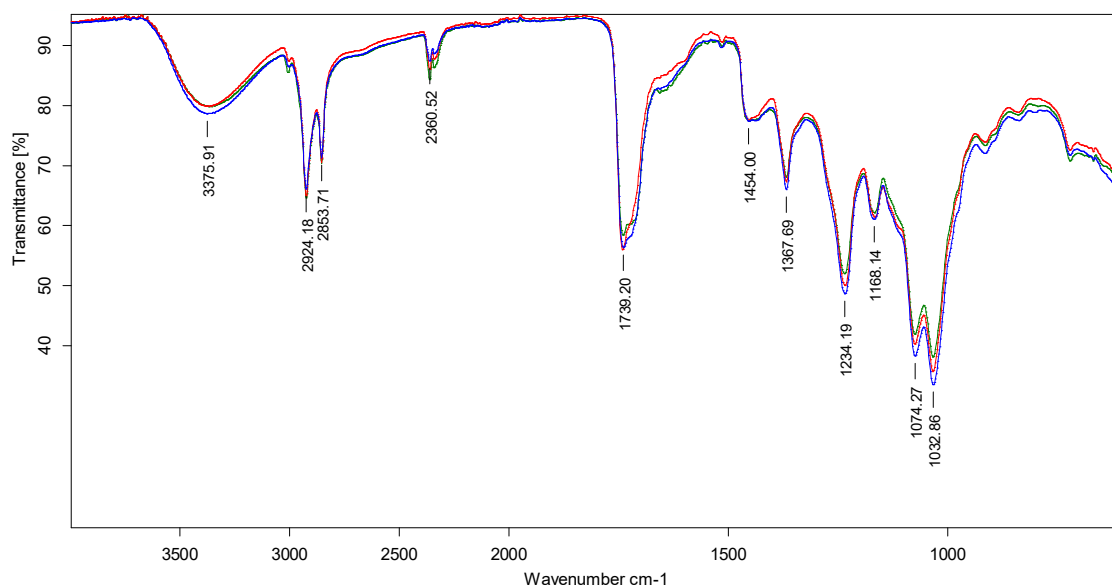


**Figure 4.13.** FTIR spectra of the SLs produced in the mixtures G+OLEIC (blue), G+OIL (green), and G+WOC (red).

### **4.3.3. Step 3: Testing wheat straw as the inert support**

In the previous steps wheat bran was used as the inert support of the fermentations and growth of fungi was observed at the later days of fermentation even after sterilization of the materials and proper cleaning of the Fermentation System I. Furthermore, wheat bran does not provide to the mixture good porosity and resistance to compaction, which are essential requirements when increasing the operation scale in solid systems. Thus, despite the good physicochemical properties of wheat straw for their use as inert support such as good WHC or its content in nitrogen and minerals, an alternative was needed. Additionally, we should not forget that wheat bran is a relative costly material used for human feeding. If the aim of this work is the valorisation of wastes or by-products to produce added-value products through a green low-cost process, the use of raw materials as wheat bran should not be considered as a reasonable option. Wheat straw was suggested as a good alternative to functioned as the inert support of the substrates selected in Step 2: MOL and WOC. Wheat straw is a low-cost material, not used for human feeding, and with a proper water holding capacity. A comparison of process dynamics between fermentations carried out with wheat bran and wheat straw is discussed in this section.

### **Experiments**

In this set of experiments, SLs were synthesized using a mixture based on MOL and WOC blended in two different inert supports: wheat bran and wheat straw. Mixtures with wheat bran were prepared as described previously in Step 2. For mixtures with wheat straw, 20 g of wheat straw were used instead of the 20 g of wheat bran. Since a total of 50 mL of media (40 mL of molasses solution + 10 mL inoculum) was added to 20 g of inert support, each gram of inert support held 2.5 mL of media. It means that fermentations were carried out at around the 100% of the WHC of the inert supports. As can be observed in Figure 4.14, wheat straw (right) provided lower bulk density and therefore higher porosity to the solid mixture. The experiment was carried out for 8 days with a continuous aeration of  $0.20 \text{ L kg}^{-1} \text{ min}^{-1}$ . Four reactors were prepared with each inert support and one replicate of wheat bran and one of wheat straw was sacrificed and used for analysis at each sampling point (days 0, 3, 5 and 8).



**Figure 4.14.** SSF mixtures based on MOL and WOC blended with wheat bran (left) or wheat straw (right).

### Process dynamics

Figure 4.15 shows the OUR profiles of the different replicates of SSF carried out using MOL and WOC blended with two different inert supports: wheat bran and wheat straw. The profiles obtained were very different: for fermentations with wheat bran maximum OUR was reached after 2 days with a value of  $2.32 \pm 0.21 \text{ mg O}_2 \text{ g}^{-1} \text{ DM h}^{-1}$  (average  $\pm$  standard deviation for 3 fermentations), while for fermentations with wheat straw maximum OUR was reached after almost 3 days with a value of  $1.31 \pm 0.13 \text{ mg O}_2 \text{ g}^{-1} \text{ DM h}^{-1}$  (average  $\pm$  standard deviation for 3 fermentations). The low variability ( $< 10\%$ ) between replicates is an indicator of the good reproducibility of the experimental data.

Figure 4.16 shows OUR and COC profiles of the SSF after 8 days for wheat bran (Figure 4.16A) and wheat straw (Figure 4.16B). The oxygen consumed at the end of the fermentation was  $0.286$  and  $0.200 \text{ g O}_2 \text{ g}^{-1} \text{ DM}$  for fermentations with wheat bran and wheat straw, respectively. In the beginning, the higher consumption of oxygen in fermentations with wheat bran suggested either that *S. bombycol* grows better in wheat bran, or either that other microorganisms were growing in this material. The growth of black fungi was observed in the latter days of fermentation with wheat bran but not with wheat straw, confirming that the extra oxygen uptake came from the growth of other microorganisms. In fact, the maximum SL yield (final value, day 8) was higher when

using wheat straw (0.107 g g<sup>-1</sup>DM or 0.178 g g<sup>-1</sup> of wet substrates) than when using wheat bran (0.068 g g<sup>-1</sup>DM or 0.113 g g<sup>-1</sup> of wet substrates). This confirms our hypothesis described in section 4.3.1 that the growth of other microorganisms in fermentations with wheat bran was either degrading the produced SLs or consuming the substrates and hindering the growth of *S. bombicola* and therefore the synthesis of SLs.

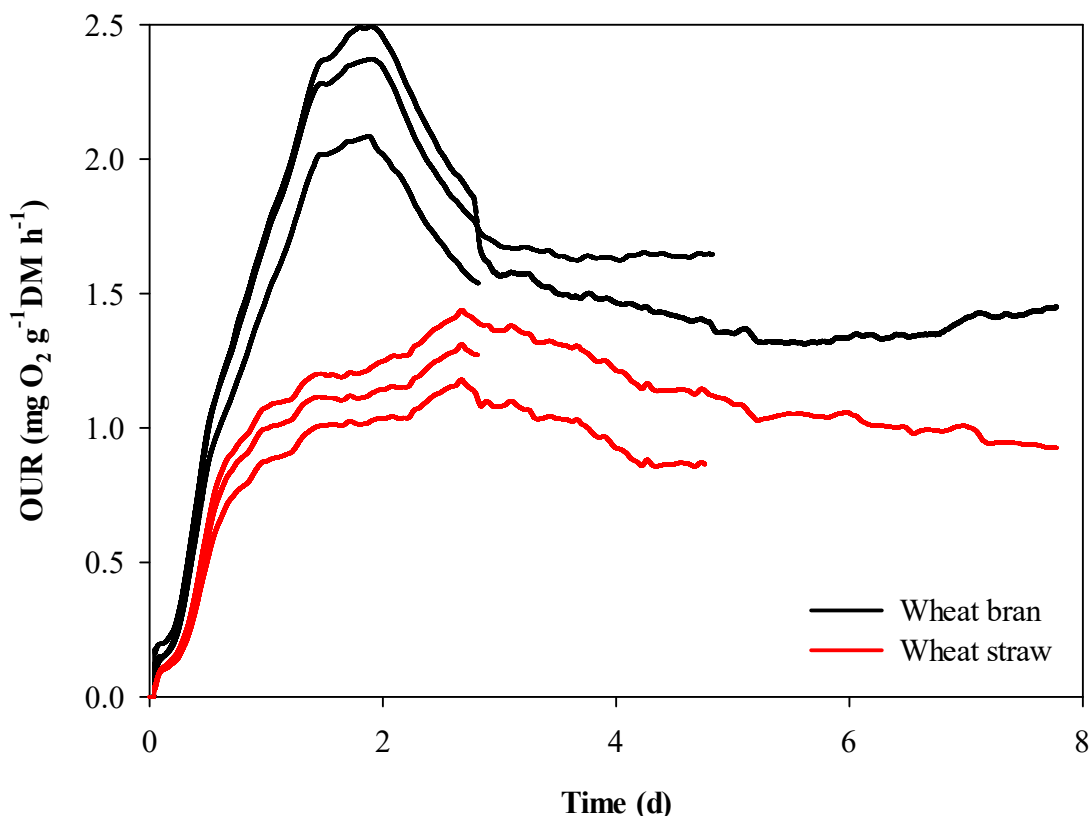


**Figure 4.15.** OUR profiles of the different replicates of fermentations with wheat bran and wheat straw.

Regarding the pH, it dropped from an initial value of 5.8 to values of 4.3 for fermentations with wheat bran and to 3.3 for fermentations with wheat straw. Water content was maintained around 50% during the experiment.

Fat degradation in 8 days (g g<sup>-1</sup>DM) was 65 and 75% for experiments with wheat bran and wheat straw, respectively (Figure 4.16). A linear relationship was found when SL yield (g g<sup>-1</sup>DM) was plotted versus COC (g O<sub>2</sub> g<sup>-1</sup>DM) and versus fat consumed (g g<sup>-1</sup>DM). Determination coefficients (R<sup>2</sup>) are shown in Table 4.4. Linear correlations between SL yield and COC and fat consumed were also found in Step 1 for

fermentations where glucose and oleic acid were used as substrates, and will be discussed in more detail in Chapter 5.

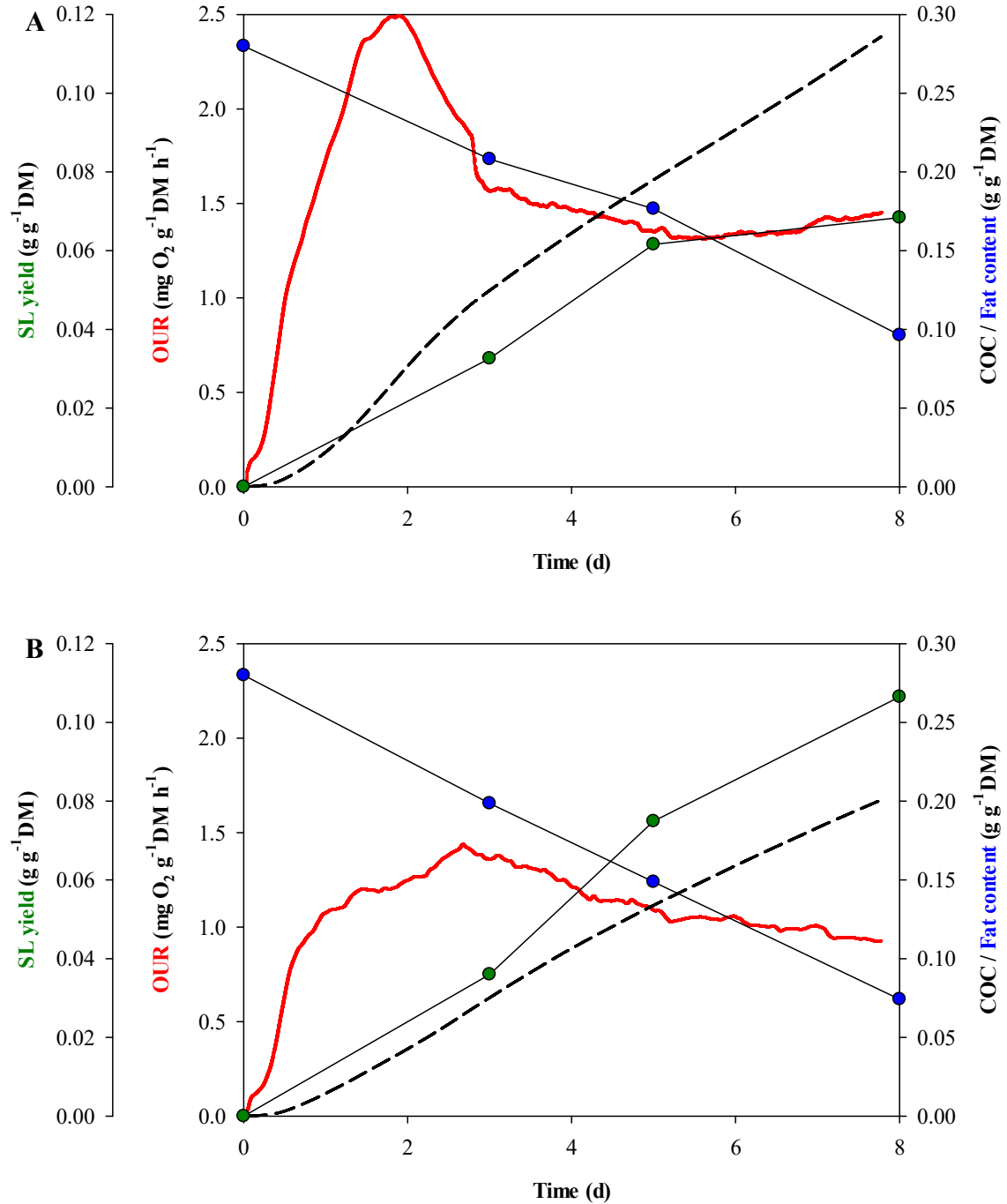


**Figure 4.16.** SSF profile of the process using wheat bran (A) and wheat straw (B) as the inert support: OUR and COC profiles and time course of SL yield and fat content.

**Table 4.4.** Determination coefficients ( $R^2$ ) obtained when SL yield ( $\text{g g}^{-1}\text{DM}$ ) was plotted versus COC ( $\text{g O}_2 \text{g}^{-1} \text{DM}$ ) and vs. fat consumed ( $\text{g g}^{-1}\text{DM}$ ).

	<b>Wheat bran</b>	<b>Wheat straw</b>
COC ( $\text{g O}_2 \text{g}^{-1}\text{DM}$ )	0.928	0.951
Fat consumed ( $\text{g g}^{-1}\text{DM}$ )	0.860	0.987

Glucose was not detected in the samples during the time course of the fermentation. As shown in Table 4.1, the glucose content of MOL constitutes a tiny 0.24% db. It is well-known that molasses have minor amounts of monosaccharides such as glucose, and are mainly constituted by sucrose and oligosaccharides (Van Bogaert et al., 2011b). Therefore, the measurement of the glucose content cannot be used for the monitoring of the consumption of sugars in a SSF process where MOL is used as the hydrophilic carbon source.

A common method used for the monitoring of sugar content in SSF processes is the DNS method (Chapter 3, section 3.5.4), which measures the reducing sugars of a sample (Cerda et al., 2016b; Maulini-Duran et al., 2015). A reducing sugar is any sugar that can act as a reducing agent because it has a free aldehyde group or a free ketone group. As shown in Table 4.1, MOL contains 4.18% reducing sugars in dry basis. Sucrose, which is one of the main components of molasses, is a disaccharide with a glycosidic bond between its anomeric carbons and thus cannot be converted to an open-chain form with an aldehyde group. Thus, sucrose is considered a non-reducing sugar, which cannot be measured by the DNS method. Therefore, this method was discarded as an option for monitoring the sugar content profile of the SSF process described in this study.

Another method used to monitor the sugars profile in SSF processes is the anthrone method (Chapter 3, section 3.5.5), which measures the total sugar content of a sample (Mohanty et al., 2009). As can be seen in Table 4.1, sugar content in MOL could be well determined by this method, and therefore the anthrone method was proposed to monitor the sugar content along the time course of the fermentation. Its efficiency to monitor the SSF system under study will be evaluated in the following chapter.

### Structural identification by FTIR

FTIR spectra of the isolated viscous products obtained using wheat straw (Figure 4.17) as the inert support was similar to the one obtained using wheat bran (Figure 4.13), which confirms that the obtained product belongs to the SLs.

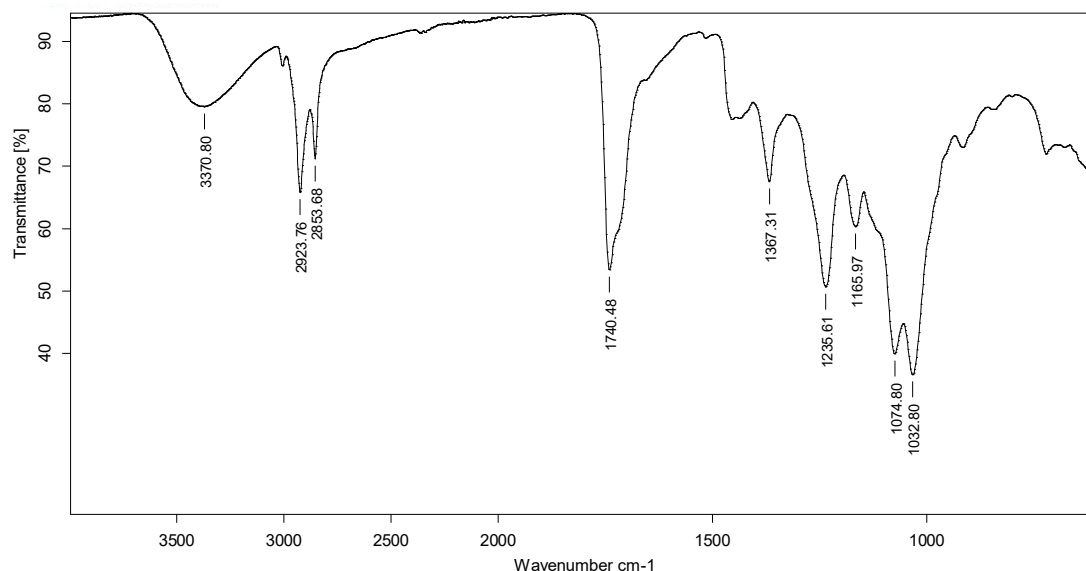


**Figure 4.17.** FTIR spectra of the SLs produced using wheat straw as the inert support.

The results obtained in this experiment confirm that wheat straw can be used instead of wheat bran as the inert support of the SSF mixture based on WOC and MOL because a higher SL yield was obtained and problems associated with fungi growth were not observed.

### 4.4. Conclusions

The feasibility of SSF to produce SLs by *S. bombicola* was proved at 0.5-L scale using both pure substrates and agro-industrial wastes and by-products. The SSF mixture based on winterization oil cake and sugar beet molasses blended with wheat straw was selected for further experiments for three main reasons. Firstly, the winterization oil cake is produced in large quantities in Spain, and in other oil-refining countries, and its potential due to its high fat content is still not properly explored. The valorization of this waste to obtain an added-value product as SLs would be a good alternative. SSF seems to be the most feasible technique for its valorisation considering the solid nature of the

winterization oil cake. Secondly, sugar beet molasses is a by-product of national origin produced in large quantities. Its high sugar content makes this substrate ideal to be used as the hydrophilic carbon source in SL synthesis, and its content in nitrogen and micronutrients such as Mg, K or Na decreases or even avoids the necessity of mineral supplementation to the yeast. Thirdly, wheat straw was selected as the inert support because it is a low-cost material, not used for human feeding, and did not support the growth of fungi as wheat bran did.

The combination of the three materials winterization oil cake, sugar beet molasses and wheat straw gives a low-cost mixture which is capable of producing SLs using the inoculum *S. bombicola*. Maximum SL yield obtained for the mixture selected was 0.107 g g<sup>-1</sup>DM at day 8 of fermentation. Further experiments for the optimization of the process in terms of the substrate ratio and the aeration rate will be performed in Chapter 5.

The fat content was properly monitored using the Soxhlet method in all cases. The results suggest that interesting correlations can be obtained between fat content or fat degradation and SL yield. However, the monitoring of the sugar content was challenging when sugar beet molasses was used as the hydrophilic substrate. The measurements of glucose or reducing sugar content were discarded because only a small fraction of the total sugars contained in the sugar beet molasses are measured by these methods. Thus, the anthrone method was selected as a promising method for the monitoring of sugars for the time course of the fermentation and its efficiency will be evaluated in the following chapter.

Finally, OUR and COC were found to be very useful tools for the follow-up of the process. In fact, correlations were found between SL yield and COC. Monitoring of the cultivation process has been identified as one of the challenges to be addressed for biosurfactant production by SSF and will be studied more in detail in the upcoming chapters.





## CHAPTER 5

---

### *Sophorolipids from winterization oil cake by SSF: process optimization*

*Part of this chapter has been published in Biochemical Engineering Journal 115, 93-100. 2016.*

*Production of sophorolipids from winterization oil cake by solid-state fermentation: Optimization, monitoring and effect of mixing.*

*Jiménez-Peñalver, P., Gea, T., Sánchez, T., Font, X.*

*Part of this chapter has been also published in two divulgation journals:*

*INFORM magazine 28 (5), 20-23. 2017.*

*Sophorolipids from a winterization oil cake.*

*Jiménez-Peñalver, P., Font, X., Gea, T.*

*Industria Química 47, 76-80. 2017.*

*Soforolípidos a partir de un residuo de winterización.*

*Jiménez-Peñalver, P., Font, X., Gea, T.*



## Summary

The present chapter contains an in-depth study of the use of winterization oil cake (WOC) and sugar beet molasses (MOL) blended with wheat straw to produce SLs under SSF using *S. bombicola* as inoculum. The feasibility of this mixture for the solid-state fermentation was proven in Chapter 4. Fermentations were performed at the 0.5-L scale and were optimized in terms of the ratio of substrates and the aeration rate using response surface methodology. The effect of inoculum size and sterilization of the SSF mixture was also assessed. The optimized SSF process (1:4 MOL:WOC mass ratio, 0.30 L kg<sup>-1</sup> min<sup>-1</sup> aeration rate, 10% (v/p) inoculum size), carried out under static conditions, was monitored for 10 days with a maximum SL yield of 0.179 g g<sup>-1</sup>DM. The effect of intermittent mixing on the process was also investigated. Mixing caused a 31% increase in SL production, with a total yield of 0.235 g g<sup>-1</sup>DM. The optimization of the process carried out in this chapter led to an increase of 120% in the SL yield with respect to the preliminary results obtained in Chapter 4. The OUR and the COC were used to monitor the biological activity of the fermentation processes. There were significant correlations between the SL yield and the oxygen and fats consumed.

## 5.1. Materials

Wheat straw was generously provided by the experimental farms at Universitat Autònoma de Barcelona (UAB) and was shredded and sieved. Particles between 5 and 30 mm were used together with MOL and WOC (Figure 5.1). Main characteristics of these materials are shown in Table 5.1. WHC of the wheat straw from UAB was 3.5 g water g<sup>-1</sup> of material, which is a 45% higher than the commercial wheat straw used in Chapter 4. In contrast, from a nutritional point of view the wheat straw from the UAB is worse since it has 50% less nitrogen and the sugar content is 5 times lower. However, nitrogen and sugars are already provided by the molasses in the mixture. Therefore, it was more convenient for us to use an inert support with higher WHC, which allowed us to work with a higher water activity in the SSF mixture as will be discussed in the next section.



**Figure 5.1.** Physical appearance of the sugar beet molasses (left), the winterization oil cake (center), and the wheat straw (right).

**Table 5.1:** Main characteristics of the substrates and the inert support.

	Substrates		Inert support
	Sugar Beet Molasses	Winterization Oil Cake	Wheat straw (UAB)
pH	6.79±0.06	4.75±0.01	7.17±0.01
Water content (%)	16.9±0.8	0	4.2±0.5
Organic matter (% db)	87.3±2.1	64.3±1.3	96.2±0.4
Fat content (% db)	n.d.	<b>65.1±1.0</b>	2.7±0.6
Sugar content (% db)	<b>78.4±2.8</b>	n.a.	2.2±0.2
Nitrogen content (% db)	<b>1.89±0.01</b>	n.d.	0.54±0.11

*Abbreviations:* db, dry basis; n.d., not detected; n.a., not analysed. Data presented as mean ± standard deviation of the sample.

## 5.2. Experiments

In Chapter 4, fermentations were performed at 0.5-L scale with a total amount of substrates of 30 g (10 g MOL + 20 g WOC) blended with 20 g of wheat straw and 10 g of toothpicks. In this chapter, the SSF mixture was slightly changed:

- Toothpicks were no longer required since the wheat straw provides enough porosity and resistance to compaction.
- The amount of wheat straw could be reduced from 20 to 14 g due to the higher WHC of this material compared with the wheat straw used in Chapter 4.

- The elimination of toothpicks and the reduction in the amount of inert support allowed to increase the amount of substrates from 30 to 45 g in the same fermentation volume.

Therefore, SSF mixtures contained 100 g of wet fermentation medium consisting of 45 g of substrates (WOC and MOL), 14 g of wheat straw as the inert support, plus 10 mL of inoculum (Chapter 3, section 3.1.2) and 40 mL of sterile distilled water. Final appearance of the mixture is shown in Figure 5.2. Fermentations were carried out at the 100% of the WHC of the wheat straw. The average bulk density of the substrate mixtures was  $250 \text{ g L}^{-1}$ , and the air filled porosity was 80%. A high value of air filled porosity enhances oxygen transfer and carbon dioxide and heat removal from the solid matrix (Ruggieri et al., 2009). Fermentation experiments were performed in 0.5-L Erlenmeyer flasks at 30 °C in the Fermentation System I (Chapter 3, section 3.2.1). The oxygen concentration in the exhaust gases was recorded and used for the calculation of the OUR and the COC (Chapter 3, section 3.3).

At sampling times, the whole content of one reactor was collected and manually homogenized with a metal spatula. Then, 5 g was used to measure pH, 10 g was used to analyse SL content, and the rest of the sample was oven-dried at 105 °C to measure the water content (Chapter 3, section 3.4 and section 3.5). The total sugar and fat contents of the dry sample was then determined (Chapter 3, section 3.5).



**Figure 5.2.** SSF mixture based on winterization oil cake and sugar beet molasses blended with wheat straw.

### 5.3. Results and discussion

#### 5.3.1 Optimizing the aeration rate and the ratio of substrates

The combined effect of two important variables (MOL:WOC mass ratio and aeration rate) for the production of SLs under this SSF process was studied and optimized through a central composite design (CCD).

#### Experiments

The effects of the ratio of substrates and the aeration rate on the production of SLs were assessed by a full experimental design consisting of 12 experiments ( $3^2$  experiments plus 3 replicates at the central point for statistical validation). The specific aeration rate (A) was fixed at 0.05, 0.175 and 0.30 L air kg<sup>-1</sup> total wet mass min<sup>-1</sup> (coded values -1, 0, 1, respectively). These values were chosen based on the background of the research group in similar processes (Almeira et al., 2015). The ratio of the substrates (S, MOL:WOC, w/w) was fixed at 1:2, 1:3 and 1:4 (coded values -1, 0, 1, respectively) and total amount of substrates was kept constant. These values were selected because the fats were expected to be the limiting substrate. The main characteristics of the mixtures are listed in Table 5.2. The yield of SLs at day 5 was selected as the objective function. Additional experiments to assess the influence of the aeration rate were performed in triplicate using a 1:4 MOL:WOC ratio. The results of the full experimental design for process optimization were statistically analysed using a central composite design (CCD) with coded values (Gea et al., 2007; Rispoli et al., 2010) and a one-way ANOVA followed by Duncan's test ( $p < 0.05$  confidence level).

**Table 5.2:** Main characteristics of the initial mixtures.

	Ratio MOL:WOC		
	1:2	1:3	1:4
pH	6.14±0.02	6.26±0.06	6.54±0.03
Water content (%)	43.7±0.8	43.8±0.9	44.7±0.9
Organic matter (% db)	78.1±0.1	75.9±0.3	74.7±0.4
Fat content (% db)	<b>33.9±0.8</b>	<b>36.1±0.2</b>	<b>39.0±0.2</b>
Sugar content (% db)	<b>16.1±1.0</b>	<b>13.4±0.8</b>	<b>10.6±1.1</b>

*Abbreviations:* db, dry basis. Data presented as mean ± standard deviation of the sample.

### Central composite design

Table 5.3 summarizes the 12 experiments performed for the experimental design. Maximum SL yield was obtained in run 12 (0.080 g g<sup>-1</sup>DM) and minimum (0.038 g g<sup>-1</sup>DM) was obtained in run 3 (Table 5.3). The low variability (< 7%) of the central points (runs 5, 7, 8, 9) is an indicator of the good reproducibility of the experimental data (Table 5.3).

**Table 5.3:** CCD matrix for the optimization of aeration rate and substrate ratio to produce SLs with the coded and real values for the variables and the experimental and predicted values for the response.

Run	A: Aeration rate (L kg <sup>-1</sup> min <sup>-1</sup> )		S: Substrate ratio (w/w)		Y: SL yield (g g <sup>-1</sup> DM)	
	Coded	Real	Coded	Real	Real	Predicted
1	-1	0.05	-1	1:2	0.052	0.051
2	-1	0.05	0	1:3	0.052	0.052
3	-1	0.05	1	1:4	0.038	0.040
4	0	0.175	-1	1:2	0.055	0.057
5	0	0.175	0	1:3	0.073	0.069
6	0	0.175	1	1:4	0.070	0.067
7	0	0.175	0	1:3	0.070	0.069
8	0	0.175	0	1:3	0.067	0.069
9	0	0.175	0	1:3	0.063	0.069
10	1	0.30	-1	1:2	0.053	0.052
11	1	0.30	0	1:3	0.075	0.074
12	1	0.30	1	1:4	0.080	0.082

The experimental data was evaluated by using analysis of variance (ANOVA) and the following polynomial equation (Equation 5.1) was obtained, which represents SL yield (Y, g g<sup>-1</sup>DM) as a function of the coded aeration rate (A) and the substrate ratio MOL:WOC (S):

$$Y = 0.07 + 0.01A + 4.79 \cdot 10^{-3}S - 5.70 \cdot 10^{-3}A^2 - 6.66 \cdot 10^{-3}S^2 + 0.01AS \quad (\text{Eq. 5.1})$$



The quadratic model was found to be significant with a F value of 24.12 ( $p < 0.001$ ) obtained by Fisher's F-test (Table 5.4). The goodness of fit of the model was checked by the determination coefficient ( $R^2$ ). The  $R^2$  value of 0.9526 suggests a good correlation between the experimental and the predicted values, and indicates that 95.26% of the total variability in SL yield could be explained by the proposed model. The predicted  $R^2$  of 0.7880 is in reasonable agreement with the adjusted  $R^2$  of 0.9131, which was found to be very close to  $R^2$ . Lack of fit was found to be non-significant ( $p = 0.6890$ ) which indicates that Equation 5.1 is adequate to predict SL yield under any set of combinations of the studied variables in the studied range.

**Table 5.4.** Analysis of variance of the fitted model obtained from the CCD for optimal SL yield ( $\text{g g}^{-1}\text{DM}$ ).

Source	Sum of squares	Degrees of freedom	Mean squares	F-value	$p$ -value	
Model	$1.60 \cdot 10^3$	6	$3.198 \cdot 10^{-4}$	24.12	0.0007	*
A	$7.36 \cdot 10^{-4}$	1	$7.365 \cdot 10^{-4}$	55.54	0.0003	*
S	$1.38 \cdot 10^{-4}$	1	$1.375 \cdot 10^{-4}$	10.37	0.0181	*
A <sup>2</sup>	$8.65 \cdot 10^{-5}$	1	$8.655 \cdot 10^{-5}$	6.53	0.0432	*
S <sup>2</sup>	$1.18 \cdot 10^{-4}$	1	$1.183 \cdot 10^{-4}$	8.92	0.0244	*
AS	$4.19 \cdot 10^{-4}$	1	$4.188 \cdot 10^{-4}$	31.58	0.0014	*
Residual	$7.96 \cdot 10^{-5}$	10	$1.326 \cdot 10^{-5}$			
Lack of fit	$2.78 \cdot 10^{-5}$	6	$9.262 \cdot 10^{-6}$	0.54	0.6890	NS
Pure error	$5.18 \cdot 10^{-5}$	4	$1.726 \cdot 10^{-5}$			
Total	$1.68 \cdot 10^{-3}$	16				

$R^2$ : 0.9526; adj  $R^2$ : 0.9131; pre  $R^2$ : 0.7780; C.V.: 5.83; adequate precision: 16.55.

\*Statistically significant (95% confident interval).

NS=Statistically not significant (95% confident interval).

Significance of the model terms in Equation 5.1 was checked by their  $p$  values. In this experiment, coefficients of linear terms A and S and quadratic terms  $A^2$  and  $S^2$  were significant ( $p < 0.05$ ), indicating that the two studied variables greatly influence the production of SLs by SSF (Table 5.4). The high F value of term A (ratio MOL:WOC) indicates that SL yield was highly influenced by this variable. Cross terms AS was also significant ( $p < 0.05$ ), which highlights a significant interaction effect between the studied variables. Figure 5.3 shows the response surface obtained from Equation 5.1. As can be observed, increasing both the aeration rate and the ratio of substrates had a positive effect on the SL yield.

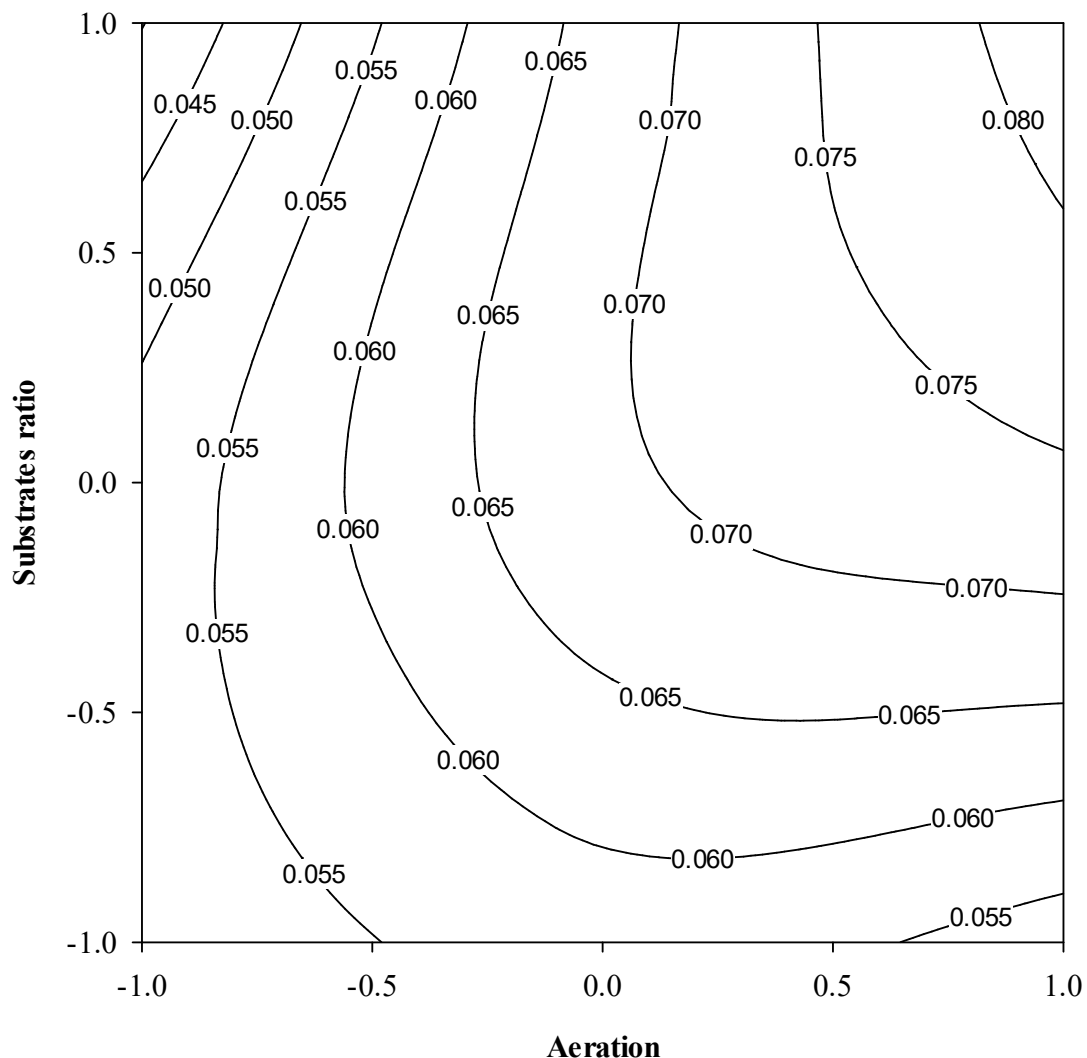


**Figure 5.3.** Response surface for SL yield ( $\text{g g}^{-1}\text{DM}$ ) obtained at different aeration rates: 0.05 (-), 0.175 (0) and 0.30 (1)  $\text{L air kg}^{-1} \text{min}^{-1}$ ; at the different ratio of substrates: 1:2 (-), 1:3 (0) and 1:4 (1) MOL:WOC.

The fitted regression model (Equation 5.1) was solved for maximum SL yield and the optimum level for each variable was found to be 1 and 1 in coded values, which corresponds with a ratio of substrates 1:4 and an aeration rate of  $0.30 \text{ L kg}^{-1} \text{ min}^{-1}$ . Under these optimum conditions predicted SL yield is  $0.082 \text{ g g}^{-1} \text{ DM}$ . The optimal ratio of substrates was 1:4, the one with the highest amount of fats and the lowest amount of sugars (Table 5.2). This suggests that fats are the key substrate for SL production in this process. Higher ratios of substrates MOL:WOC were not studied to avoid potential problems of porosity and compaction due to reduced particle size of the solid substrates. Compaction would hinder oxygen transfer in the solid mixture.

As mentioned, the optimal aeration rate was the highest studied,  $0.30 \text{ L kg}^{-1} \text{ min}^{-1}$ , confirming oxygen supply as an important parameter for this SSF. This value fell in the limit of the selected experimental range. Additional experiments repeating the aeration rate of  $0.30 \text{ L kg}^{-1} \text{ min}^{-1}$  and using higher aeration rates of  $0.60$  and  $0.90 \text{ L kg}^{-1} \text{ min}^{-1}$  were performed at a fixed 1:4 substrate ratio to check if a further increase in the aeration rate would improve SL production. However, there were no significant differences in the SL yield and COC among the three different airflows according to Duncan's test (Figure 5.4).

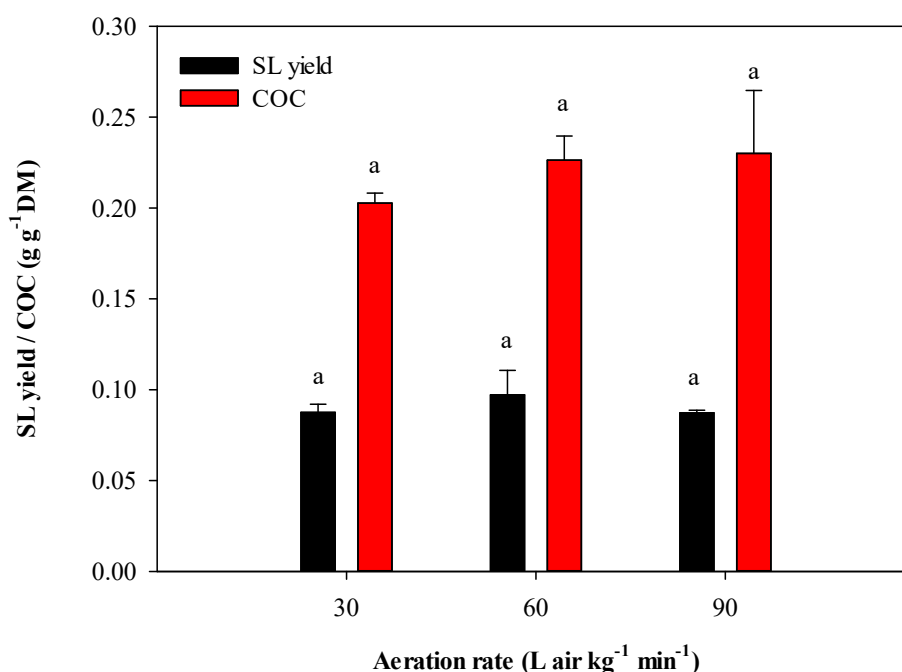


**Figure 5.4.** SL yield and COC values obtained with aeration rates of 30, 60 and  $90 \text{ L air kg}^{-1} \text{ min}^{-1}$ . Results are expressed as mean  $\pm$  standard deviation of three replicates. Means with the same letters are statistically equal according to Duncan's test ( $p < 0.05$ ).

As demonstrated by Almeida et al. (2015) and Mejias et al. (2017), low airflows can limit the biological activity, but increasing aeration over a given threshold does not further affect the fermentation. Therefore, an aeration rate of  $0.30 \text{ L kg}^{-1} \text{ min}^{-1}$  was selected for further experiments to avoid unnecessary energy costs.

### 5.3.2. Effect of inoculum size and sterilization

The inoculum size and sterilization of the fermentation mixture greatly affect the total costs of a SSF process, and therefore, the final price of the bioproduct. Both factors were evaluated in this section.

#### Experiments

Reactors were prepared under the previously optimized conditions, namely a 1:4 MOL:WOC mass ratio and an aeration rate of  $0.30 \text{ L kg}^{-1} \text{ min}^{-1}$ . Sterilization effect was evaluated by inoculating a non-sterilized SSF mixture with a 10% (v/w) of inoculum. The SSF mixture was prepared right before inoculation to minimize contamination. A reactor with a sterilized SSF mixture was used as control. Reactors were sampled at day 7.

Reactors with different percentage of inoculum (2, 6, 10 and 14% v/w) were prepared varying the amount of inoculum and distilled water to maintain the same water content (50%) of the SSF mixture. Thus, 48, 44, 40 and 36 mL of distilled water were used in fermentations using 2, 6, 10 and 14 mL of inoculum, respectively. Reactors prepared in triplicates were sampled at day 7. Results were analysed by one-way ANOVA followed by Duncan's test ( $p < 0.05$  confidence level) using SPSS 15.0 software for Windows.

#### Process dynamics

SL yield decreased around a 65% when SSF mixture was not sterilized (Figure 5.5A). An economical balance should be performed to assess if cheapen the process by non-sterilizing the SSF mixture offsets with the decrement in the production of SLs. Nevertheless, sterilization of the SSF mixture was performed in the following experiments.

The effect of inoculum size on SL yield is illustrated in Figure 5.5B. Inoculum sizes of 10 and 14% (v/w) resulted in the highest yields ( $\text{g g}^{-1}\text{DM}$ ), with no significant differences between both inoculum sizes based on Duncan's test ( $p < 0.05$ ). For practical and economic reasons, we selected an inoculum size of 10% (v/w) for the following experiments.

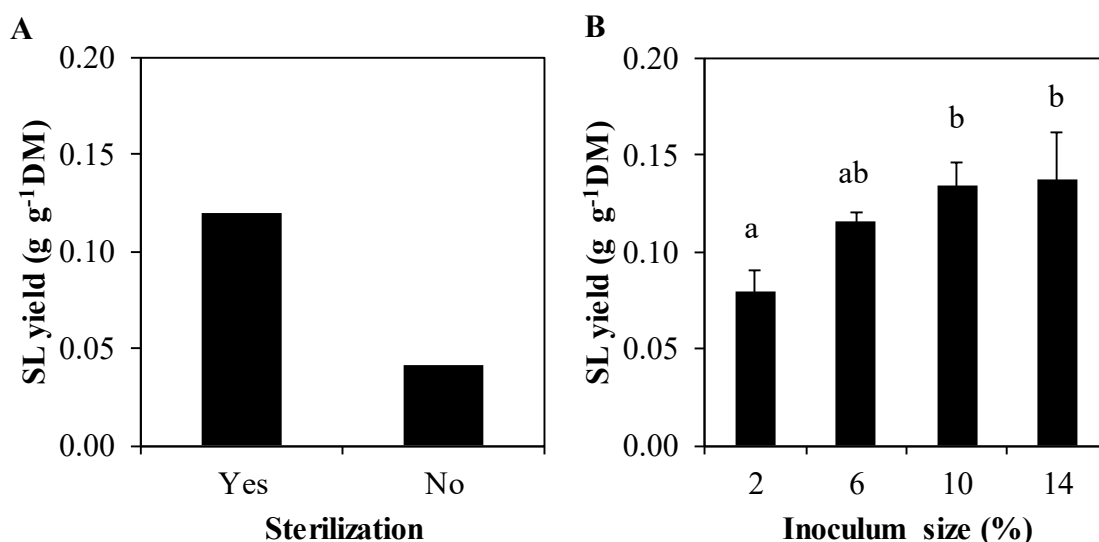


**Figure 5.5.** SL yield values obtained with and without sterilization of the SSF mixture (A) and sterilized with inoculum sizes of 2, 6, 10 and 14 % (v/p). This last are expressed as mean  $\pm$  standard deviation of three replicates. Means with the same letters are statistically equal according to Duncan's test ( $p < 0.05$ ).

### 5.3.3. Monitoring SL production under optimized conditions

The optimized SSF process was monitored for 10 days under the optimized conditions, namely a 1:4 MOL:WOC mass ratio, an aeration rate of  $0.30 \text{ L kg}^{-1} \text{ min}^{-1}$ , and an inoculum size of 10% (v/w), so as to determine the time course of SL production.

### Experiments

Six reactors were prepared and one of the reactors was sacrificed for analysis at each of the sampling points (0, 2, 4, 6, 8 and 10 days). Three consecutive extractions were performed to evaluate the efficiency of the extraction method used for SL determination.

## Process dynamics

Figure 5.6 shows the results of the OUR and COC curves and the time course of SL yield and sugar and fat content during the 10 days of fermentation. Substantial SL formation occurred by day 2 ( $0.017 \text{ g g}^{-1}\text{DM}$ ). SL yield at day 4 and day 6 was  $0.073$  and  $0.130 \text{ g g}^{-1}\text{DM}$  respectively, which agrees with the SL yield of  $0.082 \text{ g g}^{-1}\text{DM}$  predicted for day 5 according to the previous optimization. The maximum yield of  $0.172 \text{ g g}^{-1}\text{DM}$  was reached on day 8, which corresponds to  $0.191 \text{ g g}^{-1}$  of wet substrates. This yield is 60% higher than the value obtained previously in Chapter 4 (section 4.3.3), which was obtained in a first screening of this SSF process and prior to the process optimization. OUR reached its maximum value after almost 3 days ( $1.64 \pm 0.20 \text{ mg O}_2 \text{ g}^{-1}\text{DM h}^{-1}$ , average  $\pm$  standard deviation for 4 fermentations), and the oxygen consumed at the end of the fermentation was  $0.370 \text{ g O}_2 \text{ g}^{-1}\text{DM}$ .

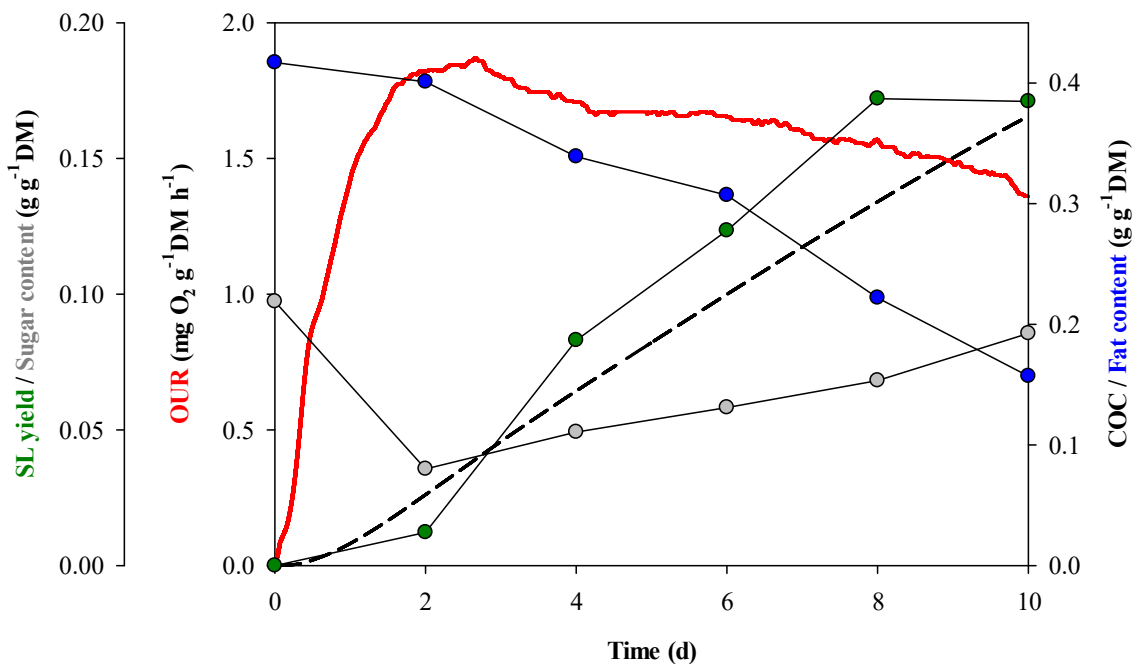


**Figure 5.6.** SSF profile of the process: OUR and COC profiles and time course of SL yield and sugar and fat content.

Figure 5.6 also shows the profile of sugar and fat content expressed as grams per gram of total dry matter in the fermentation medium. Fat content was gradually degraded and around 60% of the initial fats were consumed at the end of the fermentation. In contrast with the observed for the fat content profile, the sugar content

profile does not show a clear trend. As illustrated in Figure 5.6 two third parts of the sugar content were consumed during the first 2 days of fermentation. After that point, it seems that sugar content slightly increases with the time course of the fermentation, which apparently makes no sense. In the previous experiment carried out using glucose as the hydrophilic carbon source of the synthesis (Chapter 4, section 4.3.1) we observed that glucose was consumed in a 75% during the first 2 days of fermentation, which agrees with the observed in this experiment. However, in that case glucose was almost depleted at day 4, remaining below the 4% for the rest of the fermentation (Figure 4.7). It should be noticed that in this experiment we are measuring total sugars with the anthrone method and not only glucose with YSIS as previously done (Chapter 3, section 3.5).

Two hypothesis arise to explain the increase of the sugar. The first one points to a liberation of sugars from the wheat straw during the fermentation favoured by the moisture and the biological activity of the SSF mixture. Sugar content in the wheat straw was determined to be 2.18% db (Table 5.1). The second hypothesis is that the SLs produced are extracted to the aqueous extraction carried out for the sugar determination by the anthrone method (Chapter 3, section 3.5.5). Therefore, the sophoroses of the SLs produced are quantified as sugars. It has been reported in the literature that the anthrone method can be used as an indirect method for the quantification of SLs (Hu and Ju, 2001; Solaiman et al., 2004). Both hypothesis might be contributing to this observation. In conclusion, the measurement of the sugar content of this SSF mixture by the anthrone method cannot be used as a tool to monitor the consumption of the sugar beet molasses throughout the fermentation.

The pH dropped from an initial value of 6.4 to a value of 3.6 at day 10 of fermentation. As also observed in Chapter 4, the production of SLs is associated with a pH decrement of the SSF mixture. The water content remained at values of approximately 48% wet basis during the whole process.

### **Efficiency of the SL extraction methodology**

Three consecutive extractions were performed and quantified at each sampling point to assess the efficiency of the extraction method used for SL determination. Figure 5.7 shows the fraction of SLs extracted in each of the three extractions at each of the

sampling points along the time course of the fermentation. On average, 77% of SL yield was extracted in the first extraction, 18% in the second one, and a 5% in the last one. This results are practically identical to those obtained in the previous chapter where 78, 17 and 5% were obtained in the first, second and third extraction, respectively. In that case, SLs were produced in a different SSF mixture based on glucose and oleic acid blended with wheat bran (Chapter 4, section 4.3.1).

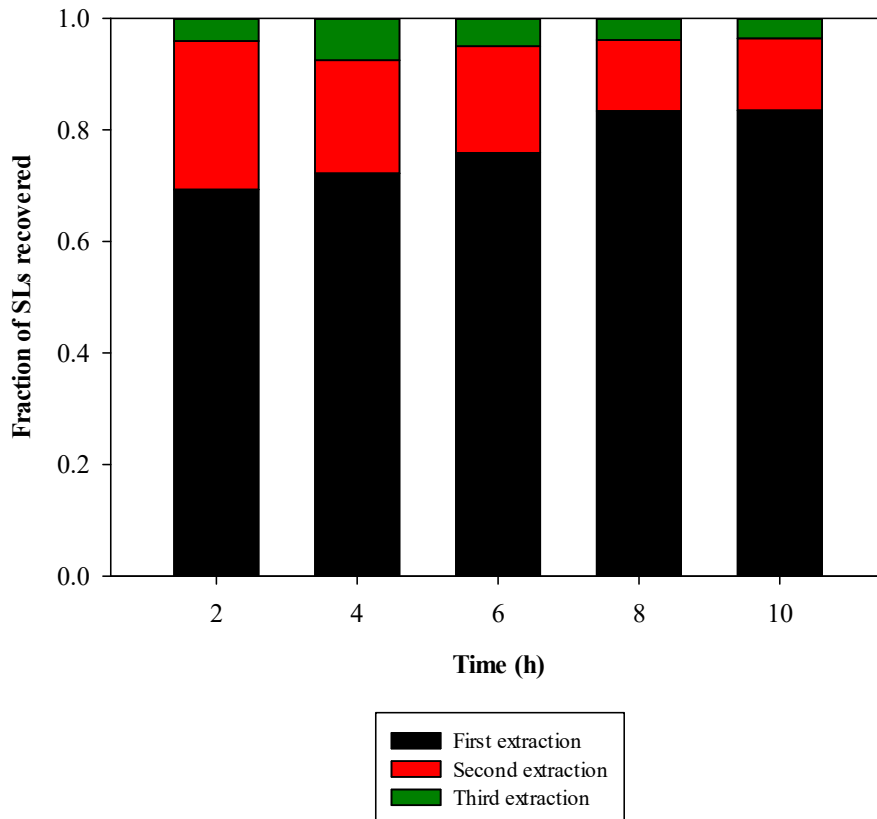


**Figure 5.7.** Fraction of SLs extracted in each of the three extractions performed at each sampling point of the time course.

As also observed in Chapter 4, a linear correlation is obtained when fat content ( $\text{g g}^{-1}\text{DM}$ ) is plotted vs. the fraction of SLs recovered of the first extraction (Figure 5.8). This correlation indicates that efficiency of the first extraction is highly dependent of the fat content of the SSF mixture: the lower the fat content, the higher recovery in the first extraction. According to the regression curve obtained ( $y = -0.647x + 0.953$ ), in a hypothetical SFF mixture without fat content, up to 95% of the SLs would be extracted in the first extraction. This value is also in agreement with the obtained in the previous chapter (Chapter 4, section 4.3.1).



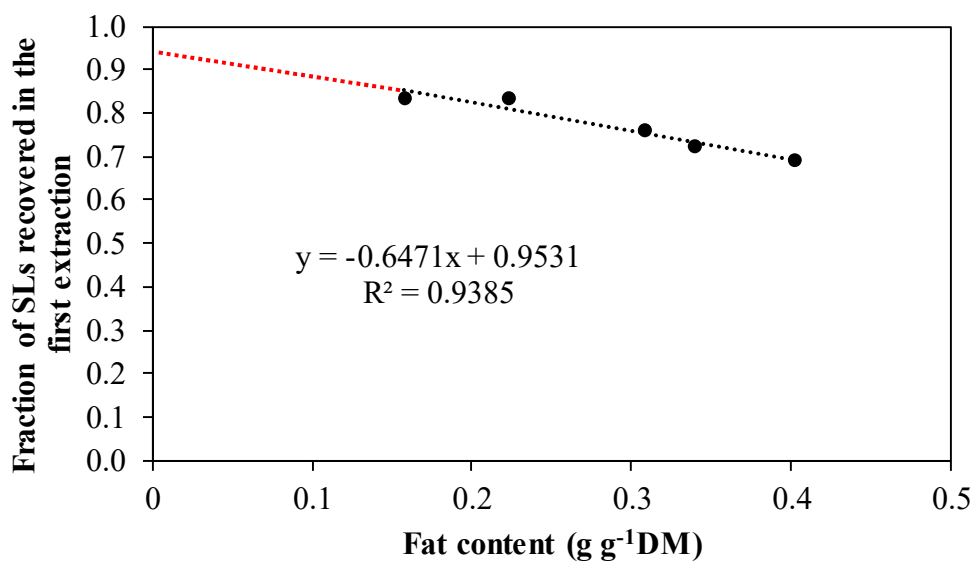


**Figure 5.8.** Fat content (g g<sup>-1</sup>DM) plotted vs. fraction of SLs recovered during the first extraction.

#### 5.3.4. Effect of intermittent mixing on SL production

In the previous experiment, around 40% of the fats remained in the reactor when maximum SL yield was achieved, which most probably corresponds with fats not accessible to the yeast. In this section, we explored the effect of intermittent mixing on the dynamics of this SSF process expecting to improve substrate bioavailability and reduce nutrients and biomass composition gradients in the solid mass (Berthe et al., 2007), and to increase the production of SLs.

#### Experiments

Two processes were performed using the optimized conditions (1:4 MOL:WOC ratio, aeration rate 0.30 L kg<sup>-1</sup> min<sup>-1</sup>, 10% (v/p) inoculum size): one static fermentation for 10 days and one fermentation with intermittent mixing for 14 days. Reactors at static conditions were sampled at days 3, 5, 7 and 10. Reactor under mixing conditions were manually mixed at days 3, 5, 7, 10 and 12. For mixing, the whole content of a flask was discharged into a 1-L glass beaker, carefully mixed with a sterile metal spatula in a laminar flow chamber, and loaded again into the Erlenmeyer flask. One reactor was sacrificed, after mixing, at each of days 5, 7, 10, 12 and 14. The process with mixing was monitored for longer time because an increase in SL production and a higher fat and oxygen consumption was expected.

### Process dynamics

Figure 5.9 shows OUR profiles of the different replicates of fermentations carried out at static and mixing conditions. OUR reached its first maximum value after almost 3 days ( $1.80 \pm 0.05 \text{ mg O}_2 \text{ g}^{-1}\text{DM h}^{-1}$ , average  $\pm$  standard deviation for 9 fermentations). The low variability ( $< 3\%$ ) between replicates is an indicator of the excellent reproducibility of the experimental data. Mixing increased the OUR, and the global maximum for fermentations at mixing conditions was reached at 7 days with a value of  $1.93 \pm 0.11 \text{ mg O}_2 \text{ g}^{-1}\text{DM h}^{-1}$  (average  $\pm$  standard deviation for 4 fermentations) (Figure 5.8). Variability between mixed replicates was below the 6%.

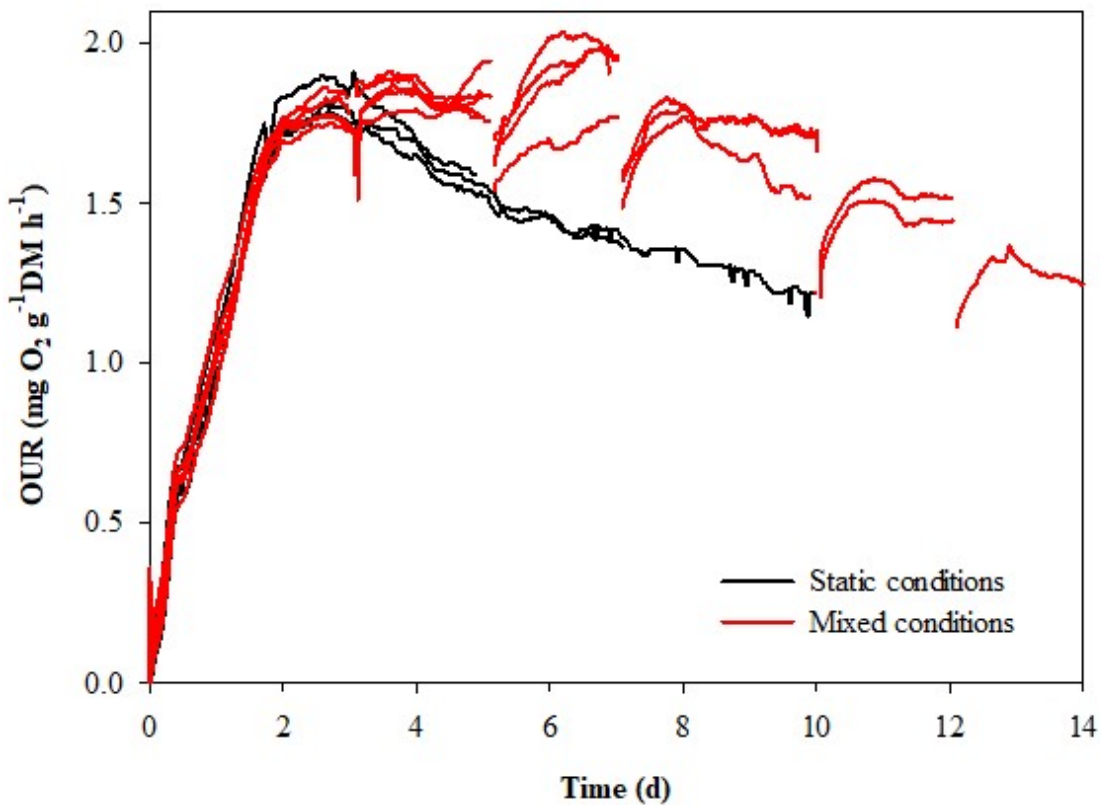


**Figure 5.9.** OUR profiles of the different replicates of fermentations at static and mixing conditions.

Mixing increased the maximum SL yield by 31% compared with fermentation under static conditions, with a total production at day 10 of  $0.235 \text{ g g}^{-1}\text{DM}$ , which corresponds to  $0.261 \text{ g g}^{-1}$  of wet substrates (Figure 5.10). It seems that SL yield slightly

decreases after day 10 of fermentation. However, the deviation between SL yield values at days 10, 12 and 14 is below the 5%, which is within the OUR deviation obtained between replicates for mixed reactors. It means that SLs are not being consumed or degraded but they remain in the solid mixture. By day 10, 22% more fats had been consumed in the mixed fermentation than in the static fermentation (Figure 5.10). This confirms that part of the fats remained in the reactor at the end of the fermentation under static conditions were not accessible for the yeast. The remaining of fats may correspond with waxes or fatty acids provided by the WOC that are not feasible for SL synthesis (Annex I).

The oxygen consumed at day 10, when maximum SL yield was obtained, was 0.330 g O<sub>2</sub> g<sup>-1</sup>DM for static reactors (Figure 5.10A), and 0.386 ± 0.006 g O<sub>2</sub> g<sup>-1</sup>DM (average ± standard deviation for 3 fermentations) for mixed reactors (Figure 5.10B). It means that oxygen consumption was 17% higher in mixed fermentations than in the non-mixed fermentations, indicating a higher biological activity when intermittent mixing is performed.

At both static and mixing conditions, pH dropped from an initial value of 6.4 to values between 3 and 3.5 after day 5. The water content remained at values of approximately 48% wet basis during the whole process, which again confirms the effectiveness of the use of humidified air in the control of the fermentation moisture.

We observed differences in the solid matrix between the mixed and the static conditions. Intermittent mixing reduced the size of the solid aggregates. From these observations, we concluded that intermittent mixing increases the bioavailability of substrates to the yeast and, therefore, more oxygen and fats are consumed and more SLs are produced. The positive effect of intermittent mixing on the biological activity of solid-state processes has been previously described (Berthe et al., 2007). These findings indicate that the SSF process could be scaled up using bioreactors with mixing systems, such as rotating drums (Rodríguez-Jasso et al., 2013). These changes would not only improve the yield of SLs but would also help to reduce channelling and overheating problems that are typically found in unmixed systems (Flodman and Nouredini, 2013).

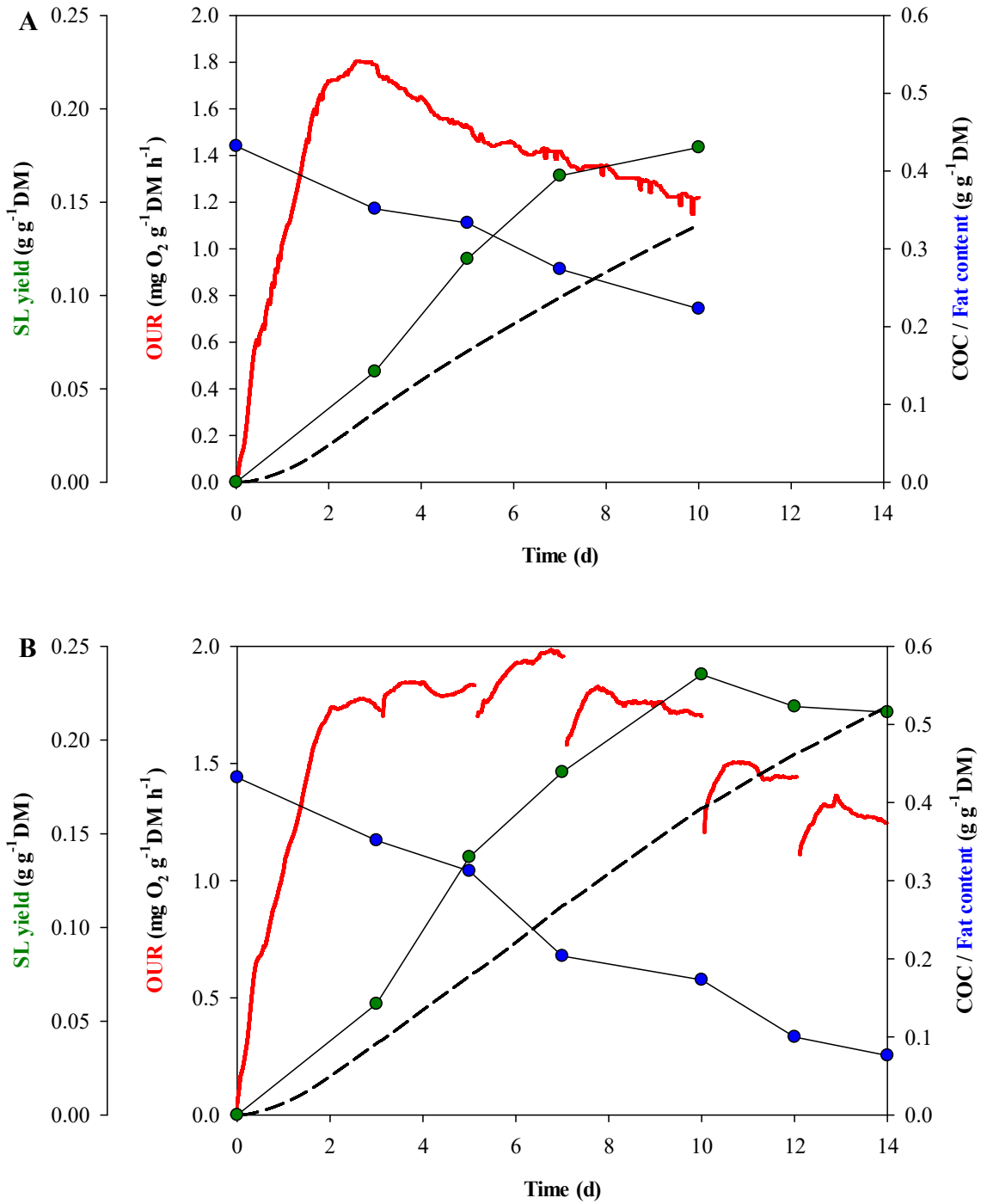


**Figure 5.10.** SSF profile of the process under static (A) and intermittently mixed (B) conditions: OUR and COC profiles and time course of SL yield and fat content.

### 5.3.5. Process monitoring variables

The monitoring of SSF processes for biosurfactant production is a challenge that must be addressed in the scale-up of such processes to commercial production scale (Krieger et al., 2010). Respiration parameters, such as OUR and COC, are useful for the monitoring of the biological activity in the fermentation medium. However, respirometry has not yet been explored to produce biosurfactant by SSF.

In order to explore the correlations between oxygen and fats consumed and SLs produced, all the experimental results reported in this chapter were compiled in the plots displayed in Figure 5.11. As illustrated in Figure 5.11A, SL yield ( $\text{g g}^{-1}\text{DM}$ ) was directly proportional to the COC ( $\text{g O}_2 \text{ g}^{-1}\text{DM}$ ), with a proportionality constant of 0.518 ( $\text{g SL per g O}_2$ ), ( $n = 47$ ,  $R^2 = 0.9545$ ,  $p < 0.001$ ). This suggests that the respiration parameter COC can be used as an indirect measurement of the production of SLs for the online monitoring of SSF. Additionally, SL yield ( $\text{g g}^{-1}\text{DM}$ ) was directly proportional to the fats consumed ( $\text{g g}^{-1}\text{DM}$ ), with a proportionality constant of 0.805 ( $\text{g SL per g fat consumed}$ ), ( $n = 35$ ,  $R^2 = 0.970$ ,  $p < 0.001$ ) (Figure 5.11B).

### 5.3.6. Process versatility

Process versatility was assessed after the optimization using WOC by using a different oil cake from the oil refining industry. Specifically, we used a bleaching oil cake (BOC), also known as spent bleaching earth, which is obtained after the discoloration of vegetable oils (Figure 5.12). We decided to carry out fermentations to test how the BOC performs as the hydrophobic carbon source of SL synthesis.

## Experiments

LIPSA (Barcelona) provided BOC having a water content of 1.3% (wet basis), an organic matter of 38.8% (dry basis) and a fat content of 28.2% (dry basis). Experiments were performed with BOC and compared to WOC, preparing both mixtures as previously described (Chapter 5, section 5.2). Given the lower fat content of BOC compared to WOC, additional experiments were undertaken to assess the influence of the ratio of substrates using 1:4, 1:8 and 1:12 MOL:BOC ratios (w/w). Reactors were sampled after 6 days of fermentation.

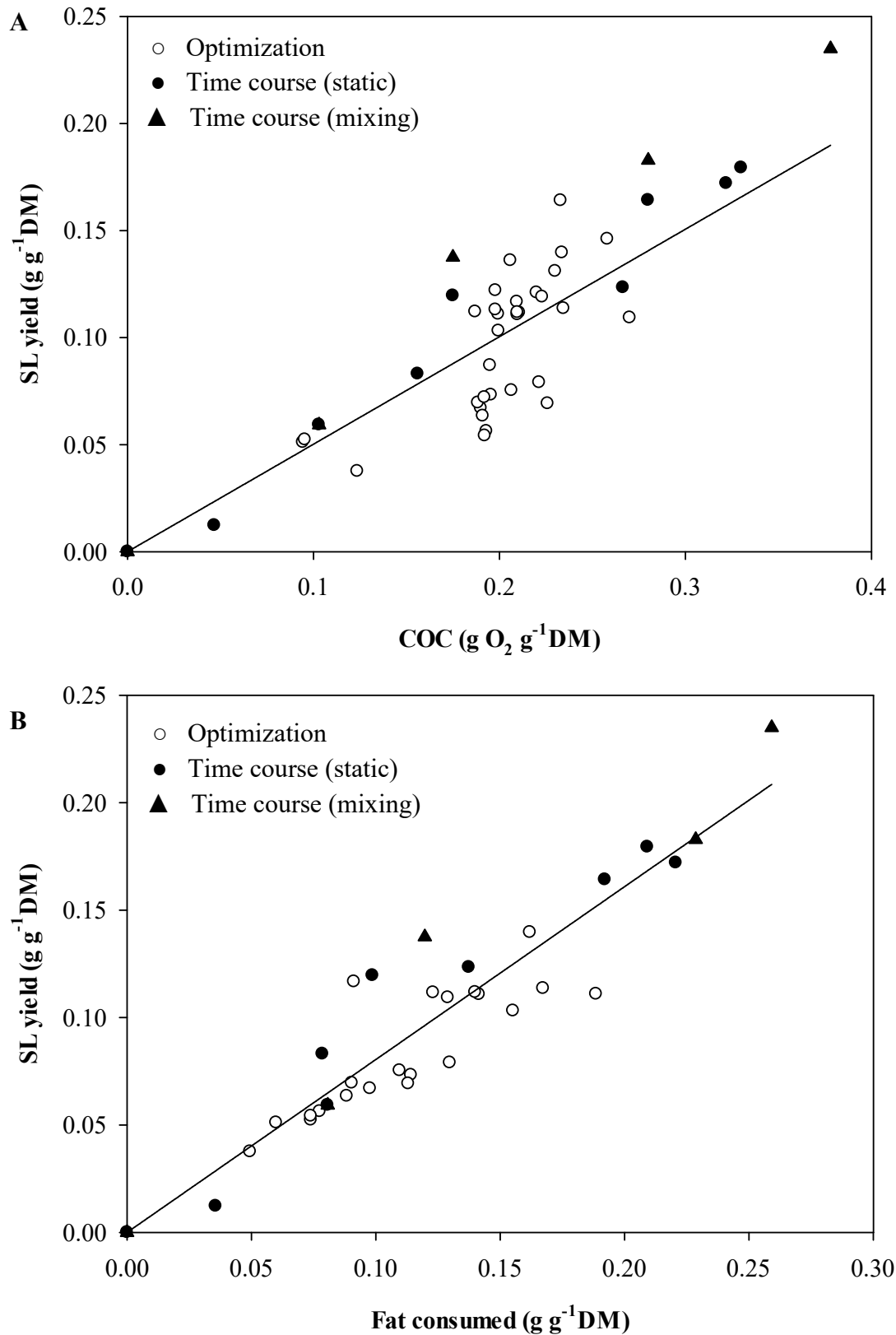


**Figure 5.11.** Correlations between SL yield vs. cumulative oxygen consumption (COC) (A) and between SL yield vs. fat consumed (B).



**Figure 5.12.** Physical appearance of the bleaching oil cake.

## Results

SL production using BOC as the hydrophobic carbon source was only 34% lower than using WOC (Figure 5.13A), which was surprising because the fat content of the BOC is 50% lower than of the WOC (Table 5.1). This suggests that there was a better bioavailability of substrates in fermentations with BOC. We observed differences between solid mixtures with WOC and BOC: fermentations with BOC did not show formation of solid aggregates as WOC did. As can be observed from Figure 5.12, BOC has thinner particles and does not show tendency to aggregate. These promising results motivated us to perform additional experiments using different ratios of MOL:BOC (w/w) increasing the ratio of BOC to check if SL yield could be improved by increasing the fat content of the SSF mixture. However, increasing the ratio of BOC decreased the SL yield (Figure 5.13B), probably because of the lower MOL content.

These results highlight the versatility of the SSF process to be used with different oil cakes from the oil refining industry. However, further optimization studies are required when changing either the hydrophobic or hydrophilic carbon source. Next chapters will focus on WOC as the hydrophobic carbon source.

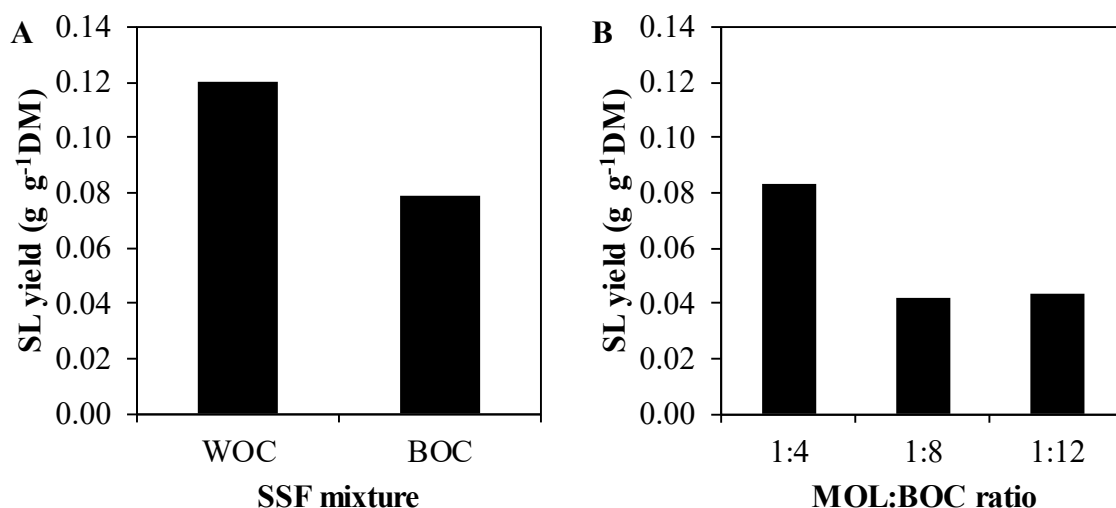


**Figure 5.13.** SL yield obtained using WOC and BOC at 1:4 MOL:OC ratio (A) and using different MOL:BOC ratios (w/w) (B).

#### 5.4. Conclusions

As demonstrated in Chapter 4, the winterization oil cake is a suitable substrate to produce sophorolipids by SSF using sugar beet molasses as co-substrate and *Starmerella bombicola* as inoculum. Optimization of the process in terms of substrate ratio (1:4 MOL:WOC), aeration rate (0.30 L kg<sup>-1</sup> min<sup>-1</sup>) and inoculum size (10% v/w) led to a 60% increment on SL yield with regards the yield obtained in Chapter 4. The sophorolipid yield at 10 days was 0.179 g g<sup>-1</sup>DM, which corresponds to 0.199 g g<sup>-1</sup> of wet substrates. Intermittent mixing (at 3, 5 and 7 days) increased SL yield 31% to 0.235 g g<sup>-1</sup>DM, which corresponds to 0.261 g g<sup>-1</sup> of wet substrates. In summary, after the experiments carried out in this chapter, the SL yield was increase in a 120% respect the preliminary results obtained in Chapter 4.

SL yield were linearly correlated with the fat content but not with the sugar content. In fact, it was observed that the anthrone method is not suitable for the measurement of the sugar content of this SSF mixture during the fermentation. SL levels were linearly correlated with the cumulative oxygen consumption, suggesting that respirometry can be a useful tool for monitoring SL production by *S. bombicola* in SSF.

Finally, the described SSF process is a promising technology to potentially valorize different oil cakes and this research could be extended to other wastes from the food and oil-refining industries.





## CHAPTER 6

---

### *Sophorolipids from winterization oil cake by SSF: scale-up*

*Part of this chapter has been presented on a conference presentation at Red Española de Compostaje Conference, 2016, Sevilla.*

*Best communication award*

*Biosurfactantes a partir de residuos del refinado de aceites por fermentación en estado sólido.*

*Jiménez-Peñalver, P., Font, X., Sánchez, T., Gea, T.*



## Summary

As demonstrated in previous chapters, the winterization oil cake and sugar beet molasses blended with wheat straw is a feasible solid mixture to produce SLs by *S. bombicola* through SSF. So far, temperature of the SSF mixtures could be well-controlled by submerging the 0.5-L scale reactors in water baths at 30 °C. However, temperature is hardly controlled at bigger scales due to the low conductivity of organic solids, which makes ineffective the use of water jackets or cooling coils. The design of large-scale bioreactors with high rates of heat removal is essential to maintain the temperature of the SSF mixture as close as possible to the optimal temperature for the microbial growth and product formation.

In this chapter, the effect of temperature in the SSF process was assessed at 0.5-L scale at values ranging from 27 to 36 °C. The results showed that SL production was negatively affected by temperatures above 30 °C. In consequence, the 40-L and 100-L bioreactors were operated with high aeration rates to favor heat removal. The scale-up to the 40-L bioreactor confirmed the robustness of the process: SLs were produced in similar yields than at lab scale with temperatures in the solid bed ranging from 25 to 36 °C and with water content gradients ranging from 35 to 60%.

However, the scale-up to the 100-L bioreactor process did not work properly, most probably due to the high temperatures over 40 °C of the solid bed and the existence of preferential air paths that hindered heat removal. Yet there are several parameters to be explored for the proper operation of the 100-L bioreactor such as the agitation regime, the airflow rate, or the humidity and temperature of the inlet air.

## 6.1. Materials

The materials used were sugar beet molasses (MOL), winterization oil cake (WOC), and wheat straw from the experimental farms at Universitat Autònoma de Barcelona (UAB). Main characteristics of MOL and WOC are detailed in Table 6.1. More information about these materials can be found in Chapter 3, section 3.1.1.

**Table 6.1:** Main characteristics of the substrates and the initial mixture.

	Substrates		Initial mixture
	Sugar Beet Molasses	Winterization Oil Cake	
pH	7.40±0.02	4.75±0.01	6.56 ± 0.01
Water content (%)	11.6±1.0	0	47.7 ± 0.8
Organic matter (% db)	74.2±0.8	60.4±0.9	80.7 ± 1.1
Fat content (% db)	n.d.	<b>59.0±0.7</b>	<b>38.4 ± 0.6</b>
Sugar content (% db)	<b>76.1±7.2</b>	n.a.	<b>11.1 ± 0.4</b>
Nitrogen content (% db)	<b>1.89±0.01</b>	n.d.	n.a.

*Abbreviations:* db, dry basis; n.d., not detected; n.a., not analysed. Data presented as mean ± standard deviation of the sample.

## 6.2. Experiments

Fermentations were carried out, unless otherwise indicated, with the optimized parameters of Chapter 5, namely: 1:4 MOL:WOC ratio (w/w), an aeration rate of 0.30 L kg<sup>-1</sup> total wet mass min<sup>-1</sup>, and an inoculum size of 10% (v/w). Solid mixtures at 0.5-L scale were prepared as previously described (Chapter 5, section 5.2). Solid mixtures for the experiments in the 40-L and 100-L bioreactors were prepared in batches of 2,000 g. First, 720 g of WOC and 280 g of wheat straw were weighted. Then, 180 g of MOL were dissolved in 800 mL of water and the solution was added to the mixture of WOC and wheat bran. The solid mixture was homogenized, introduced in a bag for sterilization, and sterilized (121 °C, 30 min) (Figure 6.1). Main characteristics of one of the initial solid mixtures prepared in this chapter is shown in Table 5.1. Similar values were obtained for the rest of the batches (data not show). These values were similar to the ones reported in Table 5.1 for the initial mixture with 1:4 MOL:WOC ratio (w/w) (Chapter 5, section 5.1).

The oxygen concentration in the exhaust gases was recorded and used for the calculation of the OUR and the COC (Chapter 3, section 3.3). pH, water content, fat content and SL yield were measured on samples according with the methodology described in Chapter 3, section 3.4 and 3.5.



**Figure 6.1.** Pictures of the SSF mixture (left) and the sterilized bags (right).

## 6.3. Results and discussion

### 6.3.1. Effect of temperature on SL production

The aim of this study was to evaluate the effect of temperature on the production of SLs and on the respiration parameter COC.

#### Experiments

Fermentation experiments were performed at lab scale in 0.5-L Erlenmeyer flasks in the Fermentation System I (Chapter 3, section 3.2.1). Fermentations were run at 30 °C for 24 h to allow the proper growth of the inoculum. Then, the temperature of the water baths was adjusted at 27, 30, 33 and 36 °C and the fermentation continued for 4 days more. The experiments were performed in triplicates. Results were analysed by one-way ANOVA followed by Duncan's test ( $p < 0.05$  confidence level) using SPSS 15.0 software for Windows.

#### Results

As shown in Figure 6.2, there were no significant differences in the SL yield among temperatures of 27 and 30 °C according to Duncan's test ( $p < 0.05$ ). These results are in agreement with those reported by Casas and García-Ochoa (1999), who found no significant differences in the SL yield obtained by SmF at 25 and 30 °C. In fact, optimal temperature for SL production was set at 21 °C (Göbbert et al., 1984), but most of the fermentations are performed at 25 or 30 °C for practical reasons (Van Bogaert et al.,

2011b). These results indicate that SL production is not hindered in a range of temperature of at 21 – 30 °C and, therefore, it could be considered to run SSFs at room temperature.

Significant differences were observed among temperatures of 30, 33 and 36 °C according to Duncan's test ( $p < 0.05$ ), showing that temperatures above 30 °C have a negative effect on the production of SLs (Figure 6.2). SL yield decreased around 65 and 80% when temperature was increased to 33 and 36 °C, respectively. These results confirm that heat removal should be considered as a critical parameter to be addressed for the scale-up of this SSF process to avoid a decrease in the SL production.

Although SL yield is greatly affected by the increase of temperature, no significant differences were observed in COC values according to Duncan's test (Figure 6.2). This suggests that an increase in temperature stresses the yeast and leads to changes in the metabolism.

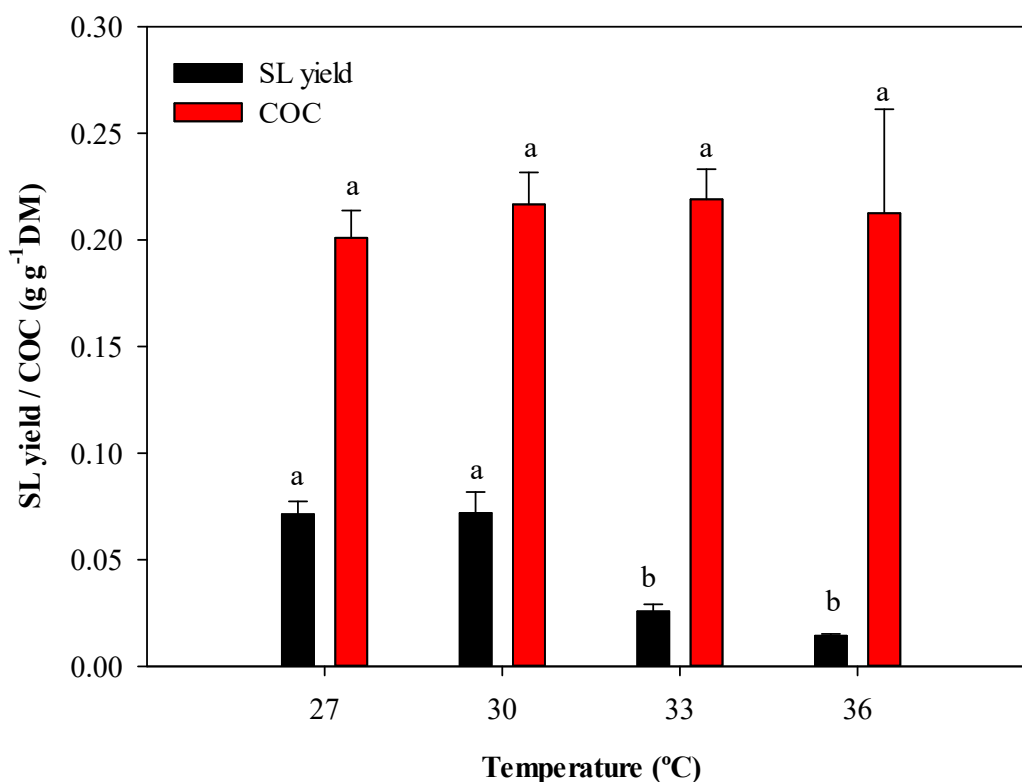


**Figure 6.2.** SL yield and COC obtained at temperatures of 27, 30, 33 and 36 °C. Results are expressed as mean  $\pm$  standard deviation of three replicates. Means with the same letters are statistically equal according to Duncan's Test ( $p < 0.05$ ).

### 6.3.2. Scale-up to the 40-L bioreactor

The SSF was scaled-up to the 40-L bioreactor with 3 trays to study the process in terms of temperature dynamics, effectiveness of high aeration rates for heat removal, water content gradients and resistance to contamination. The configuration of this bioreactor is not useful for large-scale processes but it can provide useful information about heat and mass transfer dynamics of our fermentation process.

#### Experiments

The experiments carried out in this section were performed in the 40-L bioreactor with 3 trays in the Fermentation System II (Chapter 3, section 3.2.2). Firstly, the bioreactor was copiously cleaned with bleach and, right before the beginning of the experiment, the trays were cleaned with ethanol (70%). 2,000 g of sterilized solid mixture were discharged in each tray and subsequently inoculated with fresh inoculum. This process was performed as quickly as possible to minimize the risk of contamination. Figure 6.3 illustrates some pictures of the 40-L bioreactor after inoculation.

The fermentation process with a total of 6,000 g of solid mixture was monitored for 12 days. The solid mixture of each tray was manually mixed every 2 days. Samples (30 - 40 g per tray) were taken after mixing for analysis. Temperature was on-line monitored using temperature sensors at the central point of each tray ( $r = 0$  cm). Temperature was also measured at a radius of 10 and 20 cm prior each mixing. Aeration rate of  $0.30 \text{ L air kg}^{-1} \text{ min}^{-1}$  was provided during the first 24 h. Then, the aeration rate was increased to  $0.90 \text{ L air kg}^{-1} \text{ total wet mass min}^{-1}$  to favor heat removal. Previous experiments demonstrated that SL production is not hindered by increasing the aeration rate to this value (Chapter 5, section 5.3.1). The respirometer parameters OUR and COC could not be properly calculated since the bioreactor is not completely airtight. The oxygen level was checked daily and it was confirmed that the high aeration rate provided oxygen in excess for the fermentation.

A preliminary experiment charging only one tray was done to confirm the suitability of this equipment (data not shown).





**Figure 6.3.** Pictures of the 40-L packed-bed bioreactor filled with a solid mixture based on winterization oil cake and sugar beet molasses blended with wheat straw.

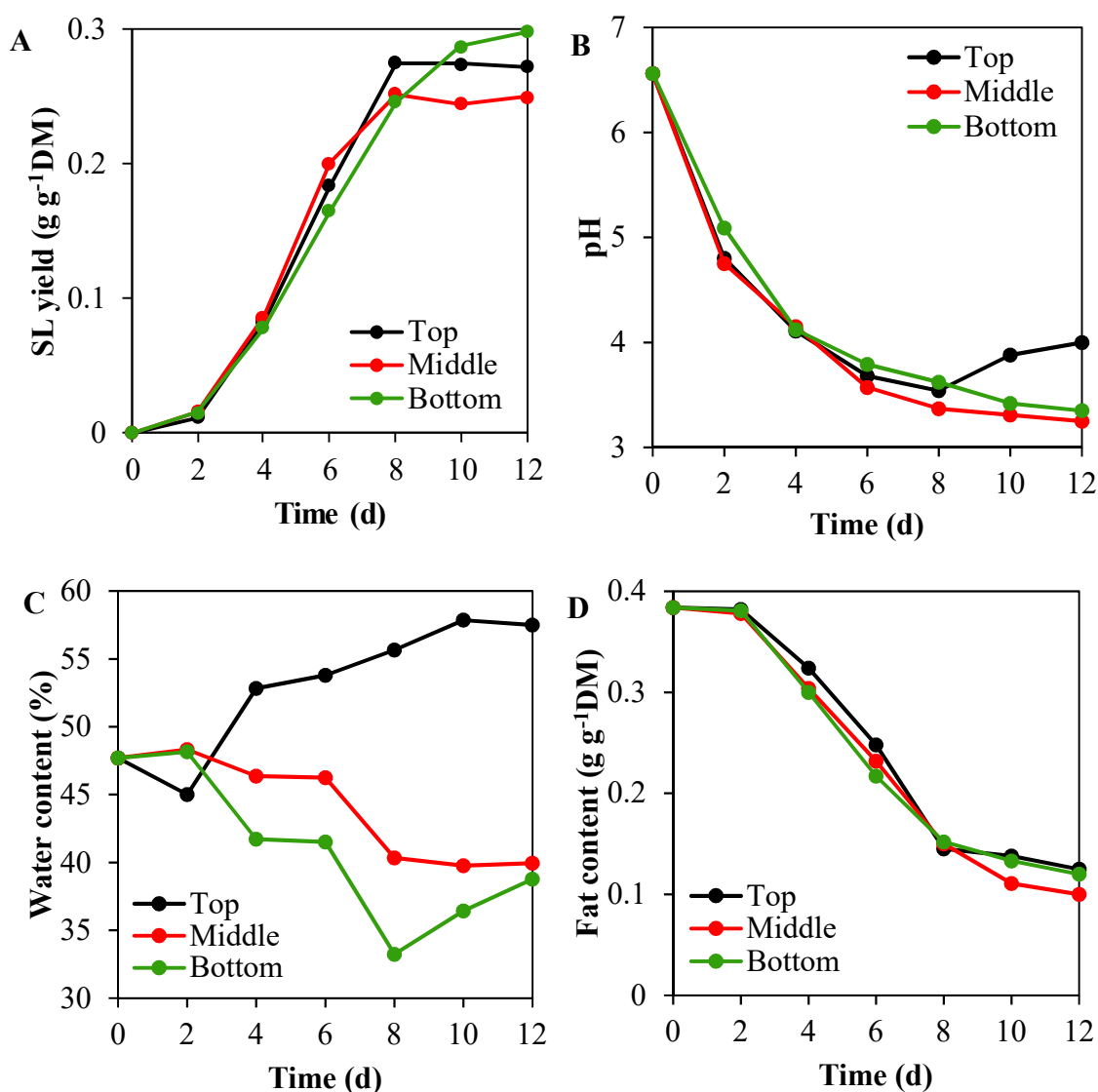
### Process dynamics

Figure 6.4 shows the time course of SL yield, pH, water content and fat content in each tray of the bioreactor during the 12 days of fermentation. The maximum SL yield was reached on day 8 of fermentation, with  $0.258 \pm 0.016$  g SLs  $g^{-1}$ DM, which corresponds to  $0.330 \pm 0.075$  g  $g^{-1}$  of substrates (Figure 6.4A). This yield is similar to that obtained at 0.5-L scale (Chapter 5, section 5.3.4).

The three trays showed similar pH profiles: pH dropped from an initial value of 6.56 to values between 3 and 4 after day 6 (Figure 6.4B). In contrast, the water content profiles were different for each tray (Figure 6.4C). While the water content in the bottom and middle trays decreased from an initial value of 48% to values around 40%, the top tray increased its water content to values close to 60%. This is a consequence of the high aeration rates, which affect the water content of the SSF mixture in the reactor creating gradients across the solid mixture (Mitchell et al., 2006). The water content removed from the bottom and middle trays condensate on the lid of the bioreactor and fell into the top tray. However, these gradients did not affect the process negatively, as can be deduced from the very similar profiles of SL yield (Figure 6.4A). Parekh and Pandit (2012) reported that SL production is optimum in a range of water content between 40 and 80% in a SSF mixture based on oleic acid and glucose blended with wheat bran.

As observed in Figure 6.4D, around 75% of the initial fats were consumed at the end of the fermentation. Fats consumed ( $g$   $g^{-1}$ DM) correlated linearly with SL yield ( $g$

$\text{g}^{-1}\text{DM}$ ), with a proportionally constant of 1.086 ( $\text{g SL per g fat consumed}$ ) ( $n = 20$ ,  $R^2 = 0.988$ ,  $p < 0.001$ ) (Figure 6.5). This plot was built using the data from Figure 6.4D plus the preliminary experiment performed with only one tray. The correlation constant obtained at 40-L scale is slightly higher than the obtained for all the experiments at 0.5-L scale (0.805). This suggests that there is a better conversion of fats into SLs in this equipment, most probably due to the frequent mixings.



**Figure 6.4.** Time course of SL yield (A), pH (B), water content (C) and fat content (D) in the different trays of the 40-L bioreactor.

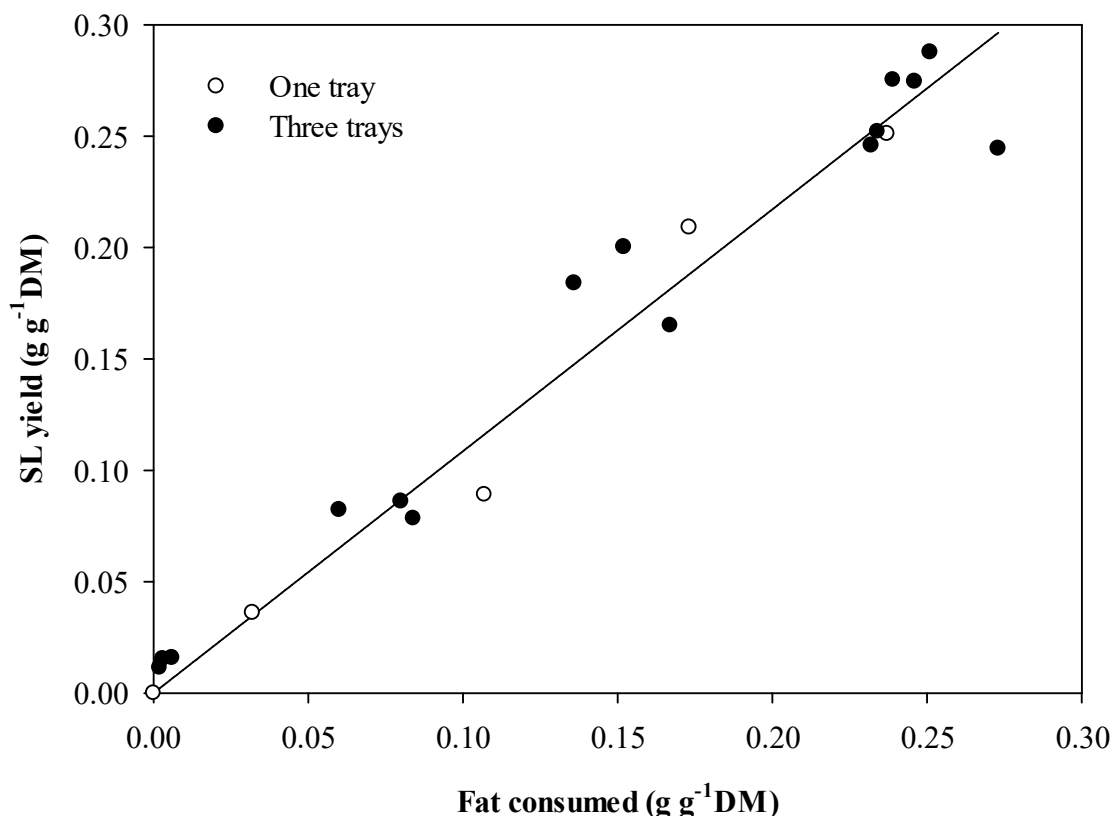


**Figure 6.5.** Correlations between SL yield and fat consumed.

Temperature dynamics, together with the excellent SL yields, were the most interesting data of this experiment. As can be observed in Figure 6.6, temperature increased rapidly during the first 2 days of SSF. It is well-known that SSF processes are associated with a temperature increase of the solid matrix due to the metabolism of the microorganisms. The yeast *S. bombicola* colonized the solid mixture during this period, as deduced from the exponential growth of the OUR curves in the experiments at 0.5-L scale (Figure 5.9). Temperatures increased after mixing as a consequence of the improvement of the substrates bioavailability to the yeast and, therefore, its metabolism.

As expected, temperature values (higher to lower) followed: middle > top > bottom. It makes sense considering that the top and the bottom trays hamper the heat removal from the middle tray. Temperature gradients were found not only between trays, but also axial gradients of temperature up to 3 °C were observed in the same tray (Figure 6.7). Temperatures above 30 °C were recorded, but SL yield was not affected, contrary to what would be expected according to the results obtained at 0.5-L scale for different

temperatures. This confirms the robustness of the process and the ability of *S. bombicola* to thrive on these somehow adverse conditions of the dynamic process: SLs were produced in similar yields than at 0.5-L scale with temperatures in the solid bed ranging from 25 to 36 °C and with water content gradients ranging from 35 to 60%.

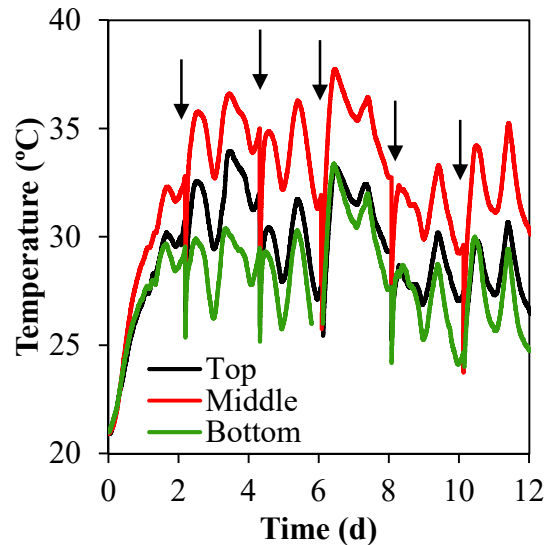


**Figure 6.6.** Temperature profiles in the different trays ( $r = 0$  cm) of the 40-L bioreactor. The arrows indicate mixings.

### 6.3.3. Scale-up to the 100-L bioreactor

The SSF process was scaled up to a 100-L intermittently-mixed bioreactor. This configuration may help to minimize the temperature and water content gradients observed in the experiment with the 40-L bioreactor.

### Experiments

The experiments carried out in this section were performed in the 100-L intermittently-mixed bioreactor in the Fermentation System III (Chapter 3, section 3.2.3). The bioreactor was copiously cleaned with ethanol (70%) before the beginning of the experiment. Each bag of 2,000 g of sterilized solid mixture was discharged in a plastic container, inoculated with fresh inoculum and introduced in the bioreactor through the hopper. This process was performed as quickly as possible to minimize the risk of contamination. The fermentation process with a total of 20,000 g of solid mixture was monitored for 4 days. The solid mixture was mechanically mixed every day (10 rpm, 5 min). Samples (30 - 40 g) were taken after mixing for analysis.

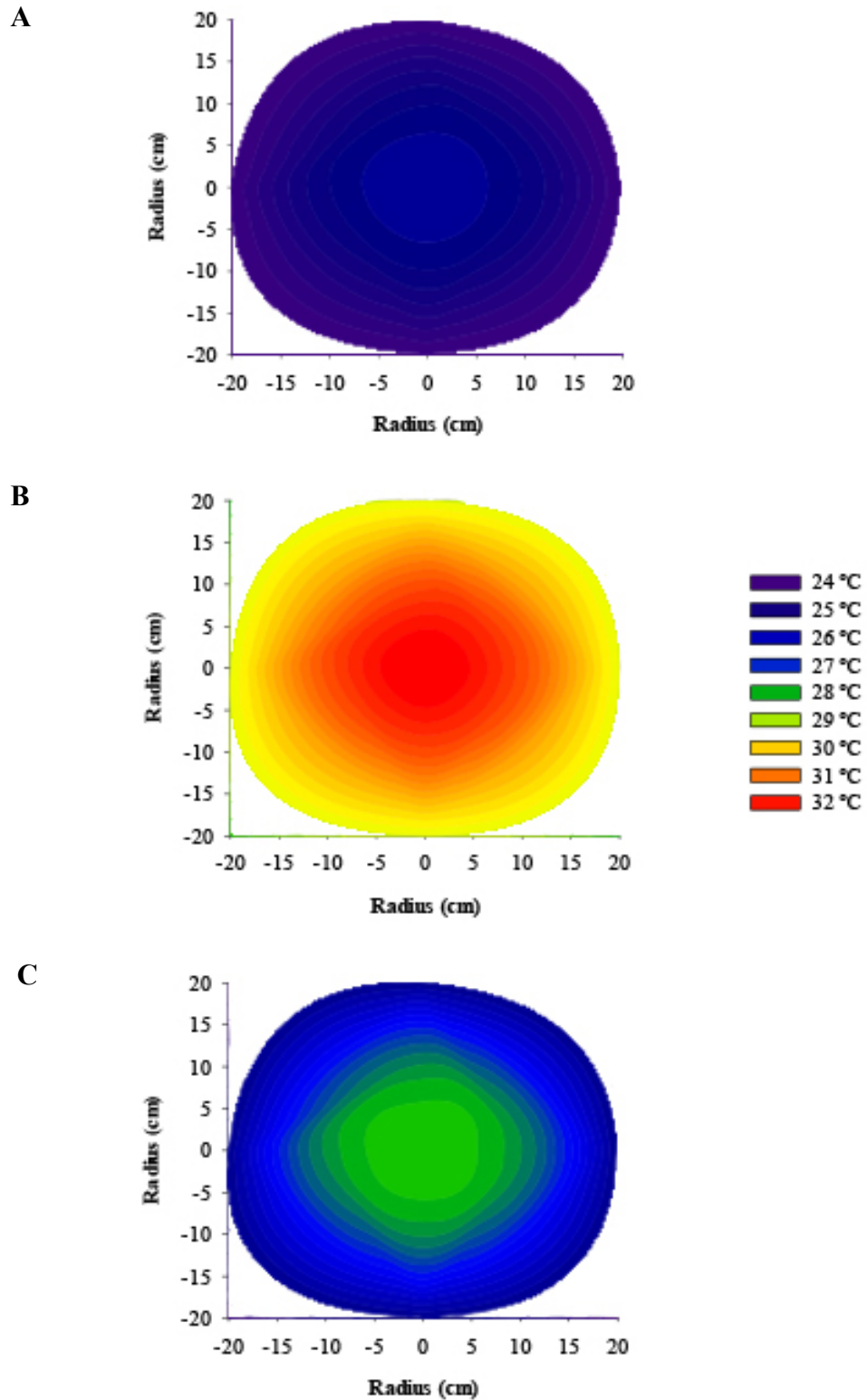


**Figure 6.7.** Temperature gradients in the top (A), middle (B) and bottom (C) tray at day 6 of fermentation.

Temperature was on-line monitored in the inlet and outlet air, and in the bioreactor. It should be reminded that the temperature sampling point of the bioreactor is close to the wall (Figure 3.9). Aeration rate of  $0.30 \text{ L air kg}^{-1} \text{ min}^{-1}$  was provided during the first 24 h. Then, the aeration rate was increased to  $0.90 \text{ L air kg}^{-1} \text{ total wet mass min}^{-1}$  to favor heat removal. A total of 3 experiments were performed under these conditions. Since the SSF profiles of the processes were very similar, the results of only one of them is shown for discussion. Some experiments described in this section were performed at 0.5-L scale in the Fermentation System I (Chapter 3, section 3.2.1).

### **Process dynamics**

Three key parameters, namely: pH, SL yield and OUR profile, have been determined in all the fermentations performed in this work to confirm the proper evolution of the process. As a reminder, Figure 6.8A shows a representative example of the time course of pH and SL yield and the OUR profile for the 4 first days of fermentation of the optimized process at 0.5-L scale. pH drops to acidic values close to 4 after day 4 and substantial SL formation already occurred by day 2 of fermentation. Also, OUR reaches its maximum value between days 2 and 3 with an OUR around  $2 \text{ mg O}_2 \text{ g}^{-1} \text{ DM h}^{-1}$ .

Figure 6.8B shows the time course of pH and SL yield and the OUR profile of the process at 100-L scale. Surprisingly, pH increased from an initial value of 6.3 to a value of 8 after day 4 and SLs were not detected at any of the samplings. However, we observed consumption of oxygen (OUR profile) which confirms the metabolic activity in the bioreactor (Figure 6.8B). Some hypotheses were considered to explain these observations.

The first hypothesis pointed to a problem of contamination of the substrates or the inoculum. However, we performed experiments in parallel at 0.5-L scale using the same initial solid mixture inoculated in the bioreactor and the process went as usual: pH dropped to acidic values and SLs were produced in yields around  $0.2 \text{ g g}^{-1} \text{ DM}$  (Table 6.2). As expected, similar results were found in fermentations carried out at  $30 \text{ }^\circ\text{C}$  and at room temperature (Table 6.2). This confirmed the absence of quality problems related to the substrates or the inoculum.

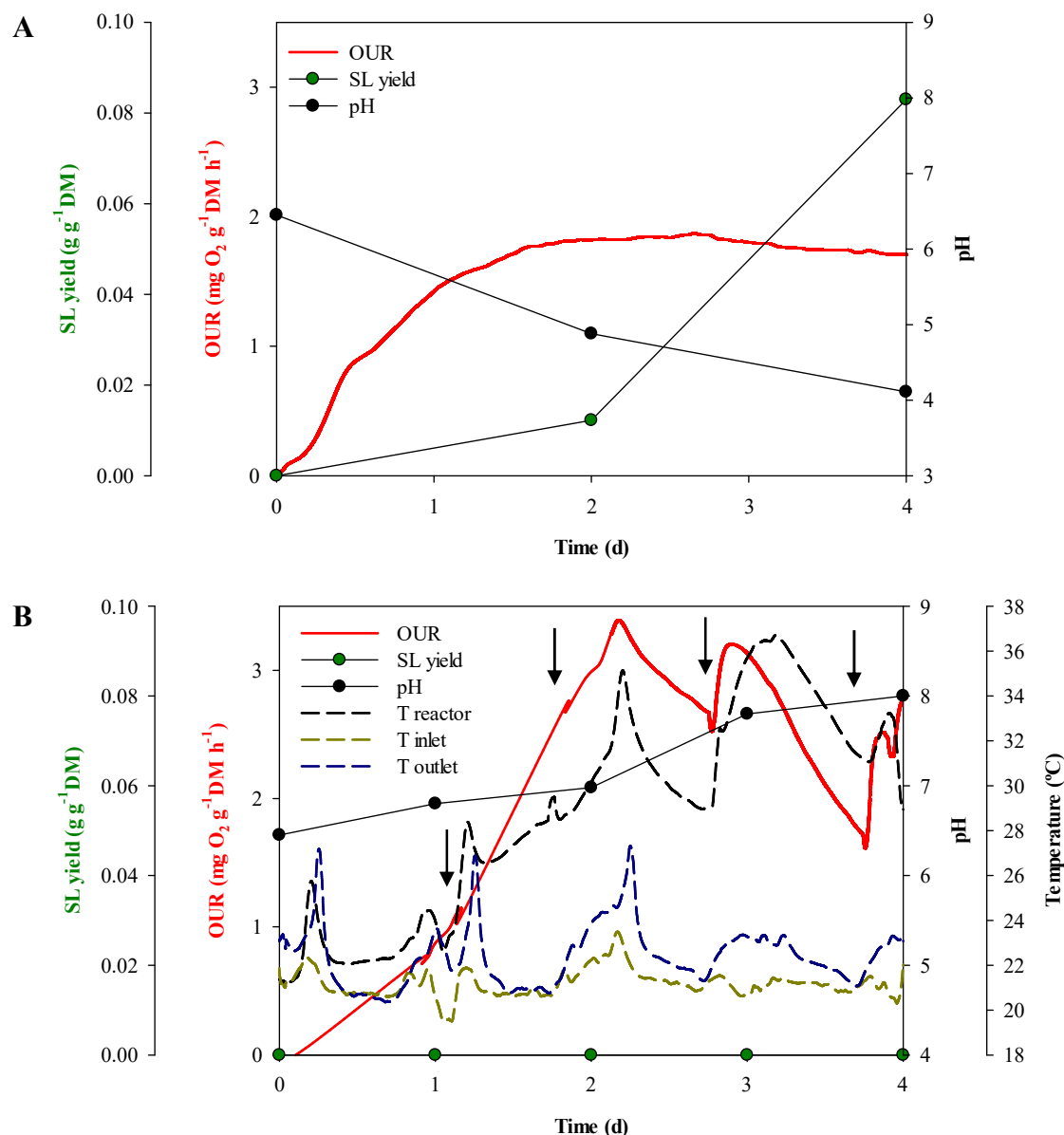


**Figure 6.8.** SSF profile of the process at 100-g (A) and 100-L (B) scale: time course of SL yield and pH, and OUR and temperature profiles. The arrows indicate mixings.

The second hypothesis suggested a problem of contamination from the air compressor used to feed the 100-L bioreactor, which is different from the one used in Fermentation Systems I and II (Chapter 3, section 3.2). For this reason, we performed an experiment with only 2,000 g of solid mixture in the 100-L bioreactor (without intermittent mixing). The pH dropped to acidic values and SLs were produced (Table 6.2). This confirmed that there was any contamination coming from the air compressor or any other part of the Fermentation System III.

**Table 6.2.** pH and SL yield at day 7 of fermentation of different experiments performed during the scale-up to the 100-L bioreactor.

SSF process	Sample (g)	pH	SL yield (g g <sup>-1</sup> DM)
Control – room temperature	100	3.82	0.199
Control – 30 °C	100	3.84	0.214
1 day – room temperature	100	4.09	0.192
1 day – 30 °C	100	4.35	0.183
100-L bioreactor	2,000	3.92	0.153

The third hypothesis pointed to the existence of preferential air paths, which may create non-aerated areas in the solid bed inhibiting the proper growth of the microorganism. Temperature of the outlet airflow was few degrees higher than the inlet airflow, but much lower than the temperature measured in the bioreactor (Figure 6.8B). Temperature of the outlet airflow increases after mixings, which suggests the presence of preferential paths (Anon, 2017). We observed that after mixing the solid was not homogeneously distributed in the reactor but a significant amount stayed on the stirrer surface leaving voids volumes that favored the pass of the air directly to the exit on top. These preferential air paths would contribute not only to the formation of non-aerated areas but also to the inefficiency of the airflow to cool down the solid bed as will be discussed below.

The fourth and final hypothesis pointed to a problem of high temperatures inside the bioreactor, which might inhibit the SSF process as discussed in section 6.3.1. As shown in Figure 6.8B, the maximum temperature recorded was reached after 3 days with a value of 36 °C. However, it should be reminded that the temperature sensor is close to the wall of the bioreactor. The peaks of higher temperature were measured after mixing indicating that there were gradients of temperature across the solid bed. For this reason, we also measured the temperature in the center of the bioreactor before mixing. As observed at 40-L scale, the highest temperatures are recorded in the center of the bioreactor. Surprisingly, temperatures ranging from 40 to 45 °C were measured. These high temperatures demonstrate the inefficiency of the airflow rate and the agitation regime to remove excess heat in the solid bed.



The agitation regime is a key parameter to be optimized. On one hand, suitable agitation would favor heat removal decreasing the temperature from the solid bed. On the other hand, it was observed that agitation favored the compaction of solids due to the mechanical strength of the stirrer. These compacted solids reached higher temperatures.

During the second fermentation process at 100-L scale, we took solids after 1 day and performed one experiment at 0.5-L scale. Interestingly, pH dropped and SLs were produced (Table 6.2). It suggests that *S. bombycola* is growing in the 100-L bioreactor but is doing a different metabolic route due to the high temperatures. However, the process is robust and the yeast is able to recover from a period of high temperatures when back to controlled conditions. Further research is needed for the proper operation of the 100-L bioreactor.

#### 6.3.4. SL production by SSF: yields

Several SSF processes have been described in Chapters 4, 5 and 6 using WOC and MOL blended with wheat straw as solid mixture. Table 6.3 summarizes the maximum SL yields obtained in the time courses.

**Table 6.3.** SL yields obtained in the time courses performed in Chapter 4, 5 and 6.

SL yield		Scale (g)	Conditions	Reference
g g <sup>-1</sup> DM	g g <sup>-1</sup> substrates			
0.107	0.178	100	First screening. Static conditions.	Chapter 4, section 4.3.3
0.179	0.199	100	SSF process optimized. Static conditions.	Chapter 5, section 5.3.4
0.235	0.261	100	SSF process optimized. Intermittent mixing.	Chapter 5, section 5.3.4
0.258	0.330	6,000	40-L bioreactor. Intermittent mixing.	Chapter 6, section 6.3.2

The maximum SL yield of the optimized process at 0.5-L scale was 0.199 g per g of wet substrates, which increased to 0.261 g per g of wet substrates when intermittent

mixing was applied. Our results are similar to those of Parekh and Pandit (2012), who obtained a maximum SL yield of 0.180 g per g of substrates using glucose and oleic acid as pure substrates (blended with wheat bran). Additionally, similar yields were obtained when the oleic acid was substituted by mango kernel fat as the hydrophobic carbon source for SL production (Parekh et al., 2012). Rashad et al. (2014) used a medium based on a mixture of sunflower oil cake and soybean oil moistened with a nutrient medium. These authors obtained a maximum yield of 0.220 g per g of substrates when using the same ethyl acetate extraction method as that used by Parekh and Pandit (2012) and in this work. However, they obtained 0.495 g per g of substrates when they improved the extraction by using a new concept based on two consecutive extractions with two different solvents: methanol and ethyl acetate. This highlights that the quantification of SL production strongly depends on the extraction method. In consequence, the efficient extraction of SLs from the solid matrix must be further studied.

These three published studies of SL production by SSF were performed using 4-14 g of substrates in 15-20 g of total wet mass. In the studies performed in Chapters 4 and 5, we increased the scale of operation to 100 g of total wet mass and used wastes instead of pure substrates, yet we still obtained yields similar to those previously reported (Parekh et al., 2012; Parekh and Pandit, 2012; Rashad et al., 2014). In Chapter 6, the process was scale-up to 6,000 g of total wet mass and the SL yield was similar than at 0.5-L scale. Additionally, these authors either moistened the media with a pH buffer or added nutrients to the solid medium (e.g., yeast extract). In our study, we avoided the use of additives to simplify and cheapen the SSF process in view of its prospective scale-up.

#### **6.4. Conclusions**

The experiments performed in this chapter confirm that the most important handicap for the scale-up of the SSF process proposed in this work is the maintenance of a temperature close to the optimum for microbial growth and product formation. Experiments performed at 0.5-L scale indicated that constant temperatures above 30 °C have a negative effect on SL production. The scale-up of the process to the 40-L bioreactor showed gradients of water content (35–60%) and dynamic temperature

gradients across the solid bed up to 36 °C. These gradients did not hinder the process and SLs were produced in similar yields than at 0.5-L, which confirmed the robustness of the system. However, the scale-up to the 100-L bioreactor process did not work properly, most probably due to the high temperatures of the solid bed and the existence of preferential air paths. The use of the selected airflow rates and the agitation regime was found to be ineffective to remove heat from the solid matrix and minimize preferential air paths.

Knowledge about heat and mass transport phenomena within the solid matrix is fundamental to bring the environmental conditions back to the optimum. Yet, there are a limited number of operating variables that can be modified. For example, we can further explore the agitation regime, the airflow rate or the humidity and temperature of the inlet air.

## CHAPTER 7

---

### *Sophorolipids from winterization oil cake by SSF: characterization*

*Part of this chapter has been published at a Spanish Journal, Industria Química 47, 76-80. 2017.*

*Soforolípidos a partir de un residuo de winterización.*

*Jiménez-Peñalver, P., Font, X., Gea, T.*

*Part of this chapter is in preparation for submitting to an international SCI journal with the tentative title: Characterization of sophorolipids from a winterization oil cake*



## Summary

Most of the results shown in this chapter correspond with the work performed in a 6-months stay in the Center for Biocatalysis and Bioprocessing at the Rensselaer Polytechnic Institute (RPI) in NY, USA. The results are an in-depth characterization of the crude SL natural mixture from the winterization oil cake (WOC) attending to their structure and their interfacial properties, namely surface tension lowering capacity, emulsion properties and displacement activity.

From a structural point of view, the SLs were characterized by FTIR, <sup>1</sup>H-NMR and LC-MS. The crude SL natural mixture was also purified and the main compounds were quantified by HPLC. These SLs produced from WOC by SSF were compared with SLs synthesized from oleic acid by SmF to assess the influence of the technology in the mixture of SLs.

The surface tension lowering capacity was studied in a water-air interface at temperatures ranging from 15 to 50 °C and the parameters minimal surface tension (mST) and critical micelle concentration (CMC) were determined. The emulsion properties were evaluated in a water-almond oil interface at different concentrations of SLs and almond oil. The average emulsion droplet sizes and the emulsion phase stability were studied for 7 days and the results were compared with those obtained for the commercial non-ionic surfactant Triton X-100. The diesel displacement activity of the SL natural mixture was studied and the results were compared with those obtained for surfactant Triton X-100.

Additionally, the crude SL natural mixture was chemically modified to obtain ethyl ester sophorolipid (EESL) and their interfacial properties were evaluated.

## 7.1. Materials

The SLs used for characterization were obtained in the laboratories of the research group at RPI where a simpler replication of the Fermentation System I (Chapter 3, section 3.2.1) was set up with capacity for 3 SSF reactors (Figure 7.1). A water bath was used to maintain the temperature at 30 °C and 3 rotameters were installed to adjust the airflow rate for each reactor. In this system, the oxygen concentration in the exhaust gases was not monitored. Fermentations were carried out at 0.5-L scale in 0.5-L Erlenmeyer Flaks using the previously optimized SSF mixture and conditions (Chapter

5). The WOC was provided as usual by the oil refinery LIPSA and sent frozen from Spain to USA. The MOL were purchased in VWR (Radnor, PA, USA) and the wheat straw was purchased in a local market. The SLs were extracted after 7 days of fermentation (Chapter 3, section 3.5.1), lyophilized overnight and stored at 4 °C. These were the crude SL natural mixture used for the characterization.

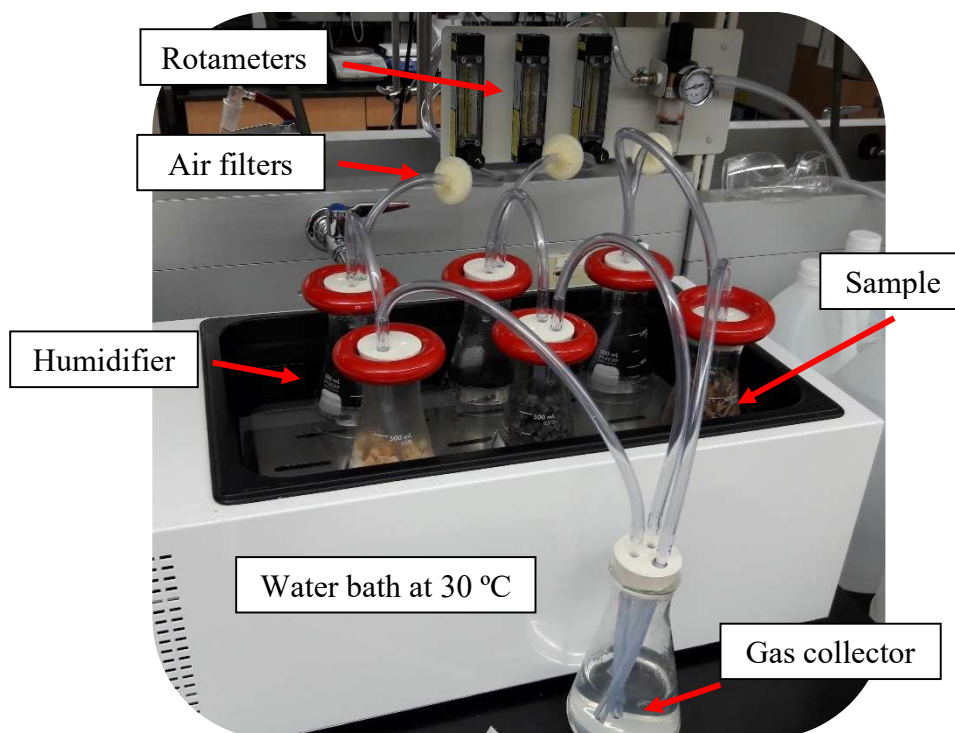


**Figure 7.1.** Setup of the SSF system at RPI.

## 7.2. Experiments

Figure 7.2 shows a scheme of the characterization performed in this Chapter. Firstly, the SLs were structurally characterized using FTIR,  $^1\text{H-NMR}$  and LC-MS, and later purified by silica gel column chromatography and quantified by HPLC. Secondly, the interfacial properties of the SLs were studied attending to their surface tension lowering capacities in a water-air interface, their emulsification properties in a water-almond oil interface, and their diesel displacement activity. Finally, the SLs were chemically modified to obtain the ethyl ester sophorolipid (EESL) and the interfacial properties of this molecule were evaluated. The structural characterization and the analysis of the interfacial properties were performed according to the methodology described in Chapter 3, section 3.6.

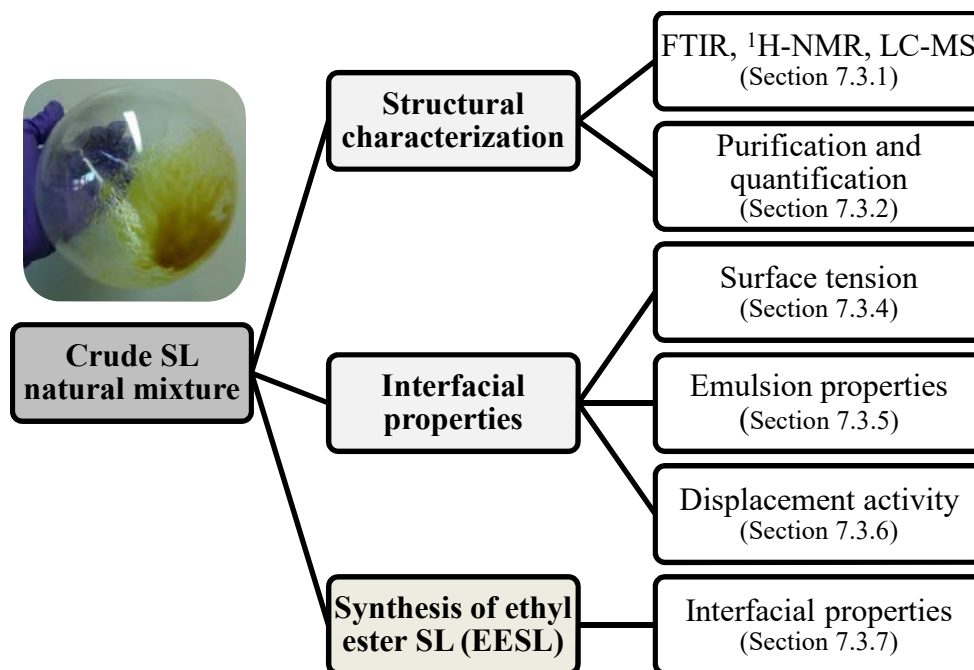


**Figure 7.2.** Scheme of the characterization performed in this Chapter.

### 7.3. Results and discussion

#### 7.3.1. Structural characterization by FTIR, <sup>1</sup>H-NMR and LC-MS

The crude SL natural mixture produced from WOC were initially identified by FTIR and <sup>1</sup>H-NMR. An LC-MS system was used to separate and identify the SLs.

##### FTIR

The FTIR spectra obtained is shown in Figure 7.3. The spectra revealed a broad band at 3396 cm<sup>-1</sup>, which corresponds to the O-H stretch (Figure 1.2). Asymmetrical stretching ( $\nu_{as}$  CH<sub>2</sub>) and symmetrical stretching ( $\nu_s$  CH<sub>2</sub>) of methylene were observed at 2924 cm<sup>-1</sup> and 2854 cm<sup>-1</sup>, respectively. The C=O absorption band at 1742 cm<sup>-1</sup> may include contributions from lactones, esters or acids. The stretch of the C-O band of C(=O)-O-C in lactones appeared at 1165 cm<sup>-1</sup>. The C=O absorption band at 1235 cm<sup>-1</sup> of acetyl esters and the band at 1367 cm<sup>-1</sup> for the symmetrical bending of the methyl groups of the acetyl esters indicate that our SL natural mixture contains acetylated sophorose moieties. The band at 1456 cm<sup>-1</sup> corresponds to the C-O-H in-plane bending of carboxylic acid (-COOH) and may indicate the presence of small quantities of unused fatty acids that were left after hexane washings or the contribution of acid SLs. The



spectra also show the absorption for C=C at  $721\text{ cm}^{-1}$ . Finally, a C-O stretch from C-O-H groups of sugars was observed at  $1034\text{-}1075\text{ cm}^{-1}$ . All the bands mentioned together with the correspondent stretch and the functional group involved are summarize in Table 7.1. The FTIR spectra shown in Figure 7.3 is like those shown previously in Chapter 4 and those reported in the bibliography (Daverey and Pakshirajan, 2010; Maddikeri et al., 2015; Parekh and Pandit, 2012; Rashad et al., 2014), which confirms that the product obtained belongs to the SLs.

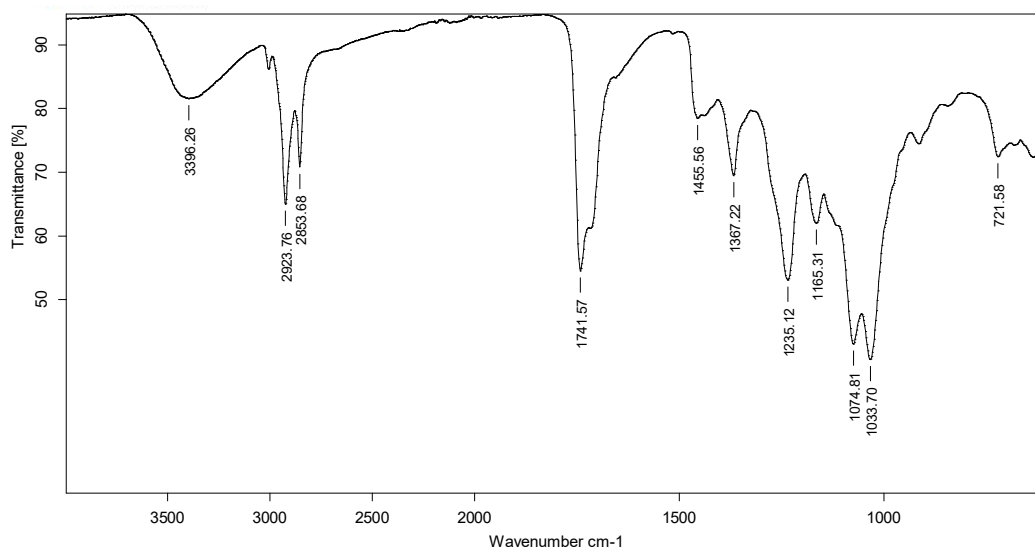


**Figure 7.3.** FTIR spectra of the SLs produced from WOC.

**Table 7.1.** Frequencies of the FTIR spectra with the correspondent stretch, functional group and structure.

Frequency ( $\text{cm}^{-1}$ )	Stretch	Functional group	Structure
3396	O-H	-OH	Acids and glucoses
2924	$\nu_{\text{as}}\text{ CH}_2$	-CH <sub>2</sub> -	Fatty acid chain moiety
2854	$\nu_{\text{s}}\text{ CH}_2$	-CH <sub>2</sub> -	Fatty acid chain moiety
1742	C=O	-C(=O)-O-X (X=H or R)	Lactones, esters and acids
1456	C-O-H	-COOH	Acids
1367	$\delta_{\text{s}}\text{ CH}_3$	R-O-C(=O)-CH <sub>3</sub>	Acetyl group
1235	C=O	R-O-C(=O)-CH <sub>3</sub>	Acetyl esters
1165	C-O	R'-C(=O)-O-R''	Lactones
1034-1075	C-O	C-O-H	Glucoses (sophorose moiety)
721	C=C	-HC=CH-	Fatty acid chain moiety

**<sup>1</sup>H-NMR**

The <sup>1</sup>H-NMR spectra of the SLs is typical of a glycolipid-type structure (Figure 7.4). The protons of the two glucoses resonated at 3.44 - 4.57 ppm. It was possible to identify the signals of the protons of glucose-H-1' (4.45 and 4.48 ppm) and glucose-H-1'' (4.54 and 4.57 ppm). These signals correspond, respectively, to the glycosidic bond between the sophorose molecule and the fatty acid chain and the glycosidic bond between the two glucoses (Figure 1.2). The protons of the (-COCH<sub>3</sub>) group resonated at 2.09 ppm. Multiple signals of protons at 1.30 ppm indicate the presence of a fatty acid chain moiety, and peaks at 5.34 ppm correspond to the vinyl group (-CH=CH-) of the fatty acid chain. All the signals mentioned together with the correspondent protons and structure are summarize in Table 7.2.

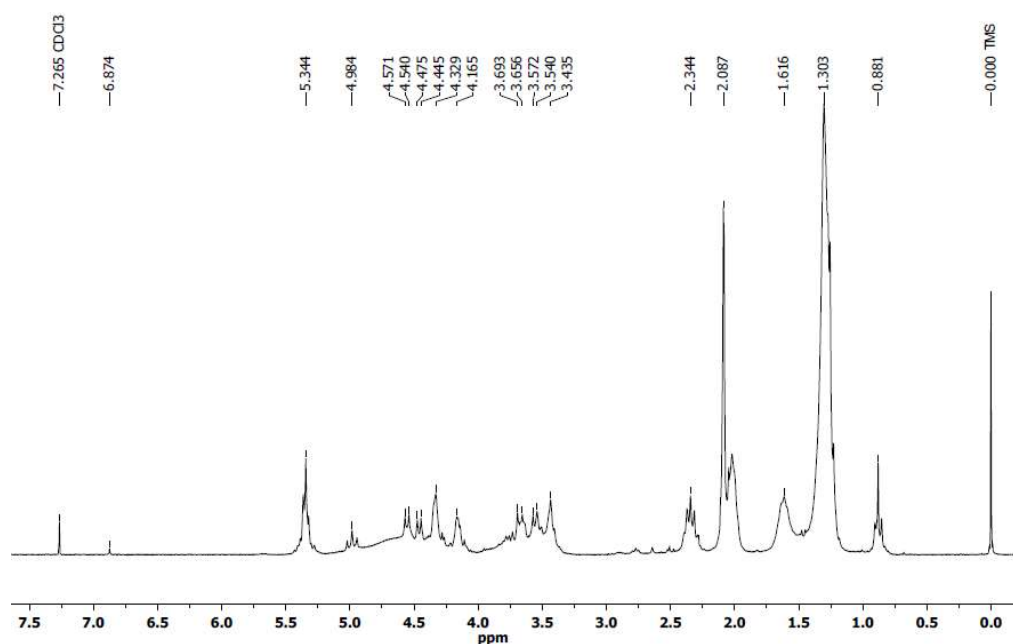


**Figure 7.4.** <sup>1</sup>H-NMR spectra of the SLs produced from WOC.

**Table 7.2.** Signals of the <sup>1</sup>H-NMR spectra with the correspondent protons and structure.

Signal (ppm)	Protons	Structure
1.30	-CH <sub>2</sub> -	Fatty acid chain moiety
2.09	-COCH <sub>3</sub>	Acetyl group
3.44-4.57	H of glucoses	Glucoses
5.34	-CH=CH-	Fatty acid chain moiety

## LC-MS

It is well-known that SLs are produced as a mixture of different molecules with two major points of variation: acetylation in the sophorose and lactonization (Figure 1.2). Also, the length of the fatty acid chains varies between 16 and 18 carbons, which may be saturated or unsaturated (Nuñez et al., 2001). The results obtained from FTIR and  $^1\text{H-NMR}$  confirm that the SL natural mixture from WOC contains both acidic and lactonic SLs, SLs acetylated in the sophorose, and SLs with fatty acid chains unsaturated. However, information about the concrete structure of the SLs and their proportion in the SL natural mixture cannot be obtained from these data. FTIR and  $^1\text{H-NMR}$  are very useful tools to easily confirm the identity of SLs but they do not provide information about the blend of molecules. Therefore, a LC-MS system was used to elucidate the structures of SLs contained in the SL natural mixture.

SLs were firstly separated by HPLC and their response was then recorded using the UV-Visible detector of the HPLC (Figure 7.5A) and the total ion chromatogram (TIC) given by the MS (Figure 7.5B). Assignment of peaks from the mass spectra to the correspondent SLs was performed attending to the mass to charge ratio ( $m/z$ ) given by the mass spectra for each peak (data not shown). As can be observed in the chromatograms, the detector of the HPLC did not record the SLs without double bonds in the fatty acid chain moiety (Figure 7.5A). Nonetheless, this chromatogram is shown because is essential for quantification purposes, as will be discussed later.

The TIC shows a complex mixture of SLs containing both diacetylated lactonic SLs (C18:0, C18:1, C18:2 and C16:0) and diacetylated acidic (C18:1) SLs (Figure 7.5B). Also, the monoacetylated lactonic C18:1 SL was observed but with lower proportion than the correspondents diacetylated structures. SLs are separated due to their hydrophobicity during the HPLC, which explains the different retention times in the chromatograms (Figure 7.5). For example, acidic SLs elucidate in the first 5 min of analysis, while the lactonic ones elucidate later. Also, the diacetylated SLs show longer retention times than the correspondent mono or non-acetylated ones. The length and the number of double bonds of the fatty acid chains also have an influence in the retention times. As can be observed in Figure 7.5B, SLs with shorter tails elucidate before (C16:0 < C18:0). Also, SLs with higher number of double bonds show shorter retention times (C18:2 < C18:1 < C18:0).

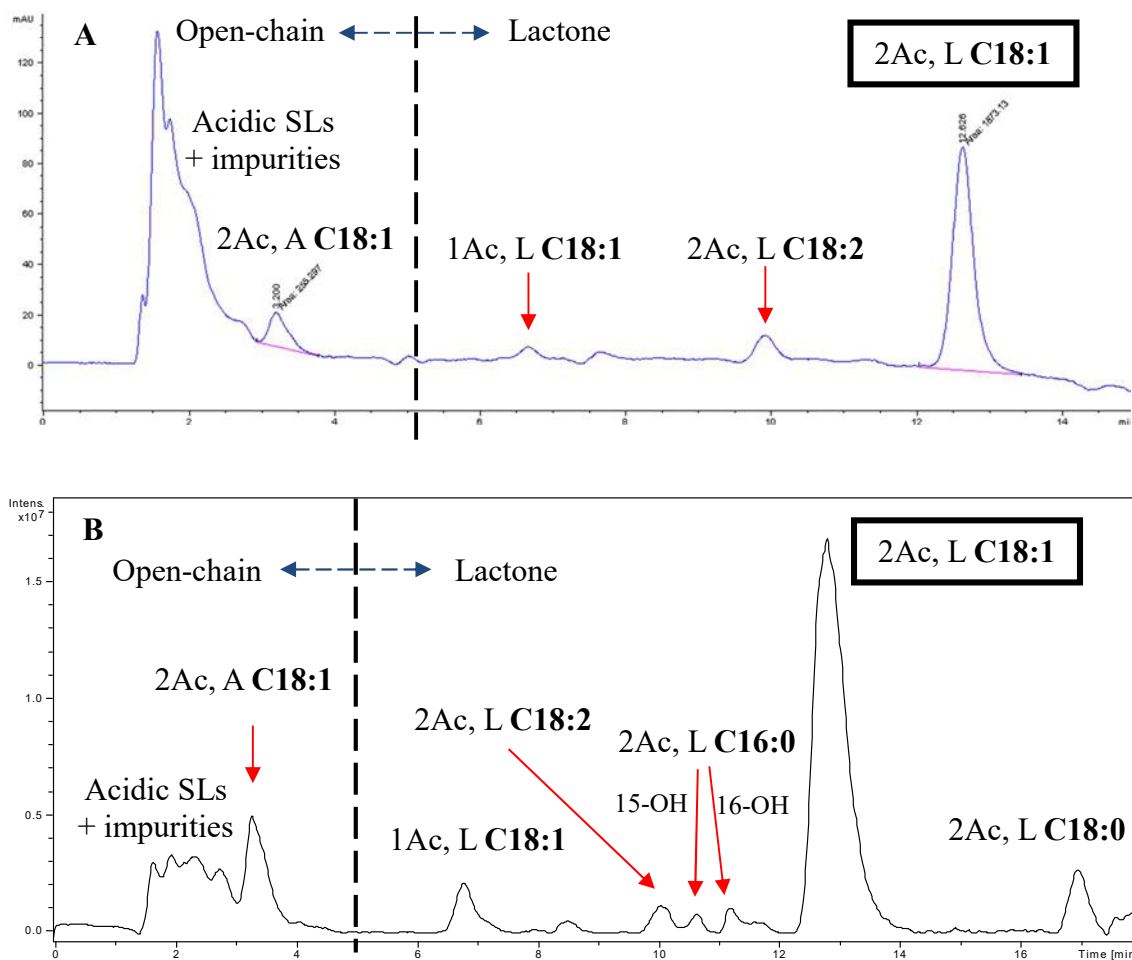


**Figure 7.5.** HPLC chromatogram (A) and total ion chromatogram (B) of the SLs produced from WOC.

Interestingly, the TIC shows two peaks with the same  $m/z$  ratio, which were assigned to the diacetylated lactonic C16:0 SL (Figure 7.5B). They are believed to differ only in the position of the hydroxyl group. The one with shorter retention time had the hydroxyl group in the subterminal position (C15), while the other at the terminal (C16) position (Davila et al., 1994; Hommel et al., 1994b; Hu and Ju, 2001). The chromatograms clearly show that the diacetylated lactonic C18:1 SL is the predominant molecule of the mixture followed by the acidic form. The abundance of these two SLs is consistent with oleic acid as the predominant fatty acid in the WOC (Table 3.1). According to the data reported in the literature, the diacetylated lactonic C18:1 SL is mostly synthesized with the hydroxyl group in the subterminal (C17) position (Figure

1.2), and only a small fraction has the hydroxyl group in the terminal (C18) position (Ashby et al., 2008; Hu and Ju, 2001). Unfortunately, both isomers could not be separated with the HPLC method used in this work. According to IUPAC rules, the proper way to name the diacetylated lactonic 17-OH C18:0 SL is: 17-L-([2'-O- $\beta$ -D-glucopyranosyl- $\beta$ -D-glucopyrosyl]oxy)-octadecanoic acid 1'-4''-lactone 6',6''-diacetate.

The subterminal/terminal ratio is dependent on the hydroxylation step of the fatty acid prior to the formation of the SL (Van Bogaert et al., 2011b). In general, this step is highly dependent on the enzyme involved in the reaction. In yeasts, the hydroxylation is typically performed by cytochrome P450 monooxygenases from the CYP52 family: some tend to hydroxylate preferably in the subterminal position and others in the terminal one (Van Bogaert et al., 2011a). Other parameters such as the length of the hydrophobic source, the *in vitro* conditions or even the temperature can affect the hydroxylation (Van Bogaert et al., 2011a).

Table 7.3 summarizes the retention times of the SLs and the correspondent structure and molecular weight. The order in the elucidation of SLs and the assignment of peaks agrees with the reported previously in the bibliography (Ashby et al., 2008; Davila et al., 1994; Hu and Ju, 2001; Nuñez et al., 2001).

**Table 7.3.** Retention times of the SLs and the correspondent structure and molecular weight.

Retention time (min)	SL structure	Molecular weight (g mol <sup>-1</sup> )
1.6 – 3	Unidentified acidic SLs	-
3.5	2Ac, acidic C18:1	706
6.8	1Ac, lactonic C18:1	664
10.1	2Ac, lactonic C18:2	686
10.8	2Ac, lactonic 15-OH C16:0	662
11.2	2Ac, lactonic 16-OH C16:0	662
12.8	2Ac, lactonic C18:1	688
17	2Ac, lactonic C18:0	690

### 7.3.2. Purification and quantification

The crude SL natural mixture was purified by silica gel column chromatography. The purified SL was found to be white crystalline in nature, which is in contrast with the amber viscous appearance of the partially purified SL (Figure 7.6). The presence of residual fatty acids or co-products of fermentation which were not eliminated with the washings with *n*-hexane might explain the amber color and the viscosity. Proper purification of the SL was checked by LC-MS. The TIC (Figure 7.7) revealed a major peak at 12.8 min which was previously attributed to the diacetylated lactonic C18:1 SL (Figure 7.5). The rest of the peaks attributed to other SLs and impurities were not observed, which confirms a proper SL purification.



**Figure 7.6.** Partially purified (left) and purified (right) SL.

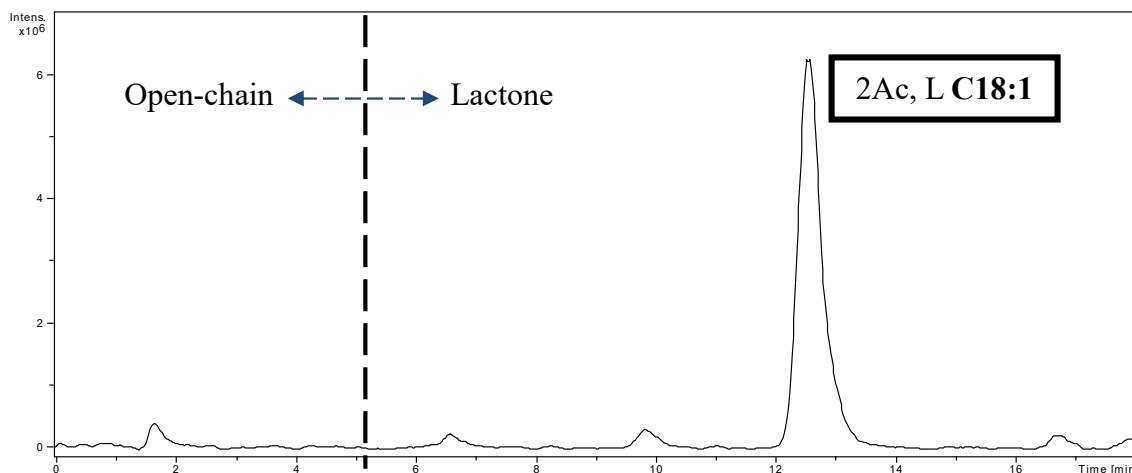


**Figure 7.7.** Total ion chromatogram (TIC) of the purified SL produced from WOC.

The isolated diacetylated lactonic C18:1 SL was used to prepare a calibration curve to determine the concentration of this molecule in the SL natural mixture (Annex II). The concentration of the correspondent acidic form was also determined by the same calibration curve assuming a similar response in the HPLC detector. The HPLC chromatogram of the SL natural mixture was used for quantification (Figure 7.5A). The results showed that 36% of the crude SL natural mixture corresponds to the diacetylated lactonic C18:1 SL and a 6% to the correspondent acidic form (Table 7.4). Hence, the ratio lactonic: acidic was 86:14. The rest of the sample is formed by small percentages of other individual SLs and impurities such as remaining oils and co-products of fermentation.

**Table 7.4.** Retention times, area and the correspondent concentration of the diacetylated acidic and lactonic C18:1 SLs.

Retention time (min)	SL structure	Area	SL concentration (g L <sup>-1</sup> )
3.5	2Ac, acidic C18:1	255	0.06
12.5	2Ac, lactonic C18:1	1873	0.36

These results indicate that approximately half of the crude SLs produced from WOC are pure SLs, and the other half are impurities. This means that the SL yields showed in this work are overestimated and are lower than what has been referenced. Surprisingly, most papers about production of SLs use the same extraction method and obtain the same honey-like compounds, which indicates that all these works may be also overestimating the yield of their fermentations (Parekh and Pandit, 2012). As far as we know, none of them has evaluated the purity of their final product, which makes very difficult to compare yields between different works. The purity of the so-called “partially purified SLs” or “crude SLs” depends on several factors as the type and the amount of fats remaining in the fermentation media, the extraction method or the number of washings with *n*-hexane.

It should be mentioned that purification of the SLs might not be always needed and will depend on the regulation involved in their final application. For example, we might use the crude SLs for environmental applications such as soil or water remediation, but not for cosmetics or biomedicine applications.

### 7.3.3. Comparison with SLs produced by SmF

The objective of this experiment was to evaluate if the technology used for SL production, SmF or SSF, influences the structures of the SLs synthesized. For that, SLs were synthesized by SmF using the pure substrates oleic acid and glucose by means of an optimized methodology of the research group at RPI. Oleic acid was selected as the hydrophobic carbon source because it is the most abundant fatty acid in the WOC (Table 3.1). As mentioned before, oleic acid is also the substrate preferred to produce SLs commercially since it gives the best yields.

The fermentation was carried out in a 5-L bioreactor with an initial working volume of 3 L and it was operated in the fed-batch mode with a total of 7 feedings of 50 g L<sup>-1</sup> of glucose and 50 g L<sup>-1</sup> oleic acid (Figure 7.8). After 10 days of fermentation the bioreactor was stopped and the fermentation mixture was separated in two phases (Figure 7.8). The top layer (1.1 L) contained 212 g L<sup>-1</sup> SLs and 388 g L<sup>-1</sup> oleic acid, while the bottom one (2.6 L) contained insignificant amounts of these compounds. The top layer was washed six times with *n*-hexane to remove the unused oleic acid and the other co-products of fermentation. Then, the SLs were extracted with ethyl acetate. The crude SL natural mixture (Figure 7.8) seemed purer than the one obtained from WOC (Figure 7.6), probably because of a higher number of washings with *n*-hexane and the higher concentration of SLs in the top phase of the fermentation media.



**Figure 7.8.** Pictures of the bioreactor during the fermentation (left), when the fermentation was stopped (center), and the SLs extracted (right).



The chromatograms of the crude SLs from SmF (Figure 7.9) were very similar to the ones of the crude SLs from WOC (Figure 7.5). Both contain acidic and lactonic SLs with different fatty acid tails being the diacetylated lactonic C18:1 SL the most abundant.

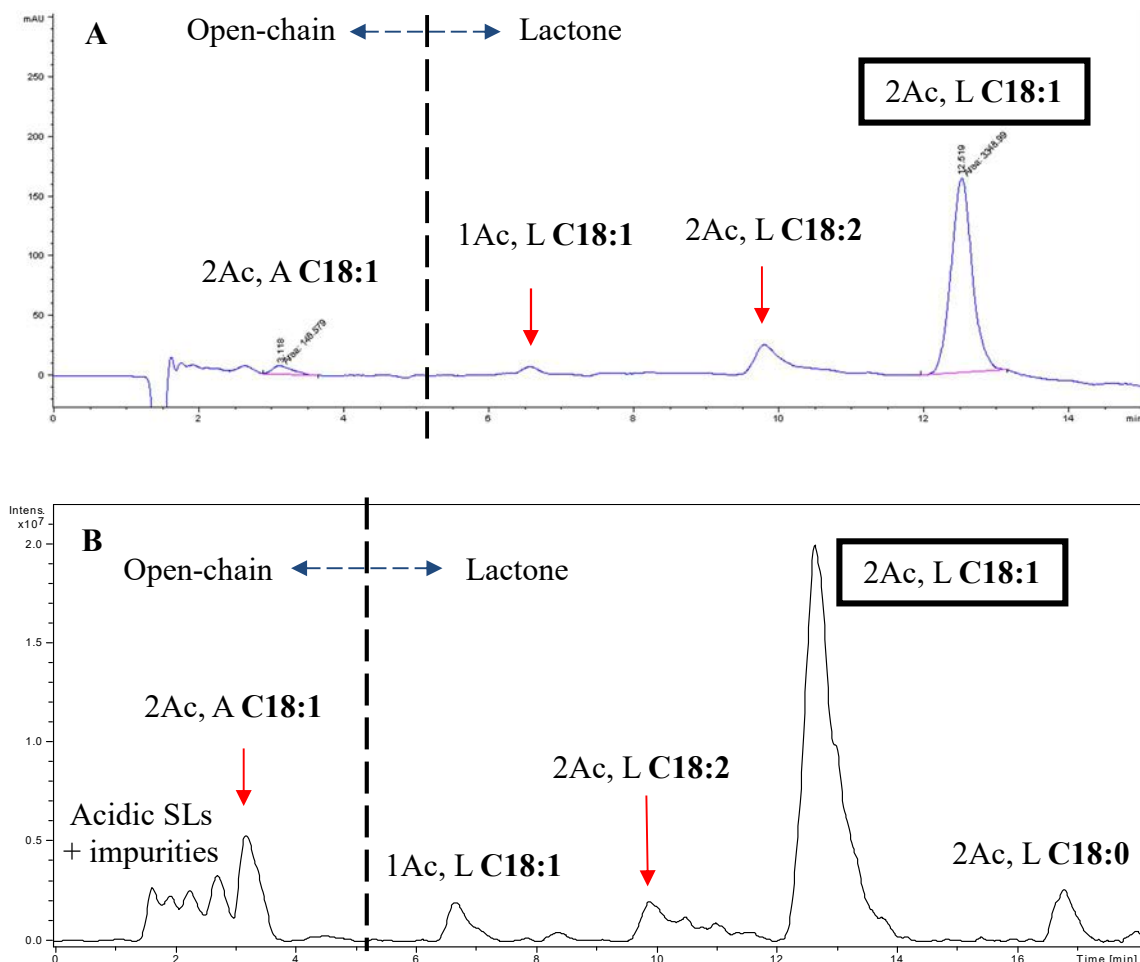


**Figure 7.9.** HPLC chromatogram (A) and total ion chromatogram (B) of the SLs produced from oleic acid.

The HPLC chromatogram (Figure 7.9A) was used to quantify the concentration of this SL (Annex II). The results showed that 64% of the partially purified SLs corresponds to the diacetylated lactonic C18:1 SL and a 4% to the correspondent acidic form (Table 7.5). Hence, the ratio lactonic: acidic was 94:6, which is similar to the one obtained for the SLs from the WOC. The other 30% of the sample might be formed by small percentages of other individual SLs and impurities such as remaining oleic acid and co-products of fermentation. The small percentage of impurities was expected

attending to the physical appearance of the crude SL natural mixture (Figure 7.8). These results indicate that the technology used for the synthesis of SLs (SmF or SSF) do not influence the structures of the SLs produced.

**Table 7.5.** Retention times, area and the correspondent concentration of the diacetylated acidic and lactonic C18:1 SLs.

Retention time (min)	SL structure	Area	SL concentration (mg mL <sup>-1</sup> )
3.5	2Ac, acidic C18:1	147	0.04
12.5	2Ac, lactonic C18:1	3349	0.64

#### 7.3.4. Surface tension lowering capacity

Surfactants, both chemical and biological, are well-known for their surface tension lowering capacity at oil-water or water-air interfaces (Krieger et al., 2010). In general, biosurfactants have a comparable performance to chemically-derived surfactants while still being non-toxic, which make them very attractive for environmental and household surfactant applications (e.g. household cleaners, removal of toxic compounds from soil). There are two fundamental parameters used to characterize surfactants in terms of their interfacial properties: minimal surface tension (mST) and critical micelle concentration (CMC). Both parameters were experimentally calculated for the crude SL natural mixture.

Figure 7.10 shows the surface tension curve obtained at different concentrations of SLs in an aqueous solution at 25 °C. As can be observed, the surface tension decreases with the increment in the concentration of SLs until the surface tension reaches a minimum, named minimal surface tension (mST). Specifically, the SLs synthesized herein decreases the surface tension from 72.0 mN m<sup>-1</sup> to 34.2 mN m<sup>-1</sup>. This value is within the range from 40 to 30 mN m<sup>-1</sup> reported in the literature for natural SLs (Develter and Lauryssen, 2010).

Critical micelle concentration (CMC) represents the concentration of surfactants above which micelles form. This parameter was calculated from the intersection of the two slopes of Figure 7.10. CMC of the SLs synthesized herein was 40.1 mg L<sup>-1</sup>, which is in agreement with the range of values from 11 to 250 mg L<sup>-1</sup> reported in the literature for SLs (Develter and Lauryssen, 2010).

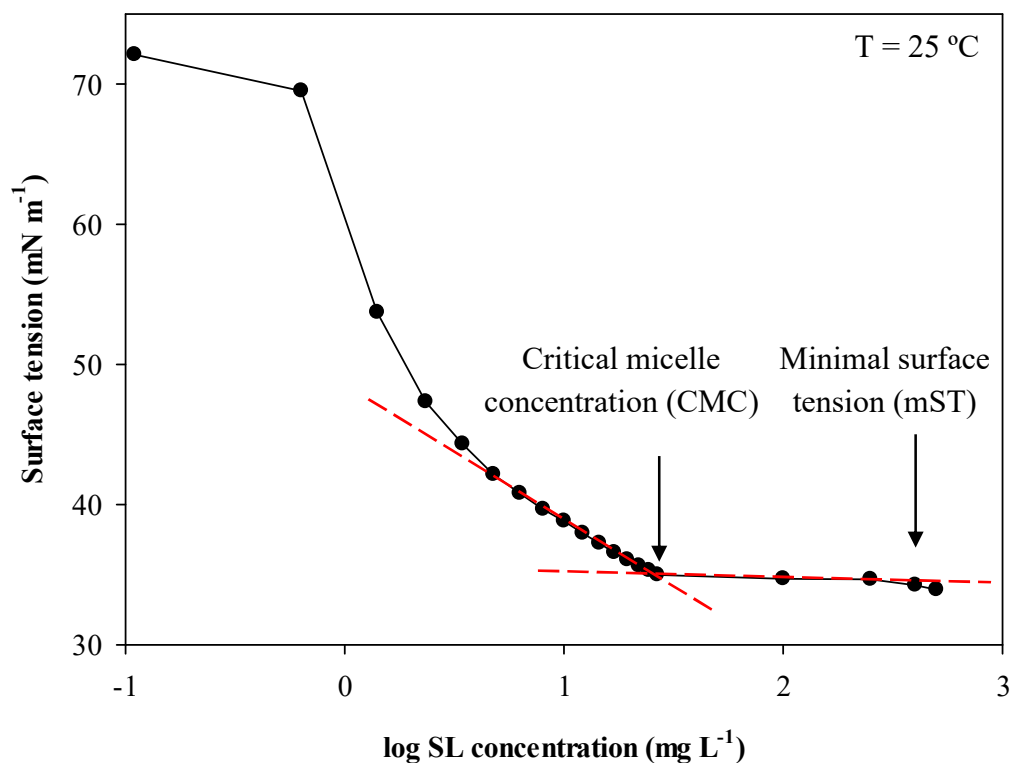


**Figure 7.10.** Surface tension curve at 25 °C of the SLs produced from WOC.

Values of mST and CMC reported in literature are mainly dependent on the composition of SLs. For example, it has been reported that a mixture of SLs displays better interfacial properties than a SL alone suggesting a natural synergism between molecules (Hirata et al., 2009). Also, it is well-known that diacetylated lactonic SLs are better lowering the mST and the CMC compared to non-acetylated acidic molecules (Lanf et al., 2000). In general, the higher the hydrophobicity of the SL hydrophobic tail, the lower the mST and the CMC (Zhang et al., 2004). As shown in Figure 7.5 and explained in section 7.3.1, the SLs produced in this work are a mixture of acidic and lactonic SLs with different fatty acid tails, which would explain the low mST and CMC values determined for the SL natural mixture. It should be remarked that surface tension analyses have been performed with crude SLs, which means that the surface tension lowering capacity of the SLs could have been affected by impurities such as fatty acids or co-product of fermentation. Surface tension analyses cannot be performed with the isolated diacetylated lactonic C18:1 SL due to the poor water solubility of lactonic SLs (Koh et al., 2016).

### Effect of temperature

The effect of temperature on the interfacial parameters mST and CMC was evaluated at temperatures ranging from 15 to 50 °C. Figure 7.11 shows the values of mST and CMC calculated from the surface tension curves of the SL natural mixture at 15, 25, 40 and 50 °C (Annex III). As can be observed, the increment in temperature disfavors the formation of micelles, which leads to an increment in the CMC values. This fact can be explained considering that the solubility of the surfactant increases with increasing temperature, and therefore more molecules can be in the solution in the free form before the micelle starts to be formed. Additionally, the increment in temperature causes an increase in the breakdown of the structured water surrounding the fatty acid chain of the SLs disfavoring the process of micellization. Thus, the formation of the micelles tends to occur at higher concentrations as the temperature increases (Chen et al., 1998).

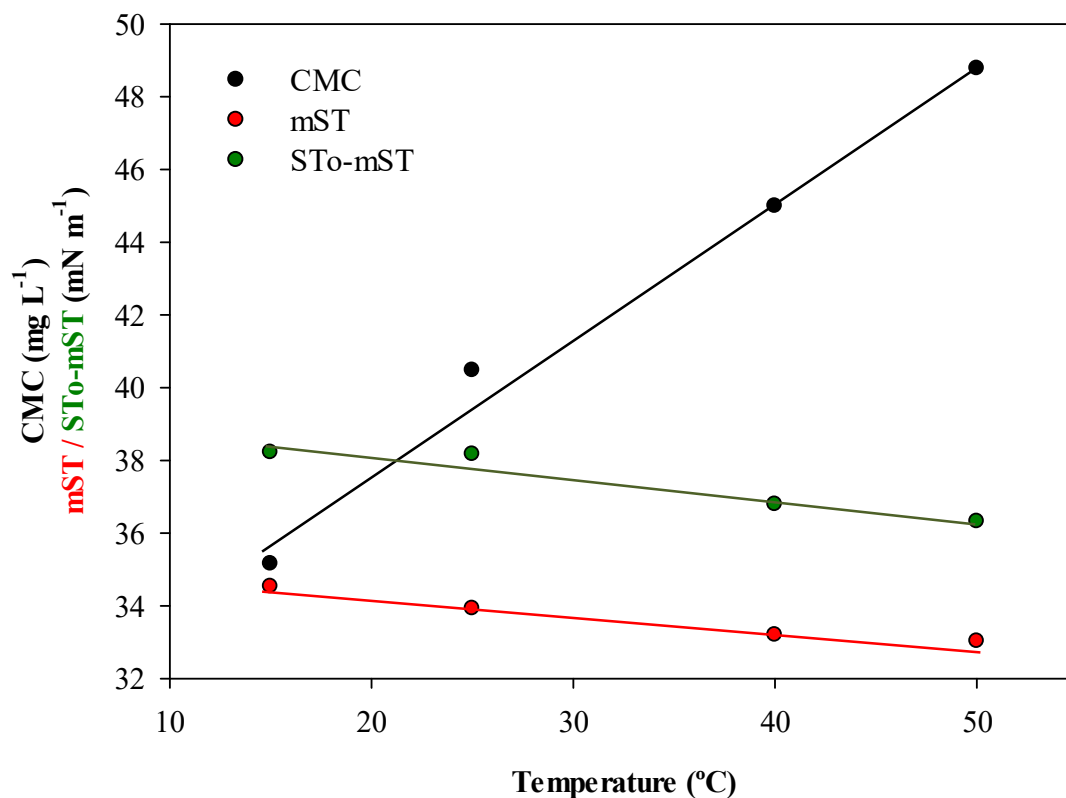


**Figure 7.11.** CMC, mST and STo-mST values at temperatures ranging from 15 to 50 °C.

The minimal surface tension slightly decreases with the increment of temperature (Figure 7.11). In general, the surface tension of an aqueous system decreases when temperature increases because cohesive forces decrease with an increase of molecular thermal activity. However, the lowering capacity of the SL natural mixture (STo-mST) decreases with the increment of temperature (Figure 7.11). These values were calculated by resting the surface tension of water at a given temperature (STo) to the mST of the surfactant at that temperature. It means that the decrement in the mST values with temperature is due to the lower STo values of the water system at increasing temperatures and not because of a better performance of the SLs. Interestingly, CMC, mST, and STo-mST values correlated linearly with temperature when these parameters were plotted together (Figure 7.11).

### 7.3.5. Emulsion properties

An emulsion is the mixture of two immiscible liquids. Such systems are thermodynamically unstable and require a surfactant to reduce the system's free energy and stabilize the interfacial area between the two phases. The emulsion properties of SLs synthesized from WOC were assessed at a water-almond oil interface in order to observe the average emulsion droplet sizes and the emulsion phase stability. Emulsions were prepared with 1, 10 or 20% almond oil by weight and 0.01 or 0.1% surfactant by total emulsion weight. Analysis of emulsions was performed immediately after emulsification and after 1 and 7 days of aging. The results were compared with those obtained for the commercial non-ionic surfactant Triton X-100.

#### Effect of SLs on the emulsion droplet size

Emulsion droplet size is an indicator of system stability. The smaller the emulsion droplet size, the more kinetically stable the emulsion and, therefore, the better the efficiency in combating thermodynamic instability (Solans et al., 2005). Figure 7.12 shows the average droplet sizes of the emulsions tested immediately after emulsification and after 1 and 7 days of aging. The average droplet sizes of SLs emulsions increase with the increment in the percentage of almond oil for a given time with mean values ranging from 500 to 5,000 nm. Similar trends have recently been reported for emulsions

with SLs using almond oil (Koh et al., 2016), lemon oil (Koh and Gross, 2016a) and paraffin oil (Koh and Gross, 2016b).

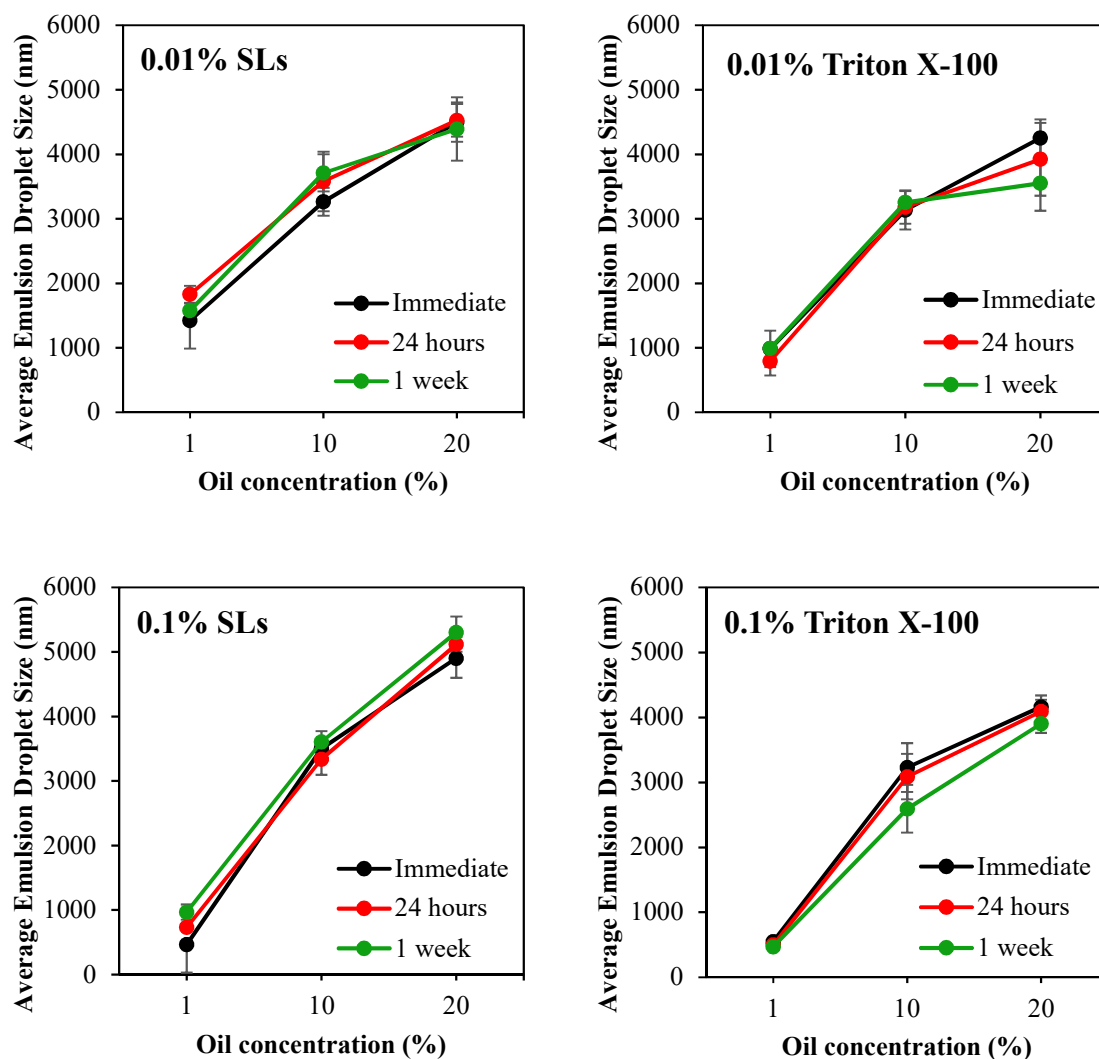


**Figure 7.12.** Average emulsion droplet sizes of water-almond oil emulsions immediately after emulsification and after 24 h and 1 week of aging. Results are expressed as mean  $\pm$  standard deviation of three replicates.

Interestingly, the average droplet sizes of 0.01% SLs emulsions showed little differences with 0.1% SLs emulsions for the same oil concentration, which indicates an excellent emulsification capacity of these molecules even at low concentrations of SLs and high concentrations of oil (Figure 7.12). In fact, the results obtained for the crude SLs from WOC are very similar to those of the commercial surfactant Triton X-100 (Figure 7.12). There is little change in the average emulsion droplet sizes from the

immediate time after emulsification to 1 and 7 days of aging when comparing emulsions with the same oil concentration (Figure 7.12). It indicates that the SLs from WOC are efficient stabilizing water-almond oil emulsions, even using 0.01% surfactant and high oil concentrations of 20% by weight.

Emulsions were systematically assessed under an optical microscope. As an example, Figure 7.13 display images of 0.1% surfactant emulsions at different oil concentrations. The emulsion droplets appear as disperse or non-interacting. The images clearly show how the emulsion droplet sizes increase with the increment in oil concentration.

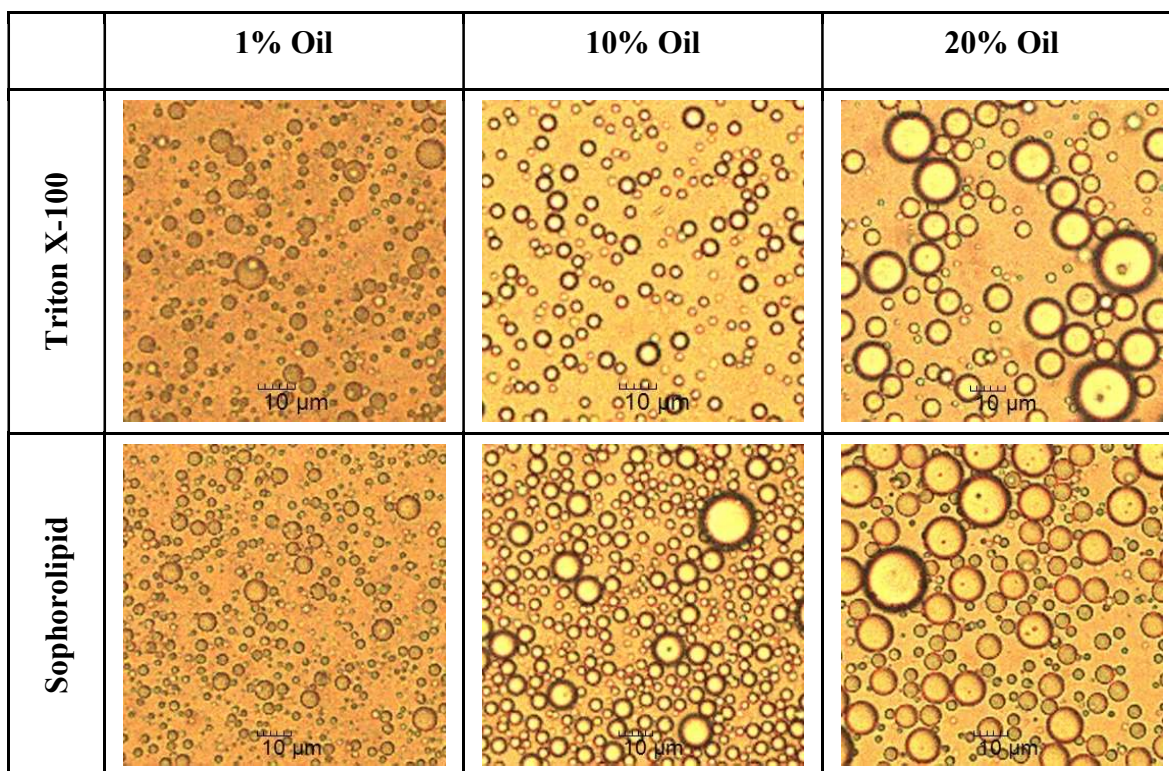














**Figure 7.13.** Optical microscopy images of water-almond oil emulsions after 7 days of aging at different oil concentrations.

### Effect of SLs on the emulsion phase stability

The emulsion phase stability is also an indicator of how a surfactant will perform as an emulsifier. Ideally, the emulsion phase should be homogeneous and without oil separation or surfactant precipitation. Emulsion phase stability was evaluated herein by taking photographs of the emulsions at the immediate time and after 1 and 7 days of

aging. Figure 7.14 shows photographs of the 10% almond oil emulsions at the different aging times. As can be observed, the images of the emulsions immediately after they were made show a large amount of foam, which obscured the separation of phases. Although none of the emulsions of this work showed oil separation or surfactant precipitation, they all show creaming (Figure 7.14), which is expected due to the small particle sizes of the emulsions (Koh et al., 2016). Little changes are observed in the creaming phase after 7 days, which indicates that the emulsion phase is stable after 1 week of aging.













	Triton X-100			Sophorolipid		
	Immediate	1 day	7 days	Immediate	1 day	7 days
0.01% surfactant						
0.1% surfactant						

**Figure 7.14.** Photographs of water-almond oil emulsions with 10% oil at immediate time and after 1 and 7 days of aging.

Physical appearance of all the emulsions tested after 7 days aging is of display in Figure 7.15. All emulsions show a homogeneous creaming phase similar to the one described above. As expected, the creaming phase is bigger at higher oil concentrations. Any of the emulsions tested showed oil separation or precipitation across the aging



times, even after 7 days for emulsions where the oil concentration was 2,000 times that of surfactant by weight.

	Triton X-100			Sophorolipid		
Oil	1%	10%	20%	1%	10%	20%
0.01% surfactant						
0.1% surfactant						

**Figure 7.15.** Photographs of water-almond oil emulsions after 7 days of aging.

### 7.3.6. Displacement activity

Oils spills, from the petrochemical industry or ships, in the marine environment are a problem of major concern due to the large surface area of sea water that cover quickly. In this section, displacement activity was determined as a measure of surfactant capacity to “herd” or push the borders of a diesel slick to decrease the surface area covered by released diesel (Buist et al., 2017). A larger displacement activity indicates that a surfactant is better able to herd an oil slick for burning (Koh et al., 2017).

Figure 7.16A and B show the diesel displacement activity of the SL natural mixture and Triton X-100 on deionized water at 30 s and 300 s after application, respectively. As can be observed, displacement activity was similar between the two time points. Diesel displacement was 1.3 cm after 300 s at 0.1 mg mL<sup>-1</sup>, while at 0.5 mg mL<sup>-1</sup> diesel

displacement was 4.3 cm. Therefore, surfactant concentration clearly affects the diesel displacement activity: the more concentrated the surfactant, the higher diesel displacement.

Triton X-100 performed better than the SL natural mixture, especially at 0.1 mg mL<sup>-1</sup>, which is in contrast with the observed in the previous sections for emulsions. These results agree with the ones published by Koh et al., (2017), who used a mixture of acidic and lactonic C18:1 SL (ratio 1:1 w/w) to displace crude oil and found a better performance of the Triton X-100. However, the use of SL esters as the ethyl ester SL and the hexyl ester SL worked similarly than the commercial surfactant Triton X-100 (Koh et al., 2017). More information about SL esters is provided in the following section.

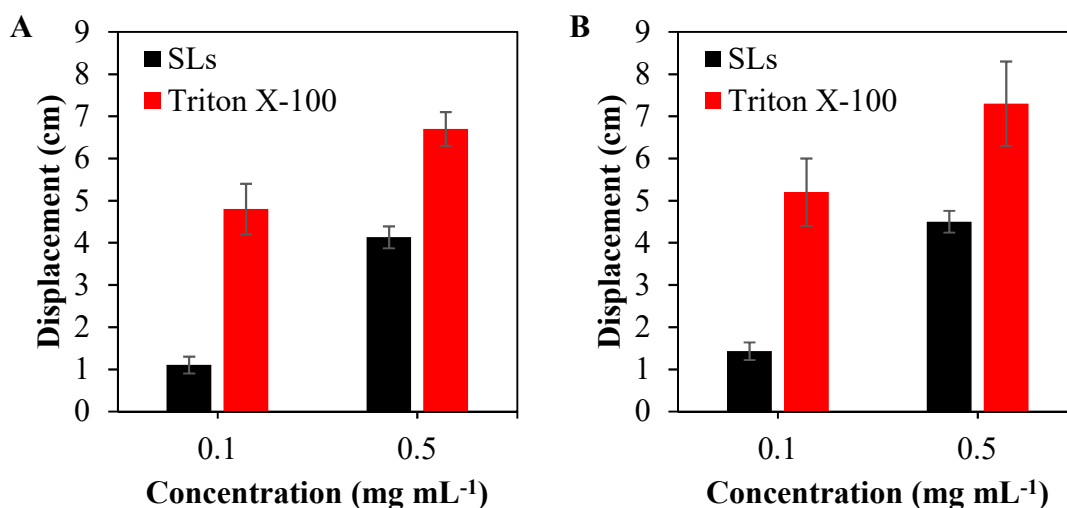


**Figure 7.16.** Diesel displacement by SLs and Triton X-100 after 30 s (A) and 300 s (B).

### 7.3.7. Interfacial properties of the ethyl ester SL

In this section, the crude SL natural mixture from WOC was chemically modified to form the ethyl ester SL (EESL) as described in Chapter 3, section 3.6.4 (Figure 7.17). It means that the fatty acid tail was enlarged from 18 to 20 carbons. It has been reported that elongation of the fatty acid tail improves the physicochemical properties of the SLs (Zhang et al., 2004). Proper synthesis and purification of the EESL was confirmed by LC-MS (Annex IV).

SL esters have shown an excellent surface tension lowering capacity. For example, the synthesized EESL decreased the surface tension in a water-air interface from 72.0 to 38.3 mN m<sup>-1</sup>, with a CMC value of 38.4 mg L<sup>-1</sup> (Annex IV). These values agree with those previously reported by Zhang et al. (2004). The same authors demonstrated that the CMC of SL esters decreases to about 1/2 per additional CH<sub>2</sub> group to the alkyl ester moiety. This improvement in their physicochemical properties can increase the performance and the market price of the SL molecules (Ashby et al., 2008; Koh et al., 2016).

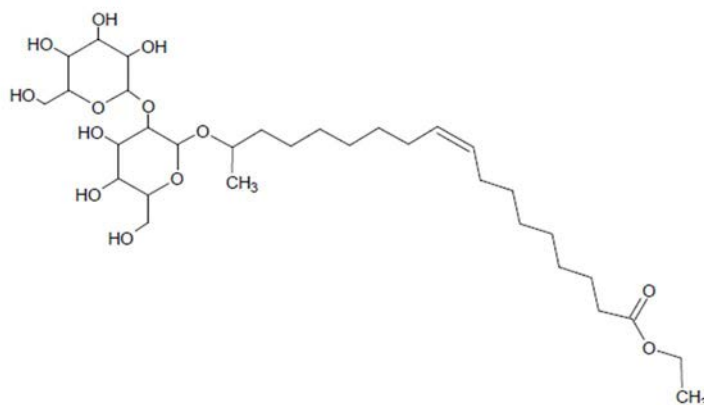


**Figure 7.17.** Molecular structure of the ethyl ester sophorolipid.

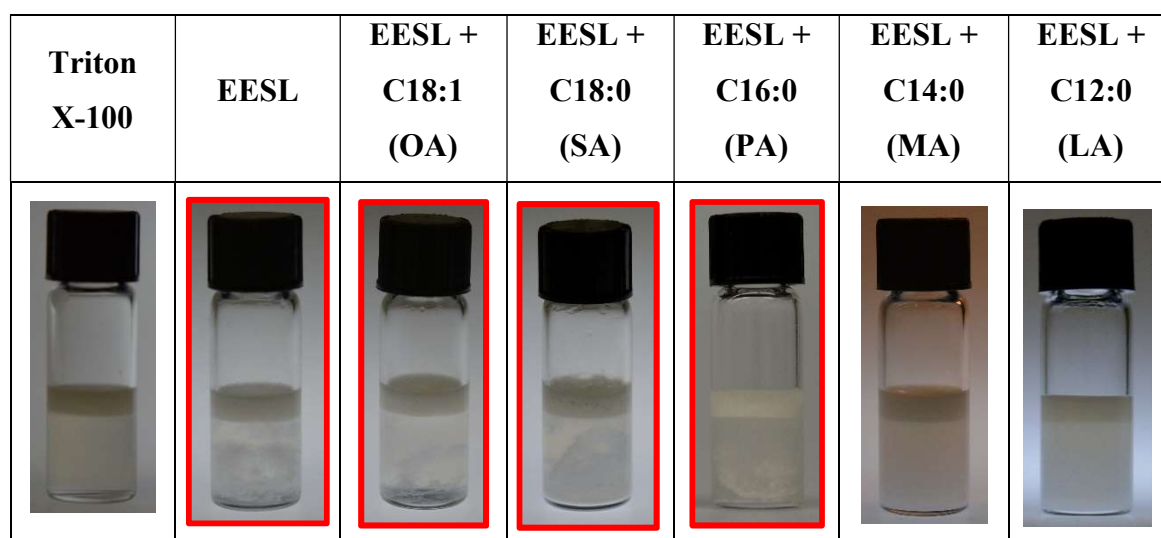
Despite the good surface tension lowering capacity of the SL esters (Zhang et al., 2004) and their excellent displacement capacity (Koh et al., 2017), their performance as emulsifiers have shown some problems associated with the emulsion phase stability such as surfactant precipitation or oil separation, which could be a drawback when formulating a new product (Koh et al., 2016; Koh and Gross, 2016a; Koh and Gross, 2016b). Co-surfactants can provide added emulsion stability by reducing interfacial tension, increasing viscosity, or improving solubility among others. The research group at RPI has previously studied the effect of using n-alkyl alcohols as co-surfactants in SL ester emulsions with interesting results (data not published).

The results shown below are focused on the effect of using fatty acids as co-surfactants in EESL emulsions. Emulsions were prepared with 10% almond or lemon oil by weight and 1% surfactant by weight. For emulsions with co-surfactants, a 0.5% surfactant by weight and a 0.5% co-surfactant by weight were used. The fatty acids tested were oleic acid (C18:1), stearic acid (C18:0), palmitic acid (C16:0), myristic acid

(C14:0) and lauric acid (C12:0). All the fatty acids were of analytical grade ( $\geq 95\%$  of purity, Sigma-Aldrich). Analysis of emulsions was performed immediately after emulsification and after 1, 7 and 28 days of aging at 25 °C. Since the photographs obtained at these days were very similar, only the photographs at day 7 are shown. The common commercial non-ionic surfactant Triton X-100 was used as reference. These results should be considered as a small contribution to a project currently being performed at RPI.

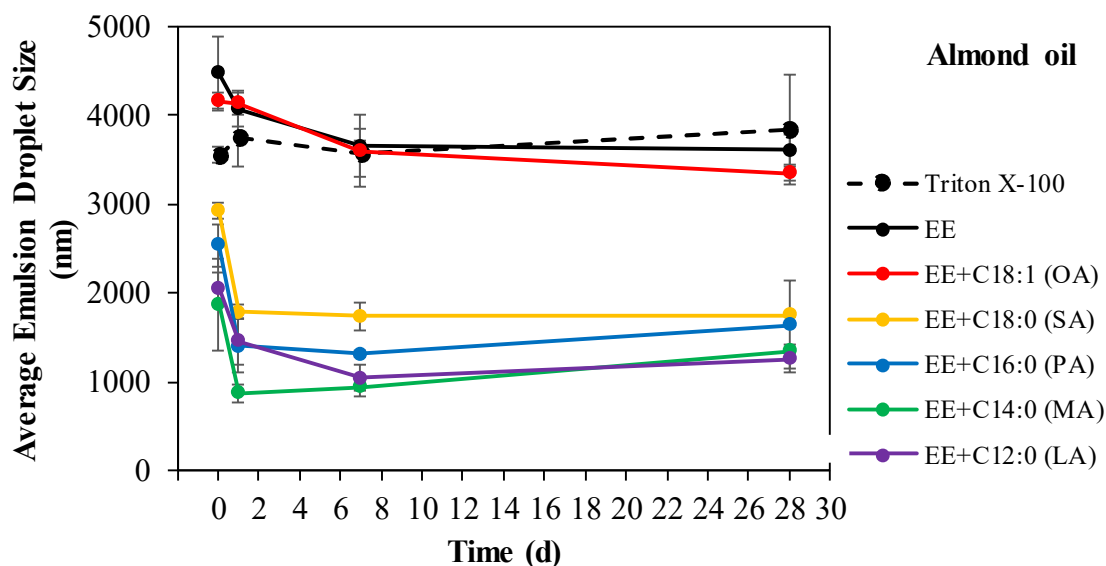
### Fatty acids as co-surfactants in almond oil emulsions

Figure 7.18 shows photographs of the almond oil emulsions of Triton X-100, EESL and EESL + fatty acids after 7 days of aging. As can be observed, EESL emulsion show surfactant precipitation. The addition of oleic acid (C18:1), the only unsaturated fatty acid tested, had any effect on the emulsion phase stability and precipitation was also observed (Figure 7.18). It makes sense considering that the oleic acid is indeed the major component of the almond oil, presented in about a 70% (Shi et al., 1999). Precipitation was also observed in two of the saturated fatty acids tested (C18:0 and C16:0), while for the other two (C14:0 and C12:0) a creamy and viscous stable phase was obtained (Figure 7.18). Since all these fatty acids are white solids, the precipitate could be fatty acid, surfactant, or a mixture of both.



**Figure 7.18.** Photographs of water-almond oil emulsions after 7 days aging. Photographs outlined in red show precipitation.

Figure 7.19 shows the mean droplet sizes of almond oil emulsions over 28 days. Similar droplet sizes of around 4,000 nm were obtained for emulsions with EESL and the commercial surfactant Triton X-100 without significant differences between them. As expected, the addition of oleic acid had any significant effect on the emulsion droplet sizes. However, the addition of the saturated fatty acids (C18:0, C16:0, C14:0 and C12:0) decreased the average emulsion droplet sizes to values ranging from 1,000 to 2,000 nm (Figure 7.19). From a kinetic point of view, smaller emulsion droplet sizes display more stable emulsions (Solans et al., 2005). In fact, all the emulsions tested showed stability for a period of 28 days. It should be noticed that the average droplet sizes immediately after emulsion formation are higher than at 1, 7 and 28 days, which is attributed to the formation of foam. The instrument used to measure droplet sizes (Chapter 3, section 3.6.3) does not distinguish between air bubbles and emulsion droplets, which will overestimate the average droplet sizes (Koh et al., 2016). It is surprising that although all the saturated fatty acids decreased the emulsion droplet sizes improving the emulsion droplet stability, only the C14:0 and the C12:0 showed an improvement in the emulsion phase stability.



**Figure 7.19.** Average emulsion droplet sizes of water-almond oil emulsions immediately after emulsification and after 1, 7 and 28 days of aging. Results are expressed as mean  $\pm$  standard deviation of three replicates.

### Fatty acids as co-surfactants in lemon oil emulsions

In contrast with the observed for almond oil emulsions, lemon oil emulsions with EESL displayed good emulsion phase stability (Figure 7.20). This is in agreement with the findings previously reported by Koh and Gross (2016a). The different behaviour between emulsions with almond and lemon oil can be attributed to the chemical compositions of the oils, which are totally different. While the almond oil is primarily composed by triglycerides of oleic acid and linoleic acid, the lemon oil is composed of a mixture of a wide variety of terpenes as limonene (Rao and McClements, 2012; Shi et al., 1999). Despite the good emulsion phase stability of lemon oil emulsions with EESL, it is interesting to study the effect of fatty acids on their emulsion properties to understand how they would perform in a new formulation.

Addition of fatty acids to lemon oil emulsions with EESL displayed stable emulsion phases without precipitation or oil separation (Figure 7.20). Figure 7.21 shows mean droplet sizes of lemon oil emulsions of Triton X-100, EESL and EESL + fatty acids over 28 days. Droplet sizes of around 1,500 nm were obtained for emulsions with only EESL, which kept stable for 28 days. These values agrees with the ones reported in the literature (Koh and Gross, 2016a). It should be noticed that emulsion droplets of lemon oil emulsions with EESL are almost 3 times smaller than the ones of almond oil emulsions using the same surfactant, which might be cause by the different chemical structures of the oils.

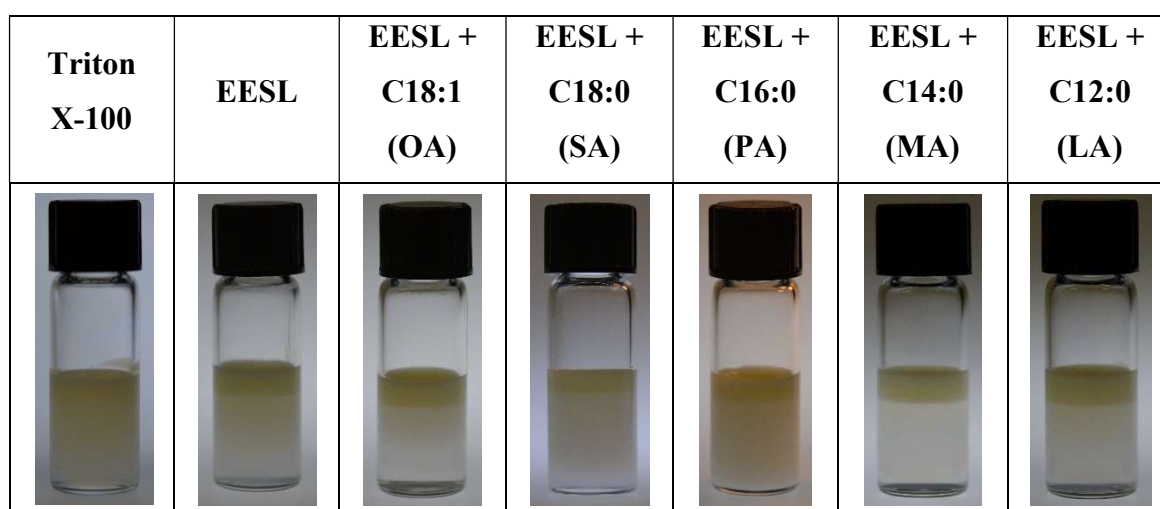


**Figure 7.20.** Photographs of water-lemon oil emulsions after 7 days aging.

The addition of fatty acids C18:1, C18:0 and C16:0 decreased the droplet sizes to 200 nm immediately after the emulsion was made. The emulsion droplets gradually increased their size during the 28 days aging to reach values above 3,000 nm (Figure 7.21). It means that the addition of these fatty acids destabilizes the emulsion droplets, which will inevitably break down in oil droplets. In contrast, the addition of fatty acids C14:0 and C12:0 gave emulsion droplets stable for the 28 days.

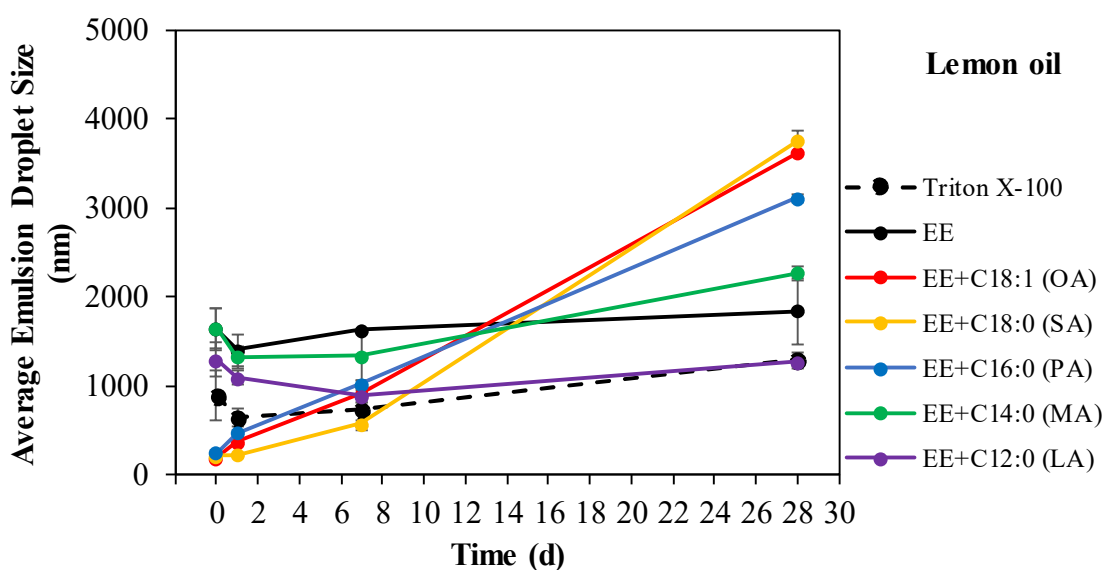


**Figure 7.21.** Average emulsion droplet sizes of water-lemon oil emulsions immediately after emulsification, after 1, 7 and 28 days of aging. Results are expressed as mean  $\pm$  standard deviation of three replicates.

#### 7.4. Conclusions

The crude SL natural mixture from WOC was characterized in terms of the structure of the SLs and their interfacial properties. LC-MS revealed a complex mixture of SLs containing both acidic and lactonic SLs with different fatty acid tails. The diacetylated C18:1 lactonic SL was found to be the most abundant SL of the mixture followed by the correspondent acidic form. This is consistent with oleic acid (C18:1) as the predominant fatty acid in the WOC. SLs produced by SmF using oleic acid showed a similar composition to the SLs produced from WOC, indicating that the technology used for their synthesis do not influence the structures of SLs.

The surface tension lowering capacity of the SLs synthesized herein was similar to those reported in the bibliography for SLs produced from other substrates under SmF.

Specifically, the SLs of this work decreased the surface tension in a water-air interface from  $72.0 \text{ mN m}^{-1}$  to  $34.2 \text{ mN m}^{-1}$ , with a critical micelle concentration value of  $40.1 \text{ mg L}^{-1}$ . The critical micelle concentration was greatly affected by temperature in a range of values from 15 to 50 °C: the higher the temperature, the higher the critical micelle concentration. These SLs showed excellent properties as emulsifiers in emulsions of almond oil, with similar results than the ones obtained for Triton X-100, a common non-ionic commercial surfactant. The emulsions were stable even when the oil concentration was 2,000 times that of surfactant by weight. The SL natural mixture was also evaluated for diesel displacement but better results were obtained for Triton X-100.

The ethyl ester SL was successfully synthesized and characterized. The use of fatty acids as co-surfactants in almond and lemon oil emulsions with the ethyl ester SL showed different effects on the overall emulsion stability, which were attributed to the chemical composition of the oils. More research is needed to understand how the fatty acids affect the interfacial properties, the viscosity or the solubility of the water-almond oil and water lemon oil emulsions with the ethyl ester SL.





## CHAPTER 8

---

### *Sophorolipids from stearic acid by SSF: process optimization and characterization*

*A modified version of this chapter has been submitted to Journal for Cleaner Production.*

*Production and characterization of sophorolipids from stearic acid by solid-state fermentation, a cleaner alternative to chemical surfactants.*

*Jiménez-Peñalver, P., Castillejos, M., Koh, A., Gross, R., Sánchez, T., Font, X., Gea, T.*

*Part of this chapter has been presented on the international congress: 10<sup>th</sup> World Congress of Chemical Engineering, 2017, Barcelona.*

*Sophorolipids from the solid-state fermentation of stearic acid.*

*Jiménez-Peñalver, P., Koh, A., Gross, R., Sánchez, T., Font, X., Gea, T.*



## Summary

This chapter focuses on SL production from stearic acid (SA, C18:0), a low-cost carbon source that is difficult to work with in SmF since it remains as a solid during fermentations due to its high melting temperature. Consequently, optimizations of SSF inoculated with *S. bombicola* were studied for conversions of SA and molasses (MOL) to SLs. Polyurethane foam (PUF) functioned as the inert support. The effect of PUF density and water holding capacity (WHC) was assessed and the process was optimized in terms of substrate and inoculum ratio. The best conditions were: PUF with a density of  $32 \text{ kg m}^{-3}$  at 75% WHC, 1.17:1 MOL/SA (w/w) and 5% (v/w) inoculum, to obtain a yield of 0.211 g SLs per g of substrates. Mass spectrometry revealed that the SLs produced herein had high contents of diacetylated acidic and lactonic C18:0 SLs. The results of interfacial properties studies revealed that C18:0 SLs had promising surface tension lowering capacity, emulsification behavior and displacement activity.

## 8.1. Materials

The substrates used for SSF were MOL and SA, which are illustrated in Figure 8.1. Characteristics of MOL are detailed in Table 6.1. SA (analytical grade > 95%) was provided from Sigma-Aldrich (St. Louis, MO, USA). Polyurethane foam of density  $25 \text{ kg m}^{-3}$  (PUF-25) was purchased from Servei Estació (Barcelona, Spain), while McMaster-Carr (Elmhurst, IL, USA) provided PUFs with densities of 32 and  $45 \text{ kg m}^{-3}$  (PUF-32 and PUF-45). PUF sheets were cut into cubes of 6x6x6 mm, copiously washed with distilled water, and then dried at  $65 \text{ }^\circ\text{C}$  overnight (Figure 8.1). PUF cubes were analysed under the scanning electron microscope (SEM) (Annex V).



**Figure 8.1.** Physical appearance of the sugar beet molasses (left), the stearic acid (center), and the PUF cubes (right).

## 8.2. Experiments

Fermentations were performed in 0.45-L cylindrical polyvinylchloride packed-bed bioreactors in the Fermentation System I (Chapter 3, section 3.2.1) containing, unless otherwise indicated, 65 mL of media (substrates, water and inoculum) impregnated in PUF cubes. Substrates (total of 30 g dry wt.) consisted of a predetermined mixture of MOL and SA. The final water content was set at 50%. The fermentation media was prepared by dissolving MOL in distilled water, and subsequently adjusting the pH to  $6.0 \pm 0.1$  with 0.1 M HCl. Then, SA was added to the media and the mixture was heated at 80 °C until stearic acid melting was complete. The PUF cubes were impregnated with the fermentation media, the resulting SSF mixture was sterilized (121 °C, 30 min) and, after cooling, was inoculated with fresh inoculum (Chapter 3, section 3.1.2).

Fermentation experiments were performed at 30 °C with an aeration rate of 0.45 L air kg<sup>-1</sup> total wet mass min<sup>-1</sup>. The oxygen concentration in the exhaust gases was recorded and used for the calculation of the OUR and the COC (Chapter 3, section 3.3). The SSF was mixed every 2 days, unless otherwise indicated, as described in Chapter 5, section 5.3.4. Intermittent mixing increases the bioavailability of substrates to the yeast favouring the production of SLs.

At sampling times, one reactor was terminated and, prior to its analysis, the collected material was manually homogenized with a metal spatula. pH and water content were determined according to Chapter 3, section 3.4. The protocol to determine SL yield was slightly modified from the one described in Chapter 3, section 3.5. When we started working with this SSF mixture, SLs did not precipitate properly after evaporation of ethyl acetate and addition of *n*-hexane for washings, probably due to the bad solubility of SA in *n*-hexane. Consequently, SA was firstly removed from the sample and then the SLs were extracted. This protocol is longer but ensures proper measurements of SL yield. Thus, SA was extracted from the fermentation mixture by mixing 10 g of the material with hexane in a 1:10 (w/v) ratio at 200 rpm for 1 h. This extraction protocol on the 10 g sample was repeated three times. Then, SLs were extracted from the fermentation by mixing 10 g of the material with ethyl acetate in a 1:10 (w/v) ratio at 200 rpm for 1 h. This extraction protocol with the 10 g sample was repeated twice. During the time course experiment (section 8.3.4), a third extraction was carried out to ensure maximum SL recovery. Solvent extractions were pooled together,

filtered through a Whatman paper Grade 1, and vacuum-dried at 40 °C with a rotary evaporator. SA content and SL yield were determined gravimetrically and expressed as g g<sup>-1</sup> substrates (Equation 3.11). Results were analysed by one-way ANOVA followed by Duncan's test ( $p < 0.05$  confidence level) using SPSS 15.0 software for Windows.

### 8.3. Results and discussion

#### 8.3.1. Effect of PUF density

PUF density is a key parameter to assess prior to further optimization of a new SSF system (Baños et al., 2009). It affects the fermentation matrix mechanical strength, substrate distribution and oxygen transfer within PUF pores. Consequently, PUF density influences microbial growth and SL production. Three PUF densities (25, 32 and 45 kg m<sup>-3</sup>; PUF-25, PUF-32 and PUF-45, respectively) were evaluated.

#### Experiments

WHC of PUF-25, PUF-32 and PUF-45 were determined in 14.5, 13.0 and 9.9 g of water per g of PUF cubes, respectively, following the methodology described in Chapter 3, section 3.4.5. Fermentations were carried out at 75% WHC for each PUF cube type based on the work of Haug et al. (1993). Thus, 6, 6.7 and 8.8 g of PUF-25, PUF-32 and PUF-45, respectively, were impregnated with the 65-mL fermentation media (Figure 8.2). The ratio of the substrates was 1:1 (15 g each), the inoculum added was 10% (v/w), and experiments were performed in triplicate for 7 days.



**Figure 8.2.** Pictures of the 3 polyurethane foam (PUF) with different densities with the 65-mL fermentation media in the reactor.

## Results

Figure 8.3 shows that PUF-32 and PUF-45 resulted in higher SL yields ( $\text{g L}^{-1}$ ) than PUF-25, with no significant differences between PUF-32 and PUF-45 based on Duncan's test ( $p < 0.05$ ). In other words, both foams would give the same SL volumetric yield. However, the highest substrate conversion was attained using PUF-32 ( $0.108 \text{ g g}^{-1}$  substrates). Furthermore, PUF-45 has 25% lower WHC than PUF-32 so, consequently, more PUF-45 cubes are needed to hold the same volume of media. For these reasons, we selected PUF-32 for the additional studies discussed below.

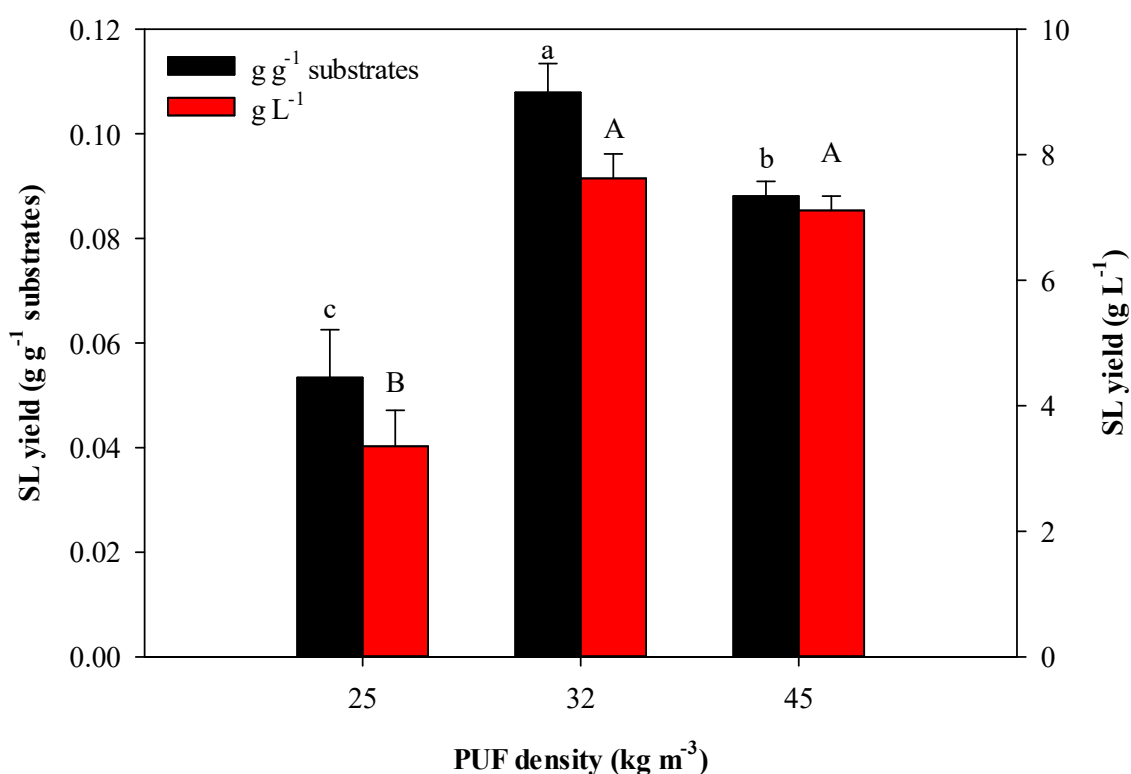


**Figure 8.3.** SL yield obtained for 3 different polyurethane foam (PUF) densities. Results are expressed as mean  $\pm$  standard deviation of three replicates. Means with the same letters are statistically equal per Duncan's test ( $p < 0.05$ ).

### 8.3.2. Optimization of substrates ratio and inoculum size

To maximize sophorolipid production with respect to the parameters MOL/SA ratio and inoculum size, experimental design was performed using Central Composite Design (CCD).

## Experiments

Ratio MOL/SA and inoculum size were evaluated at 3 levels with 5 replicates at the central point in 13 different trials (Table 8.1). The ratio MOL/SA (S, w/w) was fixed at 1:3, 1:1 and 3:1 (normalized values  $-1$ ,  $0$ ,  $1$ , respectively), and the inoculum size (I, % v/w) was fixed at 5, 10 and 15 (normalized values  $-1$ ,  $0$ ,  $1$ , respectively). SL yield ( $\text{g g}^{-1}$  substrates) at day 7 of fermentation was the response (Y). PUF cubes were saturated at the 75% WHC.

**Table 8.1.** Central Composite Design (CCD) matrix for the optimization of the ratio of substrates and inoculum size to produce SLs with the coded and real values for the variables and the experimental and predicted values for the response.

Run	S: Ratio MOL/SA		I: Inoculum size		Y: SL yield	
	(w/w)		(% v/w)		$(\text{g g}^{-1} \text{ substrates})$	
	Coded	Real	Coded	Real	Experimental	Predicted
1	1	3:1	-1	5	0.102	0.099
2	-1	1:3	1	15	0.079	0.080
3	1	3:1	0	10	0.096	0.099
4	-1	1:3	0	10	0.079	0.080
5	0	1:1	0	10	0.119	0.120
6	0	1:1	0	10	0.125	0.120
7	0	1:1	0	10	0.107	0.120
8	0	1:1	-1	5	0.114	0.120
9	0	1:1	0	10	0.117	0.120
10	1	3:1	1	15	0.097	0.099
11	-1	1:3	-1	5	0.082	0.080
12	0	1:1	1	15	0.133	0.120
13	0	1:1	0	10	0.119	0.120

## Results

The maximum and minimum SL yields obtained were run 12 ( $0.133 \text{ g g}^{-1}$  substrates) and run 2 ( $0.079 \text{ g g}^{-1}$  substrates), respectively (Table 8.1). The low variability ( $< 6\%$ ) of the central points (runs 5, 6, 7, 9, 13) is an indicator of the good



reproducibility of experimental data. The experimental data was evaluated using analysis of variance (ANOVA). The parameter inoculum size was non-significant in all the models studied indicating that this parameter is not critical over the range studied in influencing SL production. The following quadratic equation was the best fit of the experimental data and represents SL yield ( $Y$ , g g<sup>-1</sup> substrates) as a function of the ratio MOL/SA ( $S$ ):

$$Y = 0.118 + 9.345 \cdot 10^{-3}S - 0.030S^2 \quad (\text{Eq. 8.1})$$

The proposed model is significant with an  $F$  value of 41.78, obtained by Fisher's  $F$ -test, along with a very low probability value, which is significant at a 95% confidence interval (Table 8.2). The  $R^2$  value of 0.8931 indicates that the model explains 89.31% of total SL yield variability. The predicted  $R^2$  of 0.8480 is in reasonable agreement with the adjusted  $R^2$  (0.8717), which is close to  $R^2$ . Lack of fit was found to be non-significant ( $p = 0.5039$ ) which indicates that Equation 8.1 is adequate to predict SL yield under any combination of the studied variables. Coefficients  $S$  and  $S^2$  were significant ( $p < 0.05$ ) suggesting that the ratio MOL/SA is critical to SL production by SSF (Table 8.2).

**Table 8.2.** Analysis of variance of the fitted model obtained from the CCD for optimal SL yield (g g<sup>-1</sup> substrates).

Source	Sum of squares	Degrees of freedom	Mean squares	F-value	p-value	
Model	$3.421 \cdot 10^{-3}$	2	$1.710 \cdot 10^{-3}$	41.78	< 0.0001	*
A	$5.240 \cdot 10^{-4}$	1	$5.240 \cdot 10^{-4}$	12.80	0.0050	*
A <sup>2</sup>	$2.897 \cdot 10^{-3}$	1	$2.897 \cdot 10^{-3}$	70.76	< 0.0001	*
Residual	$4.093 \cdot 10^{-4}$	10	$4.093 \cdot 10^{-5}$			
Lack of fit	$2.505 \cdot 10^{-4}$	6	$4.175 \cdot 10^{-5}$	1.05	05039	NS
Pure error	$1.588 \cdot 10^{-4}$	4	$3.970 \cdot 10^{-5}$			
Total	$3.830 \cdot 10^{-3}$	12				

$R^2$ : 0.8931; adj  $R^2$ : 0.8717; pre  $R^2$ : 0.8480; C.V.: 6.08; adequate precision: 12.78.

\*Statistically significant (95% confident interval).

NS=Statistically not significant (95% confident interval).

By solving the fitted regression model (Equation 8.1) for maximum SL yield, the optimum MOL/SA (w/w) level is 0.16, which corresponds to the ratio 1.17:1 (16.2 g of MOL and 13.8 g of SA, dry basis). Since non-significant differences were observed between levels for the inoculum size (% v/w), the level -1, which corresponds with 5 % (v/w) of inoculum, was selected for practical and economic reasons. Under these conditions, the optimal predicted SL yield is 0.120 g g<sup>-1</sup> substrates.

### 8.3.3. Effect of PUF saturation in SL yield

The saturation of the inert support can also influence the SSF process. The more saturated the inert support, the more concentrated the substrates and the inoculum in the SSF mixture and, therefore, the better bioavailability of nutrients to the yeast. This would favour biomass growth and SL synthesis, improving the process volumetric yield. However, SSF mixtures that are too water saturated may block PUF pores obstructing oxygen diffusion through the matrix, which may hinder the fermentation process.

## Experiments

In this experiment, PUF-32 cubes were saturated at the 60, 75 and 90% WHC. The same amount of PUF-32 cubes were used to hold 52, 65 and 78 mL of media for fermentations at the 60, 75 and 90% WHC, respectively. The media was prepared according to the optimized values in the previous section. Experiments were performed in triplicate for 7 days.

## Results

Figure 8.4 shows that increasing WHC to 90% did not improve SL yield in terms of g L<sup>-1</sup>, with no significant differences with 75% WHC according to Duncan's test ( $p < 0.05$ ). Additionally, SSF mixtures at 90% WHC produced some leachate during the fermentation. Decreasing WHC to 60% gave significantly similar results as 75% in terms of g g<sup>-1</sup> substrates, but worse performance in terms of g L<sup>-1</sup> (Figure 8.4). Based on the above results PUF-32 was adjusted to 75% WHC for the remaining experiments.

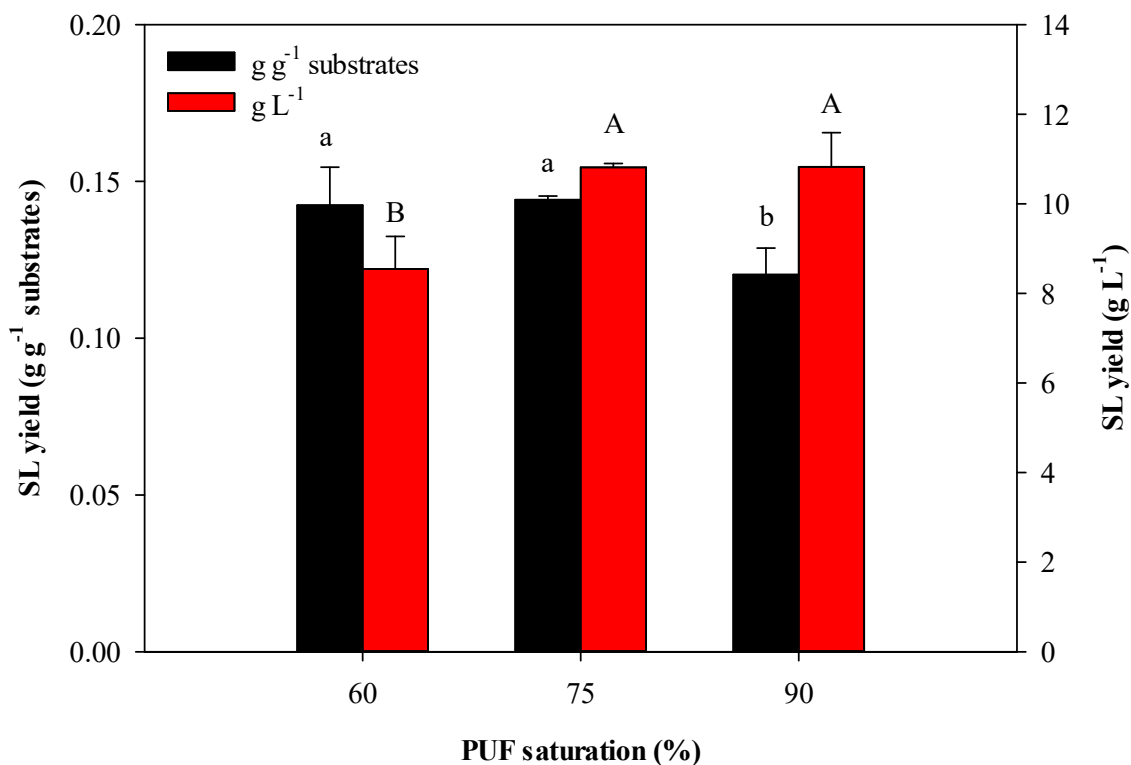


**Figure 8.4.** Effect of PUF saturation in reference to water holding capacity (WHC) on SL yield. Results are expressed as mean  $\pm$  standard deviation of three replicates. Means with the same letters are statistically equal per Duncan's test ( $p < 0.05$ ).

### 8.3.4. Time course

The optimized process was monitored for 16 days under the optimized conditions: PUF with a density of  $32 \text{ kg m}^{-3}$  at 75% WHC, 1.17:1 MOL/SA (w/w) and 5% (v/w) inoculum.

### Experiments

Eight reactors were prepared with the optimal conditions and one of the reactors was terminated for analysis at sampling points (0, 2, 3, 5, 7, 10, 13, and 16 days). In this experiment, reactors mixing was performed every day during the first week and then every 2 days until the end of the process. Analytical results are reported from triplicate samples taken from a single reactor. Viable cell number (CFUs) were determined according to Chapter 3, section 3.5.7. Scanning electron microscope (SEM) analyses were performed at days 0 (before inoculation), 2 and 7 (Chapter 3, section 3.5.8). Total

sugar content was performed as described in Chapter 3, section 3.5 with little modifications:

- Extraction of sugars from the solids was performed using wet solids instead of dried solids.
- The extraction was performed at room temperature instead of at 50 °C.
- The supernatant was extracted twice with ethyl acetate in a ratio 1:1 (v/v) to remove the SLs and avoid interferences in the analyses.

### Process dynamics

Analyses of the optimized process included SL production, substrate consumption, viable cell numbers and by respirometric methods (Figure 8.5). Substantial SL formation occurred by day 2 ( $0.079 \text{ g g}^{-1}$ ) and the maximum SL yield was on day 13 ( $0.211 \text{ g g}^{-1}$ ). Parekh et al. (2012) produced SLs from a SSF mixture consisting of glucose and stearic acid blended with wheat bran and reported a SL yield of  $0.085 \text{ g g}^{-1}$  substrates at day 10, which is 2.2 times lower than the yield obtained in this study on that day.

Gradual sugar consumption occurred until its depletion on day 7 (Figure 8.5A). In contrast, SA consumption occurred gradually such that, by day 16, 30% SA was utilized (Figure 8.5A). Remaining SA may not be easily accessible due to, for example, attachment within PUF pores. In addition, since sugar depletion occurred on day 7, further utilization of SA for SL production should slow or even stop. Interestingly, SL yield ( $\text{g g}^{-1}$  substrates) was directly proportional to SA consumed ( $\text{g g}^{-1}$  substrates), with a proportionality constant of 1.438 (g SL per g of SA consumed) ( $n=8$ ,  $R^2 = 0.985$ ,  $p < 0.001$ ). In Chapter 5 (section 5.3.5), we found that SL yield correlated with fats consumed from the WOC, the hydrophobic carbon source for SL synthesis, with a proportionality constant of 0.805 (g SL per g of fat consumed). This indicates that, in this SSF mixture with SA, there is a better conversion of the hydrophobic carbon source into SLs, probably because of higher substrate purity herein. WOC consists of waxes and triglycerides that requires metabolic conversion to fatty acids prior to use for SL formation. In contrast, stearic acid can be directly incorporated into SL molecules.

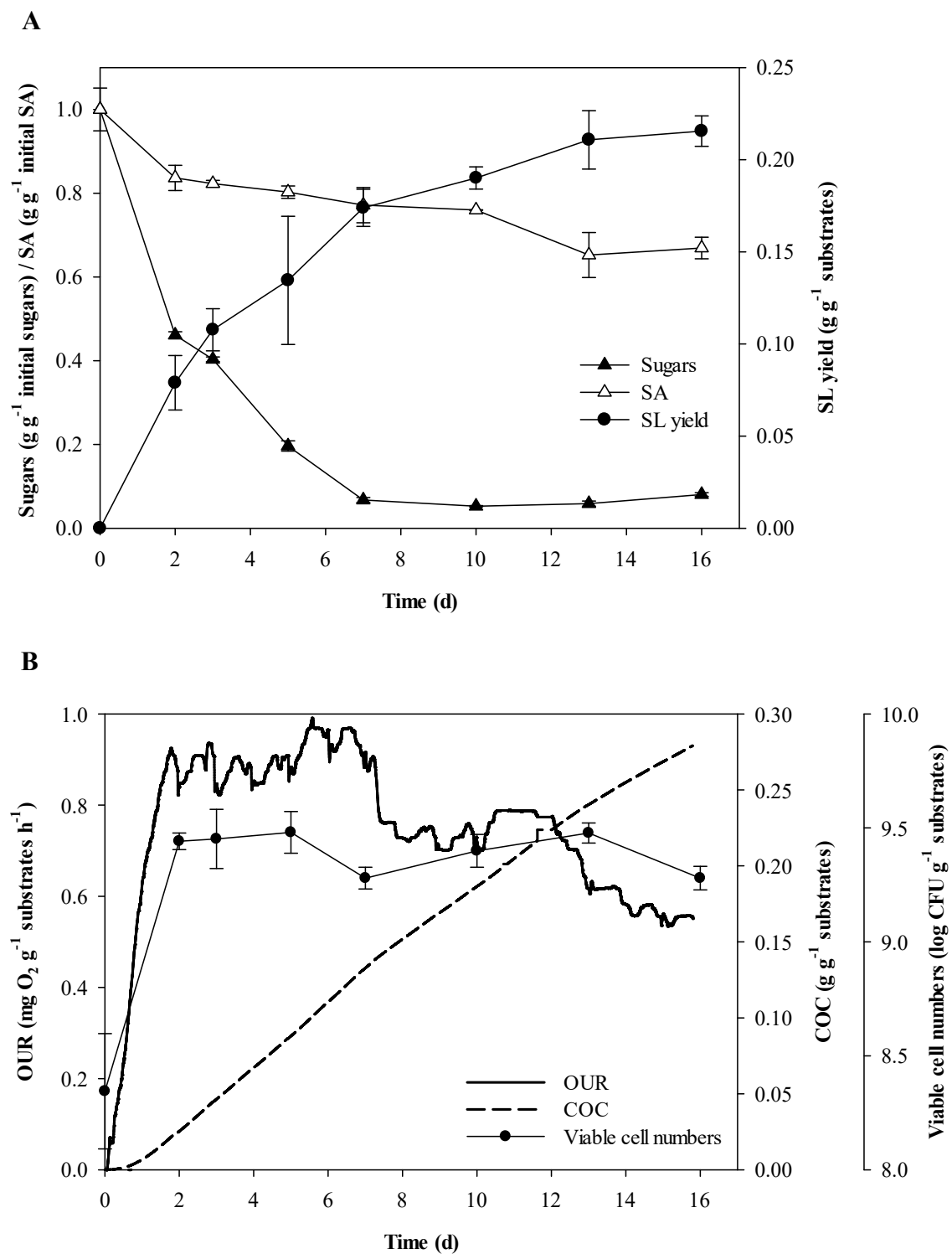


**Figure 8.5.** Solid-state fermentation profile under optimized conditions: (A) time course of SL yield, sugars and SA content; and (B) time course of viable cell numbers, oxygen uptake rate (OUR) and cumulative oxygen consumption (COC) profiles.

*S. bombicola* colonized the solid mixture within the first two days of fermentation. Viable cell numbers increased by one order of magnitude at day 2 ( $2.8 \times 10^9$  compared to  $2.4 \times 10^8$  CFU  $\text{g}^{-1}$  substrates), and no significant growth was observed after that day (Figure 8.5B). This behaviour has also been observed in SmFs with *S. bombicola* (Hu and Ju, 2001; Maddikeri et al., 2015). Figure 8.5B also shows the oxygen uptake rate (OUR) and cumulative oxygen consumption (COC) profiles of the reactor sampled at day 16. OUR reached a value of about 0.9 by day 2, and between days 2 and 7 OUR fluctuated between 0.8 to 1  $\text{mg O}_2 \text{g}^{-1} \text{substrates h}^{-1}$ . With the depletion of sugars at day 7, OUR generally decreased to day 16. Similar OUR profiles were obtained from the rest of the reactors with a variability below 6% (Figure 8.6).

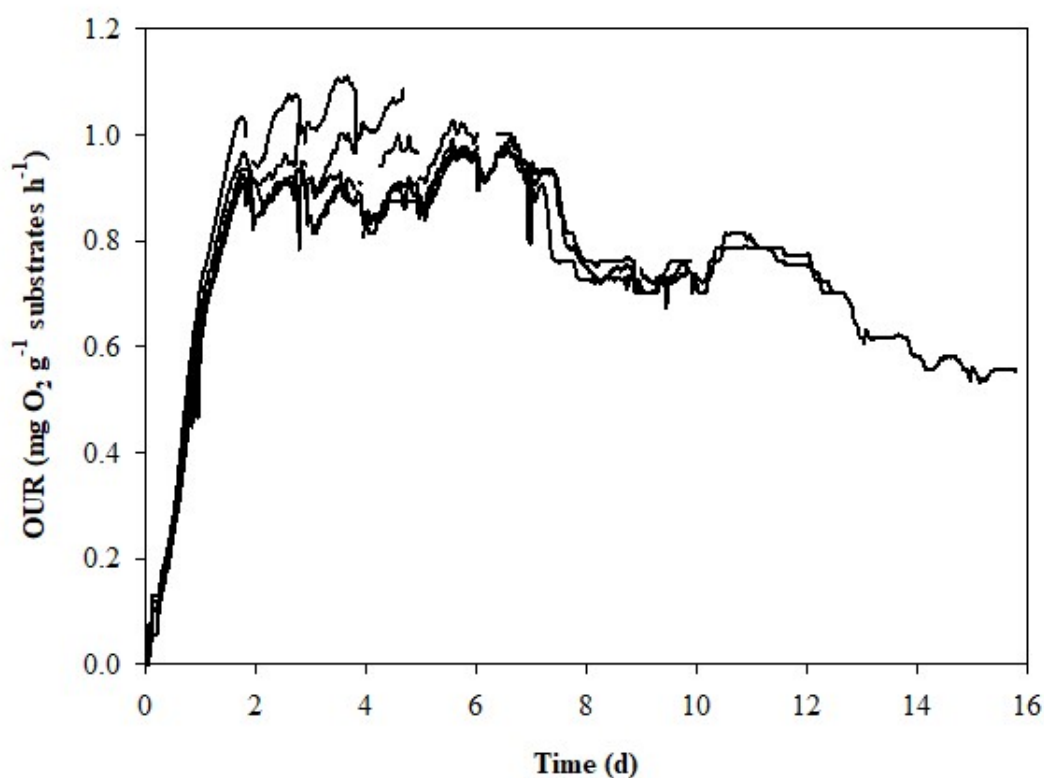


**Figure 8.6.** OUR profiles under optimized conditions.

The oxygen consumed (COC) at the end of the fermentation was  $0.280 \text{ g O}_2 \text{ g}^{-1}$  substrates. The COC values of the experiments performed with PUF-32 (optimization, effect of PUF saturation and time course until day 13) were compiled in the plot displayed in Figure 8.7. The data correlated linearly with a proportionality constant of 0.973 ( $n=27$ ,  $R^2 = 0.985$ ,  $p < 0.001$ ). In the work with WOC, correlation of SL yield with COC gave a proportionality constant of 0.518 ( $\text{g SL per g O}_2$ ) (Chapter 5, section 5.3.5). Therefore, the production of SLs per  $\text{g}$  of  $\text{O}_2$  consumed is almost the double in this SSF mixture.

The SEM images taken after the media was impregnated in PUF cubes confirmed that SA is well-distributed over the surface of the PUF cubes (Figure 8.8). The SEM images taken after 2 and 7 days of fermentation showed that *S. bombycolia* grows on the surface of the foam as dispersed individual cells (Figure 8.8). No granules or biofilm formation was observed.

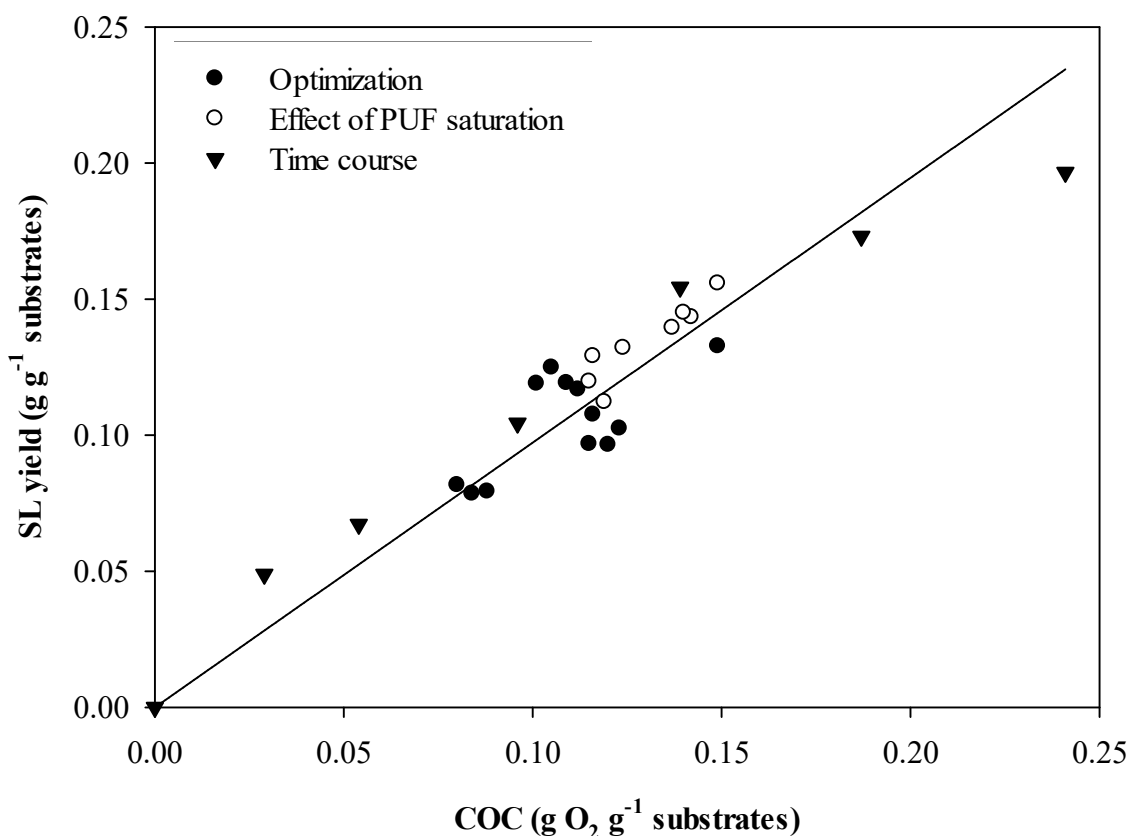


**Figure 8.7.** Correlation between SL yield and cumulative oxygen consumption (COC).

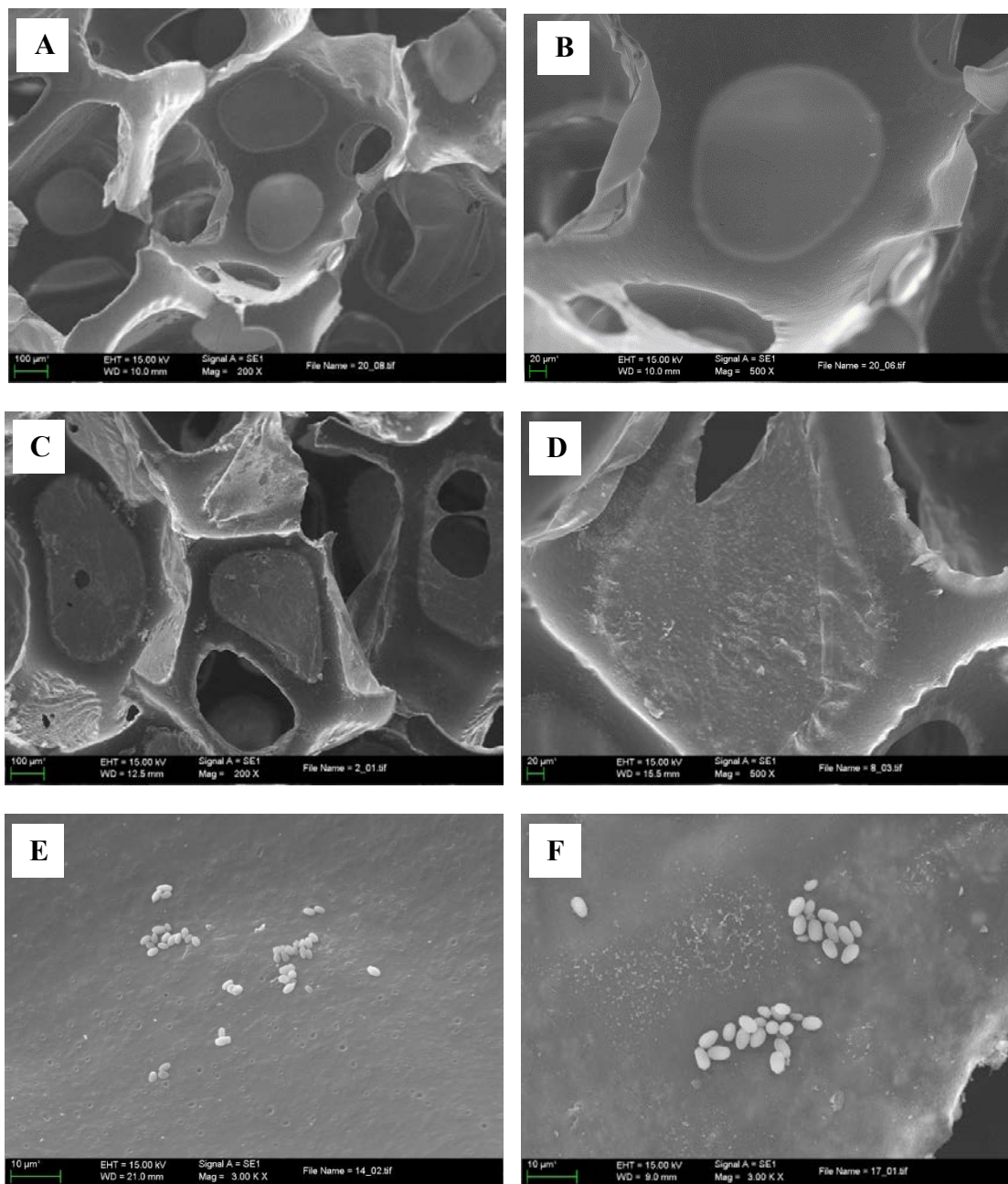


**Figure 8.8.** SEM pictures of PUF-32 (A, B), PUF-32 with the fermentation media (C, D), and PUF-32 after 2 (E) and 7 (F) days of fermentation with dispersed cells attached.



### 8.3.5. Characterization of SLs from stearic acid

Samples collected at day 7 of the time course (section 8.3.4) were used for characterization following the methodology described in Chapter 3, section 3.6.

#### Structural identification

Mass spectrometry was used to identify SL molecules contained in the SL natural mixture produced during SSFs. The mass spectrum shown in Figure 8.9 revealed that SLs consist of a complex mixture containing both diacetylated lactonic SLs (C18:0 and C18:1 with  $m/z = 689.4$  and  $687.4$ , respectively) and diacetylated acidic SLs (C18:0, C18:1 and C16:0 with  $m/z = 707.4$ ,  $705.4$  and  $679.4$ , respectively). Also, the monoacetylated acidic C18:0 SL is observed in the peak  $m/z = 665.4$  but with lower intensity than the corresponding diacetylated structures. The rest of the peaks illustrated in Figure 8.9 correspond to isotopes of the above SLs. For example, for diacetylated acidic 18:0 SL (main peak  $m/z = 707.4$ ) molecular ions ( $M^-$ ) of  $708.4$ ,  $709.4$  and  $710.4$  are observed. Assignment of the peaks from the mass spectra to the corresponding SLs is in agreement with other studies (Ashby et al., 2008; Hu and Ju, 2001).

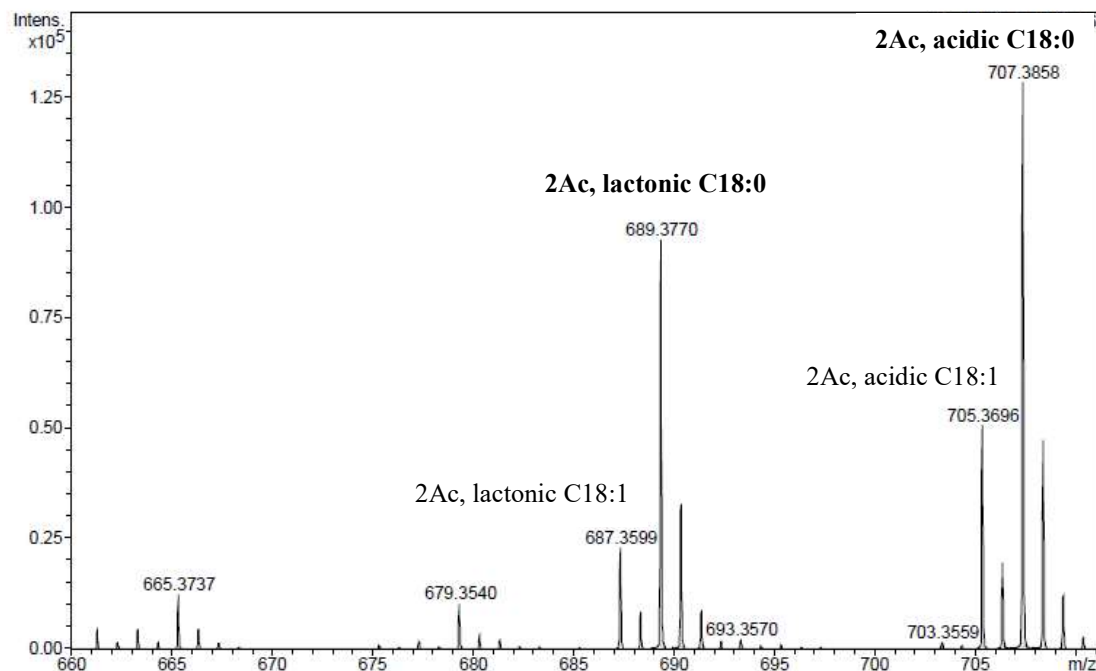
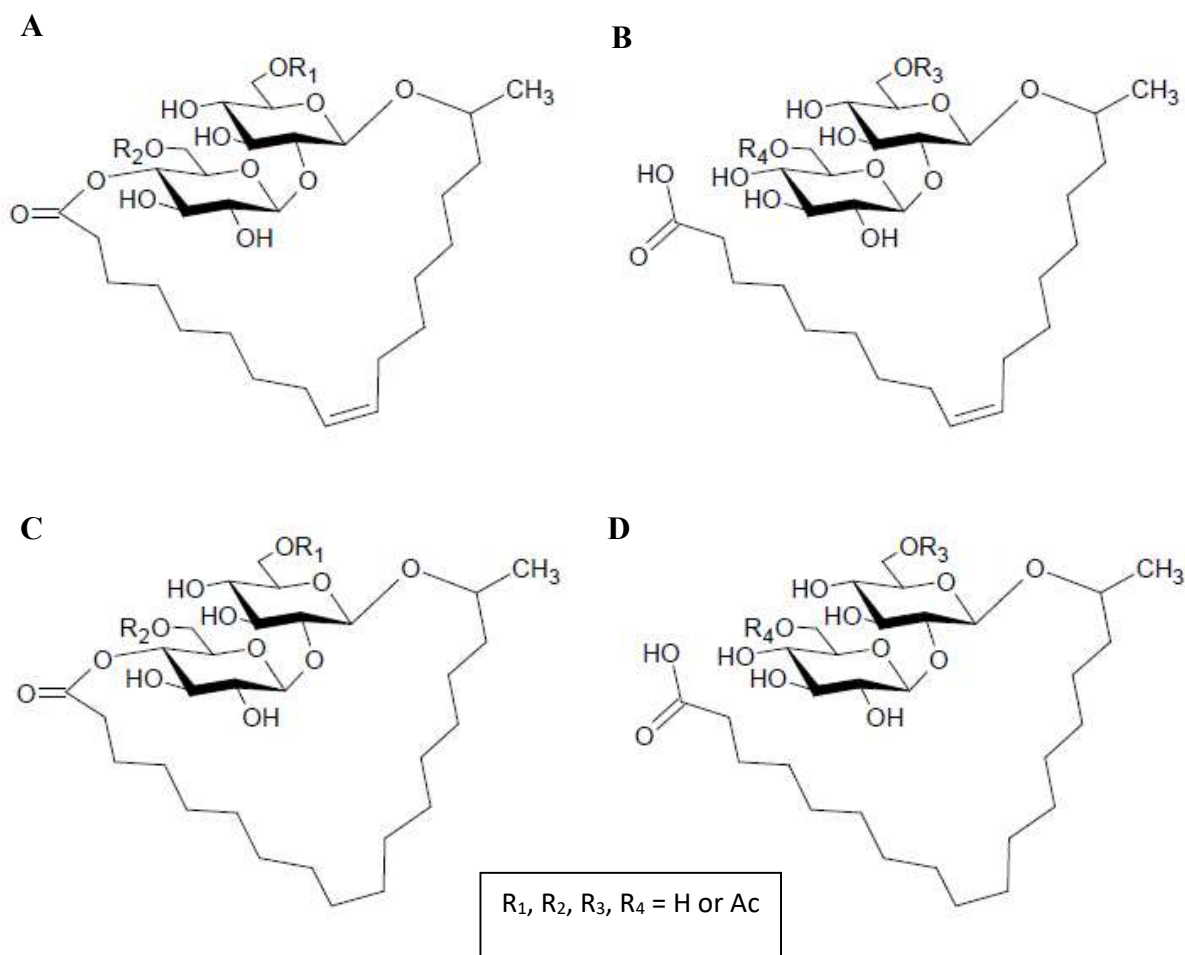


Figure 8.9 Mass spectrometry spectra of the obtained SLs.

Two peaks stand out from the others in the mass spectra:  $m/z = 689.4$  and  $707.4$ , which correspond to the diacetylated lactonic and acidic C18:0 SLs, respectively. The abundance of these two SLs is consistent with stearic acid as the predominant fatty acid in SSF fermentations. The significant presence of C18:1 SLs is due to operative fatty acid metabolic pathways of the yeast that include desaturation prior to the SL synthesis (Brett et al., 1971). Ashby et al. (2008) also produced SLs from stearic acid but by SmF instead of SSF. They also reported formation of SLs with both C18:0 and C18:1 fatty acid substituents where the latter was most abundant. Based on the work herein that uses mass spectrometry to identify the products formed, quantitation of the relative amount of SLs with C18:0 and C18:1 fatty acid substituents is not possible. The diacetylated acidic and lactonic C18:0 and C18:1 SLs are illustrated in Figure 8.10.



**Figure 8.10.** Structures of C18:1 sophorolipids (A) lactonic form and (B) free acid form, and C18:0 sophorolipids (C) lactonic and (D) free form.

### Surface tension

Natural SLs decrease the surface tension at a water-air interface from  $72.0 \text{ mN m}^{-1}$  ( $25 \text{ }^\circ\text{C}$ ) to values ranging from 40 to  $30 \text{ mN m}^{-1}$  with critical micelle concentration (CMC) values from 11 to  $250 \text{ mg L}^{-1}$  (Develter and Laurysen, 2010). The SLs synthesized by SSF herein decreased the surface tension to  $33.8 \text{ mN m}^{-1}$  with a CMC of  $37.9 \text{ mg L}^{-1}$  (Annex V). These values are within the lower range reported in the literature for natural SLs and are very similar to those reported for SLs produced using stearic acid (Ashby et al., 2008).

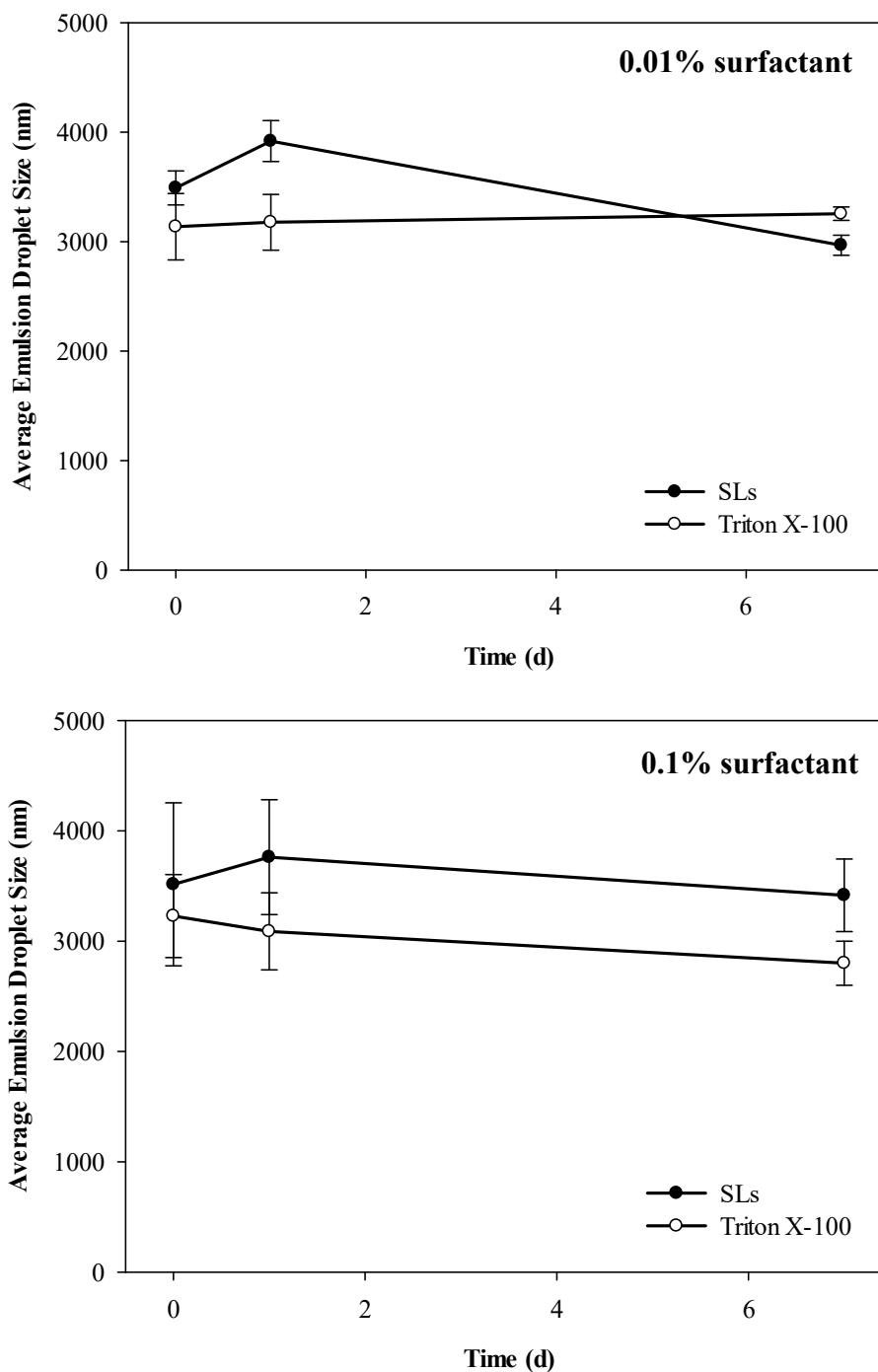
Values of minimal surface tension (mST) and CMC reported in literature are mainly dependent on the composition of SLs. It is well-known that the higher the hydrophobicity of the SL hydrophobic tail, the lower the mST and the CMC (Zhang et al., 2004). In this sense, C18:0 SLs display better interfacial properties than the most common C18:1 SLs because of the higher hydrophobicity of the tail (Ashby et al., 2008). As previously shown in Figure 8.9, SLs produced in this work are a mixture of molecules containing mainly acidic and lactonic C18:0 SLs, which would explain the low mST and CMC values obtained. As would be expected, these values were slightly lower than the ones obtained for the SL natural mixture from WOC, which was rich in C18:1 SLs (Chapter 7, section 7.3.4). Surfactants with low mST and CMC values are desirable to industry because this improves their cost-performance profile that determines their commercial viability.

### Emulsification properties

The emulsion properties of SLs synthesized from stearic acid were assessed at a water-almond oil interface in order to observe the average emulsion droplet sizes and the emulsion phase stability. Emulsions were prepared with 10% almond oil by weight and 0.01 or 0.1% surfactant by total emulsion weight. Analysis of emulsions was performed immediately after emulsification and after 1 and 7 days of aging at  $25 \text{ }^\circ\text{C}$ . Results were compared with those obtained for the commercial non-ionic surfactant Triton X-100.

Emulsion droplet size is an indicator of system stability. The smaller the emulsion droplet size, the more kinetically stable the emulsion and, therefore, the better the efficiency in combating thermodynamic instability (Solans et al., 2005). Mean droplet









sizes of SL emulsions at the immediate time point (time of formation) had values ranging from 3,000 to 4,000 nm, which were similar to those prepared using the commercial surfactant Triton X-100 (Figure 8.11).



**Figure 8.11.** Average emulsion droplet sizes immediately after homogenization and after 1 and 7 days aging. Mean  $\pm$  standard deviation of three triplicates.

All emulsion droplet sizes were stable for 7 days as is evident from the small change in emulsion droplet size from the immediate time after emulsification to 1 and 7 days of aging. Interestingly, the average droplet sizes of 0.01% SL emulsions were similar to 0.1% SL emulsions, which indicates excellent emulsification capacity even at low concentrations. This agrees with the low CMC value of the SLs of this work.

Emulsion phase stability is also an indicator of how a surfactant will perform as an emulsifier. Ideally, the emulsion phase should be homogeneous and without oil separation or surfactant precipitation. Although none of the emulsions of this work showed oil separation or surfactant precipitation, they all show creaming (Figure 8.12), which is expected due to the small particle sizes of the emulsions (Koh and Gross, 2016a). All the emulsions phases were stable for 7 days, even for emulsions where the oil concentration was 1,000 times that of surfactant by weight (Figure 8.12). No visual differences in the emulsification performance of SLs and Triton X-100 were observed.

	Triton X-100		Sophorolipid	
	1 day	7 days	1 day	7 days
<b>0.01% surfactant</b>				
<b>0.1% surfactant</b>				

**Figure 8.12.** Photographs of water-almond oil emulsions after 1 and 7 days.

### Displacement activity

Figure 8.13A and B show the diesel displacement activity of the SL natural mixture from SA and Triton X-100 on deionized water at 30 s and 300 s after application, respectively. As can be observed, displacement activity was similar between the two time points. Regarding the effect of surfactant concentration, at  $0.1 \text{ mg mL}^{-1}$ , diesel displacement was 3.3 cm at 300 s, while at  $0.5 \text{ mg mL}^{-1}$  diesel displacement was 8.0 cm at the same time point. Therefore, surfactant concentration clearly affects the diesel displacement activity: the more concentrated the surfactant, the higher diesel displacement. Triton X-100 performed better than the SL natural mixture at  $0.1 \text{ mg mL}^{-1}$ , but both surfactants show similar results at  $0.5 \text{ mg mL}^{-1}$ .

Figure 8.13 also shows the displacement activity of the SL natural mixture from WOC for comparison (Chapter 7, section 7.3.6). SLs from SA performed threefold and twofold greater than the SLs from WOC after 300 s at concentrations of  $0.1$  and  $0.5 \text{ mg mL}^{-1}$ , respectively. This confirms the better performance of the SL natural mixture from SA (rich in C18:0 SLs) compared to the conventional SL natural mixture rich in C18:1 SLs. This is in agreement with the better surface tension lowering capacity determined previously.

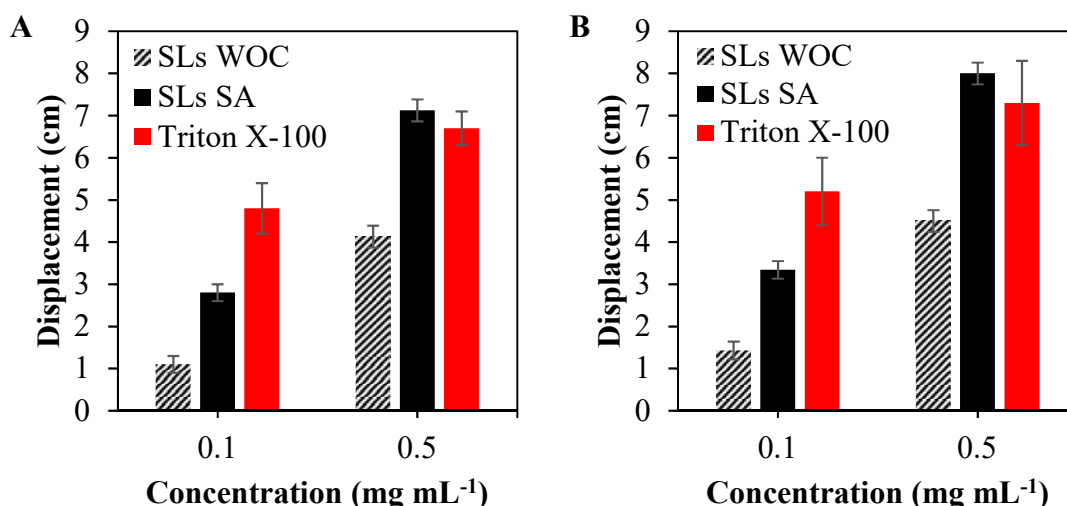


**Figure 8.13.** Diesel displacement by SLs from the winterization oil cake (WOC), SLs from stearic acid (SA) and Triton X-100 after 30 s (A) and 300 s (B).

#### 8.4. Conclusions

Sophorolipids were produced by SSF using stearic acid (C18:0) as the fatty acid carbon source and polyurethane foam as the inert support. The media cost was reduced by replacing glucose and nitrogen source (yeast extract and urea) with sugar beet molasses. Optimization of the fermentation process resulted in a sophorolipid yield of 0.211 g g<sup>-1</sup> substrates. The sophorolipids produced were mainly composed of the diacetylated acidic and lactonic C18:0 sophorolipids, which reflects a preference to form C18:0 sophorolipids when stearic acid is used as the substrate. These sophorolipids exhibited interesting interfacial properties. They decreased the surface tension at an air-water interface to 33.8 mN m<sup>-1</sup> with a CMC of 37.9 mg L<sup>-1</sup>, and showed emulsification properties in water-almond oil interfaces and diesel displacement activities similar to the commercial surfactant Triton X-100. Interestingly, the sophorolipid natural mixture from stearic acid showed better interfacial properties, namely surface tension lowering capacity and displacement activity, than the sophorolipids from the winterization oil cake. This is consistent with the higher content in C18:0 sophorolipids which are more hydrophobic and, therefore, more efficient than the conventional C18:1 sophorolipids.

## CHAPTER 9



### *Conclusions and future work*





The conclusions reached from the results obtained in this research are detailed below:

- Solid-state fermentation was as a suitable technology to produce sophorolipids by the yeast *Starmerella bombicola* using solid hydrophobic substrates as fatty acid carbon sources. Its feasibility was demonstrated herein in two different processes by using an agro-industrial residue, a winterization oil cake, and a pure substrate, stearic acid.
- Several protocols have been validated for the monitoring of the fermentation process including sugars and fats consumption and the monitoring of the yeast growth through the viable cell numbers.
- The media cost was reduced in both solid-state fermentation processes by replacing glucose and nitrogen source (yeast extract and urea) with sugar beet molasses. Molasses contains sugars (78% dry basis), nitrogen (1.9% dry basis) and small amounts of minerals as Mg, Fe, Ca, Zn and Na.
- Winterization oil cake, a residual oil cake that comes from the oil refining industry, was a feasible fatty acid carbon source to produce sophorolipids due to its high fat content (60-70%). The solid-state fermentation process was optimized at 0.5-L scale in terms of substrates ratio (1:4 molasses: winterization oil cake w/w), aeration rate ( $0.30 \text{ L kg}^{-1} \text{ min}^{-1}$ ) and inoculum size (10% v/w) to obtain a yield of 0.199 g of sophorolipids per g of substrates at day 10. Intermittent mixing (at 3, 5 and 7 days) increased sophorolipid yield by 31% to 0.261 g per g of substrates at day 10. The diacetylated lactic C18:1 sophorolipid was the most abundant sophorolipid of the mixture, followed by the correspondent acidic form. This is consistent with oleic acid (C18:1) as the predominant fatty acid in the winterization oil cake. These sophorolipids decreased the surface tension at an air-water interface to  $34.2 \text{ mN m}^{-1}$  with a critical micelle concentration of  $40.1 \text{ mg L}^{-1}$ .
- The SSF process described herein could be further extended to other oil cakes and fat-enriched wastes from food industries.

- The production of sophorolipids from winterization oil cake was proven successfully in a 40-L packed-bed bioreactor with capacity for 6 kg of solid mixture. It means that the process was scaled-up 60 times with similar sophorolipid yields than at 0.5-L scale.
- First attempts to scale-up the process to a 100-L intermittently-mixed bioreactor with capacity for 20 kg of solid mixture showed problems related with mass and heat transfer. More research is needed for the proper operation of this bioreactor.
- Sophorolipids were produced using stearic acid (C18:0) as the fatty acid carbon source and polyurethane foam as the inert support. The effect of polyurethane foam density and water holding capacity was assessed and the process was optimized at 0.5-L scale in terms of substrate and inoculum ratio. The best conditions were: polyurethane foam with a density of  $32 \text{ kg m}^{-3}$  at 75% water holding capacity, 1.17:1 molasses/stearic acid (w/w) and 5% (v/w) inoculum, to obtain a yield of 0.211 g sophorolipids per g of substrates. Sophorolipids produced herein had high contents of diacetylated acidic and lactonic C18:0 sophorolipids, which reflects a preference to form C18:0 sophorolipids when stearic acid is used as substrate. These sophorolipids decreased the surface tension at an air-water interface to  $33.8 \text{ mN m}^{-1}$  with a critical micelle concentration of  $37.9 \text{ mg L}^{-1}$ .
- The sophorolipid natural mixture from stearic acid showed better interfacial properties, namely surface tension lowering capacity and displacement activity, than the sophorolipids from the winterization oil cake. This is consistent with the higher content in C18:0 sophorolipids which are more hydrophobic and, therefore, more efficient than the conventional C18:1 sophorolipids.
- Sophorolipids from both substrates showed excellent properties as emulsifiers in emulsions of almond oil, with similar results than the ones obtained for the Triton X-100, a common non-ionic commercial surfactant. The emulsions were stable even when the oil concentration was 2,000 times that of surfactant by weight.

- Oxygen uptake rate and cumulative oxygen consumption were found to be very useful tools for the on-line monitoring of production of sophorolipids by *S. bombicola* in SSF processes. Monitoring of the cultivation process had been identified as one of the challenges to be addressed for biosurfactant production by solid-state fermentation. In this work, correlations between sophorolipid yield and cumulative oxygen consumption were obtained herein for solid-state fermentations with the winterization oil cake and stearic acid. Proportionally constants of 0.518 and 0.973 (g sophorolipid per g of O<sub>2</sub>) were obtained for fermentations with winterization oil cake and stearic acid, respectively. This indicated that the production of sophorolipids per g of O<sub>2</sub> consumed was almost the double using stearic acid.
- Sophorolipid yield also correlated with fat consumed in both solid-state fermentation processes. Proportionally constants of 0.805 and 1.438 (g sophorolipids per g of fat consumed) were obtained for processes with winterization oil cake and stearic acid, respectively. This indicated that there was a better conversion of the fatty acid carbon source into sophorolipids when using stearic acid, probably because of higher substrate purity.

Regarding future work, there are several issues which should be addressed prior the commercial viability of this process. Some of the research objectives that will be studied by the PhD student Alejandra Rodriguez are detailed below:

1. The screening of other oil cakes from different oil refining industries suitable to produce sophorolipids. By the end of this thesis, the research group has received two new winterization oil cakes with fat contents around 50%, which are lower than the winterization oil cake used herein (60-70%). We have also received two oil cakes called “bleaching oil cakes” or “spent bleaching earths” with fat contents ranging from 25 to 30%. All these oil cakes will be evaluated as potential fatty acid carbon sources to produce sophorolipids. Additionally, polyurethane foams will be studied as inert supports of these fermentations instead of wheat bran.

2. The study of an economic and environmentally friendly methodology for the downstream. In this work, sophorolipids have been extracted from the solid mixture using ethyl acetate and hexane as an analytical tool to measured sophorolipid yield. However, this methodology is unfeasible to be used in large-scale processes since a huge amount of solvents would be needed, even if they are recycled, and the final solids would be impregnated in solvent hampering their disposal or valorization. Supercritical fluid extraction could be presented as an alternative. This technology has been studied for the recovery of other products from solid-state fermentation processes but not for biosurfactants (Martins et al., 2011). Additionally, SLs might be extracted using buffers and separated using membranes.

3. The setup of a HPLC method for an accurate monitoring of the sophorolipid production. In this work, sophorolipid yield has been determined gravimetrically and their structural characterization has been performed just in few samples in a work performed during a research stay. HPLC provides very relevant information about the structures and purity of the sophorolipids produced.

4. The exploration of conditions for the proper operation of the 100-L intermittently-mixed bioreactor. There are some operating variables that can be explored such as the agitation regime, the airflow rate or the humidity and temperature of the inlet air. All these conditions will be studied in a 20-L intermittently-mixed bioreactor prior the final scale-up to 100-L scale.


## *References*

---




- Abraham J, Gea T, Sánchez A. 2013. Potential of the solid-state fermentation of soy fibre residues by native microbial populations for bench-scale alkaline protease production. *Biochem Eng J* 74:15–19.
- Abraham J, Gea T, Sánchez A. 2014. Substitution of chemical dehairing by proteases from solid-state fermentation of hair wastes. *J Clean Prod* 74:191–198.
- Acmite Market Intelligence. 2013. Global Surfactant Market, Market Report, 3rd Edition.
- Adani F, Ubbiali C, Generini P. 2006. The determination of biological stability of composts using the Dynamic Respiration Index: The results of experience after two years. *Waste Manag* 26:41–48.
- Almeira N, Komilis D, Barrena R, Gea T, Sánchez A. 2015. The importance of aeration mode and flowrate in the determination of the biological activity and stability of organic wastes by respiration indices. *Bioresour Technol* 196:256–262.
- Ashby RD, Nuñez A, Solaiman DKY, Foglia TA. 2005. Sophorolipid biosynthesis from a biodiesel co-product stream. *J Am Oil Chem Soc* 82:625–630.
- Ashby RD, Solaiman DKY, Foglia TA. 2008. Property control of sophorolipids: Influence of fatty acid substrate and blending. *Biotechnol Lett* 30:1093–1100.
- Ballardo C, Abraham J, Barrena R, Artola A, Gea T, Sánchez A. 2016. Valorization of soy waste through SSF for the production of compost enriched with *Bacillus thuringiensis* with biopesticide properties. *J Environ Manage* 169:126–131.
- Baños JG, Tomasini A, Szakács G, Barrios-González J. 2009. High lovastatin production by *Aspergillus terreus* in solid-state fermentation on polyurethane foam: An artificial inert support. *J Biosci Bioeng* 108:105–110.
- de Barros EM, Carvalho VM, Rodrigues THS, Rocha MVP, Gonçalves LRB. 2017. Comparison of strategies for the simultaneous saccharification and fermentation of cashew apple bagasse using a thermotolerant *Kluyveromyces marxianus* to enhance cellulosic ethanol production. *Chem Eng J* 307:939–947.
- Berthe L, Druilhe C, Massiani C, Tremier A, de Guardia A. 2007. Coupling a respirometer and a pycnometer, to study the biodegradability of solid organic wastes during composting. *Biosyst Eng* 97:75–88.
- Bisht KS, Gross RA, Kaplan DL. 1999. Enzyme-mediated regioselective acylations of sophorolipids. *J Org Chem* 64:780–789.




- 
- 
- Bordas F, Lafrance P, Villemur R. 2005. Conditions for effective removal of pyrene from an artificially contaminated soil using *Pseudomonas aeruginosa* 57SJ rhamnolipids. *Environ Pollut* 138:69–76.
- Brett D, Howling D, Morris LJ, James AT. 1971. Specificity of the fatty acid desaturases: The conversion of saturated to monoenoic acids. *Arch Biochem Biophys* 143:535–547.
- Buist I, Potter S, Nedwed T, Mullin J. 2017. Herding surfactants to contract and thicken oil spills in pack ice for in situ burning. *Cold Reg Sci Technol* 67:3–23.
- Camilios-Neto D, Bugay C, de Santana-Filho AP, Joslin T, de Souza LM, Sasaki GL, Mitchell DA, Krieger N. 2011. Production of rhamnolipids in solid-state cultivation using a mixture of sugarcane bagasse and corn bran supplemented with glycerol and soybean oil. *Appl Microbiol Biotechnol* 89:1395–1403.
- Cerda A, El-Bakry M, Gea T, Sánchez A. 2016a. Long term enhanced solid-state fermentation: Inoculation strategies for amylase production from soy and bread wastes by *Thermomyces* sp. in a sequential batch operation. *J Environ Chem Eng* 4:2394–2401.
- Cerda A, Martínez ME, Soto C, Zúñiga ME, Poirrier P. 2016b. Methanisation of spent maqui berry pomace via enzymatic treatment. *Renew Energy* 87:326–331.
- Cerda A, Gea T, Vargas-García MC, Sánchez A. 2017. Towards a competitive solid state fermentation: Cellulases production from coffee husk by sequential batch operation and role of microbial diversity. *Sci Total Environ* 589:56–65.
- Chen J, Song X, Zhang H, Qu Y. 2006. Production, structure elucidation and anticancer properties of sophorolipid from *Wickerhamiella domercqiae*. *Enzyme Microb Technol* 39:501–506.
- Chen LJ, Lin SY, Huang CC, Chen EM. 1998. Temperature dependence of critical micelle concentration of polyoxyethylenated non-ionic surfactants. *Colloids Surf A* 135:175–181.
- Cirigliano MC, Carman GM. 1984. Isolation of a bioemulsifier from *Candida lipolytica*. *Appl Environ Microbiol* 48:747–750.
- Daniel H, Reuss M, Sylatak C. 1998. Production of sophorolipids in high concentration from deproteinized whey and rapeseed oil in a two stage fed batch process using *Candida bombicola* ATCC 22214 and *Cryptococcus curvatus* ATCC 20509. *Biotechnol Lett* 20:1153–1156.
- Das K, Mukherjee AK. 2007. Comparison of lipopeptide biosurfactants production by *Bacillus subtilis* strains in submerged and solid state fermentation systems using a


- cheap carbon source: Some industrial applications of biosurfactants. *Process Biochem* 42:1191–1199.
- Daverey A, Pakshirajan K. 2009. Production of sophorolipids by the yeast *Candida bombicola* using simple and low cost fermentative media. *Food Res Int* 42:499–504.
- Daverey A, Pakshirajan K. 2010. Sophorolipids from *Candida bombicola* using mixed hydrophilic substrates: production, purification and characterization. *Colloids Surf B Biointerfaces* 79:246–253.
- Davila AM, Marchal R, Vandecasteele JP. 1994. Sophorose lipid production from lipidic precursors: Predictive evaluation of industrial substrates. *J Ind Microbiol* 13:249–257.
- Deshpande M, Daniels L. 1995. Evaluation of sophorolipid biosurfactant production by *Candida bombicola* using animal fat. *Bioresour Technol* 54:143–150.
- Develter DWG, Lauryssen LML. 2010. Properties and industrial applications of sophorolipids. *Eur J Lipid Sci Technol* 112:628–638.
- Díaz De Rienzo MA, Banat IM, Dolman B, Winterburn J, Martin PJ. 2015. Sophorolipid biosurfactants: Possible uses as antibacterial and antibiofilm agent. *N Biotechnol* 32:720–726.
- Dolman BM, Kaisermann C, Martin PJ, Winterburn JB. 2017. Integrated sophorolipid production and gravity separation. *Process Biochem* 54:162–171.
- European Union. 2003. Directive 2003/53/EC of the European Parliament and of the Council of 18 June 2003. *Off J Eur Union* 178:24–27.
- Faria NT, Marques S, Fonseca C, Ferreira FC. 2015. Direct xylan conversion into glycolipid biosurfactants, mannosylerythritol lipids, by *Pseudozyma antarctica* PYCC 5048T. *Enzyme Microb Technol* 71:58–65.
- Felse PA, Shah V, Chan J, Rao KJ, Gross R. 2007. Sophorolipid biosynthesis by *Candida bombicola* from industrial fatty acid residues. *Enzyme Microb Technol* 40:316–323.
- Finkler ATJ, Biz A, Oliveira Pitol LO, Medina BS, Luithardt H, Luz LFL, Krieger N, Mitchell DA. 2017. Intermittent agitation contributes to uniformity across the bed during pectinase production by *Aspergillus niger* grown in solid-state fermentation in a pilot-scale packed-bed bioreactor. *Biochem Eng J* 121:1–12.
- Flagella Z, Rotunno T, Tarantino E, Di Caterina R, de Caro A. 2002. Changes in seed yield and oil fatty acid composition of high oleic sunflower (*Helianthus annuus* L.) hybrids in relation to the sowing date and the water regime. *Eur J Agron* 17:221–230.

- 
- 
- Fleurackers SJJ. 2006. On the use of waste frying oil in the synthesis of sophorolipids. *Eur J Lipid Sci Technol* 108:5–12.
- Flodman HR, Nouredini H. 2013. Effects of intermittent mechanical mixing on solid-state fermentation of wet corn distillers grain with *Trichoderma reesei*. *Biochem Eng J* 81:24–28.
- García-Ochoa F, Casas JA. 1999. Unstructured kinetic model for sophorolipid production by *Candida bombicola*. *Enzyme Microb Technol* 25:613–621.
- Gautam P. 2002. Microbial production of extra-cellular phytase using polystyrene as inert solid support. *Bioresour Technol* 83:229–233.
- Gea T, Ferrer P, Alvaro G, Valero F, Artola A, Sánchez A. 2007. Co-composting of sewage sludge: fats mixtures and characteristics of the lipases involved. *Biochem Eng J* 33:275–283.
- Göbbert U, Lang S, Wagner F. 1984. Sophorose lipid formation by resting cells of *Torulopsis bombicola*. *Biotechnol Lett* 6:225–230.
- Gorin PAJ, Spencer JFT, Tulloch AP. 1961. Hydroxy fatty acid glycosides of sophorose from *Torulopsis Magnoliae*. *Can J Chem* 39:846–855.
- Haba E, Pinazo A, Pons R, Pérez L, Manresa A. 2014. Complex rhamnolipid mixture characterization and its influence on DPPC bilayer organization. *Biochim Biophys Acta - Biomembr* 1838:776–783.
- Haug RT. 1993. *The Practical Handbook of Compost Engineering*. Boca Raton, Florida: Lewis Publishers.
- Hernández-Rodríguez B, Córdova J, Bárzana E, Favela-Torres E. 2009. Effects of organic solvents on activity and stability of lipases produced by thermotolerant fungi in solid-state fermentation. *J Mol Catal B Enzym* 61:136–142.
- Hirata Y, Ryu M, Igarashi K, Nagatsuka A, Furuta T, Kanaya S, Sugiura M. 2009. Natural synergism of acid and lactone type mixed sophorolipids in interfacial activities and cytotoxicities. *J Oleo Sci* 58:565–572.
- Hommel RK, Weber L, Weiss A, Himmelreich U, Rilke O, Kleber HP. 1994a. Production of sophorose lipid by *Candida (Torulopsis) apicola* grown on glucose. *J Biotechnol* 33:147–155.
- Hommel RK, Stegner S, Kleber HP, Weber L. 1994b. Effect of ammonium ions on glycolipid production by *Candida (Torulopsis) apicola*. *Appl Microbiol Biotechnol* 42:192–197.

- Hu Y, Ju L-K. 2001. Sophorolipid production from different lipid precursors observed with LC-MS. *Enzyme Microb Technol* 29:593–601.
- Kim YB, Yun HS, Kim EK. 2009. Enhanced sophorolipid production by feeding-rate-controlled fed-batch culture. *Bioresour Technol* 100:6028–6032.
- Klekner V, Kosaric N, Zhou QH. 1991. Sophorose lipids produced from sucrose. *Biotechnol Lett* 13:345–348.
- Knepper TP, de Voogt P, Barcelo D. 2003. Analysis and fate of surfactants in the aquatic environment. *Wilson & Wilson's Comprehensive Analytical Chemistry*, vol 40. Amsterdam: Elsevier.
- Koh A, Gross R. 2016a. A versatile family of sophorolipid esters: Engineering surfactant structure for stabilization of lemon oil-water interfaces. *Colloids Surfaces A Physicochem Eng Asp* 507:152–163.
- Koh A, Gross R. 2016b. Molecular editing of sophorolipids by esterification of lipid moieties: Effects on interfacial properties at paraffin and synthetic crude oil-water interfaces. *Colloids Surfaces A Physicochem Eng Asp* 507:170–181.
- Koh A, Linhardt RJ, Gross R. 2016. Effect of sophorolipid n-alkyl ester chain length on its interfacial properties at the almond oil-water interface. *Langmuir* 32:5562–5572.
- Koh A, Wong A, Quinteros A, Desplat C, Gross R. 2017. Influence of sophorolipid structure on interfacial properties of aqueous - arabian light crude and related constituent emulsions. *J Am Oil Chem Soc* 94:107–119.
- Koneman EW, D. AS, Janda MW, Schreckenberger PC, Winn W. C. 2006. Introduction to Microbiology. In: *Color atlas and textbook of diagnostic microbiology*.
- Konishi M, Yoshida Y, Horiuchi J. 2015. Efficient production of sophorolipids by *Starmerella bombicola* using a corncob hydrolysate medium. *J Biosci Bioeng* 119:317–322.
- Krieger N, Neto DC, Mitchell DA. 2010. Production of Microbial Biosurfactants by Solid-State Cultivation. In: Ramkrishna S, editor. *Biosurfactants*. New York: Springer. p 203–210.
- Lang S, Brakemeier A, Heckmann R, Spöckner S, Rau U. 2000. Production of native and modified sophorose lipids. *Chim Oggi* 18:76–79.
- Maddikeri GL, Gogate PR, Pandit AB. 2015. Improved synthesis of sophorolipids from waste cooking oil using fed batch approach in the presence of ultrasound. *Chem Eng J* 263:479–487.


- 
- 
- Mahanty B, Pakshirajan K, Dasu VV. 2006. Production and properties of a biosurfactant applied to polycyclic aromatic hydrocarbon solubilization. *Appl Biochem Biotechnol* 134:129–41.
- Mann RM, Bidwell JR. 2001. The acute toxicity of agricultural surfactants to the tadpoles of four Australian and two exotic frogs. *Environ Pollut* 114:195–205.
- Martin del Campo M, Camacho RM, Mateos-Díaz JC, Müller-Santos M, Córdova J, Rodríguez JA. 2015. Solid-state fermentation as a potential technique for esterase/lipase production by *Halophilic archaea*. *Extremophiles* 19:1121–1132.
- Martínez O, Sánchez A, Font X, Barrena R. 2017. Valorization of sugarcane bagasse and sugar beet molasses using *Kluyveromyces marxianus* for producing value-added aroma compounds via solid-state fermentation. *J Clean Prod* 158:8–17.
- Martins S, Mussatto SI, Martínez-Avila G, Montañez-Saenz J, Aguilar CN, Teixeira JA. 2011. Bioactive phenolic compounds: Production and extraction by solid-state fermentation. A review. *Biotechnol Adv* 29:365–373.
- Mata-Gómez M, Mussatto SI, Rodríguez R, Teixeira JA, Martinez JL, Hernandez A, Aguilar CN. 2015. Gallic acid production with mouldy polyurethane particles obtained from solid state culture of *Aspergillus niger* GH1. *Appl Biochem Biotechnol* 176:1131–1140.
- Maulini-Duran C, Abraham J, Rodríguez-Pérez S, Cerda A, Jiménez-Peñalver P, Gea T, Barrena R, Artola A, Font X, Sánchez A. 2015. Gaseous emissions during the solid state fermentation of different wastes for enzyme production at pilot scale. *Bioresour Technol* 179:211–218.
- Mejias L, Komilis D, Gea T, Sánchez A. 2017. The effect of airflow rates and aeration mode on the respiration activity of four organic wastes: Implications on the composting process. *Waste Manag* 65:22–28.
- Miller GL. 1959. Use of dinitrosalicylic acid reagent for determination of reducing sugar. *Anal Chem* 31:426–428.
- Mitchell DA, Berovič M, Krieger N. 2006. Solid-state fermentation bioreactors: Fundamentals of design and operation. Berlin: Springer Berlin Heidelberg.
- Mnif I, Elleuch M, Chaabouni SE, Ghribi D. 2013. *Bacillus subtilis* SPB1 biosurfactant: Production optimization and insecticidal activity against the carob moth *Ectomyelois ceratoniae*. *Crop Prot* 50:66–72.
- Mohanty SK, Behera S, Swain MR, Ray RC. 2009. Bioethanol production from mahula (*Madhuca latifolia* L.) flowers by solid-state fermentation. *Appl Energy* 86:640–644.

- Morita T, Konishi M, Fukuoka T, Imura T, Kitamoto D. 2007. Microbial conversion of glycerol into glycolipid biosurfactants, mannosylerythritol lipids, by a basidiomycete yeast, *Pseudozyma antarctica* JCM 10317T. *J Biosci Bioeng* 104:78–81.
- Mukherjee S, Das P, Sen R. 2006. Towards commercial production of microbial surfactants. *Trends Biotechnol* 24:509–15.
- Mussatto SI. 2017. Challenges in building a sustainable biobased economy. *Ind Crops Prod* 106:1–2.
- Mussatto SI, Aguiar LM, Marinha MI, Jorge RC, Ferreira EC. 2015. Economic analysis and environmental impact assessment of three different fermentation processes for fructooligosaccharides production. *Bioresour Technol* 198:673–681.
- Nalini S, Parthasarathi R, Prabudoss V. 2016. Production and characterization of lipopeptide from *Bacillus cereus* SNAU01 under solid state fermentation and its potential application as anti-biofilm agent. *Biocatal Agric Biotechnol* 5:123–132.
- Nalini S, Parthasarathi R. 2014. Production and characterization of rhamnolipids produced by *Serratia rubidaea* SNAU02 under solid-state fermentation and its application as biocontrol agent. *Bioresour Technol* 173:231–238.
- Núñez A, Ashby R, Foglia TA, Solaiman DKY. 2001. Analysis and characterization of sophorolipids by liquid chromatography with atmospheric pressure chemical ionization. *Chromatographia* 53:673–677.
- Ooijkaas LP, Weber FJ, Buitelaar RM, Tramper J, Rinzema A. 2000. Defined media and inert supports: Their potential as solid-state fermentation production systems. *Trends Biotechnol* 18:356–360.
- Parekh VJ, Pandit AB. 2012. Solid state fermentation (SSF) for the production of sophorolipids from *Starmerella bombicola* NRRL Y-17069 using glucose, wheat bran and oleic acid. *Curr Trends Biotechnol Pharm* 6:418–424.
- Parekh VJ, Patravale VB, Pandit AB. 2012. Mango kernel fat: A novel lipid source for the fermentative production of sophorolipid biosurfactant using *Starmerella bombicola* NRRL -Y 17069. *Ann Biol Res* 3:1798–1803.
- Peng Y, Totsingan F, Meier MAR, Steinmann M, Wurm F, Koh A, Gross RA, Kim YB, Yun HS, Kim EK. 2015. Sophorolipids: Expanding structural diversity by ring-opening cross-metathesis. *Eur J Lipid Sci Technol* 117:6028–6032.
- Ponsá S, Gea T, Sánchez A. 2010. Different indices to express biodegradability in organic solid wastes. *J Environ Qual* 39:706–712.

- 
- 
- Pornsunthorntawe O, Arttaweeporn N, Paisanjit S, Somboonthanate P, Abe M, Rujiravanit R, Chavadej S. 2008. Isolation and comparison of biosurfactants produced by *Bacillus subtilis* PT2 and *Pseudomonas aeruginosa* SP4 for microbial surfactant-enhanced oil recovery. *Biochem Eng J* 42:172–179.
- Procter and Gamble. 2017. Working toward zero. Link <https://us.pg.com/sustainability/environmental-sustainability/focused-on/waste>. Last time consulted: 26/09/17.
- Radzuan MN, Banat IM, Winterburn J. 2017. Production and characterization of rhamnolipid using palm oil agricultural refinery waste. *Bioresour Technol* 225:99–105.
- Randhawa KKS, Rahman PKSM. 2014. Rhamnolipid biosurfactants-past, present, and future scenario of global market. *Front Microbiol* 5:1-7.
- Rao J, McClements DJ. 2012. Impact of lemon oil composition on formation and stability of model food and beverage emulsions. *Food Chem* 134:749–757.
- Rashad MM, Nooman MU, Ali MM, Mahmoud AE. 2014. Production, characterization and anticancer activity of *Candida bombicola* sophorolipids by means of solid state fermentation of sunflower oil cake and soybean oil. *Grasas Aceites* 65(2):e017.
- Rispoli FJ, Badia D, Shah V. 2010. Optimization of the fermentation media for sophorolipid production from *Candida bombicola* ATCC 22214 using a simplex centroid design. *Biotechnol Prog* 4:938–944.
- Rodríguez-Jasso RM, Mussatto SI, Sepúlveda L, Agrasar AT, Pastrana L, Aguilar CN, Teixeira JA. 2013. Fungal fucoidanase production by solid-state fermentation in a rotating drum bioreactor using algal biomass as substrate. *Food Bioprod Process* 91:587–594.
- Roelants SLKW, Ciesielska K, De Maeseneire SL, Moens H, Everaert B, Verweire S, Denon Q, Vanlerberghe B, Van Bogaert INA, Van der Meer P, Devreese B, Soetaert W. 2016. Towards the industrialization of new biosurfactants: Biotechnological opportunities for the lactone esterase gene from *Starmerella bombicola*. *Biotechnol Bioeng* 113:550–559.
- Ron EZ, Rosenberg E. 2001. Minireview. Natural roles of biosurfactants 3(4):229-236.
- Ruggieri L, Gea T, Artola A, Sánchez A. 2009. Air filled porosity measurements by air pycnometry in the composting process: a review and a correlation analysis. *Bioresour Technol* 10:2655–2666.
- Samad A, Zhang J, Chen D, Liang Y. 2015. Sophorolipid production from biomass hydrolysates. *Appl Biochem Biotechnol* 175:2246–2257.

- Santis-Navarro A, Gea T, Barrena R, Sánchez A. 2011. Production of lipases by solid state fermentation using vegetable oil-refining wastes. *Bioresour Technol* 102:10080–4.
- Sathi Reddy K, Yahya Khan M, Archana K, Gopal Reddy M, Hameeda B. 2016. Utilization of mango kernel oil for the rhamnolipid production by *Pseudomonas aeruginosa* DR1 towards its application as biocontrol agent. *Bioresour Technol* 221:291–299.
- Scott TA, Melvin EH. 1953. Determination of Dextran with Anthrone. *Anal Chem* 25:1656–1661.
- Seghal Kiran G, Anto Thomas T, Selvin J, Sabarathnam B, Lipton AP. 2010. Optimization and characterization of a new lipopeptide biosurfactant produced by marine *Brevibacterium aureum* MSA13 in solid state culture. *Bioresour Technol* 101:2389–2396.
- Shah V, Doncel GF, Seyoum T, Eaton KM, Zalenskaya I, Hagver R, Azim A, Gross R. 2005. Sphorolipids, microbial glycolipids with anti-human immunodeficiency virus and sperm-immobilizing activities. *Antimicrob Agents Chemother* 49:4093–4100.
- Shah V, Jurjevic M, Badia D. 2007. Utilization of restaurant waste oil as a precursor for sphorolipid production. *Biotechnol Prog* 23:512–515.
- Shi Z, Fu Q, Chen B, Xu S. 1999. Analysis of physicochemical property and composition of fatty acid of almond oil. *Chinese J Chromatogr* 17:506–507.
- Simione FP. 2009. Thermo Scientific nalgene and nunc cryopreservation guide. Thermo Fisher Scientific Inc.
- Singh A, Van Hamme JD, Ward OP. 2007. Surfactants in microbiology and biotechnology: Part 2. Application aspects. *Biotechnol Adv* 25:99–121.
- Slivinski CT, Mallmann E, de Araújo JM, Mitchell DA, Krieger N. 2012. Production of surfactin by *Bacillus pumilus* UFPEDA 448 in solid-state fermentation using a medium based on okara with sugarcane bagasse as a bulking agent. *Process Biochem* 47:1848–1855.
- Soares A, Guieysse B, Jefferson B, Cartmell E, Lester JN. 2008. Nonylphenol in the environment: A critical review on occurrence, fate, toxicity and treatment in wastewaters. *Environ Int* 34:1033–1049.
- Soberón-Chávez, G. 2011. *Biosurfactants: From genes to application*. Germany:Springer



- 
- 
- Solaiman DKY, Ashby RD, Zerkowski JA, Foglia TA. 2007. Simplified soy molasses-based medium for reduced-cost production of sophorolipids by *Candida bombicola*. *Biotechnol Lett* 29:1341–1347.
- Solaiman DKY, Ashby RD, Nuñez A, Foglia TA. 2004. Production of sophorolipids by *Candida bombicola* grown on soy molasses. *Biotechnol Lett* 26:1241–1245.
- Solans C, Izquierdo P, Nolla J, Azemar N, Garcia-Celma MJ. 2005. Nano-emulsions. *Curr Opin Colloid Interface Sci* 10:102–110.
- Spencer JF, Gorin PA, Tulloch AP. 1970. *Torulopsis bombicola* sp. n. *Antonie Van Leeuwenhoek* 36:129–133.
- Takahashi M, Morita T, Wada K, Hirose N, Fukuoka T, Imura T, Kitamoto D. 2011. Production of sophorolipid glycolipid biosurfactants from sugarcane molasses using *Starmerella bombicola* NBRC 10243. *J Oleo Sci* 60:267–273.
- Thaniyavarn J, Chianguthai T, Sangvanich P, Roongsawang N, Washio K, Morikawa M, Thaniyavarn S. 2008. Production of sophorolipid biosurfactant by *Pichia anomala*. *Biosci Biotechnol Biochem* 72:2061–2068.
- The US Department of Agriculture and The US Composting Council. 2001. Test methods for the examination of composting and compost. Houston: Edaphos International.
- Thomas L, Larroche C, Pandey A. 2013. Current developments in solid-state fermentation. *Biochem Eng J* 81:146–161.
- Van Bogaert INA, Develter D, Soetaert W, Vandamme EJ. 2008. Cerulenin inhibits de novo sophorolipid synthesis of *Candida bombicola*. *Biotechnol Lett* 30:1829–1832.
- Van Bogaert INA, Soetaert W. 2011. Sophorolipids. In: Soberón-Chávez, G, editor. *Biosurfactants*, *Microbiol. Monogr.* 20. Berlin, Germany: Springer-Verlag. p 179–210.
- Van Bogaert INA, Groeneboer S, Saerens K, Soetaert W. 2011a. The role of cytochrome P450 monooxygenases in microbial fatty acid metabolism. *FEBS J* 278:206–21.
- Van Bogaert INA, Zhang J, Soetaert W. 2011b. Microbial synthesis of sophorolipids. *Process Biochem* 46:821–833.
- Van Bogaert INA, Buyst D, Martins JC, Roelants SLKW, Soetaert WK. 2016. Synthesis of bolaform biosurfactants by an engineered *Starmerella bombicola* yeast. *Biotechnol Bioeng* 113:2644–2651.

- Van Hamme JD, Singh A, Ward OP. 2006. Physiological aspects. Part 1 in a series of papers devoted to surfactants in microbiology and biotechnology. *Biotechnol Adv* 24:604–20.
- Varesche MB, Zaiat M, Vieira RF, Vazoller RF, Foresti E. 1997. Microbial colonization of polyurethane foam matrices in horizontal-flow anaerobic immobilized-sludge reactor. *Appl Microbiol Biotechnol* 48:534–538.
- Velioglu Z, Ozturk Urek R. 2015. Optimization of cultural conditions for biosurfactant production by *Pleurotus djamor* in solid state fermentation. *J Biosci Bioeng* 120(5):526–531
- Wang S, Mulligan CN. 2009. Rhamnolipid biosurfactant-enhanced soil flushing for the removal of arsenic and heavy metals from mine tailings. *Process Biochem* 44:296–301.
- Winterburn JB, Martin PJ. 2012. Foam mitigation and exploitation in biosurfactant production. *Biotechnol Lett* 34:187–195.
- Yazid NA, Barrena R, Komilis D, Sánchez A. 2017. Solid-state fermentation as a novel paradigm for organic waste valorization: A review. *Sustain* 9:1–28.
- Yazid NA, Barrena R, Sánchez A. 2016. Assessment of protease activity in hydrolysed extracts from SSF of hair waste by and indigenous consortium of microorganisms. *Waste Manag* 49:420–426.
- Zhang L, Somasundaran P, Singh SK, Felse AP, Gross R. 2004. Synthesis and interfacial properties of sophorolipid derivatives. *Colloids Surfaces A Physicochem Eng Asp* 240:75–82.
- Zhi Y, Wu Q, Xu Y. 2017. Production of surfactin from waste distillers' grains by co-culture fermentation of two *Bacillus amyloliquefaciens* strains. *Bioresour Technol* 235:96–103.
- Zhou Q-H, Kosaric N. 1995. Utilization of canola oil and lactose to produce biosurfactant with *Candida bombicola*. *J Am Oil Chem Soc* 72:67–71.
- Zhu Z, Zhang F, Wei Z, Ran W, Shen Q. 2013. The usage of rice straw as a major substrate for the production of surfactin by *Bacillus amyloliquefaciens* XZ-173 in solid-state fermentation. *J Environ Manage* 127:96–102.
- Zhu Z, Zhang G, Luo Y, Ran W, Shen Q. 2012. Production of lipopeptides by *Bacillus amyloliquefaciens* XZ-173 in solid state fermentation using soybean flour and rice straw as the substrate. *Bioresour Technol* 112:254–260.



---

Zouari R, Ellouze-Chaabouni S, Ghribi-Aydi D. 2014. Optimization of *Bacillus subtilis* SPB1 biosurfactant production under solid-state fermentation using by-products of a traditional olive mill factory. *Achiev Life Sci* 8:162–169.

## *Annexes*





## I. Fat characterization of the winterization oil cake



lluis jané busquets  
laboratori d'anàlisi s.l.

nif. B61817615  
tel - fax 937211325  
lluis.jane@ljbilab.com  
www.ljbilab.com



LABORATORIO RECONOCIDO - HIRAO 2014  
MFAO, Sociedad Rectora  
del Mercado de Futuros  
del Aceite de Oliva, S.A.



Reconocido por el  
Consejo Oleícola Internacional  
para análisis físico-químico  
(01/12/16-30/11/17)



ENAC  
ENSAYOS  
Nº 918/LE1868

Los ensayos y actividades marcados  
con un (\*) no están amparados por la  
acreditación de ENAC

Luís Jané Busquets Laboratori d'Anàlisi S.L.  
c/ St Llorenç, 27 baixos 08192 Sant Quirze del Valles (Bcn)

UNIVERSITAT AUTÒNOMA DE BARCELONA  
Campus UAB Edifici A Area d'Economia i Finances  
08193 - Bellaterra  
BARCELONA

Registro Mercantil de Barcelona Tomo 31582 - Folio 73 Hoja B194757 - Incripción 1ª C.I.F. B-61817615

Nº de Informe: 42081

## INFORME DE ENSAYO

### Identificación de la Muestra

Fecha Recepción	25/07/2017	Fecha Emisión Informe	27/07/2017
Fecha Inicio Análisis	25/07/2017	Fecha Final Análisis	27/07/2017
Tipo de muestra	GRASA		
Referencia:	20.07.17		

Determinaciones/Ensayos	Resultados	Procedimiento	Metodología
<b>Composición de Ácidos Grasos (Cuantitativo %) + Trans</b>			
Ac. Láurico	0,01 %	PNT-RT-04	CG-FID
Ac. Mirístico	0,05 %	PNT-RT-04	CG-FID
Ac. Palmítico	4,62 %	PNT-RT-04	CG-FID
Ac. Palmitoleico	0,18 %	PNT-RT-04	CG-FID
Ac. Margárico	0,03 %	PNT-RT-04	CG-FID
Ac. Margaroleico	0,03 %	PNT-RT-04	CG-FID
Ac. Esteárico	2,77 %	PNT-RT-04	CG-FID
Ac. Oleico	80,88 %	PNT-RT-04	CG-FID
Ac. Linoleico	7,67 %	PNT-RT-04	CG-FID
Ac. Aráquico	1,27 %	PNT-RT-04	CG-FID
Ac. Linolénico	0,12 %	PNT-RT-04	CG-FID
Ac. Gadoleico	0,23 %	PNT-RT-04	CG-FID
Ac. Behénico	1,56 %	PNT-RT-04	CG-FID
Ac. Erúxico	<0,01 %	PNT-RT-04	CG-FID
Ac. Lignocérico	0,58 %	PNT-RT-04	CG-FID
Isómeros Trans Oleicos	0,01 %	PNT-RT-04	CG-FID
Isómeros Trans Linoleicos y Linolénicos	0,02 %	PNT-RT-04	CG-FID
<b>Ceras C36 - C62</b>			
* C36	10 mg/kg	PNT-RT-41	CG-FID
* C38	8 mg/kg	PNT-RT-41	CG-FID
* C40	71 mg/kg	PNT-RT-41	CG-FID
* C42	1.334 mg/kg	PNT-RT-41	CG-FID
* C44	6.922 mg/kg	PNT-RT-41	CG-FID
* C46	9.733 mg/kg	PNT-RT-41	CG-FID
* C48	7.259 mg/kg	PNT-RT-41	CG-FID
* C50	4.809 mg/kg	PNT-RT-41	CG-FID
* C52	3.775 mg/kg	PNT-RT-41	CG-FID
* C54	2.121 mg/kg	PNT-RT-41	CG-FID
* C56	1.265 mg/kg	PNT-RT-41	CG-FID
* C58	787 mg/kg	PNT-RT-41	CG-FID
* C60	460 mg/kg	PNT-RT-41	CG-FID

Inscrito en el Registro de Laboratorios Agroalimentarios de Cataluña del Departamento de Agricultura, Ganadería, Pesca y Alimentación como laboratorio acreditado en el sector de aceites y grasas.  
Inscrito en el Registro de Laboratorios de Salud Ambiental, Alimentaria y de control oficial de Cataluña como laboratorio acreditado con el Nº918/LE1868.

El laboratorio tiene a disposición del cliente que la solicite, la incertidumbre de los ensayos cuantitativos.

Este informe de ensayo corresponde únicamente a la muestra recibida y analizada.

Los resultados se consideran propiedad del cliente y no deberán reproducirse ni total ni parcialmente sin la aprobación por escrito del laboratorio.

Página 1 de 2



lluis jané busquets  
laboratori d'anàlisi s.l.

nif. B61817615  
tel - fax 937211325  
lluis.jane@ljbllab.com  
www.ljbllab.com



LABORATORIO RECONOCIDO - PERIÓ 2014  
MFAO, Sociedad Rectora  
del Mercado de Futuros  
del Aceite de Oliva, S.A.



Reconocido por el  
Consejo Oleícola Internacional  
para análisis físico-químico  
(01/12/16-30/11/17)



**ENAC**  
ENSAYOS  
Nº 918/LE1868

Los ensayos y actividades marcados  
con un (\*) no están amparados por la  
acreditación de ENAC

Nº de Informe: 42081

### INFORME DE ENSAYO

Determinaciones/Ensayos	Resultados	Procedimiento	Metodología
* C62	152 mg/kg	PNT-RT-41	CG-FID
* De la C36 hasta la C42	1.423 mg/kg	PNT-RT-41	CG-FID
* De la C44 hasta la C62	37.283 mg/kg	PNT-RT-41	CG-FID
* De la C36 hasta la C62	38.706 mg/kg	PNT-RT-41	CG-FID

Responsable Técnico del Laboratorio,  
Anna Jané.

Registro Mercantil de Barcelona Tomo 31582 - Folio 73 Hoja B194757 - Inscrición 1ª C.I.F. B-61817615

Inscrito en el Registro de Laboratorios Agroalimentarios de Cataluña del Departamento de Agricultura, Ganadería, Pesca y Alimentación como laboratorio acreditado en el sector de aceites y grasas.  
Inscrito en el Registro de Laboratorios de Salud Ambiental, Alimentaria y de control oficial de Cataluña como laboratorio acreditado con el Nº918/LE1868.

El laboratorio tiene a disposición del cliente que la solicite, la incertidumbre de los ensayos cuantitativos.  
Este informe de ensayo corresponde únicamente a la muestra recibida y analizada.

Los resultados se consideran propiedad del cliente y no deberán reproducirse ni total ni parcialmente sin la aprobación por escrito del laboratorio.

Página 2 de 2

## II. Calibration curves

### Reducing sugar content (DNS method)

Calibration curve and calculation done for the reducing sugar content – DNS method described in Chapter 3, section 3.5.4.

**Table II.1.** Standard curve prepared from 2 g L<sup>-1</sup> glucose solution.

Tube	Standard (mL)	Distilled water (mL)	Reagent (mL)	Concentration (g L <sup>-1</sup> )
1	0.100	0.900	3	0.2
2	0.250	0.750	3	0.5
3	0.375	0.625	3	0.75
4	0.500	0.500	3	1
5	0.750	0.250	3	1.5
6	1	0	3	2

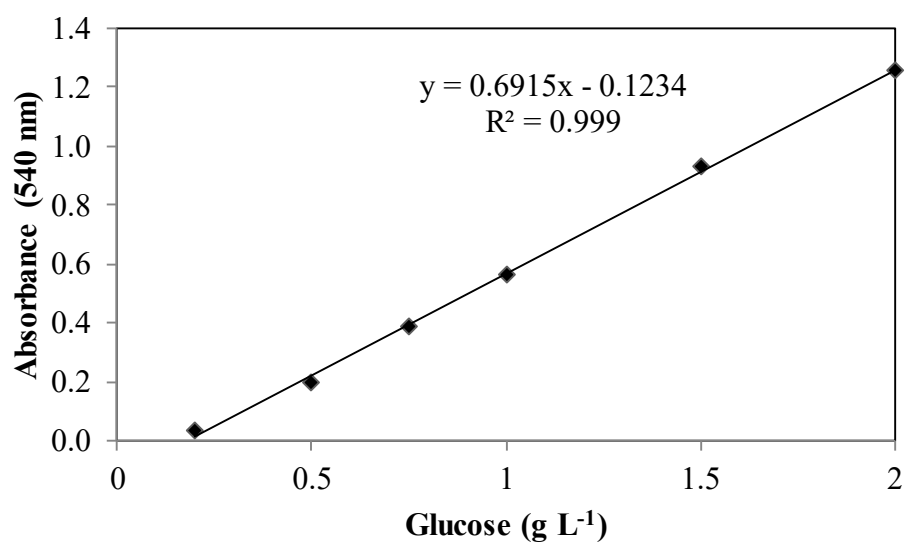


**Figure II.1.** Calibration curve for reducing sugar content. Absorbance = f (concentration)

$$\text{Absorbance (540 nm)} = -0.1234 + 0.6915 * \text{concentration (g L}^{-1}\text{)}$$



### Total sugar content (anthrone method)

Calibration curve and calculation done for the total sugar content – anthrone method described in Chapter 3, section 3.5.5. Only one sample is showed. Every new set of measurements, the calibration curve was re-done.

**Table II.2.** Standard curve prepared from 0.1 g L<sup>-1</sup> glucose solution.

Tube	Standard (mL)	Distilled water (mL)	Reagent (mL)	Concentration (g L <sup>-1</sup> )
0	0	1	4	0
1	0.2	0.8	4	0.02
2	0.4	0.6	4	0.04
3	0.6	0.4	4	0.06
4	0.8	0.2	4	0.08
5	1	0	4	0.1

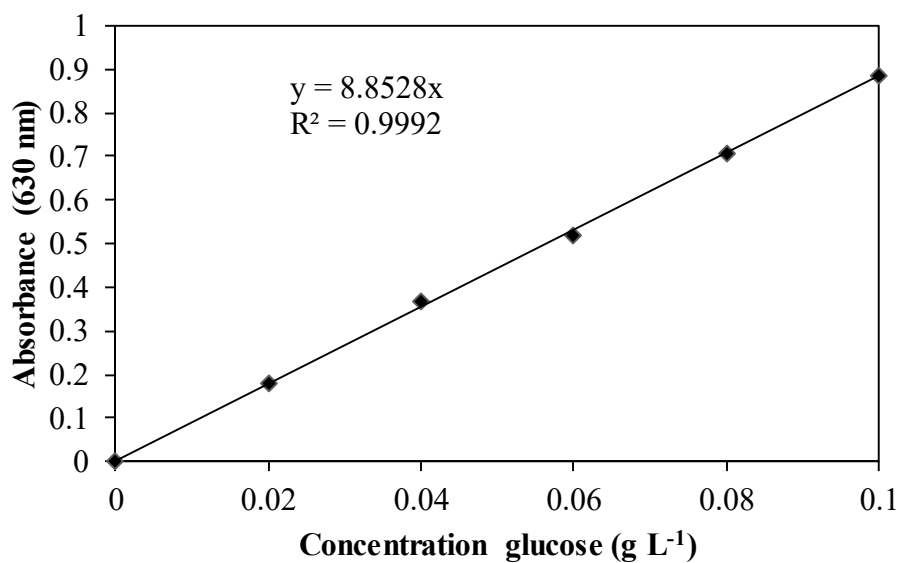


**Figure II.2.** Calibration curve for total sugar content. Absorbance = f (concentration)

$$\text{Absorbance (630 nm)} = 8.8528 * \text{concentration (g L}^{-1}\text{)}$$

### Sophorolipid content

Calibration curve performed with the purified diacetylated lactonic C18:1 SL (Chapter 7, section 7.3.2). The calibration curve was prepared using concentrations ranging from 0 to 1 g L<sup>-1</sup> and their response was measured with the UV-Vis detector of the HPLC. HPLC chromatograms and the resulting calibration curve is shown in Figure I.3 and I.4, respectively.

**Table II.3.** Standard curve prepared from 1 g L<sup>-1</sup> pure SL solution.

Tube	Standard (mL)	50:50 (v/v) Acetonitrile:water (mL)	Concentration (g L <sup>-1</sup> )
0	0	1	0
1	0.4	0.6	0.4
2	0.7	0.3	0.7
3	1	0	1

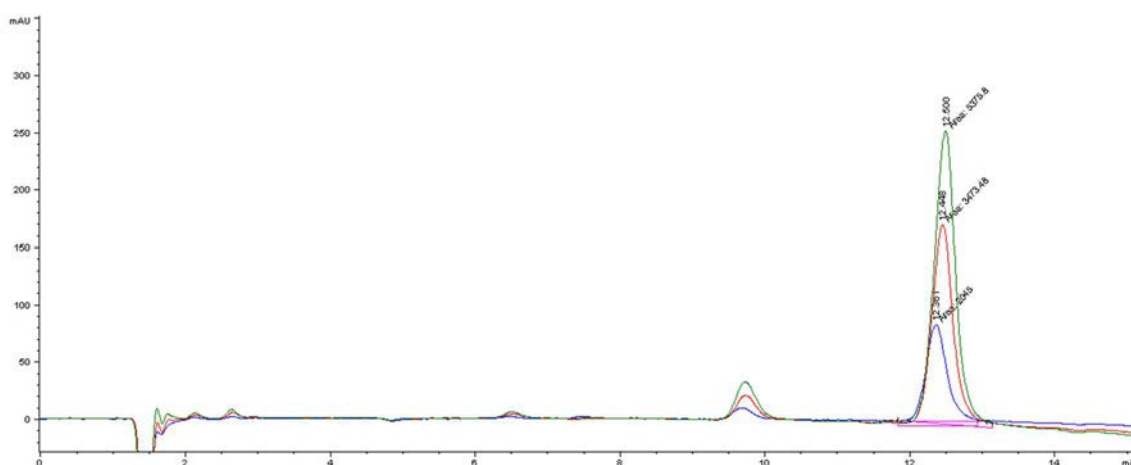


**Figure II.3.** HPLC chromatograms of the diacetylated lactonic C18:1 SL at concentrations of 0.4 (blue), 0.7 (red) and 1 (green) g L<sup>-1</sup>.

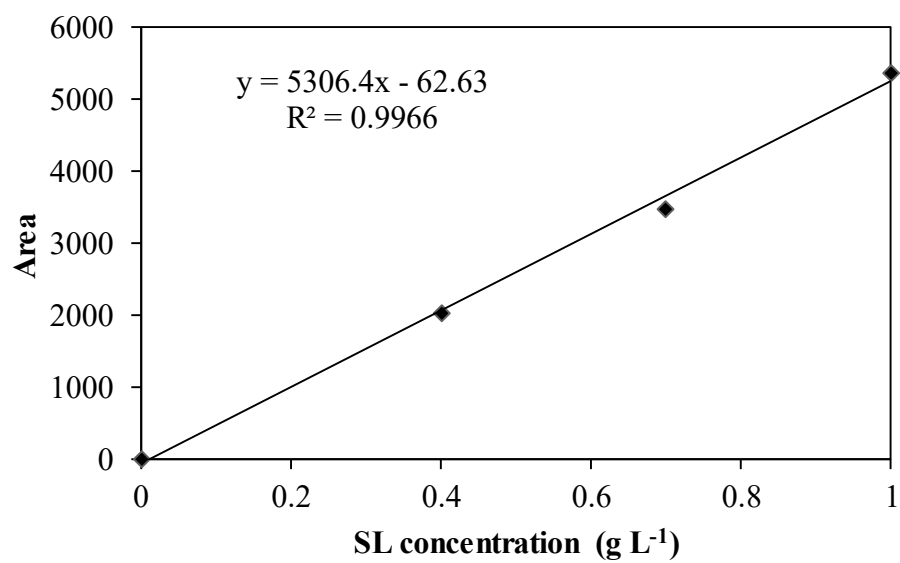


**Figure II.4.** Calibration curve for the diacetylated lactonic C18:1 SL. Area = f (concentration)

$$\text{Area} = -62.6 + 5306.4 * \text{concentration (g L}^{-1}\text{)}$$

### III. Surface tension curves at temperatures ranging from 15 to 50 °C

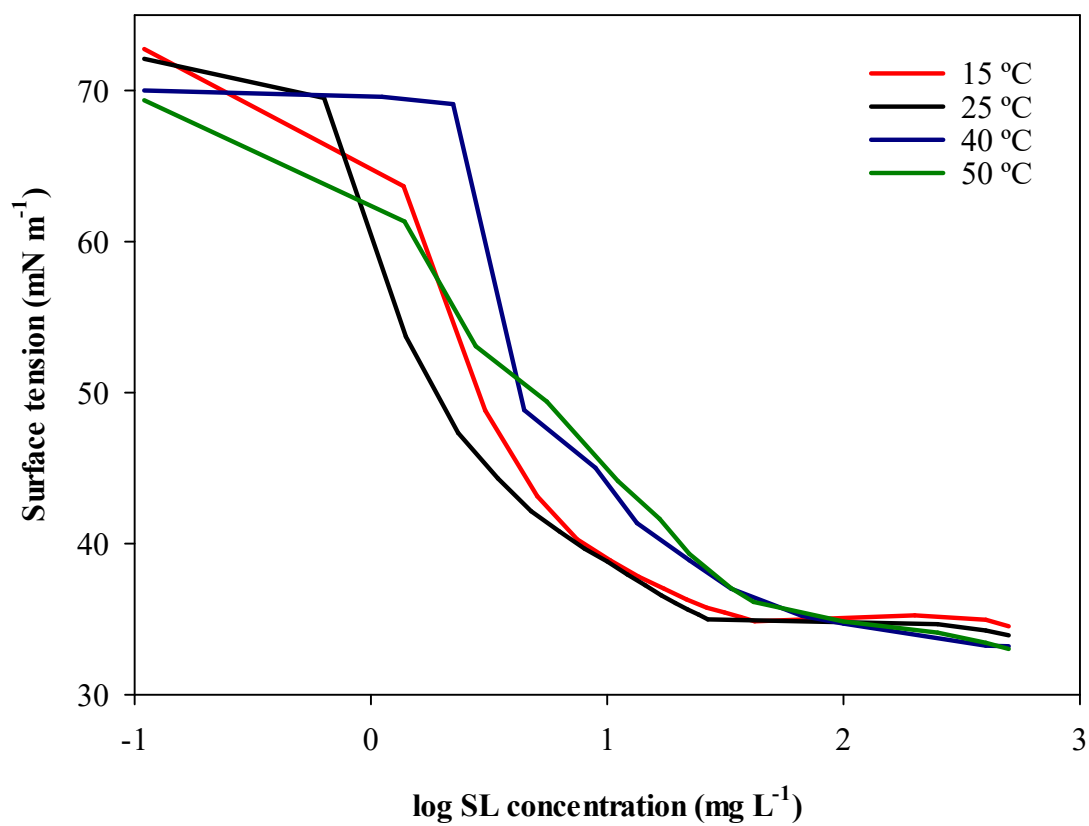


**Figure III.** Surface tension curves obtained for the SLs from WOC at 15, 25, 40 and 50 °C.



#### IV. Ethyl ester SL characterization

The EESL was analysed by LC-MS. The molecule elucidated at 4.3 min in the acidic region (Figure IV.1A) with a  $m/z$  of 1300.2 (Figure IV.1B) which corresponds to the adduct  $[2M-H]^-$  and confirms the synthesis of the EESL (M.W.  $650 \text{ g mol}^{-1}$ ).  $^1\text{H}$  and  $^{13}\text{C}$  NMR of EESL has previously been published (Bisht et al., 1999).

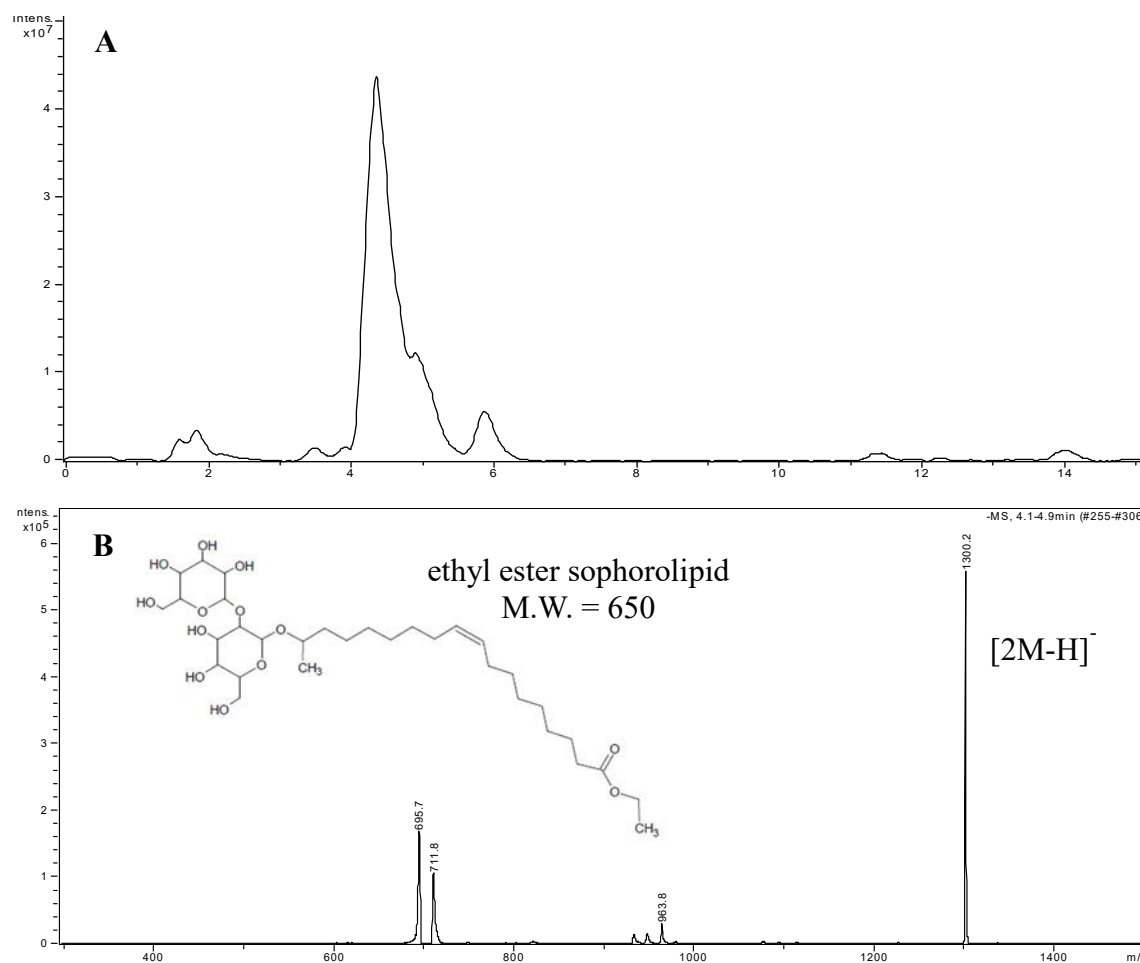


**Figure IV.1.** Total ion chromatogram (A) and mass spectra (B) of the EESL synthesized.



Figure IV.2 shows the surface tension curve obtained for the EESL.

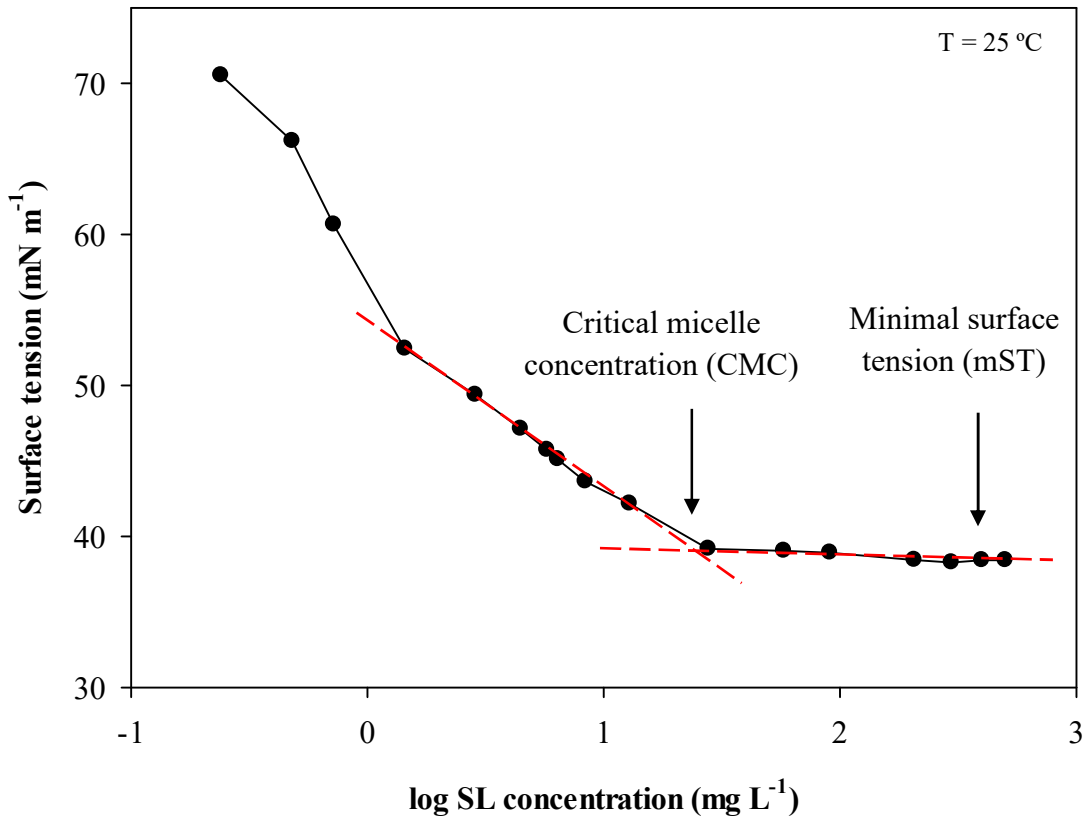


**Figure IV.2.** Surface tension curve at 25 °C of the synthesized EESL.



## V. Scanning electron microscope pictures of polyurethane foam cubes

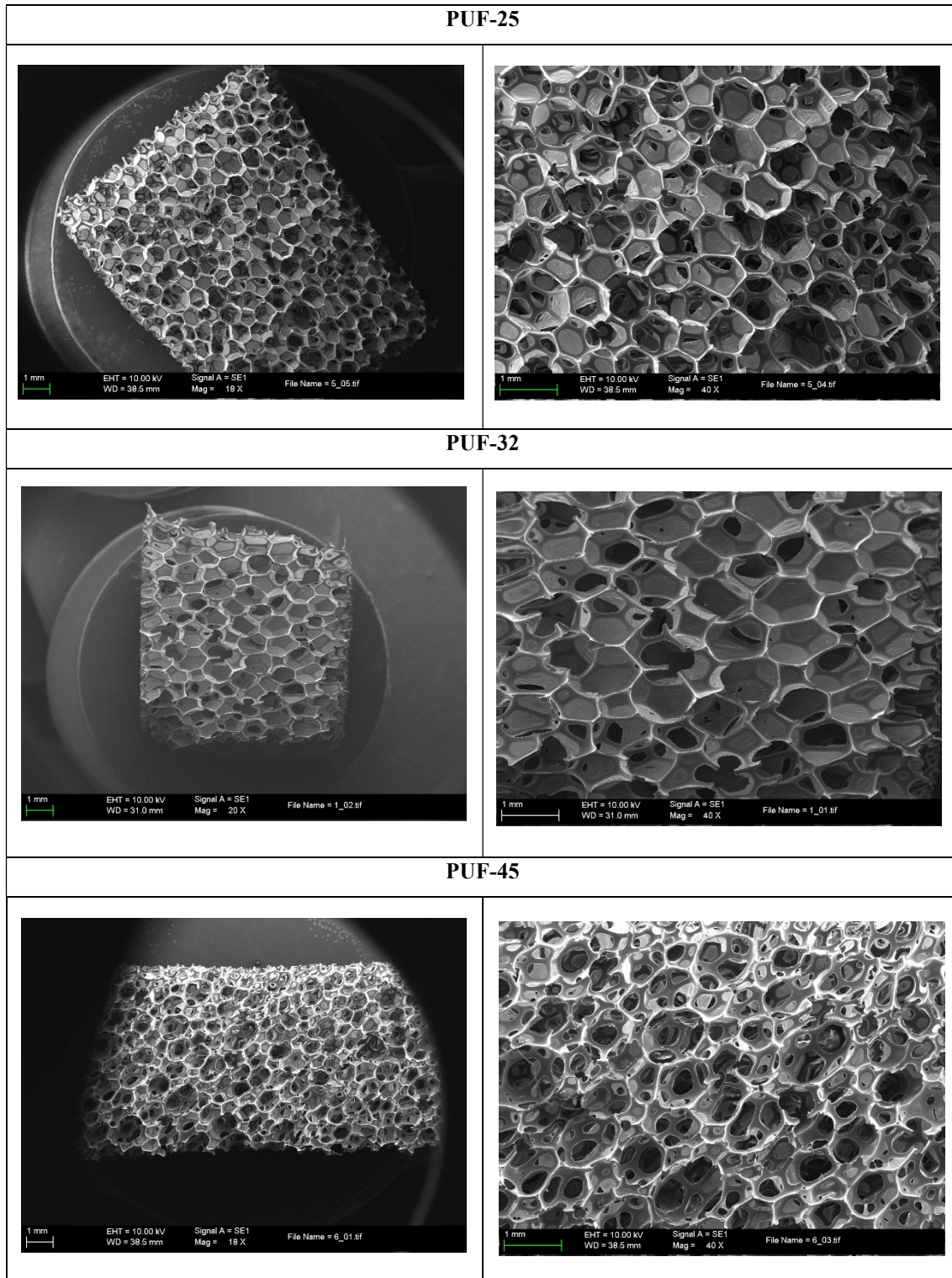


**Figure V.** Scanning electron microscope (SEM) pictures of polyurethane foam (PUF) cubes of different densities





## VI. Surface tension curve of the SLs from stearic acid

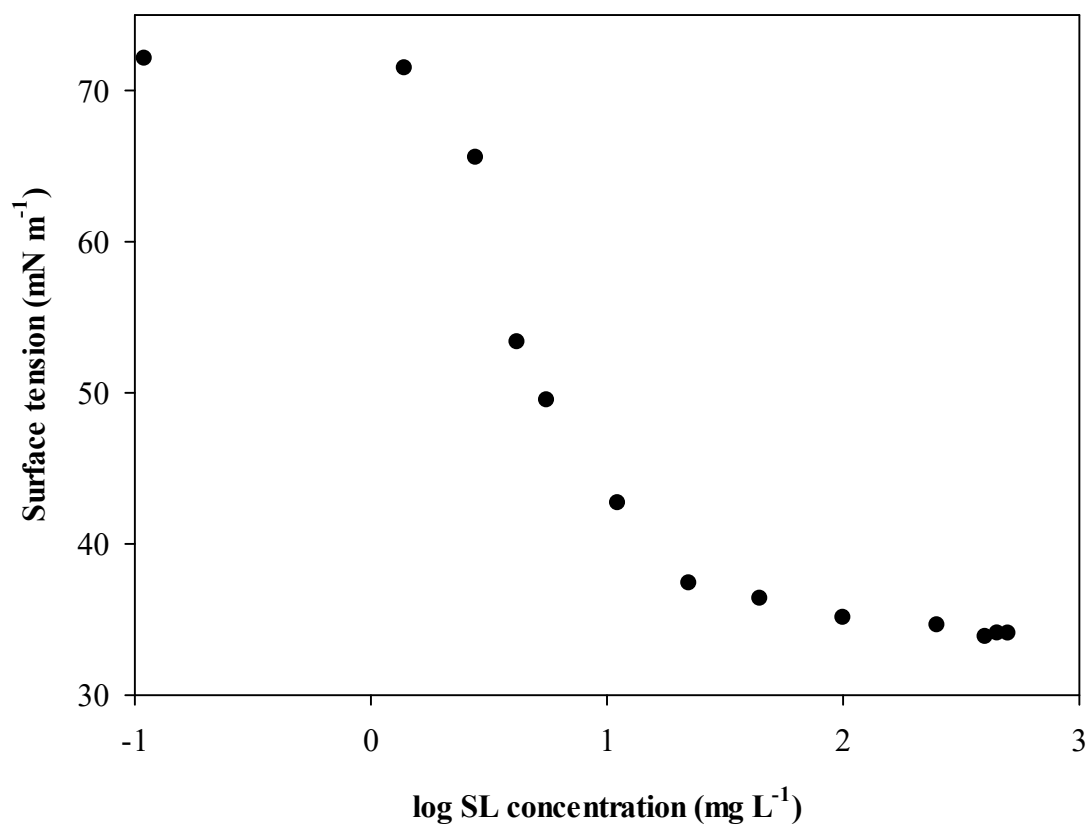


**Figure VI.** Surface tension curve of the SLs from stearic acid.